

## **PLEASE NOTE**

*The negative microfilm copy of this dissertation was prepared and inspected by the school granting the degree. We are using this film without further inspection or change. If there are any questions about the content, please write directly to the school.*

## **INFORMATION TO USERS**

The following explanation of techniques is provided to help clarify markings or notations which may appear on this reproduction.

1. The sign or "target" for pages apparently lacking from the document photographed is "Missing Page(s)". If it was possible to obtain the missing page(s) or section, they are spliced into the film along with adjacent pages. This may have necessitated cutting through an image and duplicating adjacent pages to assure complete continuity.
2. When an image on the film is obliterated with a round black mark, it is an indication of either blurred copy because of movement during exposure, duplicate copy, or copyrighted materials that should not have been filmed. For blurred pages, a good image of the page can be found in the adjacent frame. If copyrighted materials were deleted, a target note will appear listing the pages in the adjacent frame.
3. When a map, drawing or chart, etc., is part of the material being photographed, a definite method of "sectioning" the material has been followed. It is customary to begin filming at the upper left hand corner of a large sheet and to continue from left to right in equal sections with small overlaps. If necessary, sectioning is continued again—beginning below the first row and continuing on until complete.
4. For illustrations that cannot be satisfactorily reproduced by xerographic means, photographic prints can be purchased at additional cost and inserted into your xerographic copy. These prints are available upon request from the Dissertations Customer Services Department.
5. Some pages in any document may have indistinct print. In all cases the best available copy has been filmed.

**University  
Microfilms  
International**  
300 N. Zeeb Road  
Ann Arbor, MI 48106



**Microfilmed by Univ. of Wisconsin-Madison  
Memorial Library, Collection Maintenance Office** 84-21945

**PALSSON, Bernhard Orn**  
**MATHEMATICAL MODELLING OF DYNAMICS AND CONTROL**  
**IN METABOLIC NETWORKS**

The University of Wisconsin-Madison, Ph.D., 1984

**University Microfilms International Ann Arbor, Michigan 48106**

**© 1984 Bernhard Orn Palsson**

**All rights reserved.**



MATHEMATICAL MODELLING OF DYNAMICS AND CONTROL  
IN METABOLIC NETWORKS

A thesis submitted to the Graduate School of the  
University of Wisconsin-Madison in partial fulfillment of  
the requirements for the degree of Doctor of Philosophy

by

BERNHARD ORN PALSSON

Degree to be awarded: December 19\_\_\_\_ May 19\_\_\_\_ August 19 84\_\_\_\_

Approved by Thesis Reading Committee:

S. N. Ljungdahl  
Major Professor

July 30th, 1984  
Date of Examination

W. Harmon Ray

Dale F. Rudd

Robert M. Bock  
Dean, Graduate School



MATHEMATICAL MODELLING OF DYNAMICS AND CONTROL  
IN METABOLIC NETWORKS

by

BERNHARD ORN PALSSON

A thesis submitted in partial fulfillment of the  
requirements for the degree of

DOCTOR OF PHILOSOPHY  
(Chemical Engineering)

at the

UNIVERSITY OF WISCONSIN - MADISON

1984

 Copyright by Bernhard Orn Palsson 1984

All Rights Reserved

**to Mahshid Akasheh**

MATHEMATICAL MODELLING OF DYNAMICS AND CONTROL  
IN METABOLIC NETWORKS

BERNHARD ORN PALSSON

Under the Supervision of Professor Edwin N. Lightfoot

ABSTRACT

The intermediary metabolism, a large network of self-regulated enzyme catalyzed reactions, forms a fundamental entity in living systems. Its dynamics and regulation have long been of central physiological importance and of much philosophical concern. Malfunction of regulation is pathologically important.

Prediction of dynamic response and elucidation of control strategy of self-regulatory mechanisms, in this otherwise well studied reaction network, has yet to be achieved. Such study seems timely in view of rapidly developing biotechnology where metabolic dynamics play a central role, in as diverse areas as fermentation, chemotherapy and design of genetically engineered organisms; hence they naturally form a fundamental aspect.

It is the main purpose of this thesis to initiate such a study and explore the utility of chemical engineering expertise to tackle

this important problem. Presented here are initial stages of a comprehensive hierarchical modelling process which starts with simple systems, where basic physico-chemical laws apply, and then seeks to identify and describe key characteristics as compactly and economically as possible at each stage. The thesis is divided into two parts: biochemical dynamics and biochemical regulation.

The study of biochemical dynamics begins with the simple Michaelis-Menten reaction mechanism, which has mathematically intractable mass action kinetic description. Through judicious scaling and linearization an assessment of the validity of approximate descriptions, such as the quasi-steady state and quasi-equilibrium solutions, and the parametric sensitivity of the dynamics are obtained. This approach is extended to dimeric enzymes and a sequence of Michaelis-Menten reactions, where the overall dynamics can be expressed in terms of temporal moments which in turn give the important relationship between individual kinetic properties and overall response.

The study of regulation also starts with the simplest systems possible: single biochemical control loops where the end-product of a reaction chain feedback regulates the first reaction. Local stability and bifurcation analyses show two types bifurcations: for feedback activation multiple steady states exist and for feedback inhibition sustained oscillations appear. Both situations are postulated of being capable of carrying out important physiological functions: multiple steady states form a rudimentary decision making

mechanism whereas feedback inhibition can generate temporal signals.

JUL 31 1984

Approved: E.N. Lightfoot  
Professor Edwin N. Lightfoot

Date: 30 July, '84

## ACKNOWLEDGEMENTS.

During the course of preparing this thesis my mind has wandered back over the years that I have spent here in Madison. Several people come to my mind whose help and support I enjoyed both personally and professionally and to whom I would like to express my deepest gratitude.

The most important source of support came from my wife Mahshid Akasheh who through many difficult periods stood firmly by my side and was always ready to accept the high priority given to my professional efforts. It is to her that this thesis is dedicated. Our daughter Shireen Maria, born here in Madison, has given me many enjoyable moments. My parents, Pall Vigkonarson and Erna Arnar offered continuous flow of encouragement and help through these years, as they always have.

On the professional level I am indebted to the faculty and my fellow graduate students from whom I have learned so much over the years. From the day (May 1980) I proposed the study presented herein my major advisor, Professor E. N. Lightfoot, has been a continuous source of inspiration, suggestions and recommendations. His superb sense for organization and ability to extract the essentials from any problem brought for him have always motivated me; skills which I

hope that I have been able to acquire, even in modest amounts. I have learned from him what high-quality research is and how to communicate effectively research results, both verbally and in writing.

Two other faculty members have contributed immensely to my professional training. Professor Manfred Morari has ingrained into my mind the important concepts of control theory and the frequent discussions that we have had through the years always filled me with inspiration. Professor Morari's perceptive view of control theory shaped, in an important way, my thinking about biological regulation. I have been fortunate to have the opportunity to know him personally and we have spent many enjoyable hours on the tennis court together. More indirectly I have learned from Professor W. Harmon Ray and his group of graduate students about the fascinating world of dynamics of chemically reacting systems and how they are analyzed in mathematical terms. Acquiring this knowledge certainly had a major impact on the work presented herein. Furthermore I, and the department as a whole, benefited enormously from his leadership as department chairman.

My interactions with two other faculty members, Professors R. B. Bird and D. F. Rudd, have been both professionally rewarding and personally enjoyable.

Professor Sigmundur Gudbjarnason and Jónas Hallgrímsson M. D. of the University of Iceland introduced me to the exciting world of biochemistry and applied medical research. My professional career was significantly influenced by my experience in their laboratory.

I have been fortunate to have had the opportunity to be a part of and interact with the diverse group of truly outstanding graduate students here at Wisconsin. Two of my colleagues which I have had special pleasure of knowing are Bramie Lenhoff and Phil Lewellen. Their scholarly approach, strive for excellence and keen eye for detail helped to shape my way of thinking and that has left its mark on the work presented herein. Bramie Lenhoff selflessly gave generous portions of his time to help me with the wide spectrum of problems that I encountered; his seemingly encyclopedic knowledge about almost any topic often served as a reliable source of information.

Many other of my colleagues have lend me a helping hand and made my stay in Madison pleasant. I would like to single out, Costas Economou, Allan Hatton, Jim Rawlings, Tad Taylor and Magnús Sigurdsson for special mention.

Two members of the staff at the Chemical Engineering Department have been especially helpful. The resourceful Todd Ninman provided me with invaluable help both with software and hardware problems during many frustrating moments. Diane Peterson, with her constant strive for perfection, helped me preparing many manuscripts.

Financial support came from various sources. These include: Rotary International, the American Scandinavian Foundation, the Graduate School at the University of Wisconsin, and the Engineering Experiment Station. In times of need the generous Icelandic Student Loan Fund made funds available.

## TABLE OF CONTENTS

	Page
<b>Abstract</b>	iii
<b>Acknowledgements</b>	vi
<b>List of Figures</b>	xv
<b>List of Tables</b>	xx
<b>CHAPTER 1 - Introduction.</b>	<b>1</b>
<b>1.1. Properties of Living Matter.</b>	<b>2</b>
1.1.1. Formation of living matter.	2
1.1.2. Definition of "alive".	5
<b>1.2. A Brief Description of the Intermediary Metabolism.</b>	<b>8</b>
1.2.1. Early discoveries.	8
1.2.2. Mass flow.	10
1.2.3. Energy flow.	12
1.2.4. Regulation.	14
<b>1.3. Engineering and Living Systems.</b>	<b>23</b>
1.3.1. Motivation - general considerations.	23
1.3.2. Motivation - some specifics	24
<b>1.4. Mathematical Modelling of Metabolic Activity.</b>	<b>28</b>
1.4.1. Irreversible thermodynamics.	29
1.4.2. Bifurcation analysis.	30
1.4.3. Local analysis.	31
1.4.4. Numerical simulations.	32

PART I.	
Biochemical Dynamics	34
CHAPTER 2 - Simple Enzymatic Reaction Mechanisms: Michaelis-Menten Kinetics.	35
2.1. Michaelis-Menten Kinetics.	35
2.1.1. The reaction mechanism.	35
2.1.2. Kinetic description.	36
2.1.3. Scaling.	38
2.1.4. The dimensionless parameters.	39
2.2. Quasi-Stationary Analysis.	42
2.3. Linear Analysis.	43
2.3.1. Linear analysis - General procedure.	43
2.3.2. The stationary solution.	45
2.3.3. Linearization of the Michaelis-Menten model.	46
2.3.4. The eigenvalues.	47
2.3.5. The normal modes.	52
2.3.6. Influence of dimensionless parameters on dynamics.	57
2.4. Singular Perturbations.	62
2.5. Numerical solutions.	65
2.5.1. Batch Kinetics.	65
2.5.2. Open systems.	73
2.6. Discussion and Conclusions.	79
2.7. Summary.	85
CHAPTER 3 - Michaelis-Menten Kinetics - A Review.	87
3.1. Simple Approximations.	89
3.1.1. The quasi-steady state assumption.	89
3.1.2. The quasi-equilibrium approximation.	91
3.2. Error Analysis.	92
3.2.1. Analytical error estimation.	93
3.2.2. Numerical error analysis.	98
3.3. Transient Solutions.	101
3.4. Improved stationary solutions.	111

CHAPTER 4 - Dynamic Behavior of Simple Homotropic Enzymes.	117
4.1. Development of a Kinetic Model.	119
4.1.1. The reaction mechanism.	119
4.1.2. Kinetic description.	120
4.1.3. Scaling.	121
4.1.4. The dimensionless groups.	122
4.1.5. The non-cooperative dimer.	124
4.1.6. Solution strategies.	125
4.2. The Stationary Point.	126
4.3. Quasi-steady State Analysis.	130
4.4. Linear Analysis.	131
4.4.1. Linearization of the dimeric model.	132
4.4.2. The eigenvalues.	133
4.4.3. The modes.	135
4.5. Discussion and Conclusions.	147
4.6. Summary.	149
Chapter 5 - Linear Reaction Sequences.	150
5.1. Linear Analysis.	151
5.1.1. Kinetic description.	152
5.1.2. Scaling	152
5.1.3. The steady state equations.	155
5.1.4. Linearization.	155
5.1.5. Modal analysis.	157
5.2. Moments and Model Reduction.	165
5.2.1. Definition and meaning of temporal moments.	165
5.2.2. Evaluation of the moments.	167
5.2.3. The moments of $g_X$ .	171
5.2.4. Frequency response.	174
5.2.5. Model reduction - the method of moments.	175
5.3. Discussion and Conclusions.	184
5.3.1. Trials and tribulation of metabolic modellers.	184
5.3.2. The time constants.	187
5.3.3. Species interactions.	189
5.4. Summary	189

PART II.	
Biochemical Regulation	191
CHAPTER 6 - Single Biochemical Control Loops:	
Local Stability Analysis	192
6.1. Objectives and Approach.	195
6.1.1. System definition.	196
6.1.2. Kinetic description.	197
6.1.3. Interpretation.	198
6.1.4. Scaling.	200
6.2. The Dynamic Operator $C(\mathcal{D})$ .	201
6.2.1. General operators.	201
6.2.2. Linear operators - Transfer functions.	202
6.3. Local Stability Analysis.	204
6.3.1. Linearization.	204
6.3.2. The eigenvalues.	205
6.4. Discussion.	213
6.5. Summary.	217
CHAPTER 7 - Single Biochemical Control Loops:	
Positive Feedback.	219
7.1. The Single Biochemical Control Loop.	223
7.2. Kinetic Descriptions of Regulatory Enzymes.	224
7.2.1. The Lumped Controller.	225
7.2.2. The Symmetry Model.	228
7.3. Loops with Lumped Controllers.	229
7.3.1. Linear removal rate.	230
7.3.2. Michaelis-Menten removal rate.	236
7.4. Loops with the Symmetry Model.	245
7.4.1. Linear removal rate.	246
7.4.2. Michaelis-Menten removal rate.	250
7.5. Discussion.	251
7.6. Summary.	257

CHAPTER 8 - Single Biochemical Control Loops: Negative Feedbak.	259
8.1. The Single Biochemical Control Loop.	263
8.1.1. Mathematical model.	263
8.1.2. Local stability analysis.	263
8.1.3. Kinetic description of regulatory enzymes.	264
8.1.4. Kinetic description of the removal rate.	266
8.1.5. Stability of bifurcated solutions.	266
8.2. Loops with Lumped Controllers.	271
8.2.1. Linear removal rate.	271
8.2.2. Constant removal rate	277
8.2.3. Michaelis-Menten removal rate.	279
8.2.4. Computations of bifurcated solution brances.	284
8.3. Loops with the Symmetry Model.	288
8.3.1. Linear removal rate.	292
8.3.2. Constant removal rate	294
8.3.3. Michaelis-Menten removal rate.	294
8.4. Discussion.	297
8.5. Summary	300
CHAPTER 9 - Mathematical Modelling of Feedback Inhibition: A review.	302
9.1. The Goodwin Equations.	303
9.2. Stability Analysis of the Goodwin Equations.	306
9.2.1. The characteristic equation.	306
9.2.2. Hopf bifurcation.	309
9.2.3. Popov's theorem.	314
9.2.4. The second method of Lyapunov.	319
9.2.5. Harmonic balancing.	324
9.2.6. Computational search.	326
9.3. Modifications of the Goodwin Equations.	327
9.3.1. Time delays.	327
9.3.2. Different intermediate rate laws.	329
9.4. Power Law Kinetics.	332

<b>CHAPTER 10 - Conclusions and Recommendations.</b>	<b>335</b>
<b>10.1 Conclusions.</b>	<b>336</b>
10.1.1. Biochemical reacion dynamics.	336
10.1.2. Biochemical regulation.	340
<b>10.2. Recommendations.</b>	<b>344</b>
10.2.1. Branched pathways.	344
10.2.2. Hierarchical loops.	345
<b>References</b>	<b>347</b>
<b>Appendix A - Diffusional Effects.</b>	<b>363</b>
<b>Appendix B - On the Dynamics of Two Dimensional Linear Systems.</b>	<b>365</b>
<b>Appendix C - Numerical Evaluation of the Frequency Response.</b>	<b>368</b>
<b>Appendix D - Evaluation of Parameters for Low Order Transfer Functions.</b>	<b>373</b>
<b>Appendix E - Program Listings.</b>	<b>376</b>
Transient response of the Michaelis-Menten reaction mechanism (chapter 2).	378
Frequency response of a sequence of irreversible Michaelis-Menten reactions (chapter 5).	387
Local stability analysis of single biochemical control loops (chapter 8).	400

## LIST OF FIGURES

	Page
<b>Figure 1-1.</b> Illustration of the probable course of evolution.	3
<b>Figure 1-2.</b> Schematic illustrating the central role of metabolism in problems of practical importance.	7
<b>Figure 1-3.</b> Schematic illustrating the overall function of the intermediary metabolism.	11
<b>Figure 1-4.</b> Schematic illustration showing the main pathways and intermediates of energy metabolism.	13
<b>Figure 1-5.</b> Schematic of interacting metabolic and epigenic control loops.	16
<b>Figure 2-1.</b> Relative relaxation times for Michaelis-Menten kinetics.	50
<b>Figure 2-2.</b> The modal matrix and the time constants for the Michaelis-Menten mechanism as functions of the Quasi-steady state number.	58
<b>Figure 2-3.</b> The modal matrix and the time constants for the Michaelis-Menten mechanism as functions of the steady state concentration of the substrate.	59
<b>Figure 2-4.</b> The modal matrix and the time constants for the Michaelis-Menten mechanism as functions of the Stickyness number.	60
<b>Figure 2-5.</b> The modal matrix and the time constants for the Michaelis-Menten mechanism as functions of the overall equilibrium constant.	61
<b>Figure 2-6.</b> Dynamic decoupling during the transient phase of Michaelis-Menten kinetics and the zeroth order inner perturbation solution for batch systems.	66
<b>Figure 2-7.</b> Dynamic decoupling during the stationary phase of Michaelis-Menten kinetics and the quasi-steady	

state solution for batch systems.	69
Figure 2-8. The quasi-equilibrium solution for Michaelis-Menten kinetics in batch systems.	71
Figure 2-9. The quasi-steady state solution for Michaelis-Menten kinetics in open systems.	74
Figure 2-10. The quasi-equilibrium solution for Michaelis-Menten kinetics in open systems.	77
Figure 3-1. Quasi-steady state motion in the phase plane.	97
Figure 3-2. The relaxation deficit.	99
Figure 3-3. The relaxation time.	99
Figure 3-4. The relaxation error.	99
Figure 3-5. Region of applicability of the quasi-steady state assumption.	100
Figure 3-6. The unified solution to Michaelis-Menten kinetics.	107
Figure 3-7. The singular perturbation solution for $Q_s = .1$ .	109
Figure 3-8. The singular perturbation solution for $Q_s = 1$ .	110
Figure 4-1. The stationary solution of the dimeric model and location of inflection point.	128
Figure 4-2. The stationary solution of the dimeric model and the location maximum flux.	129
Figure 4-3. Regions of complex eigenvalues for the dimeric model.	136
Figure 4-4. Modal matrix and time constants for the dimeric model as they vary with the Binding number.	139
Figure 4-5. The quasi-equilibrium assumption for the dimeric model and the Binding number.	140
Figure 4-6. Modal matrix and time constants for the dimeric model as they vary with the Affinity ratio.	142
Figure 4-7. Modal matrix and time constants for the dimeric model as they vary with the Affinity ratio, while $B_Af$ is constant.	143
Figure 4-8. Modal matrix and time constants for the dimeric	

model as they vary with the Acceleration number.	144
Figure 5-1. The modal matrix and the time constants as a function of the Binding number for a two reaction chain.	162
Figure 5-2. Transient solutions for the two reaction chain at different Binding numbers.	162
Figure 5-3. The influence of the Binding number on the Nyquist plot for the two reaction chain.	176
Figure 5-4. Illustration of model reduction using method of moments.	181
Figure 5-5. Illustration of how the linear reduced model fails to represent chain dynamics as deviation from the steady state increases.	185
Figure 6-1. The single biochemical control loop.	194
Figure 6-2. Location of the loci marking the onset of dynamic bifurcations and corresponding root locus.	210
Figure 6-3. Influence of transfer function order time delays on the occurrence of dynamic bifurcations.	211
Figure 7-1. The single biochemical control loop.	221
Figure 7-2. Multiplicities in loops with the lumped controller and a linear removal rate.	232
Figure 7-3. Illustration of steady state conditions for a loop with a lumped controller and linear removal rate and how they are influenced by the ratio $\Lambda/\kappa$ .	234
Figure 7-4. Regions of multiple steady states for a loop with the lumped controller and Michaelis-Menten removal rate.	238
Figure 7-5. Multiplicities for loop with the lumped controller and Michaelis-Menten removal rate.	242
Figure 7-6. Multiplicities in loops with the lumped controller and a Michaelis-Menten removal rate.	244
Figure 7-7. Critical values Acceleration numbers and the allosteric constant for the appearance of multiple steady state solutions for a loop with the symmetry model and linear removal.	248

Figure 7-8. Regions of unique and multiple steady state solutions for loops with the symmetry model and linear removal rate.	249
Figure 7-9. Critical values of the acceleration number and the allosteric constant for the appearance of multiple steady state solutions for a loop with the symmetry model and Michaelis-Menten removal.	252
Figure 8-1. Regions of instability for the linear limit of a loop with the lumped controller.	274
Figure 8-2. The effects of the damping factor $\xi$ on the shape on the instability region for a loop with the lumped controller and linear removal rate.	275
Figure 8-3. Instability regions for the saturation limit for a loop with the lumped controller.	278
Figure 8-4. Instability regions for a loop with the lumped controller and Michaelis-Menten removal rate.	280
Figure 8-5. Bifurcation solution branches and limit cycles for a loop with the lumped controller and Michaelis-Menten removal rate.	285
Figure 8-6. Bifurcation solution branches and limit cycles for a loop with the lumped controller and Michaelis-Menten removal rate.	289
Figure 8-7. Regions of possible dynamic instabilities for a loop with the symmetry model and linear removal rate.	295
Figure 8-8. Instability regions for a loop with the symmetry model and linear removal rate.	296
Figure 8-9. Instability regions for a loop with the symmetry model and with Michelis-Menten removal.	298
Figure 9-1. Eigenvalues for the Goodwin equations.	312
Figure 9-2. Graphical illustration of Popovs theorem.	315
Figure 9-3. Regions of linear and global stability for the Goodwin equations.	318
Figure 9-4. Amplitude and period for oscillatory solutions in the Goodwin equations.	320

Figure 9-5. Amplitude for oscillatory solutions in the Goodwin equations.	321
Figure 9-6. Graphical illustration of Lyapunov functions.	323
Figure 9-7. Nyquist plot for the Goodwin equations illustrating the influence of increasing time delays.	328
Figure 9-8. Root locus plot for the Goodwin equations.	331
Figure C-1. Frequency content of the $n^{\text{th}}$ order ramp pulse.	370
Figure C-2. Frequency content of the $n^{\text{th}}$ order triangular pulse.	372

## LIST OF TABLES

	Page
Table 1-1. Known examples of feedback inhibition of biosynthetic pathways.	18
Table 5-1. Moments for the transfer functions of a sequence of irreversible Michaelis-Menten reactions.	172
Table 5-2. Low order transfer functions and their parameters given in terms of their moments.	180
Table 6-1. Linear operators used to represent reaction chains.	203
Table 9-1. Higher order bifurcations in the Goodwin equations.	312
Table 9-2. Global stability in the Goodwin equations.	317

## CHAPTER 1

## INTRODUCTION

During the past four to five decades the area of biology dealing with the structure and function of cellular components, collectively called molecular biology, has grown rapidly. Advances in experimental techniques and other areas of the natural sciences have enabled the molecular biologist to reveal the main features of the molecular structure and function of living matter. These advances extend from the early investigations of enzymatic activity to the recent highly exciting manipulations of genetic material. One aspect of cellular function, metabolic transformations, received particular attention early on and a complex network of carefully regulated interacting reactions is found to underlie metabolic activity. Today most of these chemical reactions have been individually characterized.

The study presented herein is the first step in a comprehensive modelling effort aimed at elucidating the salient dynamic features of metabolic networks. This is in turn seen as a logical point of departure for the long-term goal of putting the description of the dynamics and control characteristics of living organisms on a sound

physico-chemical basis. It is seen as a move in the direction towards the fundamentals of biotechnology, which seems to be entering a new era driven by the success of molecular biology.

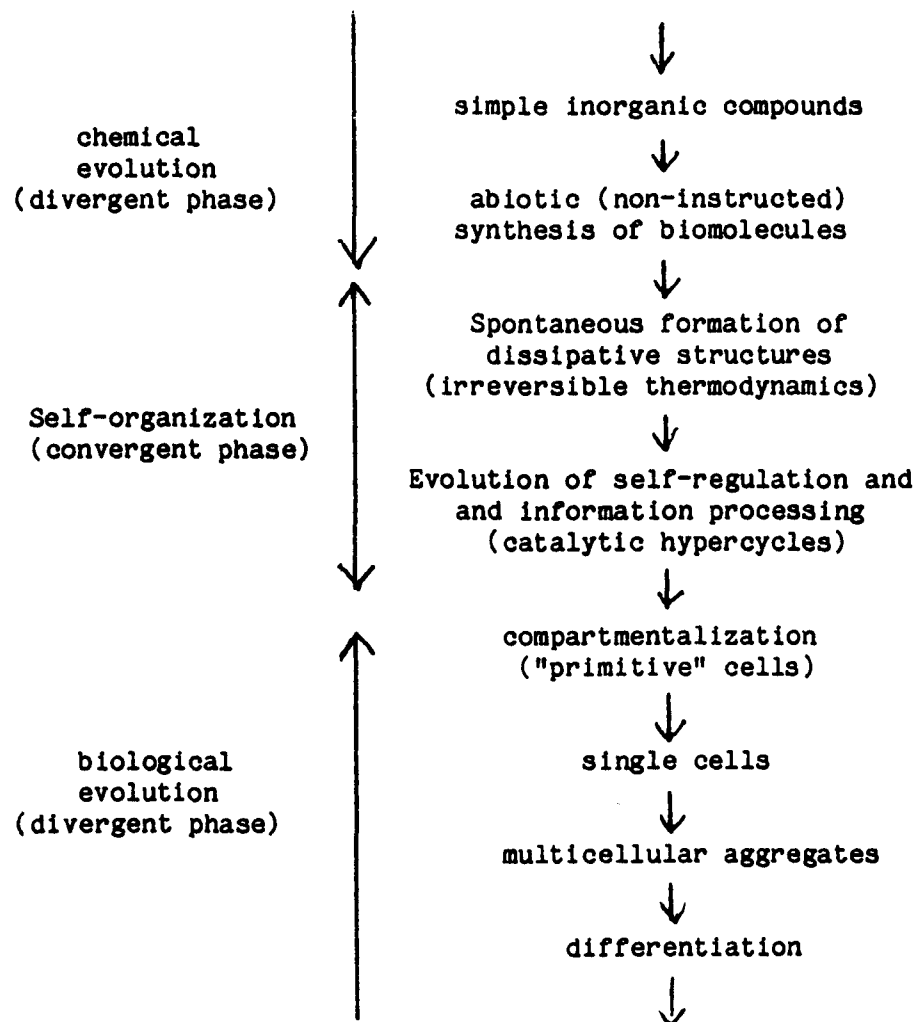
In this introductory chapter I hope to convince the reader that such development is timely and that chemical engineers, because of their unique training in both the basic sciences as well as engineering aspects, can make significant contributions to such a study. We will start out by discussing the basic features of living matter and how it is believed to have arisen from inanimate sources. The intention, by contrasting the two, is to make explicit the fundamental differences between inanimate and living matter and outline the disciplines and techniques needed to analyse the basics of "bio-systems".

### 1.1. Properties of Living Matter.

#### 1.1.1. Formation of living matter.

The probable process of formation and evolution of the living process is schematically shown in figure 1-1. The formation of simple biological molecules, such as amino acids, nucleotides and monosaccharides, from simple compounds such as those believed to be present in the "primordial organic soup", was demonstrated in 1953 with the landmark work of Stanley Miller. His now classical studies on simulated primitive atmosphere in a spark-discharge apparatus

Figure 1-1. Illustration of the probable course of evolution.



confirmed the earlier hypotheses of the soviet biologist A. I. Oparin and the english biochemist J. B. S. Haldane that abiotic formation of biomolecules could take place under these conditions.

The subsequent processes leading to formation of macromolecules, such as protein and nucleic acids, and, even more so, the instructed synthesis of protein are at present ill-understood. However it is clear that some process of self-organization must have taken place. Recently the basic forces leading to such phenomena have become better understood through fundamental developments of irreversible thermodynamics. Ilya Prigogine and the so-called Brusselles school have extended the study of irreversible thermodynamics (Glansdorff and Prigogine, 1971, Nicolis and Prigogine, 1977 and Prigogine and Stengers, 1983) from the well studied linear region around the equilibrium state to systems that are removed sufficiently far from equilibrium so that significant non-linearities appear. Under these conditions chemically reacting systems are shown to be capable of self-organization, or the formation of so-called "dissipative structures", which are viewed as dynamic counterparts of equilibrium structures.

Not only must physical self-organization have occurred but also a capability to accumulate information and to use it for regulatory purposes must have evolved. Mechanisms for the flow of information and the formation of regulation have been postulated by M. Eigen of W-Germany (Eigen, 1971, Eigen and Schuster, 1981) in the form of so-called catalytic hypercycles. Basically catalytic hypercycles are

coupled self-replicating units which acquire the capability of self-organization and evolve to a state where the production rate of all chemical species involved is dynamically controlled. Catalytic hypercycles are believed to represent the minimum structured organization for a chemically reacting system to accumulate, maintain and process information, such as the information embedded in the genome.

Following the formation of such simple structures and the subsequent compartmentalization leading to the formation of "primitive cells" is biological evolution. The basic driving force during evolution has traditionally been understood in terms of the Darwinian principle of natural selection. More recently the basics of biological evolution are associated with preservation of information in the DNA molecule. The information giving the organism the greatest survival potential prevails. Basically it allows for proper response to external disturbances, or regulatory control, and internal decision making, or servo control.

#### 1.1.2. Definition of "alive".

Armed with these basic notions I next examine more closely the properties that an organism must possess in order to be considered "alive". I follow the Russian biologist A. I. Oparin who, in 1926, postulated the three, now generally accepted, criteria;

- a) metabolism, the ability to use "food" molecules and transform,

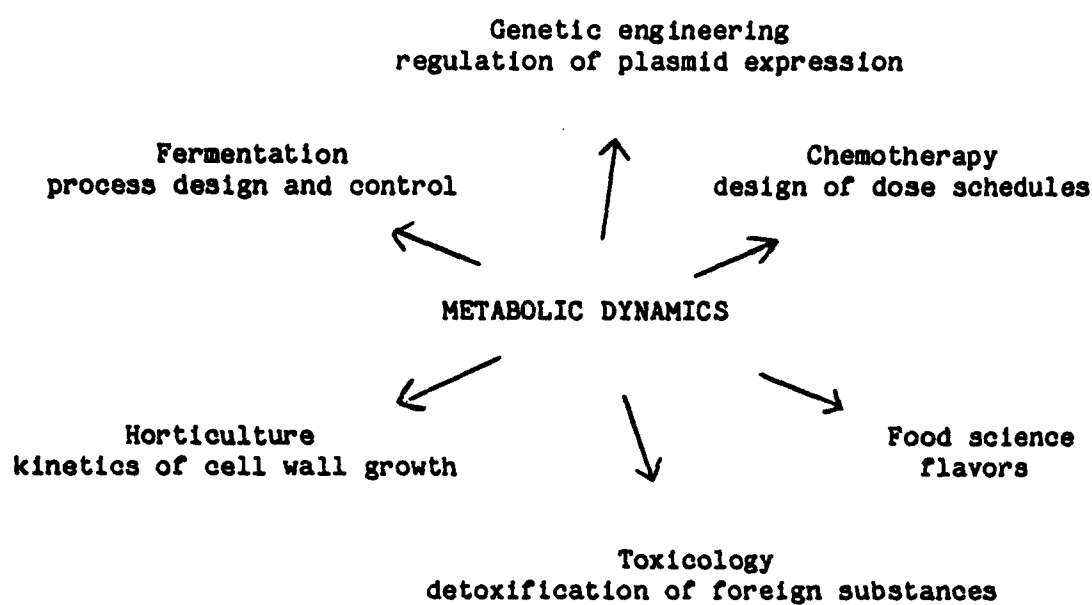
or change (the word metabolism comes from the Greek word *metabolē* (*μεταβολή*) meaning change), them into various products necessary for growth and maintenance of the cell. The information embedded in the genome directs processing of this continuous flux of mass and energy through the cell to maintain its "dissipative" state; in other words living systems are open, in a thermodynamic sense, with respect to mass and energy.

b) self-reproduction, the ability to reproduce itself thus transmitting the information it possesses into a copy of itself. Living systems seem to be metastable, or even unstable, and eventually break down and cease to exist. Hence by self-reproduction the survival of the genetic information for another biological time increment, a generation, is made possible.

c) mutability, the ability to change genetic inheritance while maintaining viability. The transfer of information by reproduction is not always exact. Hence changes in the information content will occur, and the process of natural selection will determine whether the changes occurring are preserved or disappear.

The first property, metabolism, has been the most important one for the biochemical engineer. Many areas of biotechnology, figure 1-2, are directly or indirectly concerned with metabolic dynamics. Furthermore today we have the capability to manipulate genes and induce the properties that we desire to see in an organism. In other words we would like, in a literal sense, to direct evolution into the

**Figure 1-2. Schematic illustrating the central role of metabolism in problems of practical importance.**



path that best suits our interests. We need to kinetic analysis to guide us through and assess the effects of changes in these complex systems and to assist us in the regulation of the altered organisms.

Metabolism is therefore the natural place to begin our study. I shall first describe the main features of metabolism (section 1.2) and then go on to outline more specifically our goals and motivation (section 1.3), and approach to modelling (section 1.4).

Recapitulation. The purpose of the above discussion is to introduce the reader to the fundamental properties of the systems with which the biochemical engineer must deal; they are highly organized and complex dynamic entities that exhibit coherent behavior (capable of carrying out both servo and regulatory control) in order to maintain their dissipative state. Furthermore they possess the capability to evolve towards more survivable structures. Hence kinetic analysis of metabolic activity will inevitably concentrate on dynamics and control.

## 1.2. A Brief Description of the Intermediary Metabolism.

### 1.2.1. Early discoveries.

The first observations of enzymatic activity, during the past century, sparked widespread controversy (Segal, 1959). It was not until fermentation by yeast extract, observed accidentally in 1897, that it became generally accepted that intact living matter is not

necessary for biological reactions to occur. These findings were then followed by extensive research on various chemical transformations carried out by living organisms.

In the 1930s intensive investigations by German biochemists established the sequence of chemical reactions that take place when glucose is degraded. This pathway is now known as glycolysis and is a central part of cellular metabolism. It is frequently called the Embden-Meyerhof pathway, after the investigators that contributed most to its establishment. In 1937 H. A. Krebs postulated the tricarboxylic acid (TCA) cycle, often called the Krebs cycle, following a long history of experimentation and brilliant reasoning. This reaction sequence is now known to be the major part of energy metabolism, or the adenosine nucleotide 5' tri-phosphate (ATP) generating activity, along with the electron transport system (ETS).

Most of the other important pathways, both catabolic (or degradative) and anabolic (or biosynthetic), were subsequently established, and the role of cofactors, such as ATP, nicotinamide diadenine nucleotide (NADH) and nicotinamide diadenine nucleotide phosphate (NADPH), in energy transduction realized.

All this information is now conveniently compiled in the form of metabolic charts, found on the walls of most biochemical laboratories, which basically represents an extremely complex system of mass and energy flows carefully coordinated through self-regulation.

### 1.2.2. Mass flow.

The mass flow structure for degradation and biosynthesis of the largest classes of biomolecules, i. e. amino acids, lipids, sugars and nucleotides, is now well established and surprisingly little species variation exists, especially among higher organisms. The size of the reaction network is, however, enormous. For instance Watson (1976) estimates that cells even as simple as the bacterium Escherichia coli contains approximately three to six thousand metabolic species, most likely around five thousand. Approximately half of those are "small" molecules, such as intermediates of reaction pathways, metabolites, and the remainder are macromolecules, including enzymes and other proteins.

The intermediary metabolism, which is of concern herein, is most briefly, and somewhat loosely, defined as the sum of all the enzymatic reactions pertaining to the transformation of substrate, or food, molecules into the essential building blocks of macromolecular synthesis, and other vital products for growth and maintainance. It can be divided into two basic sectors, figure 1-3. One sector carries out the degradation of substrates via a series of converging pathways which lead to a set of relatively few metabolites of central importance. These metabolites are then either "burned", to completion to yield  $\text{CO}_2$  and  $\text{H}_2\text{O}$ , or to a fermentation product, or fed into the other main sector, whose function is to synthesize monomers, or building blocks, for macromolecular biosynthesis. This block is a set of diverging pathways originating from these central metabolites

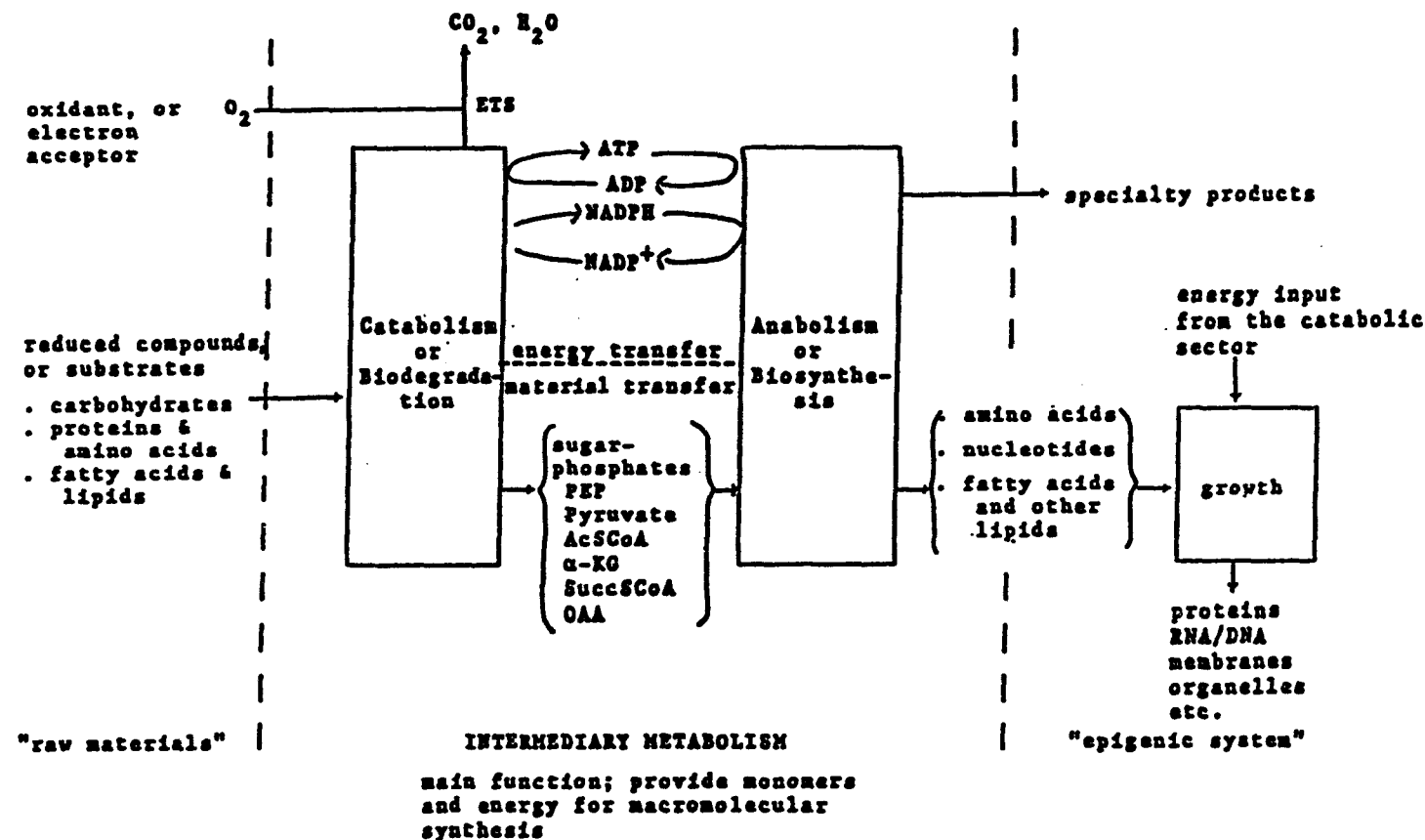


**FIGURE 1-3.** A schematic illustrating the central location of the intermediary metabolism in cellular function (modified from Atkinson, 1977)

to monomers like amino acids.

The catabolic sector -- discussed here since it is simpler than the complex biosynthetic part of the intermediary metabolism -- naturally divides into three stages, see figure 1-4. Roughly, the first stage consists of a set of degradative pathways converging towards the intermediate AcCoA. This molecule is then fed into the second stage, the TCA cycle yielding FADH and NADH whose redox potentials are used to generate ATP in the third and final stage, the ETS. The first stage is physically separated from the two latter stages in eucaryotic cells, the first occurring in the cytoplasm but the second and third in an organelle the mitochondrion, often called the powerhouse of the cell.

### 1.2.3. Energy flow.

Another key aspect of the intermediary metabolism is the energy transduction that takes place within the network. The degradative pathways are energy yielding, whereas their biosynthetic counterparts are energy requiring and the energy transduction between the two is through high-energy/high-redox potential compounds called cofactors. These compounds, the most important of which are ATP, NADH and NADPH, are able to store chemical energy, as energy-rich phosphate bonds in ATP, or as high redox potential in NADH and NADPH. Energy and redox potential is extracted by these cofactors during degradation and is then used to drive biosynthetic reactions.

In addition to the energy required for biosynthesis the cell has

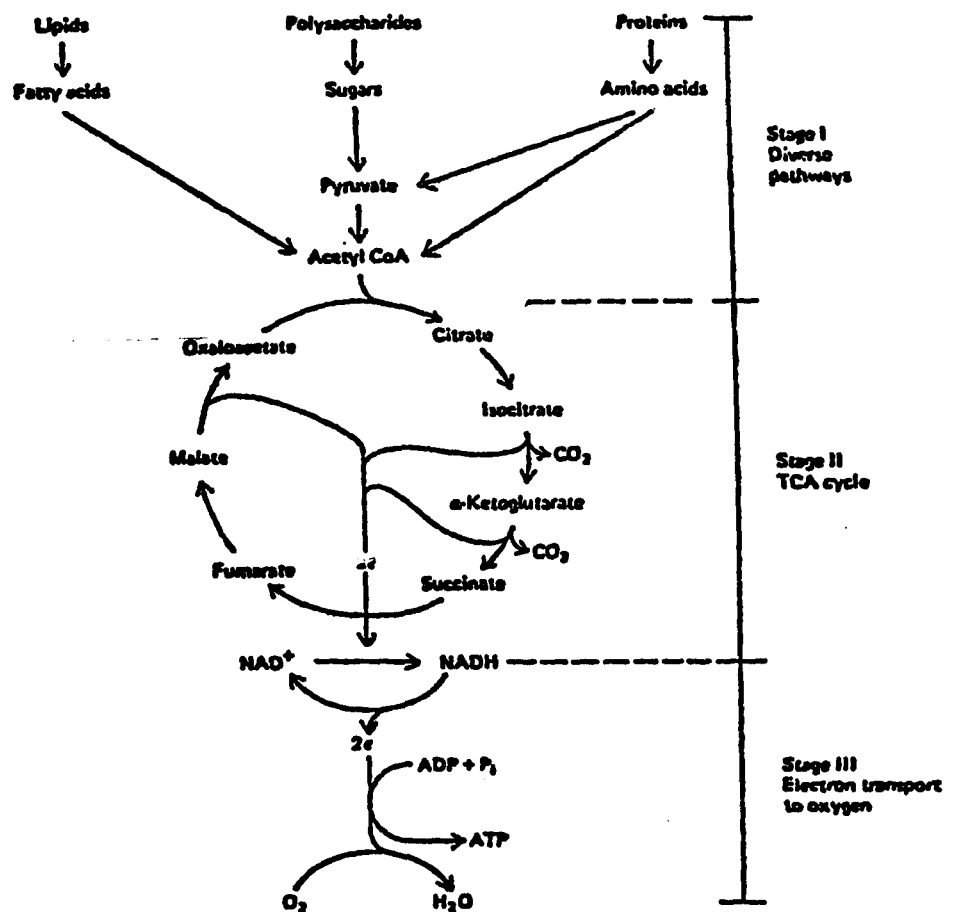


**FIGURE 1-4.** A schematic illustration of the main intermediates and pathways of energy metabolism.

several other energy requiring activities. To generate this energy a fraction of the mass flow through the catabolic part is run through the TCA cycle and the ETS resulting in full oxidation and then released as carbon dioxide and water.

The convenience of the coupling agents is clear since they provide stoichiometric decoupling between the cata-and-anabolism, and thus assume a central role in cellular metabolism. This led D. Atkinson to postulate the adenyl energy charge (Atkinson 1970, 1971, 1977) as the prime indicator of the metabolic state. The energy charge is defined as the ratio of the occupied "ports" for phosphate bonds to the total available ports in the adenyl nucleotide phosphate pool. If all the adenine nucleotide phosphate pool is in the ATP form the energy charge is unity, and the system is fully charged. On the other hand when all the adenine nucleotide phosphate pool is in the AMP form the energy charge is zero, and no energy is stored in the system. For in vivo situations the energy charge is typically in the range .8-.95. Such a lumped indicator can only give limited information as discussed in Purich and Fromm (1973), but nevertheless it seems to be a key indicator of the metabolic state and it also plays a major regulatory role as we shall discuss below.

#### 1.2.4. Regulation.

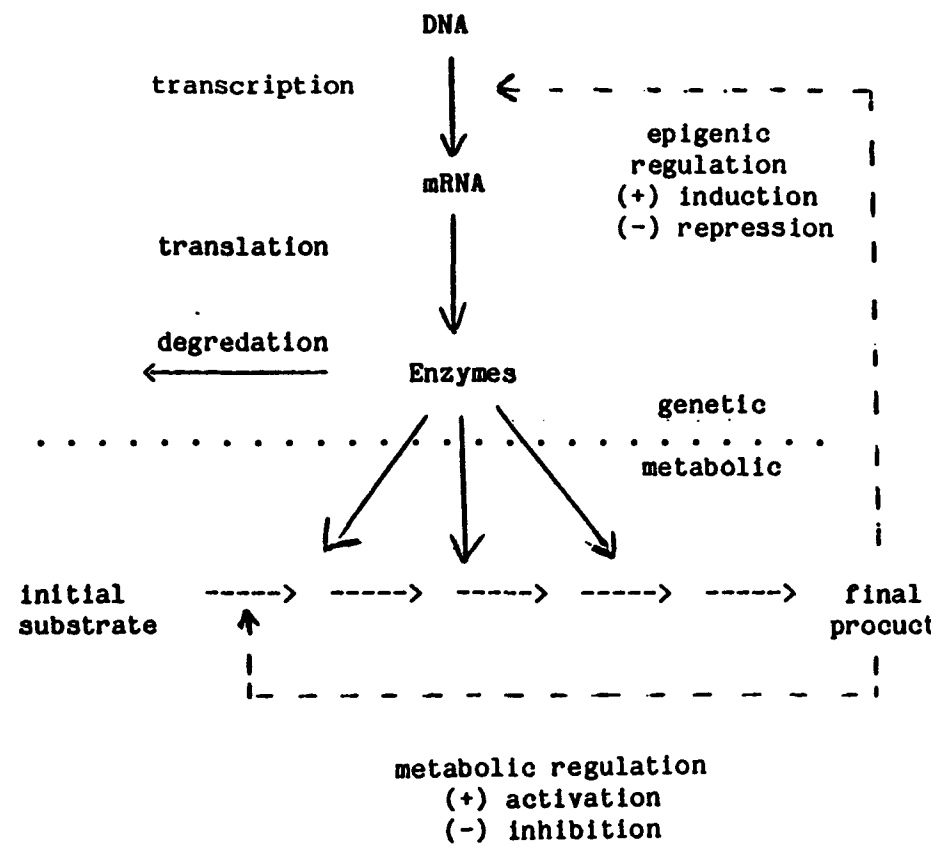
Perhaps the most unique feature of living systems is their ability to regulate their own function. Regulation of metabolism is mainly concerned with the modulation of reaction rates of key

reactions which allows for control over the fluxes through the various pathways. This modulation of reaction rates and metabolic fluxes is achieved by controlling the activity and concentration of key enzymes. These two kinds of control are illustrated in figure 1-5 where in this case the end product of a reaction sequence both feedback regulates the first reaction in the sequence and it also controls the production rate of the enzymes, that catalyse the reactions in the sequence. Control on both levels can be positive (called induction of gene expression and activation of enzyme activity) or negative (called repression in the case of epigenic regulation and inhibition in the case of enzyme regulation).

The time scales of metabolic level control (regulation of enzyme activity), are typically much shorter than those for genetic level control (regulation of enzyme synthesis), in the order of minutes and hours respectively (Goldbeter and Caplan, 1976). Normally the regulation of genetic activity is considered as coarse control of metabolism whereas regulation at the metabolic level is viewed as fine tuning. An extensive account of the principles of metabolic regulation is given in Herman et al., (1980).

Modulation of enzyme activity. Regulation of metabolic activity was probably first observed by Dische in 1940 (see Krebs, 1972) but the significance of this regulation, of hexokinase activity by phosphoglyseric acid in red blood cells, was not appreciated for many years. In the mid 1950s the role of end products of metabolic pathways in the regulation of their own synthesis through modulation

**Figure 1-5. Schematic of interacting metabolic and epigenetic control loops.**



of enzyme activity was demonstrated. These studies were carried out with bacteria and showed feedback inhibition in the amino acid biosynthetic pathways (Roberts et al., 1955, Umbarger, 1956, Yates and Pardee, 1956).

Following the discovery of feedback inhibition by metabolites it has been demonstrated for numerous situations, table 1-1. Feedback regulation is probably the most common mechanism of metabolic regulation; it is especially common in the biosynthetic pathways and the enzymes where the regulation is exerted normally catalyze the first reaction of a pathway. Extensive discussion of the individual pathways is found in the literature; these include fatty acid synthesis (Volpe and Vagelos, 1976, Katiyar and Porter, 1977, Block and Vance, 1977); purine synthesis (Wyngaarden and Kelly, 1978); pyrimidine synthesis (Levine et al., 1974), and so forth.

Cofactors play a central role in metabolic regulation. Since they are involved in both energy generating and dissipative processes the relative ratios between the high and low energy forms is particularly important and is in fact the rationale behind Atkinson's energy charge. The energy charge has been found to be a key regulatory parameter (e. g. Atkinson, 1977), in particular it is found to be important in coordinating catabolism and anabolism.

As experimental data on regulatory enzymes accumulated it became apparent that their catalytic properties were quite different from those of enzymes catalysing unregulated reactions. They are normally found to be large enzymes composed of several subunits, called

Table 1.1: Examples of Feedback Inhibition of Enzymes Involved in Biosynthetic Pathways

Reaction	Inhibitor	Tissue	References
1. Phosphoserine $\rightarrow$ serine	Serine	Rat liver	Borkenhagen and Kennedy (1958), Neuhaus and Byma (1958)
2. Phosphoribosyl pyrophosphate + glutamate $\rightarrow$ phosphoribosylamine	ATP (purine ribotides)	Pigeon liver	Wyngaarden and Ashton (1959)
3. Beta-hydroxy-beta-methyl glutarate $\rightarrow$ mevalonic acid	Cholesterol	Human liver	Siperstein and Fagan (1964)
4. Fructose-6-P $\rightarrow$ Fructose-1,6-difP + ADP	Citrate	Rabbit muscle	Passonneau and Lowry (1963)
5. Phosphoenolpyruvate + ADP $\rightarrow$ Pyruvate + ATP	Fatty acyl-CoA	Rat heart	Totsuka and Takenaka (1969)
6. Acetyl-CoA + CO <sub>2</sub> + ATP $\rightarrow$ malonyl-CoA + ADP + P <sub>i</sub>	Palmitoyl-CoA	Chick liver	Goodridge (1973)
7. Aspartate + carbamylphosphate $\rightarrow$ ureidosuccinate	Uridine cytidine derivatives (especially UMP and CMP)	Rat liver	Bourget and Tremblay (1972)
8. ATP + CO <sub>2</sub> + Glutamine $\rightarrow$ carbamyl-P + ADP + P <sub>i</sub>	UTP	Mouse spleen	Tatibana and Ito (1967)
9. ATP + CO <sub>2</sub> + "NH <sub>3</sub> " $\rightarrow$ carbamyl-P + ADP + P <sub>i</sub>	GTP	Rat liver	Kerson and Appel (1968)
10. Glutamine + phosphoribosyl pyrophosphate $\rightarrow$ glutamate + phosphoribosylamine	AMP, IMP, GMP	Rat liver	Katunuma et al. (1970)
11. Glucose + ATP $\rightarrow$ Glucose-6-P + ADP	Free fatty acids (and CoA derivatives)	Rat liver	Weber et al. (1968)
12. Acetyl-CoA + oxaloacetate $\rightarrow$ citrate	Long chain acyl-CoAs	Rat liver Pig heart	Tubbs (1963) Wieland and Weiss (1963)
13. Carbamylaspartic acid $\rightarrow$ dihydrocrotonic acid	CMP, d-CMP	Ehrlich ascites cells	Bresnick and Blatchford (1964)

From Cohn, R.M., M. Yudkoff, and P. D. Mc Namara,  
 "Servomechanisms and Oscillatory Phenomena" in Principles of  
 Metabolic Control in Mammalian Systems, R. H. Herman et al  
 eds., Plenum (1980).

oligomeric enzymes with multiple binding sites for both substrate and effectors (inhibitors/activators). The effectors are generally found to bind at different sites than the substrates, which may be located on a different subunit. The regulation is then caused by a conformational change induced by the binding of the effector which modifies the activity of catalytic site. This phenomenon is called allosterism, following the suggestions of Monod et al., (1963) and evidence allosteric behavior is now abundant (Citri, 1973).

Similarly interaction between catalytic sites are observed.

Unique kinetic behavior is displayed by allosteric enzymes which is caused by the interactions between binding sites for both effector and substrate on a single enzyme molecule. Substrate sites interact so that binding of a molecule can either enhance or suppress subsequent binding of another molecule of the same species, a catalytic feature called positive and negative cooperativity respectively (see chapter 4). Several models have been proposed to explain cooperative kinetic behavior. The two most commonly used models for allosteric enzymes are the elegant symmetry model of Monod et al., (1965) and the more complex sequential model of Koshland et al., (1966). The kinetics of allosteric enzymes are reviewed in Whitehead (1970), Hammes and Wu (1974) and Kurganov (1983).

Feedback regulation through allosterism has been extensively studied. It is, however, not the only means of regulation of enzyme activity, although it is probably the most common one Sols (1981). Others, such as compartmentalization, covalent modifications of

enzymes, enzyme activation by inorganic ions, to name a few, have also been found. These different regulatory mechanisms are discussed extensively in Stadtman (1966, 1970).

Modulation of enzyme concentration. In addition to feedback regulation of enzymatic activity, metabolites are also involved in the regulation of enzyme synthesis. The investigations of regulation of expression of the Lac operon in E. coli (see Jacob and Monod, 1961) was a prototype for study of regulation at the genetic level. Initial studies revealed that the synthesis of the enzymes necessary to degrade lactose can be induced by the presence of the lactose molecule. This regulation occurs via a complex regulatory mechanism that includes a specific protein which interacts with a regulatory site on the DNA molecule. It has been found that, in general, genetic level control also involves allosteric behavior.

The control of DNA transcription by metabolites occurs basically via two opposite mechanisms. One is repressive where the effector molecule prevents enzyme synthesis. The other mechanism is inductive where the effector molecule stimulates the production of enzymes. The Lac operon, whose enzymes degrade lactose, is induced by the lactose molecule. The mechanism of induction is common in the regulation of enzymes catalysing reactions in the catabolic sector. On the other hand end product repression of enzyme synthesis seems to be the prevalent mode in the anabolic part of the intermediary metabolism. This mode of regulation is common in the biosynthetic pathways leading to amino acids, purines and pyrimidines.

Following the period of pioneering studies of metabolic and genetic regulation a vast amount of information regarding metabolic regulation in diverse organisms accumulated. The main motivation for these studies was the early realization that different organisms had evolved different kinds of regulation for the same pathway: in contrast with the species invariance of metabolic reaction sequences, the regulatory mechanisms for the same chemical transformations are highly species variable.

Periodic operation or dynamic instabilities. The intermediary metabolism has traditionally been viewed as a process operating in a stable steady fashion. Although periodic behavior of living systems on macroscopic scale is observed, it is not until relatively recently that metabolic oscillations have been detected. The best studied examples are glycolytic oscillations in yeast and muscle, mitochondrial oscillations, and the cAMP-oscillator in Dictyostelium discoideum, see reviews in Higgins (1967), Hess and Boiteux (1971), Chance, Pye, Ghosh and Hess (1973), Hess, Boiteux and Busse (1975), Goldbeter and Nicolis (1976), Goldbeter and Caplan (1976).

Although some investigators have postulated a physiological role for metabolic oscillations it is not always clear whether they serve any purpose or whether this phenomena is simply a manifestation of the regulatory structure employed. For instance dynamic instabilities in yeast glycolysis are only observed over a narrow range of throughput fluxes, above and below which the oscillations disappear. It is conceivable that the organism is simply not "designed" to operate in

a stable fashion under these conditions and the "installed" control structure simply cannot achieve stable operation under the imposed circumstances. In fact it has been suggested that many diseases are the result of breakdown of physiological regulation (MacKay and Glass, 1977).

On the other hand mitochondrial oscillations and cAMP driven oscillations in D. discoideum appear to have a well defined physiological role, in the latter case associated with the process of differentiation.

Recapitulation. In brief the intermediary metabolism is a complex network of interacting reaction sequences containing thousands of chemical species, and it functions in a volume whose dimensions are in the order of microns. In spite of the large number of reactions and its apparent complexity the underlying mass flow structure -- which is much the same throughout the living world -- is relatively well understood. The basic functions of the intermediary metabolism is to provide an adequate energy supply, in the form of high-energy compounds, and monomers for macromolecular synthesis.

A key feature is that the network is kept functioning via an evolved self-regulatory mechanism. This is accomplished by modulation of catalytic activity of key reactions within the network, mostly by metabolites and/or cofactors. The regulatory structure, in contrast to the mass flow structure, is found to be species specific. Dynamic systems, like the intermediary metabolism, are more prone to show static/dynamic instabilities as their degree complexity grows.

Evolution towards more sophisticated metabolic systems is therefore expected to have proceeded towards a system possessing fairly robust regulation which allows for stable operation in an unpredictable environment. Breakdown of regulation results in "dynamic" disease (Mackey and Glass, 1977).

### 1.3. Engineering and Living systems.

#### 1.3.1. Motivation - general considerations.

The special characteristics of living systems present both challenges and opportunities to engineers, and the discussion of these is one of the primary concerns of this thesis. Although normal human curiosity about the splendidly complex reaction networks upon which we depend for our existence may in itself justify a dynamic study, there are also many practical reasons of quite classical engineering nature as well. They result basically from the fact that almost all applied interests in biological systems center either around deliberately perturbing them or suppressing unwanted perturbations. In the first class are processes that we want to modify to serve our needs, such as fermentations and agriculture, and the second class represents our efforts to prevent others from doing so to us, e. g. medicine.

We are therefore basically interested in very complex and highly interactive dynamic structures with the important goal of

understanding and predicting their response. Here we are specifically interested in metabolic networks and their complexity makes it difficult to achieve this goal without some systematic modelling effort: a goal that is of so much practical importance as well as of basic scientific interest. The apparent lack of systematic tractable modelling techniques for dynamics and control in metabolic reaction networks has motivated us to exploit the chemical engineering expertise to tackle this problem.

### 1.3.2. Motivation - some specifics.

More specifically there are basically two reasons for undertaking a comprehensive a modelling study of metabolic activity:

The first one originates from basic scientific interest. We are simply interested in how metabolic neworks function dynamically and what principles underlie their design. There are several questions to be answered. For example: "how can such complex systems operate in a stable fashion in face of the wide variety of disturbances occurring in their natural environment?" More specific physiological questions are: "how does a metabolic pathway respond to an external signal (e. g. a drug) ?", or "which enzymes are important in regulating the flux through a particular pathway and concentrations of some specific intermediates ?", or even "which enzymes are instrumental in the regulation of key (i. e. energy and redox inventories) metabolic functions ?", and so forth.

The second reason is more practically oriented and is more in the line of motivation for engineers. Figure 1-2 lists some of the areas of possible applications. Three more specific examples are:

Control of fermenters. We must take into account the dynamics of living organisms whenever we are concerned with processes whose time scales overlap those exhibited by the organism of interest in a significant way. A straightforward example is the control of fermentation processes where we shall most probably find explicit consideration of hitherto neglected metabolic transients be important to commercial success. The fermentation literature is full of comments about the inadequacy of presently used process descriptions and the spectrum of process time scales in fermenters overlaps with those exhibited by the underlying metabolic events (for instance in classical fermentations the process time scales include those of macro and micromixing which overlap with metabolic ones). Metabolic transients are expected to play a key role in the production of proteins with genetically engineered organism via cloning. Here the focus is directly on the genetic and metabolic regulation.

Chemotherapy. As drug delivery gets more sophisticated we increasingly need to know the response of a tissue -- or equivalently the associated metabolic network -- to the local concentration of drug. Currently much effort is devoted towards the development of "third generation" drug delivery systems or

"controlled drug release". The basic idea is to monitor some physiological variable which, directly or indirectly, can be used to assess the progress of the therapy. This information is then fed back to a "controller" or a decision making unit which determines the amount of drug to be released at every instant in time. The simplest example would be the release of insulin in diabetics. The controlling device will initially, most likely, be an external device, that is located outside the patients body. More sophisticated schemes would eventually be internal. Such closed loop control is to be contrasted to the open loop drug delivery policies that are currently used (that is administer so and so much drug at such and such time).

To assess the tissue response, which is referred to as pharmacodynamics, and evaluate the meaning of measured signals one needs a model of the underlying metabolic events. Such metabolic models would be used to guide the drug release, where they will serve an equivalent function as process models do in the process control of chemical industries. Pharmacodynamics are the next step beyond pharmacokinetics -- which deal with the dynamics of drug distribution in the body -- that give us the local concentration at the tissue site of drug; an area that chemical engineers have already contributed significantly to. Again models of metabolic dynamics are expected to play a key role.

Deliberately altered or defective/deficient enzymes. The assessment of altered kinetic properties, either deliberately or

through genetic defects, on metabolism is of major concern.

In the former case one is interested in altering a particular enzyme in an organism, through genetic engineering. To determine which kinetic properties are desirable, aiding in the selection of the new gene, and to assess the changes in function brought about by the new enzyme, one needs a metabolic model.

In the latter case we want to know how do enzyme defects/deficiencies change the metabolic response of the cell or organism in question. A specific question may for instance be; does a defective/deficient individual respond adversely, when a response from a healthy individual is not adverse, to a particular drug treatment or any other particular stress ? The simple metabolism of the mammalian red blood cell -- which has been so useful in many pioneering studies in biochemistry -- offers a tractable starting point.

In both cases a metabolic model will play a key role.

To date these examples are necessarily somewhat vague and their intrinsic problems and difficulties have been only incompletely identified and described. Such a situation is expected at these primary stages of this research and our currently primitive understanding. However we feel that the indications of future benefits resulting from a systematic dynamic investigation of metabolism are in fact quite strong. A strong motivation has come from an analogous investigation into the dynamics and control of the much simpler structures in the chemical industry.

#### 1.4. Mathematical Modelling of Metabolic Activity.

Although metabolic dynamics have been little studied by engineers they have been studied by biochemists/physiologists resulting in valuable literature (see reviews in Chance, Higgins and Garfinkel 1962, Garfinkel, Garfinkel, Pring, Green and Chance 1970, Reich and Sel'kov 1974, 1981, Heinrich, Rapoport and Rapoport 1977, Garfinkel and Kohn 1980 Wright and Kelly 1981, and Carson, Cobelli and Finkelstein, 1983). Here we shall describe some of the approaches used for metabolic modeling.

It is clear from the outset that all biological systems are sufficiently complex to defy exact description. Furthermore the extent of available and obtainable data is too fragmentary and inexact to permit drawing detailed conclusions about system behavior: we must settle for identifying and characterizing only major features. One should therefore avoid straightforward simulation procedures for the large number of stiff differential equations that must be included in such an approach. We feel that such procedure has its main value in testing more tractable descriptions for well defined model systems.

To reduce both computational difficulties as well as to facilitate conceptualization of metabolic networks we are embarking on a hierarchical modelling process, starting with the simplest elements, and seeking to identify and describe key characteristics as compactly and economically as possible at each stage. This is a hierarchical process increasingly laborious but with more details

obtained at each stage at the cost of increasing loss of overview and quickly exceeding available data.

We start with the conceptual framework given by irreversible thermodynamics.

#### 1.4.1. Irreversible thermodynamics.

Perhaps the most significant advances in theoretical biology, over the last decades, is the highly non-trivial demonstration that the origin and maintainance of the highly ordered state of living matter can be explained from macroscopic physics. These remarkable developments, coming from the so-called "Brussels" school, provide an explanation for the appearance and evolution of structure, and for the coherent behavior of living organisms. These results are in sharp contrast to the traditional belief of classical physics that every physiochemical system must invariably evolve towards equilibrium. Equilibrium is characterized by maximal disorder at the molecular level, and for living matter equilibrium means a non-functioning state, or death.

The key to opening up the realm of physics and chemistry to the apparently contradicting behavior of living system came from the extension of classical thermodynamics to non-equilibrium thermodynamics that extend beyond the linear region around the equilibrium point. These developments are described in details in Glansdorff and Prigogine (1971) and Nicolis and Prigogine (1977) and more qualitatively in Prigogine and Stengers (1983).

Within this framework there is little place for "mysteries", and functioning self-organized structures arise from the basic laws of physics. These ideas are, as expected, still controversial. Many still advocate the view that life is a result of a sequence of highly improbable events, and maintained through a mechanism of "Chance and Necessity" (Monod, 1970). This well known text of Monod probably best describes this view.

The two necessary ingredients for obtaining these non-trivial results of self-organization are, that the systems exchange mass with the environment that is, they are open, and that reactions taking place within the system possess non-linear kinetics. In fact it can be shown that linear kinetics will always have an asymptotically stable equilibrium point regardless of system complexity (Hearon, 1953, Wei and Prater, 1962 and Rosen, 1970). In view of the physical picture of the intermediary metabolism, outlined above, one can readily see that these two ingredients are in fact the essential features of intermediary metabolism.

#### 1.4.2. Bifurcation analysis.

To separate the parameter spaces into regions of the different kinds of dynamic behavior, such as unique or multiple asymptotically stable steady states and stable or unstable limit cycles, one must locate the loci where the transition from one pattern to another takes place. This is possible using bifurcation analysis which gives the onset of qualitative change in model behavior. Herein I shall

look for static/dynamic bifurcations the two simplest types of bifurcations (chapters 6,7 and 8).

Bifurcation analysis gives us essentially qualitative information which tells us what type of dynamic behavior is expected for a given parameter combination. To get more detailed information one must work harder.

#### 1.4.3. Local analysis.

Once the parameter spaces have been divided into regions of different kinds of dynamic behavior one would like to know more about the properties of the steady states in the different regions. These studies fall into two such basic catagories.

Regulatory properties. To obtain information about the systemic properties of metabolic networks it is necessary to evaluate the interactions between the different fluxes and the metabolites affecting them. Mathematically these interactions can be expressed in terms of sensitivity coefficients, which give the variation in a flux to an infinitesimal change in a regulatory parameter, see Higgins (1964), Kascer and Burns (1973, 1979), Heinrich and Rapoport (1974, 1975), Kascer (1981). This type of analysis has been useful in analysing the properties of metabolic networks, such as futile cycles (Heinrich et al., 1977) and the characteristics of biochemical oscillations (Kohn et al., 1979).

Dynamic properties. Herein, in chapters 2, 4 and 5, I present linear analysis including full modal analysis the investigate the dynamic properties of enzymatic reactions. This technique gives us the relaxation times of the reactions and how significantly the different concentration species move on the time scales involved. This analysis is found to be particularly useful for five purposes;

- 1) to examine the influence of model parameters on the dynamics,
- 2) as a guide to simplification, such as the application of the quasi-steady state and quasi-equilibrium assumptions,
- 3) for approximations to transient response,
- 4) to estimate the relative timescales of reaction and diffusion, and
- 5) to relate overall kinetic properties to individual ones.

#### 1.4.4. Numerical simulations.

To get the full transient behavior one has to numerically integrate the full set of differential equations describing the metabolic network under consideration - a major computational undertaking. The high number of variables and parameters makes it very difficult to draw meaningful conclusions from the obtained results. Therefore the system of equations under investigation should first be examined along the lines discussed above.

Full dynamic simulations of metabolic networks have been attempted by several investigators. The majority of these studies are approached by writing down the quasi-steady state rate laws for

all enzymatic reactions in a particular reaction network of interest.

Given the complexity of even the simplest metabolic networks, this very quickly generates computationally intractable models. One of the main difficulties lies in the distribution of time scales within the system. This causes the differential equations to be, what is known as "stiff" and results in immense computational effort.

Another major obstacle in this modelling approach is the large number of physical parameters needed to simulate the models. These are, if available, normally obtained in part from in vitro studies, and they may not be applicable to the in vivo situation being modelled.

Metabolic simulations and the associated difficulties are discussed and reviewed in Chance et al., (1962), Garfinkel et al., (1970), Park (1974), Garfinkel and Kohn (1980) and Wright and Kelly (1981).

**PART I**

**BIOCHEMICAL DYNAMICS**

## CHAPTER 2

## SIMPLE ENZYMATIC REACTION MECHANISMS:

## MICHAELIS-MENTEN KINETICS

Our modelling efforts begin with the kinetics of simple enzymatic reactions, which have been much studied but which exhibit surprisingly complex and mathematically intractable behavior. Our goals are both to develop simple and reliable methods for describing their kinetics and to examine the effects of the very large number of parameters affecting their behavior.

2.1. Michaelis-Menten Kinetics.2.1.1. The reaction mechanism.

We begin the discussion with the simplest enzymatic reaction mechanism, first proposed by Henri (1903) but known as Michaelis-Menten kinetics after Michaelis and Menten (1913). A good historical account of the early developments is found in Segal (1959).

The most general form of this mechanism is described by



The reaction scheme basically involves reversible binding of a substrate (S) to an enzyme (E) to form an intermediate complex (X), which in turn breaks down reversibly to form the product (P) and to regenerate the free enzyme (E). Many studies assume that the rate constant  $k_{-2}$  is zero, and that is the original, or irreversible, Michaelis-Menten reaction mechanism. If the system exchanges mass with the surroundings transport of substrate and product across system boundaries is accounted for by the input (I) and removal (R) fluxes.

### 2.1.2. Kinetic description.

The situation of most interest here involves mass flow of substrate species across the system boundaries, but with the enzyme species contained within these boundaries. Then a mass balance on the enzyme species holds at all times,

$$e_t = e + x \quad (2)$$

where  $e_t$  is the total concentration of enzyme (we shall let lower case letters denote the concentration of species defined by the corresponding upper case letter).

By use of the law of mass action the differential equations governing the system dynamics can now be written as

$$\frac{ds}{dt} = -k_1 e_t + k_{-1} x + k_1 s x + I \quad (3)$$

$$\frac{dx}{dt} = k_1 e_t s - (k_{-1} + k_2 + k_1 s + k_{-2} p) x + k_{-2} e_t p \quad (4)$$

$$\frac{dp}{dt} = k_2 x - k_{-2} e_t p + k_{-2} x p - R \quad (5)$$

where the mass balance on the enzyme species has been used to eliminate the concentration of the free enzyme (E).

In the present study we focus on reaction kinetics, and for convenience assume that the total mass of substrate and substrate derived species remain essentially time independent. This assumption is of course exact for batch systems and provides a suitable basis for our present purposes. For open systems we require that the input and removal rates are equal. The basic differential equations (3) - (5) are then no longer independent because of a mass balance on the substrate species

$$s_t = s + x + p \quad (6)$$

which defines the total amount substrate,  $s_t$ . This model thus has two degrees of freedom, and we choose the substrate and the enzyme complex as the independent variables. Then

$$\frac{ds}{dt} = -k_1 e_t s + k_{-1} x + k_1 s x + I, \quad s(0)=s_0 \quad (7)$$

$$\begin{aligned} \frac{dx}{dt} = & k_{-2} e_t s_t + (k_1 - k_{-2}) e_t s - (k_{-1} + k_2 + k_{-2}(s_t + e_t)) x \\ & - (k_1 - k_{-2}) s x + k_{-2} x^2, \quad x(0)=x_0 \end{aligned} \quad (8)$$

More complex mass exchange situations can of course occur, but these can only be considered in the context of a larger system.

Spatial variations in species concentrations are neglected here as they are believed to be un-important (see appendix A).

### 2.1.3. Scaling.

The mass action kinetic model contains a very large number of parameters which combined with the non-linearity of the rate equations have hampered efforts to obtain a satisfactory overall perspective of this system. We start our analysis by scaling system description and concentrating individual parameters into the smallest number of combinations possible. In doing this we try to maintain a clear distinction between intrinsic properties and externally imposed restraints. Hence we use the scaled variables

$$\sigma = \frac{s}{K_m}, \quad \chi = \frac{x}{e_t}, \quad \epsilon = \frac{e}{e_t}, \quad \pi = \frac{p}{K_m}$$
(9)

$$\Psi = \frac{I}{k_2 e_t}, \quad \Omega = \frac{R}{k_2 e_t}, \quad \tau = k_1 e_t$$

where,  $K_m = (k_{-1} + k_2)/k_1$ , is the well known Michaelis-Menten constant. Here we have scaled the functions I and R to the forward ( $k_2 e_t$ ) saturation velocity forcing the fluxes to be less than unity. Both  $\chi$  and  $\epsilon$  are scaled relative to the total enzyme concentration,  $e_t$ , so that  $\chi$  and  $\epsilon$  both fall in the range [0,1]. Furthermore in vivo metabolite concentrations are normally close to or below their  $K_m$  value, (Segel, 1975, Atkinson, 1977) which leaves  $\sigma$  of the order of

unity or smaller.

Substituting these scaled variables into the differential equations one obtains

$$\frac{ds}{d\tau} = -\sigma + \left(\frac{1}{1+St}\right)x + \sigma x + \left(\frac{St}{1+St}\right)\psi \quad s(0) = \sigma_0 \quad (10)$$

$$\begin{aligned} Qs \frac{dx}{d\tau} &= \frac{StQs}{K_{eq}Mr} + \left(1 - \frac{St}{K_{eq}}\right)\sigma - \left(1 + \frac{StQs}{K_{eq}}\left(\frac{1}{Mr} + 1\right)\right)x \\ &\quad - \left(1 - \frac{St}{K_{eq}}\right)\sigma x + \frac{StQs}{K_{eq}}x^2 \quad x(0) = x_0 \end{aligned} \quad (11)$$

with a dimensionless mass balance on the substrate species

$$\mu_t = \frac{Qs}{Mr} = \sigma + Qsx + \pi \quad (12)$$

where  $\mu_t = s_t/K_m$ . The dimensionless groups appearing are

$$Qs = \frac{e_t}{K_m}, \quad Mr = \frac{e_t}{s_t}, \quad St = \frac{k_2}{k_{-1}}, \quad K_{eq} = \frac{k_1 k_2}{k_{-1} k_{-2}} \quad (13)$$

#### 2.1.4. The dimensionless parameters.

One should note that our choice of scaling parameters is not unique; alternatives are found in Heineken, Tsuchia and Aris (1967), Otten (1974), Reich and Sel'kov (1974) and Meiske (1978). We have made our selection for basically two reasons.

- 1) The scaling enables separation of the dimensionless groups into three categories. Two of the groups,  $Qs$  and  $Mr$  are measures of concentration and may vary for the same enzyme system.  $St$  and  $K_{eq}$

contain only kinetic parameters and are intrinsic properties of the reaction system. Finally the scaled throughput ratios,  $\Psi$  and  $\Omega$ , represent conditions forced on the system.

2) The dimensionless groups appearing have well defined significance, and we can conveniently organize a physically meaningful discussion around them:

a) If  $Q_s$ , which describes the total amount of the enzyme relative to  $K_m$ , is small relative to unity one can safely assume quasi-steady behavior (see section 2.3.5 below). Hence we name this group the "Quasi-steady state number". For in vivo situations  $Q_s$  may approach, and even exceed, unity, since for most metabolic enzymes the value of the constant  $K_m$  is of the order  $10^{-5} - 10^{-3}$  M while enzyme concentrations may approach the millimolar range. On the other hand for in vitro kinetic experiments the total enzyme concentration is usually very low, ( $e_t = 10^{-10}$  to  $10^{-8}$  M, Srere, 1967, 1970, Masters 1977) and the value of  $Q_s$  is then very small ( $Q_s = 10^{-7} - 10^{-3}$ ).

b) The second mass related group is the ratio of total concentration of enzyme species to total substrate species,  $e_t/s_t$ , a parameter we call the "Mass ratio". The expected in vivo range of this group is probably less than unity but may approach, and even exceed, unity in some instances. For in vitro experiments this ratio is typically very small, and it has been considered as a criterion for the validity of the quasi-steady state assumption

under these conditions (e.g. Laidler, 1955, Heineken et al., 1967, Lim, 1973)

c) The parameter St is a measure of the relative ease of product formation from the intermediate complex as opposed to reversion to free enzyme and substrate. It may be called the "Stickyness number" since enzymes with larger values of this ratio than unity are frequently referred to as "sticky" enzymes. On the other hand if St is small, the substrate does not stick well to the enzyme and comes off it easily.

For most metabolic enzymes  $K_m$  approaches the disassociation constant,  $K_s = k_{-1}/k_1$ , of the substrate to the enzyme (Atkinson, 1977). Since  $K_m = K_s(1+St)$  this implies that St is small. The listing of kinetic data in Hammes and Schimmel (1970) and Mahler and Cordes (1971) supports this suggestion, and physiological values of St seem to fall in the range  $10^{-4} - 10^{-2}$  for typical metabolic enzymes.

d) The second kinetic group is the equilibrium constant,  $K_{eq}$ , for the overall reaction  $S \rightleftharpoons P$ .  $K_{eq}$  is normally expected to be in excess of unity.

e) The main interest in the mass exchange terms here is their steady state value, which is expected to be less than half of the saturation velocity. Frequently under in vivo conditions enzymes operate far below their saturation velocities.

The formulation is now complete and as compact as possible within the kinetic assumptions made. The description is in the form of two simultaneous non-linear differential equations which can be shown to have no closed form analytical solution for  $\Omega = \Psi = 0$  (Hommes, 1962, Darvey, Klotz and Ritter, 1978). Although special cases can be solved exactly or by approximate means, one must in general resort to numerical techniques to obtain exact solutions. We now proceed to examine and compare approximate solution procedures, beginning with the familiar quasi-steady state approach.

## 2.2. Quasi-Stationary Analysis.

The most widely used simplification in enzyme kinetics is the quasi-steady state assumption, first applied to the Michaelis-Menten mechanism by Briggs and Haldane (1925). It is obtained by ignoring transient changes in the concentration of the intermediate X and is implemented by equating its time derivative to zero, in equations 8 and 11. This procedure is especially simple for closed ( $\Psi = 0$ ) irreversible ( $k_{-2} \rightarrow 0$ ) systems where it permits the elimination of x between equations 10 and 11. The result is the famous hyperbolic Michaelis-Menten rate equation

$$\frac{da}{dt} = - \frac{St}{1+St} \frac{a}{1+a} \quad (14)$$

This equation can be integrated with the initial condition  $a(0) = a_0$

to give the so-called progress curve

$$\frac{St}{1+St} = \alpha_0 - \alpha + \ln(\alpha_0/\alpha) \quad (15)$$

For closed reversible systems similar procedure applies (Alberty, 1959), but for open systems, the norm for in vivo situations, this procedure is essentially numerical. The quasi-steady state assumption considerably reduces computational effort, but inspite of repeated analysis (see review in chapter 3), its range of validity is not yet well defined. We examine this question via linear analysis in next the section.

### 2.3. Linear Analysis.

#### 2.3.1. Linear analysis - General procedure.

In general dynamic systems such as ours are described by a set of non-linear ordinary differential equations as

$$\frac{dx}{dt} = f(x) + \psi(t) \quad (16)$$

where x is a n-dimensional vector containing the state variables, f(x) is a n-dimensional non-linear function and ψ is a vector containing the forcing function. After linearization such equations take the form

$$\frac{d\bar{x}'}{dt} = J\bar{x}' + \underline{\psi}'(t) \quad (17)$$

where  $J$  ( $j_{ik} = df_i/dx_k$ , where  $j_{ik}$  is the  $ik^{\text{th}}$  element of  $J$ ) is the so-called Jacobian matrix,  $\underline{x}'$  ( $= \underline{x} - \bar{x}$ ) is a state vector expressing deviations from the steady state  $\bar{x}$ , about which the equations have been linearized. Similarly  $\underline{\psi}' = \underline{\psi} - \bar{\underline{\psi}}$ . The solution to this set of equations, for the initial condition  $\underline{x}' = \underline{x}_0'$ , is

$$\underline{x}'(t) = e^{Jt} \underline{x}_0' + \int_0^t e^{J(t-\tau)} \underline{\psi}'(\tau) d\tau \quad (18)$$

Here the first term represents a decay of the unforced system and the integral term arises from the forcing function.

The Jacobian matrix can normally be diagonalized by the transformation  $J = M\Lambda M^{-1}$ , where  $\Lambda$  is a diagonal matrix of eigenvalues and the matrices  $M$  and  $M^{-1}$  are composed of the eigenvectors and eigenrows, respectively. Substituting this transformation into equation 18 and defining the modes as  $\underline{m} = M^{-1}\underline{x}'$  one obtains,

$$\underline{m}(t) = e^{\Lambda t} \underline{m}_0 + \int_0^t e^{\Lambda(t-\tau)} \underline{\theta}(\tau) d\tau \quad (19)$$

Here  $\underline{\theta}(\tau)$  ( $= M^{-1}\underline{\psi}'(\tau)$ ) is the linearly transformed forcing function.

The transformed equation, 19, describes a set of decoupled variables,  $\underline{m}_i$ , each moving on its own time scale, as defined by its eigenvalue  $\lambda_i$ , and influenced by its own forcing function,  $\theta_i$ . The matrix  $M^{-1}$  characterizes the transformation of  $\underline{x}'$  to  $\underline{m}$  and as we will see below it provides significant insight into kinetic behavior.

### 2.3.2. The stationary solution.

For the Michaelis-Menten reaction scheme the stationary point is found by equating the time derivative of equations 10 and 11 to zero. We have then three independent equations, two from equations 10 and 11

$$0 = -\bar{\sigma} + \frac{1}{1+St}\bar{x} + \sigma\bar{x} + \frac{St}{1+St}\bar{\psi} = f_1(\bar{\sigma}, \bar{x}, \bar{\psi}, St) \quad (20)$$

$$\begin{aligned} 0 &= \bar{x}^2 - (1 + \frac{1}{Mr} + \frac{K_{eq}}{StQs})\bar{x} + (\frac{K_{eq}}{St} - 1)\frac{\bar{\sigma}}{Qs}\bar{x} + \frac{1}{Mr} + (\frac{K_{eq}}{St} - 1)\frac{\bar{\sigma}}{Qs} \\ &= f_2(\bar{\sigma}, \bar{x}, Qs, Mr, K_{eq}/St) \end{aligned} \quad (21)$$

and a mass balance

$$0 = \bar{\sigma} + Qs\bar{x} + \bar{\pi} - \frac{Qs}{Mr} = f_3(\bar{\sigma}, \bar{x}, \bar{\pi}, Qs, Mr) \quad (22)$$

These equations have four dimensionless parameters ( $Qs$ ,  $Mr$ ,  $St$ ,  $K_{eq}$ ) and four variables ( $\bar{\sigma}$ ,  $\bar{x}$ ,  $\bar{\pi}$ ,  $\bar{\psi}$ ), eight quantities in all. Hence we must specify five of these eight quantities and solve for the remaining three. Furthermore at steady state we have  $\bar{\epsilon} = 1 - \bar{x}$ ,  $\bar{\psi} = \bar{\Omega}$ , and the flux is bounded as  $\bar{\psi} \in [-1/St, \bar{\sigma}/(1+\bar{\sigma})]$ .

Here we choose to specify  $Qs$ ,  $St$ ,  $K_{eq}$ ,  $\bar{\sigma}$  and  $\bar{\psi}$  since reasonable estimates for these quantities under in vivo conditions are at hand. Solving the equations for the remaining three yields

$$\bar{x} = \frac{(1+St)\bar{\sigma} - St\bar{\psi}}{(1+St)\bar{\sigma} + 1} \quad (23)$$

$$\bar{\pi} = \frac{K_{eq}}{1+St\bar{\psi}}(\bar{\sigma} - \bar{\psi}(1+\bar{\sigma})) \quad (24)$$

$$Mr = \frac{Qs}{\bar{\sigma} + Qs\bar{\chi} + \bar{\pi}} \quad (25)$$

In several important limits these results simplify.

- 1) Saturation behavior ( $\bar{\sigma} \rightarrow \infty$ ). This limit applies when the substrate concentration becomes very large and  $\bar{\chi} \rightarrow 1$ .
- 2) Irreversible reaction ( $k_{-2} \rightarrow 0$ , or  $K_{eq}/St \rightarrow \infty$ ). In this limit  $f_2 = f_2(\bar{\sigma}, \bar{\chi})$  and the results simplify to

$$\bar{\epsilon} = 1 - \bar{\chi} = 1 - \bar{\Psi} = \frac{1}{1 + \bar{\sigma}} \quad (26)$$

We note here that the assumption of constant  $s_t$  is not necessary in this limit since the product does not influence the rest of the reaction and it can accumulate without changing the dynamics of  $\sigma$  and  $\chi$ . Also note that in this limit  $\bar{\sigma}$  and  $\bar{\Psi}$  are not independent.

- 3)  $St = K_{eq}$  ( $k_1 = k_{-2}$ ). In this limit the solution simplifies because  $f_2$  becomes independent of  $\bar{\sigma}$ . Here an analytical solution to the transient behavior is attainable (Miller and Alberty, 1958).

### 2.3.3. Linearization of the Michaelis-Menten model.

The non-linear terms in the mass action kinetic description of the Michaelis-Menten mechanism may be linearized by a Taylor series expansion around the stationary point as

$$\sigma\chi = \bar{\sigma}\bar{\chi} + \bar{\chi}(\sigma-\bar{\sigma}) + \bar{\sigma}(\chi-\bar{\chi}) + (\sigma-\bar{\sigma})(\chi-\bar{\chi}) \quad (27)$$

$$\chi^2 = \bar{\chi}^2 + 2\bar{\chi}(\chi-\bar{\chi}) + (\chi-\bar{\chi})^2 \quad (28)$$

Omitting the quadratic terms and substituting the remaining ones into

equations 10 and 11 gives a liner description with a Jacobian matrix

$$J = \begin{bmatrix} -\bar{\epsilon} & \frac{1+St\bar{\psi}}{(1+St)\bar{\epsilon}} \\ \frac{(1-St/K_{eq})\bar{\epsilon}}{Qs} & -\frac{1+StQs\bar{\epsilon}^2/K_{eq}}{Qs\bar{\epsilon}} \end{bmatrix} \quad (29)$$

and with

$$\text{tr}(J) = -\frac{1+(1+St/K_{eq})Qs\bar{\epsilon}^2}{Qs\bar{\epsilon}} < 0 \quad (30)$$

$$\det(J) = \frac{St(Qs\bar{\epsilon}^2)}{QsK_{eq}} + \frac{1-\bar{\psi}}{1+St} + \frac{1}{K_{eq}}\left(\frac{1+St\bar{\psi}}{1+St}\right) > 0 \quad (31)$$

Here we have chosen  $\bar{\epsilon}$  as our independent concentration variable, since the algebra is much simpler than when  $\bar{\sigma}$  is used;  $\bar{\epsilon}$  is readily obtained from the steady state equations if  $\bar{\sigma}$  is given.

#### 2.3.4. The eigenvalues.

In our case there are two eigenvalues, hence two characteristic relaxation times, which provide useful insight into system dynamics.

These eigenvalues  $\lambda_1, \lambda_2$  of the Jacobian are given by

$$\lambda_1, \lambda_2 = \frac{1}{2}(\text{tr}(J) \pm \sqrt{\text{tr}(J)^2 - 4\det(J)}) \quad (32)$$

They can be shown, using equations 30 and 31, to be real negative, and it follows that the equilibrium point is a stable node, also see Darvey and Matlak (1967). Our next step is to establish the relative magnitudes of the time constants and their dependence on system

parameters.

Order of magnitude analysis. We now seek parameter combinations for which the two time constants are well separated which is important from a practical standpoint as a necessary condition for the existence of fast and slow variables. We shall find this situation to exist for almost all conditions of interest to us. As shown in appendix B analytical approximations to the eigenvalues in equation 32 may be obtained when a parameter  $\delta$  given by

$$\delta = 4\det(J)/\text{tr}(J)^2 \quad (33)$$

is small. The time constants may then be approximated by

$$\tau_1 = -1/\lambda_1 \rightarrow -\text{tr}(J)/\det(J) \quad (34)$$

$$\tau_2 = -1/\lambda_2 \rightarrow -1/\text{tr}(J) \quad (35)$$

Since  $\delta$  is small under many parameter combinations separation of time scales frequently occurs and approximate expressions for the time constants can be obtained. Some limits of interest are;

I)  $Q_s \rightarrow 0$  ( $e_t \ll K_m$ )

$$\tau_1 = \frac{1}{St\bar{\epsilon}\left(\frac{1-\bar{\Psi}}{1+St} + \frac{1}{K_{eq}}\left(\frac{1+St\bar{\Psi}}{1+St}\right)\right)} \quad (36)$$

$$\tau_2 = Q_s\bar{\epsilon} \quad (37)$$

Hence the motion on the faster time scale, represented by  $\tau_2$ , becomes very rapid whereas the slower time scale  $\tau_1$  remains unaffected.

II)  $\bar{\sigma} \rightarrow \infty$  ( $\bar{\epsilon} \rightarrow 0$  reaction in the saturation region). Here the approximate time constants are the same as given by equations 36 and 37. Here not only does the motion of the faster time scale accelerate, due to rapid movement of the enzyme species, but the slower time scale becomes very long representing the insensitivity of zeroth order behavior to variations in the substrate concentration.

III)  $St \rightarrow 0$  (binding step much faster than the product release)

$$\tau_1 = \frac{1}{St\bar{\epsilon}} \left( \frac{1}{\frac{1}{K_{eq}} + \frac{1-\bar{\psi}}{1+Qs\bar{\epsilon}^2}} \right) \quad (38)$$

$$\tau_2 = Qs\bar{\epsilon}/(1+Qs\bar{\epsilon}^2) \quad (39)$$

Hence the slower time scale, represented by  $\tau_1$ , becomes very long while the faster one  $\tau_2$  remains unaffected.

IV)  $St \rightarrow \infty$  (the binding step much slower than product release).

$$\tau_1 = \frac{Qs\bar{\epsilon}}{Qs\bar{\epsilon}^2 + \bar{\psi}} \quad (40)$$

$$\tau_2 = \frac{K_{eq}}{St\bar{\epsilon}} \quad (41)$$

Here the faster time scale  $\tau_2$  shortens while the slower one remains unaffected.

These limiting cases are useful in assessing the importance of diffusional effects, see appendix A.

Figure 2-1.

Relative magnitudes of the two time constants of Michaelis-Menten kinetics. Loci of constant ratios between the two time constants ( $\tau_2/\tau_1$ ) in the St,Qs-plane, for typical values of the dimensionless parameters,  $K_{eq} = 1000$ ,  $\bar{\sigma} = 1$ ,  $\bar{\Psi} = .25$ .

region (1),              ratio  $< 10^{-3}$ ,

region (2),  $10^{-3} < \text{ratio} < 10^{-2}$ ,

region (3),  $10^{-2} < \text{ratio} < 10^{-1}$ , and

region (4),  $10^{-1} < \text{ratio}$ ,

where the ratio is  $(\tau_2/\tau_1)$ . These results are not very sensitive to variations in these parameters, except when  $K_{eq}$  drops below unity.

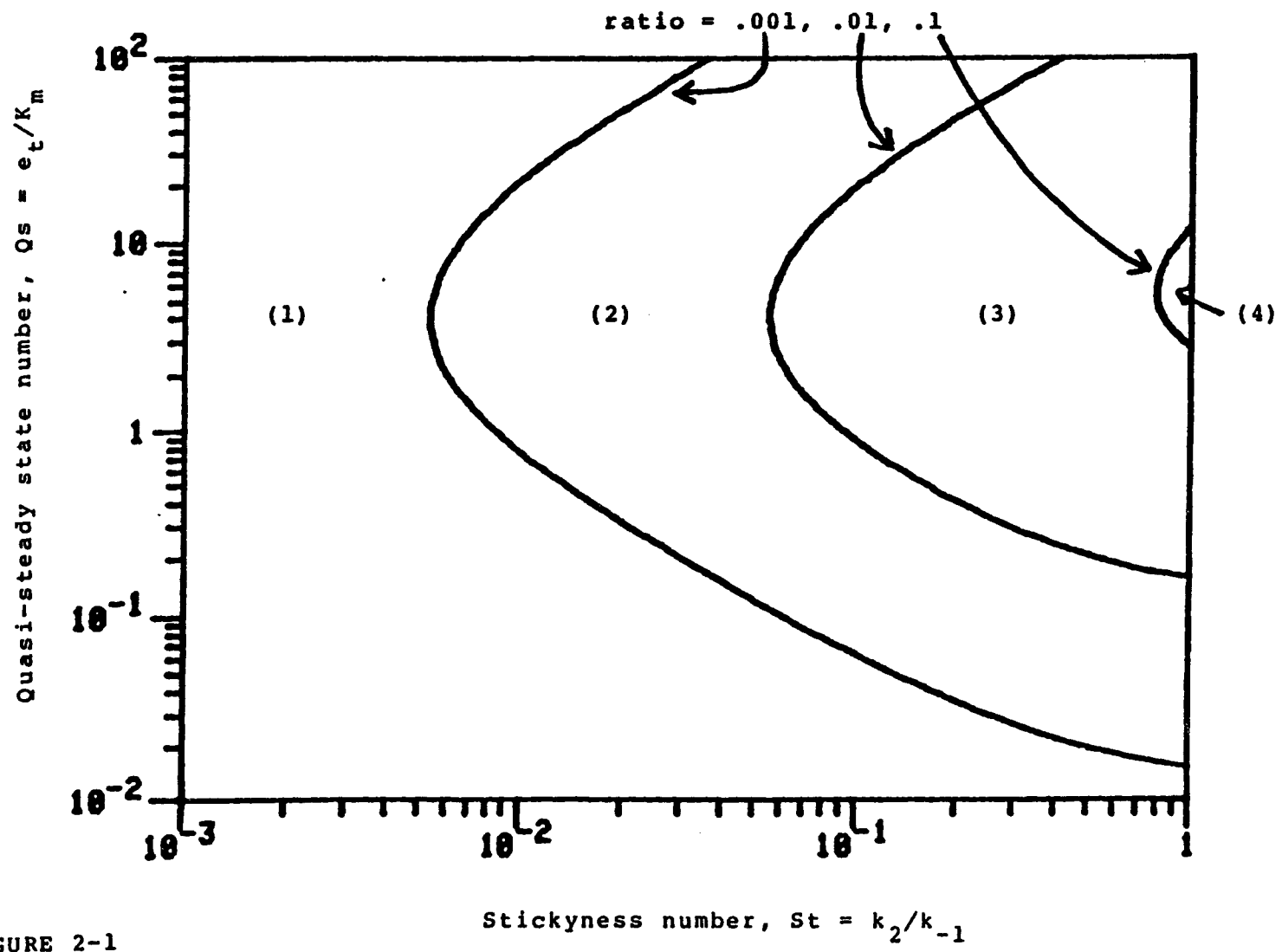


FIGURE 2-1

We have computed the time constant ratio

$$\frac{\tau_1}{\tau_2} = \frac{1-\sqrt{1-\delta}}{1+\sqrt{1-\delta}} \quad (42)$$

over the parameter space. Typical results, figure 2-1, show that for physiological ranges of the dimensionless groups the time constants are well separated.

### 2.3.5. The normal modes.

The dynamic behavior of our system is perhaps best understood by examining the dynamically independent normal modes, of the linear description, and how they relate to the original concentration variables. As discussed in section 2.3.1 and appendix B this relationship is given by

$$\begin{pmatrix} m_1 \\ m_2 \end{pmatrix} = M^{-1} \begin{pmatrix} o' \\ x' \end{pmatrix} = \begin{pmatrix} u_{11} & u_{12} \\ u_{21} & u_{22} \end{pmatrix} \begin{pmatrix} o' \\ x' \end{pmatrix} = \begin{pmatrix} u_{11}o' + u_{12}x' \\ u_{21}o' + u_{22}x' \end{pmatrix} \quad (43)$$

The relative magnitudes of the elements of each row in  $M^{-1}$  may be interpreted as measures of interaction (appendix B). Assessing these interactions is important since in the limits where they are small, in particular where time scale separation occurs simultaneously, approximate solutions may be obtained since the modes will then approximate the actual variables.

The matrix  $M^{-1}$  is comprised of the eigenrows as  $M^{-1} = (\underline{u}_1, \underline{u}_2)^t$ , where  $\underline{u}_1 = (u_{11}, u_{12})$  and  $\underline{u}_2 = (u_{21}, u_{22})$ , and where the eigenrows are defined by,  $\underline{u}_i(J - \lambda_i I) = \underline{0}$ . The relative magnitudes of the elements

in the eigenrows are

$$c_1 = \frac{u_{12}}{u_{11}} = \frac{\lambda_1 - j_{11}}{j_{12}} \quad c_2 = \frac{u_{21}}{u_{22}} = \frac{j_{12}}{\lambda_2 - j_{11}} \quad (44)$$

and  $c_1$  and  $c_2$  the desired measures of interactions, appendix B. It is conceptually useful to assign a weight of unity to the concentration variable that contributes more to a mode, hence we define

$$\begin{aligned} u_1 &= (1, c_1) \text{ for } c_1 < 1 \\ &= (c_1^{-1}, 1) \text{ for } c_1 > 1 \end{aligned} \quad (46)$$

$$\begin{aligned} u_2 &= (c_2, 1) \text{ for } c_2 < 1 \\ &= (1, c_2^{-1}) \text{ for } c_2 > 1 \end{aligned} \quad (45)$$

which is possible by appropriate scaling of the eigenrows, see appendix B. Here we have chosen  $m_2$  as the faster mode, since  $\chi$  is expected to be the fast changing variable.

Order of magnitude analysis. We now seek parameter combinations under which the interaction parameters  $c_1$  and  $c_2$  are small since under these conditions the concentration variables will approximate the modes and hence will be dynamically decoupled. In particular such behavior is useful when time scale separation occurs simultaneously, as we shall see below. Then approximate values for  $c_1$  and  $c_2$  are

$$c_1 = -\frac{j_{11} + j_{12}j_{21}}{j_{21}(j_{11} + j_{22})} \quad c_2 = \frac{j_{21}}{j_{22}} \quad (46)$$

by using equations 34 and 35 along with  $\text{tr}(J) = j_{11} + j_{22}$  and  $\det(J) = j_{11}j_{22} - j_{12}j_{21}$ . Substituting the expressions for the elements of

the Jacobian matrix from equation 29 into equation 46 we obtain

$$c_1 = Qs^2 \frac{\epsilon^2 + \frac{1}{Qs} \left(1 - \frac{St}{K_{eq}}\right) \left(\frac{1+St\Psi}{1+St}\right)}{\left(1 - \frac{St}{K_{eq}}\right) \left(1 + \left(1 + \frac{St}{K_{eq}}\right) Qs\epsilon^2\right)} \quad (47)$$

$$c_2 = -\frac{\epsilon^2}{\frac{1 - \frac{St}{K_{eq}}}{1 + \frac{StQs\epsilon^2}{K_{eq}}}} \quad (48)$$

Examination of limits I-IV leads to some very important results.

I)  $Qs \rightarrow 0$ ,  $\Rightarrow c_1 \rightarrow 0$ . In this limit the first mode and  $\sigma$  become identical since  $\chi$  does not contribute to  $m_1$ . As shown above the time scales are well separated in this limit, and hence  $\sigma$  emerges as a slow variable that moves independently of  $\chi$ . This is then a case of one-way decoupling where movement of  $\chi$  will not cause  $\sigma$  to move but  $\chi$  adjusts quickly to changes in  $\sigma$ . Hence when one is interested in motion on the slower time scale the dynamics of  $\chi$  are unimportant and ignoring them will not introduce significant errors.

This is precisely what the quasi-steady state assumption does, and hence it is expected to produce satisfactory results in this limit. Note, however, that the quasi-steady state assumption differs from this result stating that the rates of production and removal of the intermediate become equal after a short transient period. The more realistic interpretation that we arrive at via the linear analysis is that this simplification is really based on

reduced dynamic interactions between the concentration species accompanied by time scale separation.

II)  $\bar{\sigma} \rightarrow \infty$ ,  $\Rightarrow c_2 \rightarrow 0$ . In this limit, where the flux approaches its saturation limit, the enzyme is saturated with substrate and the reaction displays effectively zeroth order kinetics. Here we have an opposite situation to limit I) namely the motion on the fast time scale is dominated by  $\chi$  decoupled from  $\sigma$ . Hence when considering motion on the shorter time scale one can for all practical purposes consider  $\sigma$  to be constant during this period. The motion of the substrate is on the slower time scale and corresponds to the zeroth order removal.

III)  $St \rightarrow 0$ . In this limit time scale separation occurs and the interaction coefficients become  $c_1 = Qs$  and  $c_2 = -\bar{\epsilon}^2$  hence we expect two independent dynamic variables to appear as

$$m_1 = \sigma + Qs\chi \quad (\text{slow}) \quad (49)$$

$$m_2 = -\bar{\epsilon}^2\sigma + \chi \quad (\text{fast}) \quad (50)$$

Combining equations 10 and 11 in these ratios we get

$$\frac{dm_1}{d\tau} = \frac{d(\sigma + Qs\chi)}{d\tau} = -\frac{d\pi}{d\tau} = \frac{-St}{1+St}(\chi - \psi) \quad (51)$$

by the use of the mass balance, equation 12, and

$$Qs \frac{dm_2}{d\tau} = (1 + \bar{\epsilon}^2 Qs)(\sigma - \frac{1}{1+St}\chi - \sigma\chi) \quad (52)$$

Mode 2 moves much faster than  $m_1$  and by relaxing its dynamics we get

$$\frac{\sigma(1-\chi)}{\chi} = \frac{1}{1+St} \quad (53)$$

which in dimensioned form is

$$\frac{se}{x} = \frac{k_{-1}}{k_1} = K_s \quad (54)$$

which simply is the equilibrium relationship for substrate binding. Hence we conclude that when St is small the binding step equilibrates fast. Applying the quasi-equilibrium assumption then gives

$$\frac{dm_1}{d\tau} = - \frac{d\pi}{d\tau} = - \frac{St}{1+St} \left( \frac{\sigma}{\frac{1}{1+St} + \sigma} - \psi \right) \quad (55)$$

which in dimensioned form is

$$\frac{dp}{dt} = \frac{k_2 e_t s}{K_s + s} \quad (56)$$

for closed systems, which is the original equation derived by Michaelis and Menten (1913) by using the quasi-equilibrium assumption. Hence we have the remarkable result that the quasi-equilibrium assumption can be rationally interpreted and justified using modal analysis.

Linearizing and rearranging equation 52 gives

$$\left( \frac{-\epsilon Qs}{1+\epsilon^2 Qs} \right) \frac{dm_2}{d\tau} = -m_2 \quad (57)$$

which suggests that the equilibrium is reached with the time constant of equation 39 (which is the same quantity as in the parentheses multiplying the derivative of  $m_2$  in equation 57). Then the quasi-equilibrium state moves with a relaxation time given by

equation 38 and its motion can be described by equation 55 or 56.

IV)  $St \rightarrow \infty$ . Here  $c_1, c_2 \rightarrow 0$  leading to analogous simplifications as in limits I) and II).

For,  $St = K_{eq}$ ,  $c_2 = 0$ , an exact solution is attainable, since  $c_2$  is identically zero. Here the differential equation for  $x$  is independent of  $\sigma$ . For open systems this means that any perturbations in  $\sigma$ , as brought about by changing  $\Psi$ , will not move  $x$  which is now truly stationary. Hence  $\sigma$  is readily obtained, and the quasi-steady state assumption is exact. For batch systems the solution for this limit was presented by Miller and Alberty (1958).

### 2.3.6. Influence of the dimensionless groups on dynamic behavior.

From the above discussion it is clear that simultaneous consideration of the time constants and the modal matrix  $M^{-1}$ , figures 2-2,3,4 and 5, provide an excellent basis for interpreting reaction dynamics. In figures 2-2,3,4 and 5 we present computations of the time constants and the modal matrix where we have chosen parameter values typical for metabolic enzymes and we show their influence by varying one at the time.

- a) As shown in figure 2-2 at small  $Q_s$  numbers the 1,2-element of  $M^{-1}$  becomes small and the faster time constant becomes fast, which leads to quasi-stationary behavior as discussed above.
- b) As seen in figure 2-3 the substrate concentration mainly influences the 2,1-element of  $M^{-1}$  and the ratio between the time

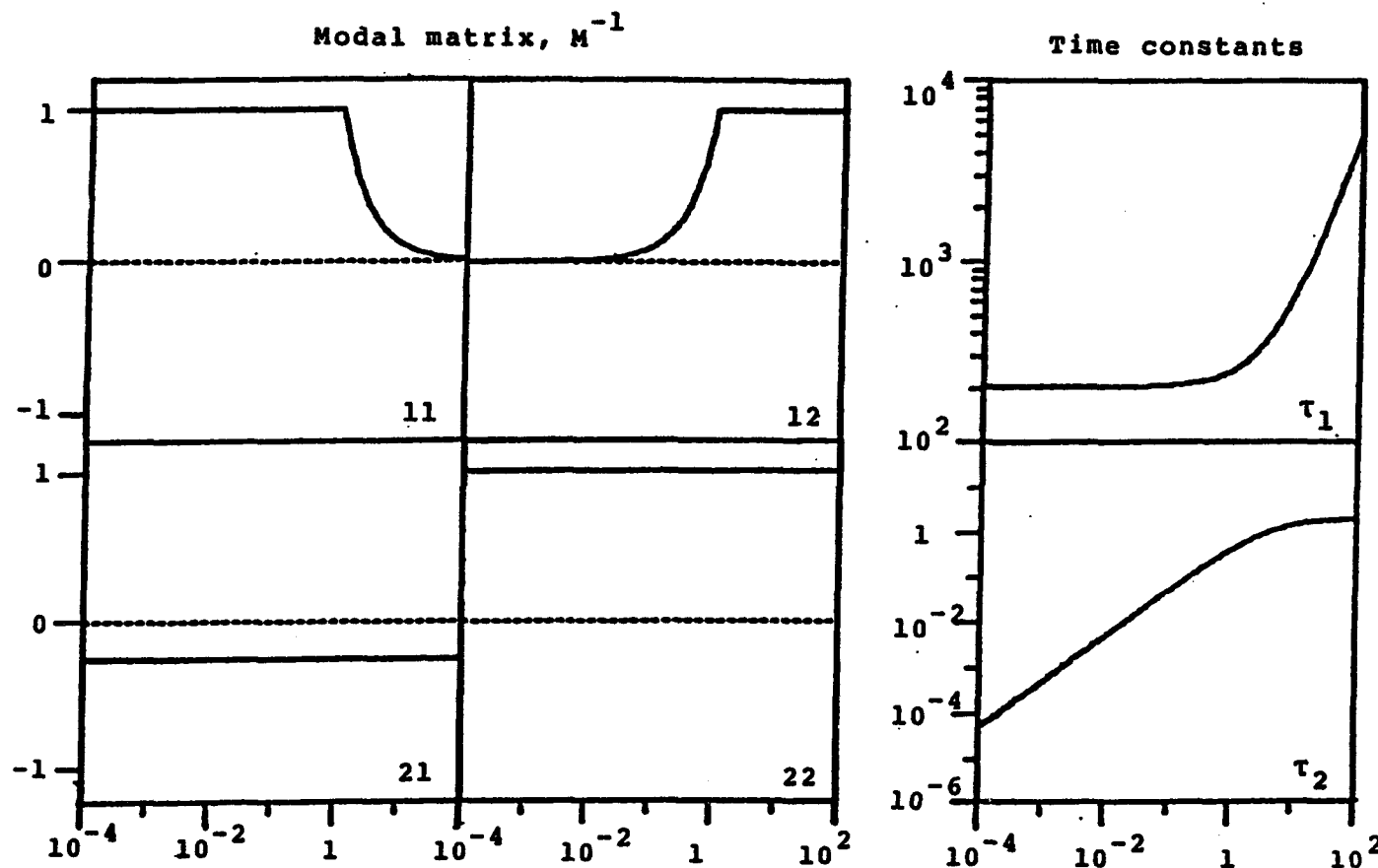


Figure 2-2. The modal matrix and the time constants as functions of the quasi-steady state number,  $Q_s$ . The other dimensionless are  $St = .01$ ,  $K_{eq} = 1000$ ,  $Mr = .01$ ,  $\Psi = .25$ ,  $\sigma = 1$ .

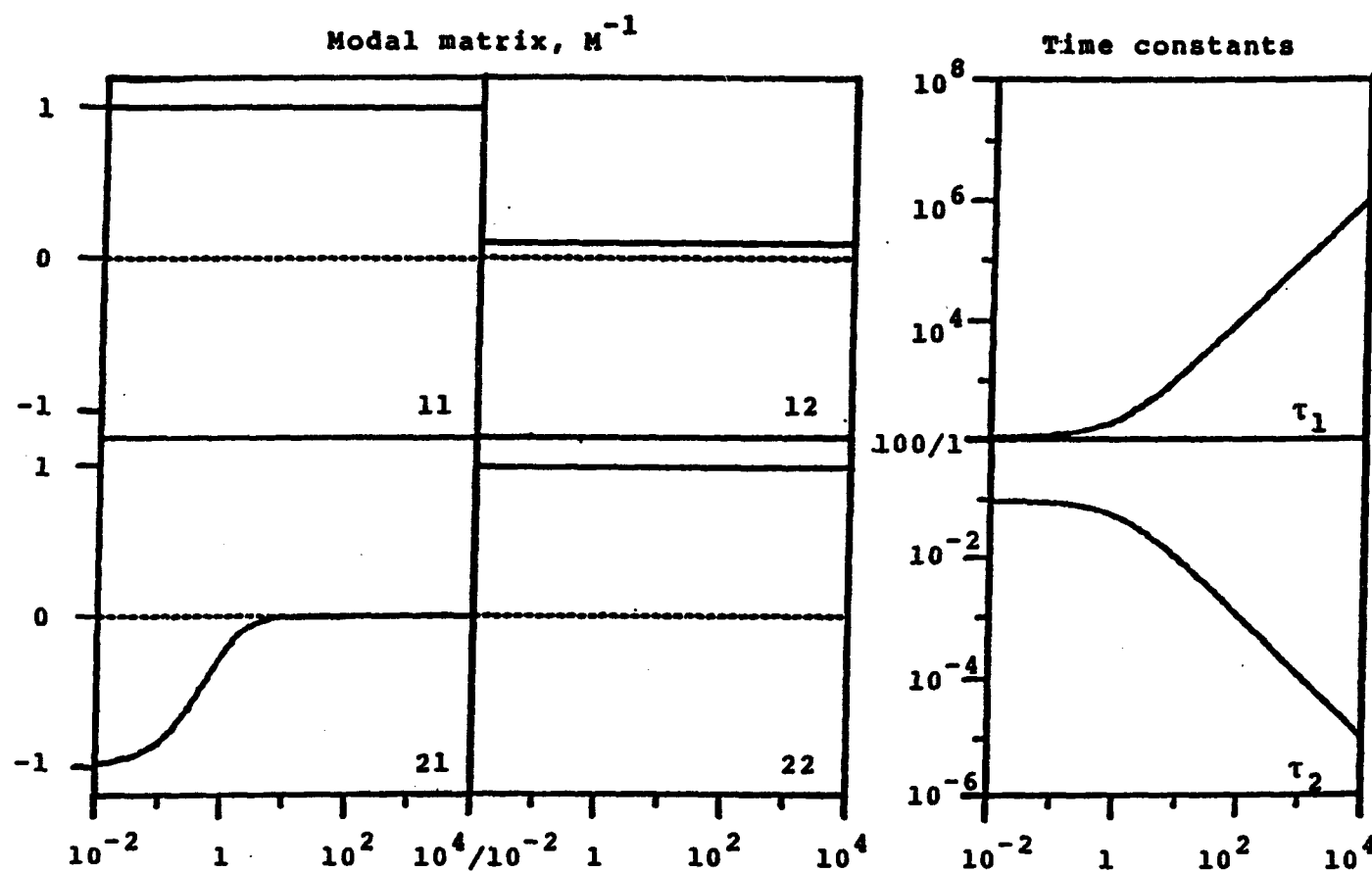


Figure 2-3. The modal matrix and the time constants as functions of the steady state concentration of the substrate,  $\bar{o}$ . The other dimensionless are  $St = .01$ ,  $K_{eq} = 1000$ ,  $Q_s = .1$ ,  $M_r = .01$ ,  $\bar{\Psi} = .25$ .

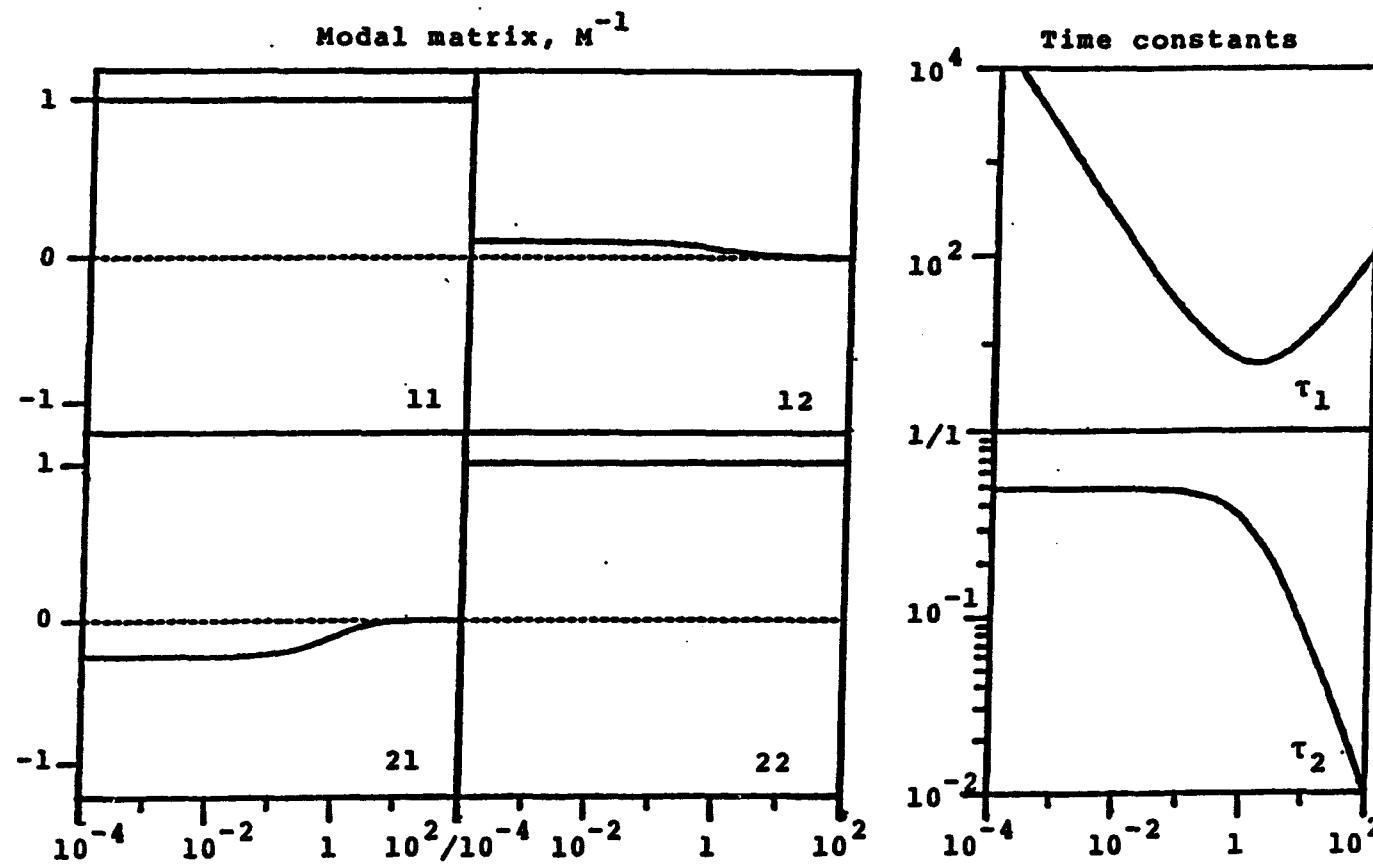


Figure 2-4. The modal matrix and the time constants as functions of the stickiness number,  $St$ . The other dimensionless are  $K_{eq} = 1000$ ,  $Q_s = .1$ ,  $M_r = .01$ ,  $\bar{\gamma} = .25$ ,  $\bar{\sigma} = 1$ .

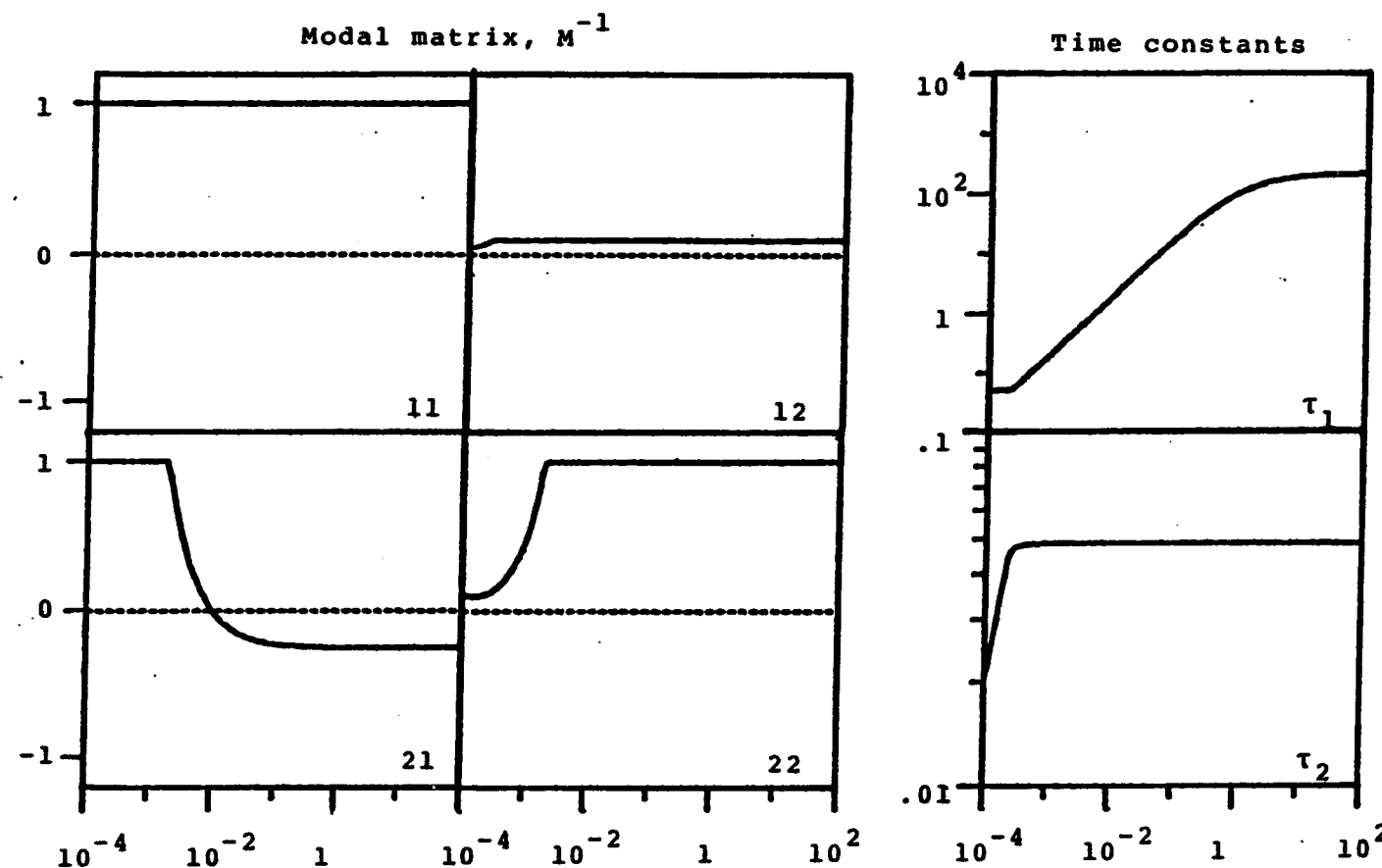


Figure 2-5. The modal matrix and the time constants as functions of the overall equilibrium constant,  $K_{eq}$ . The other dimensionless are  $St = .01$ ,  $Qs = .1$ ,  $Mr = .01$ ,  $\Psi = .25$   $\sigma = 1$ .

constants as discussed previously. This decoupling leads to a justification for using a zeroth order inner perturbation solution as discussed in the following section.

c) At low St numbers the interaction coefficients reach finite values which as discussed above leads to quasi-equilibrium behavior. At high St numbers all interactions between  $\sigma$  and  $\chi$  disappear and quasi-steady state analysis will be applicable, figure 2-4.

d) The equilibrium constant influences the second mode in a peculiar way, figure 2-5. At high  $K_{eq}$  values the second mode is dominated by  $\chi$  but as  $K_{eq}$  drops the 2,1-element changes sign, at  $K_{eq} = St$ , and eventually  $\sigma$  dominates the behavior of mode 2. We also note that the 2,1-element moves quickly through zero indicating that the exact solution of Miller and Alberty (1958) would rapidly lose applicability as  $K_{eq}$  deviates from St.

Through the full linear analysis we have been able to put the quasi-steady state and quasi-equilibrium assumption into perspective, and next we shall use it to gain insight into another major development, the use of singular perturbation theory.

#### 2.4. Singular Perturbations.

Quasi-steady state analysis is intimately related to the theory of singular perturbations (Bowen, Acrivos and Oppenheim, 1963), basically because the quasi-steady state solution often is the first

term in an asymptotic series solution. This technique has been useful in analysing batch kinetics, and particularly extensive results are at hand for irreversible Michaelis-Menten kinetics (Heineken et al., 1967, Lin and Segel, 1974, Meiske 1978).

The solution procedure basically involves a separation of the transient response into two separate time regions, an "inner region" containing the rapid transients, and an "outer region" representing the slower motion. An asymptotic series solution is then formulated, as a power series in a small parameter, in each time regime. For the irreversible limit the zeroth order term in the outer solution is the quasi-steady state solution, and it is obtained by equating the perturbation parameter to zero. The zeroth order term in the inner region is obtained by assuming the substrate species concentration to be constant at the initial value during the transient phase. The zeroth order inner and outer solutions are then spliced together. This solution procedure was first presented by Wong (1965), and it was put into the framework of singular perturbation theory by Heineken et al., (1967), who also provided the full solution.

The perturbation parameter used by Heineken et al., (1967) is  $Mr = e_t/s_t = Qs/\mu_t < Qs/\bar{a}$ , and this ratio has been taken as an indicator of the applicability of the quasi-steady state assumption (e.g. Laidler, 1955, Heineken et al, 1967, Lim, 1973). If  $Mr$  is small the quasi-steady state assumption is believed to give good results.

The linear analysis provides us with an insight into the dynamic

interactions between the concentration variables and hence sheds light on the basic assumptions of the singular perturbation approach. If  $c_2$  is small the substrate is not expected to move significantly during the transient phase of the reaction, and the smallness of  $c_2$  can be used as a measure of applicability for the zeroth order inner solution. On the other hand if  $c_1$  is small  $\chi$  is not expected to move to any significant extent on the slower time scale and  $\chi$  would adjust rapidly to any changes in  $\sigma$  without disturbing the motion of  $\sigma$ . Under these circumstances the zeroth order outer solution is expected to adequately represent events on the slower time scale.

Both these decoupling features are found when the ratio  $Qs/\bar{\sigma}$  is small, given that  $Qs$  is small (i.e.  $e_t \ll K_m$ ) and that  $\bar{\sigma}$  is large (i.e.  $\bar{s} \gg K_m$ ). The former criterion ( $Qs$  small) is especially important here since it will predict the utility of the quasi-stationary analysis. Crooke, Tanner and Aris (1979) have also argued that  $Qs$  is an important indicator for the applicability of the quasi-steady state assumption.

Next we provide a rigorous test of the above discussion via direct integration of the differential equations and comparison with approximate solutions.

## 2.5. Numerical solutions.

### 2.5.1. Batch Kinetics.

Here we examine the time course of the reaction for typical in vitro kinetic experiments, where only substrate is initially present, and the enzyme is added at time zero,  $c(0) = c_0$  and  $x(0) = 0$ .

The inner solution. We now wish to test the prediction that  $c_2$  indicates the applicability of the zeroth order inner solution. The behavior of the reaction during the transient period is shown in figure 2-6 as it depends on  $c_0$ . The figure clearly shows that as the substrate concentration increases, or  $c_2$  decreases, less and less motion of the substrate is observed during the transient period, and furthermore the zeroth order inner solution converges to the exact motion.

The outer solution. Likewise the constant  $c_1$  reflects how the enzyme complex influences the motion of the substrate during the slower phase. As shown in figure 2-7 the motion of  $c$  during the stationary phase is less and less influenced by  $x$  as  $Q_s$  drops ( $c_1 = Q_s$ ). Hence the zeroth order outer solution, or quasi-stationary analysis, is applicable if  $Q_s$  is small.

The quasi-equilibrium solution. Figure 2-8 shows the product concentration profile as computed from the exact model and by applying the quasi-equilibrium assumption. As predicted by modal

Figure 2-6.

Dynamic behavior of the Michaelis-Menten reaction mechanism during the transient phase illustrating one-way dynamic decoupling.

a) The dynamic behavior of  $x$  during the transient phase for  $x_0 = 0$ ,  $K_{eq} = 1000$ ,  $St = .01$ ,  $Qs = .1$ ,  $Mr = .01$  and varying  $\sigma_0$ .

$$(1) \sigma_0 = .1, \tau_2 = .0834, c_2 = -.915$$

$$(2) \sigma_0 = 1, \tau_2 = .0476, c_2 = -.500$$

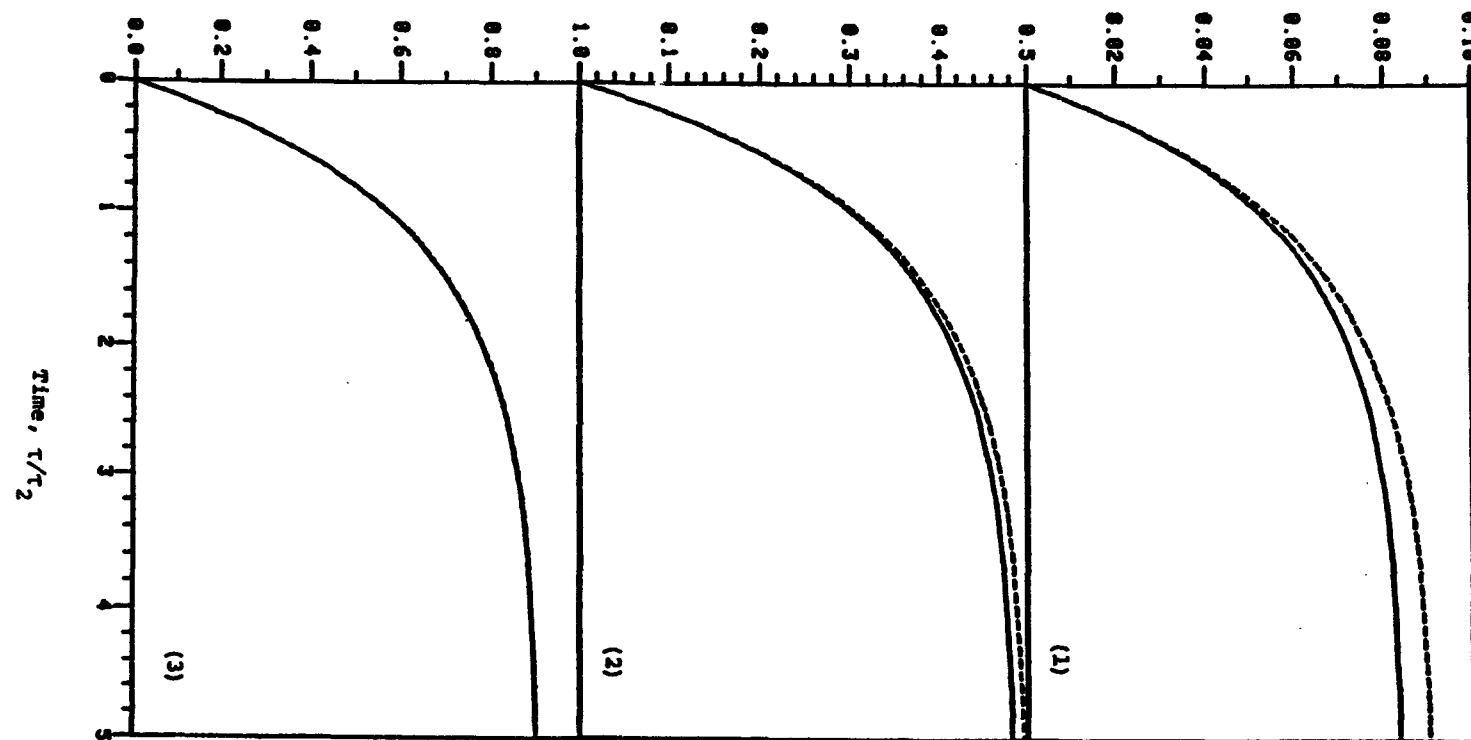
$$(3) \sigma_0 = 10, \tau_2 = .0090, c_2 = -.091.$$

Note that the time is scaled in terms of the faster time constant. The solid line represents the exact solution and the dashed line represents the zeroth order inner solution (which assumes the substrate concentration to be constant,  $\sigma = \sigma_0$ ).

b) Motion of the  $\sigma$  during the transient phase. As  $\sigma_0$  grows the motion of  $\sigma$  becomes less significant during the transient phase.

FIGURE 2-6a.

Concentration of the intermediate complex,  $\chi$ .



Percent deviation from initial conditions,  $100 \times (\sigma - \sigma_0) / \sigma_0$

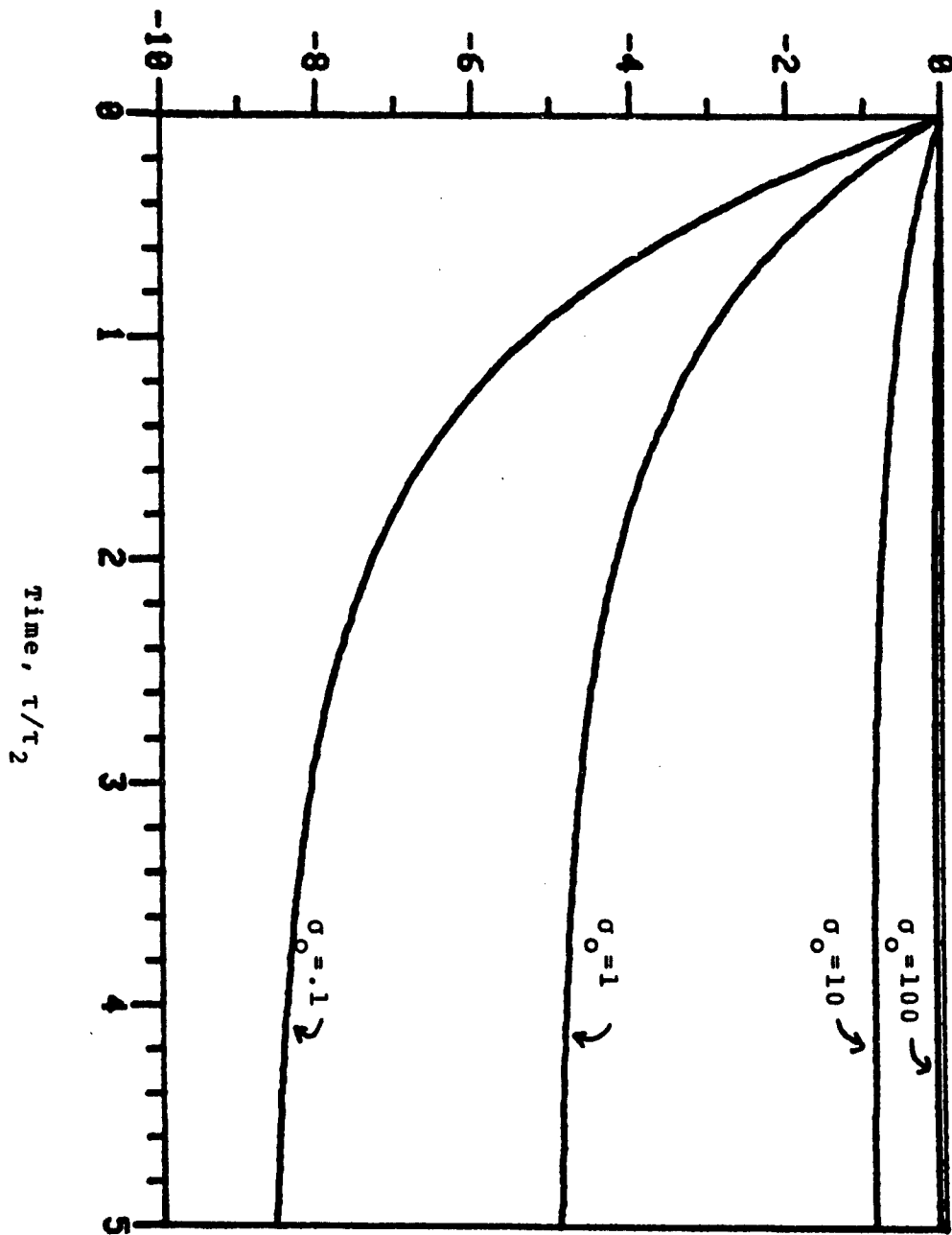


FIGURE 2-6b

Figure 2-7.

The dynamic behavior of  $\sigma$  during the stationary phase for  $a_0 = 1$ ,  $x_0 = 0$ ,  $K_{eq} = 1000$ ,  $St = .01$ ,  $Mr = .01$  and varying  $Q_s$ :

- (1)  $Q_s = 1$ ,  $\tau_1 = 274$ ,  $c_1 = .996$
- (2)  $Q_s = .1$ ,  $\tau_1 = 210$ ,  $c_1 = .0995$
- (3)  $Q_s = .01$ ,  $\tau_1 = 202$ ,  $c_1 = .00995$

Note that the time is scaled in terms of the slower time constant.  
The solid line represents the exact solution and the dashed line  
represents the quasi-steady state solution.

FIGURE 2-7.

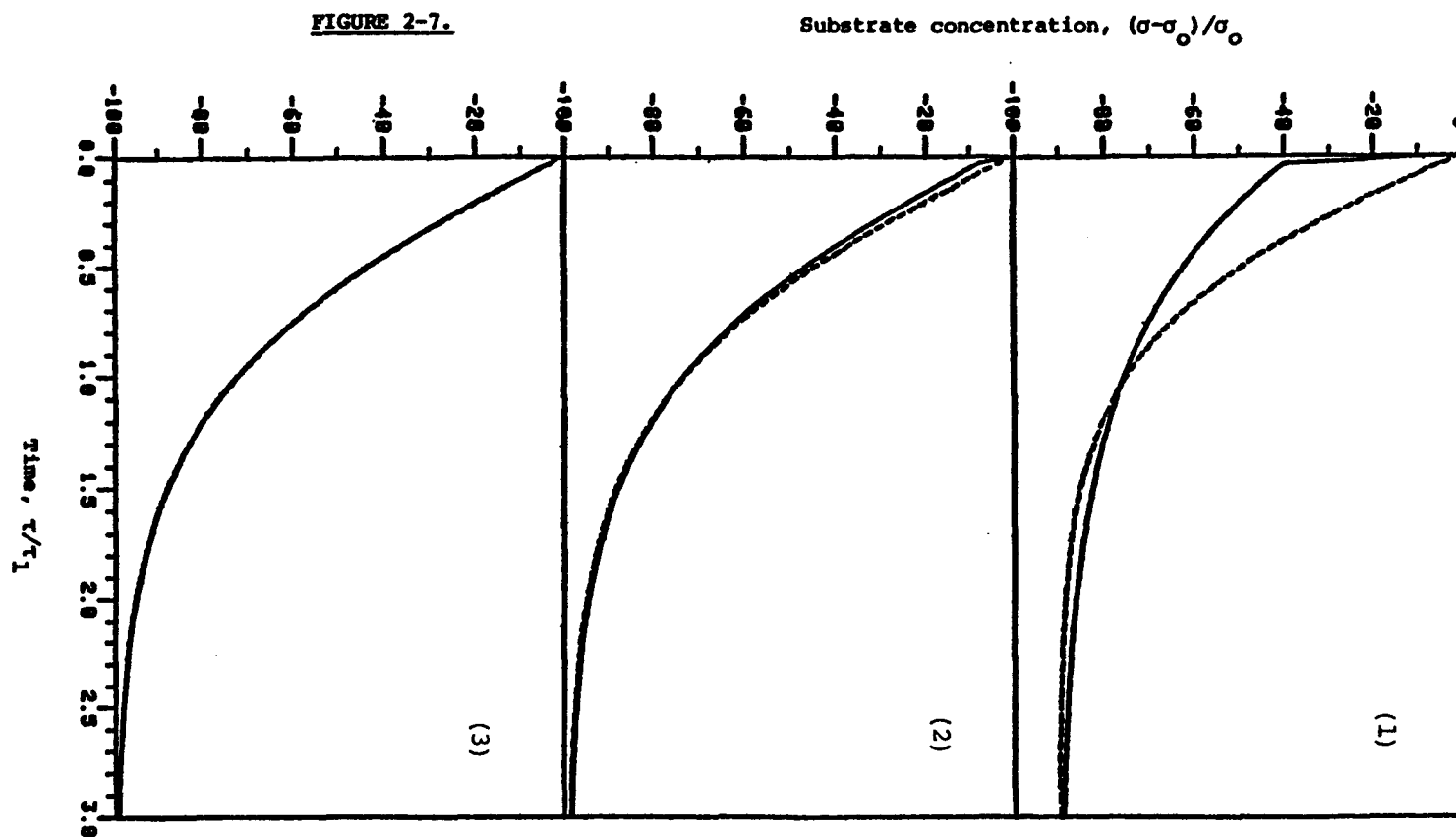


Figure 2-8.

The dynamic behavior of  $\pi$  as obtained from: the exact numerical solution (the solid line) and by using the quasi-equilibrium solution (the dotted line).

$$(1) St = 10, \tau_1 = 2.92, c_2 = -.603$$

$$(2) St = 1, \tau_1 = 5.65, c_2 = -.549$$

$$(3) St = .1, \tau_1 = 32.7, c_2 = -.508$$

Note that the time is scaled in terms of the slower time constant.

The value  $c_2$  that represents quasi-equilibrium is  $-.5$ . Other parameters are:  $a_0 = 1$ ,  $x_0 = 0$ ,  $Q_s = 1$  and  $K_{eq} \rightarrow \infty$ .

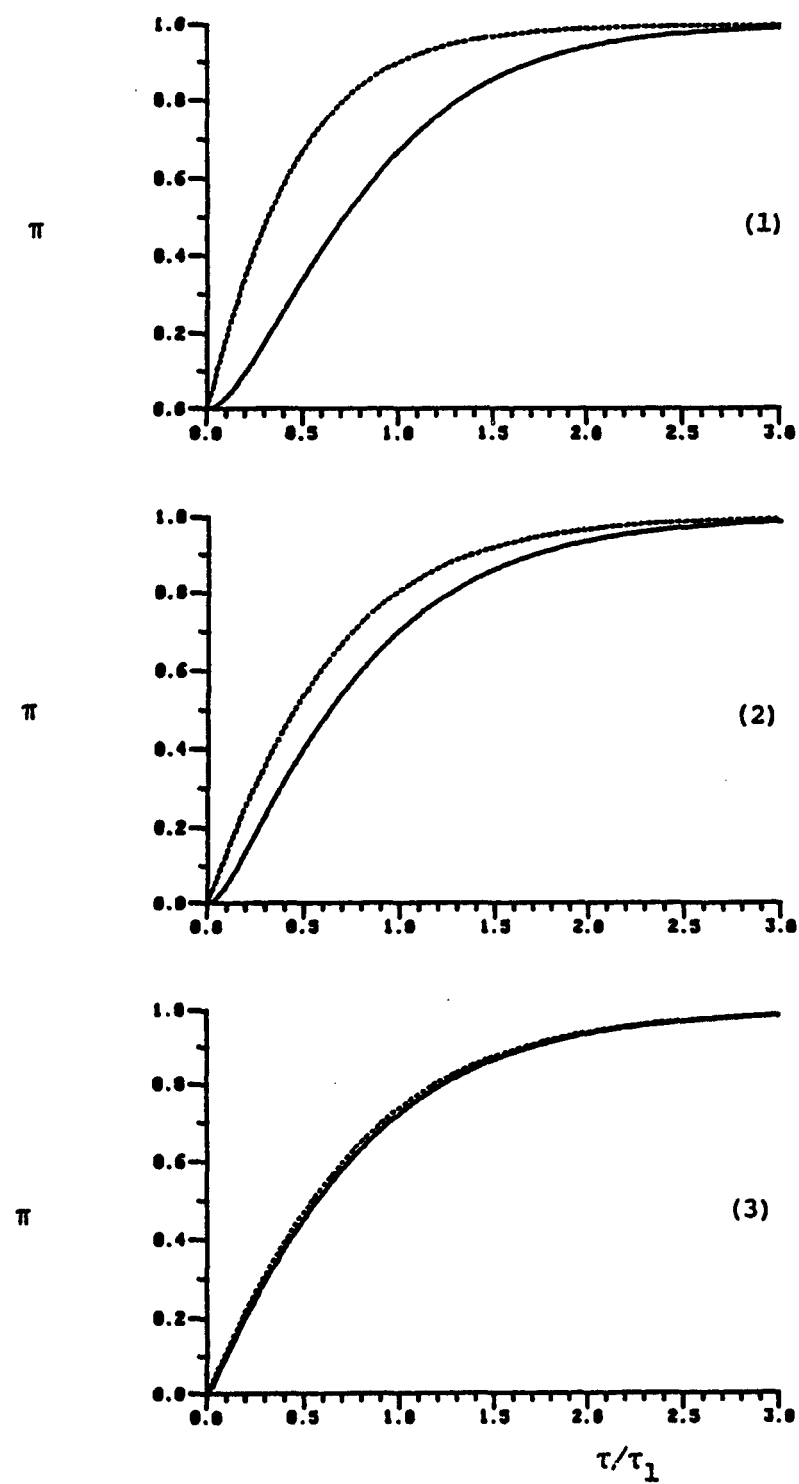


FIGURE 2-8.

analysis in section 2.3.5 the quasi-equilibrium solution converges to the exact one as  $S_t$  drops. For  $S_t$  less than .01-.05 the two solutions are indistinguishable (this can also be seen from figure 2-4 since the elements of the modal matrix do not change appreciably below  $S_t$  of .01-.05).

### 2.5.2. Open systems.

We now look at the transient response under typical in vivo conditions, figure 2-9. In vivo the reaction operates around some steady state, and we are interested in the dynamic behavior around this steady state and here we start out with the reaction in the steady state and impose a disturbance in the input flow rate. In figure 2-9 we show two possible approximate solutions: the quasi-steady state and the linear solutions.

The quasi-stationary solution. As already discussed the quasi-stationary analysis is mainly dependent on the magnitude of the  $Q_s$  number and as shown in figure 2-9 the quasi-steady state solution diverges from the exact solution as  $Q_s$  increases. Our numerical results indicate that in general for  $Q_s$  number larger than about .1 the quasi-steady state solution starts to diverge from the exact one and can give a seriously misleading representation of the exact motion. As a rule of thumb when  $Q_s$  is less than about .01-.1 the quasi-steady state solution is quite good.

There is a major difference between the dynamic behavior of open

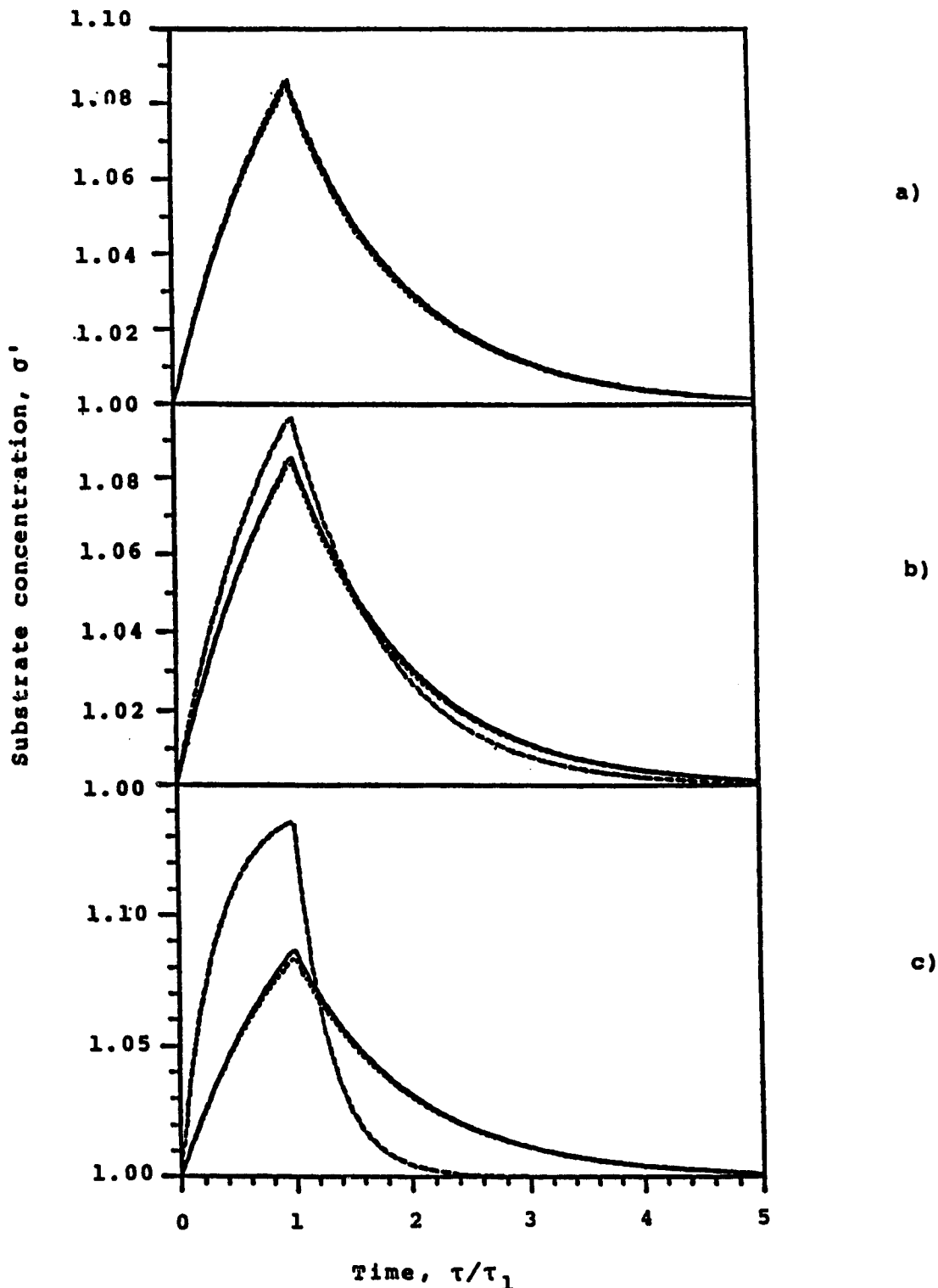
Figure 2-9.

The dynamic behavior of  $\sigma$  during the stationary phase for Michaelis-Menten kinetics with net mass exchange with the environment. The parameters are  $K_{eq} = 1000$ ,  $St = .01$ ,  $\bar{\Psi} = .5$  and  $\bar{\sigma} = 1$  and:

- (1)  $Q_s = .1$ ,  $\tau_1 = 276$ ,
- (2)  $Q_s = 1$ ,  $\tau_1 = 336$ ,
- (3)  $Q_s = 10$ ,  $\tau_1 = 936$ .

Note that the time is scaled in terms of the slower time constant. The solid line represents the exact solution, the dotted line represents the quasi-steady state solution, and the dashed line represents the linear solution.

FIGURE 2-9



and batch systems due to the differences in the initial conditions.

Unlike batch systems in vivo situations are normally in a steady state and the reaction is moved away from this state by perturbations in the input flux. Hence under in vivo the reaction starts out with  $x$  in the stationary state and the rapid transients are less noticeable, compared to batch situations where the enzyme species starts out far away from the quasi-stationary state.

The linear solution. The other approximate solution shown in figure 2-9 is the linear solution, equation 18. This solution represents the exact solution reasonably well from modest deviations from steady state regardless of parameter values (Guertin, Sørensen and Stewart, 1977, have also pointed out that linearization can be more reliable than the quasi-steady state assumption). However it becomes less reliable when the deviation from the steady state become appreciable, and in particular if the reaction is moved into the saturation range where the deviations from linearity are most severe (see chapter 5).

The quasi-equilibrium solution. In figure 2-10 we show how the quasi-equilibrium solution approaches the exact one as  $St$  drops. A major drawback of the quasi-equilibrium solution for open systems is evident: the differential equations under the quasi-equilibrium assumption do not satisfy the steady state conditions! Unlike the quasi-steady state assumption, which relaxes the dynamics of the intermediate enzyme complex and it is therefore by definition in the

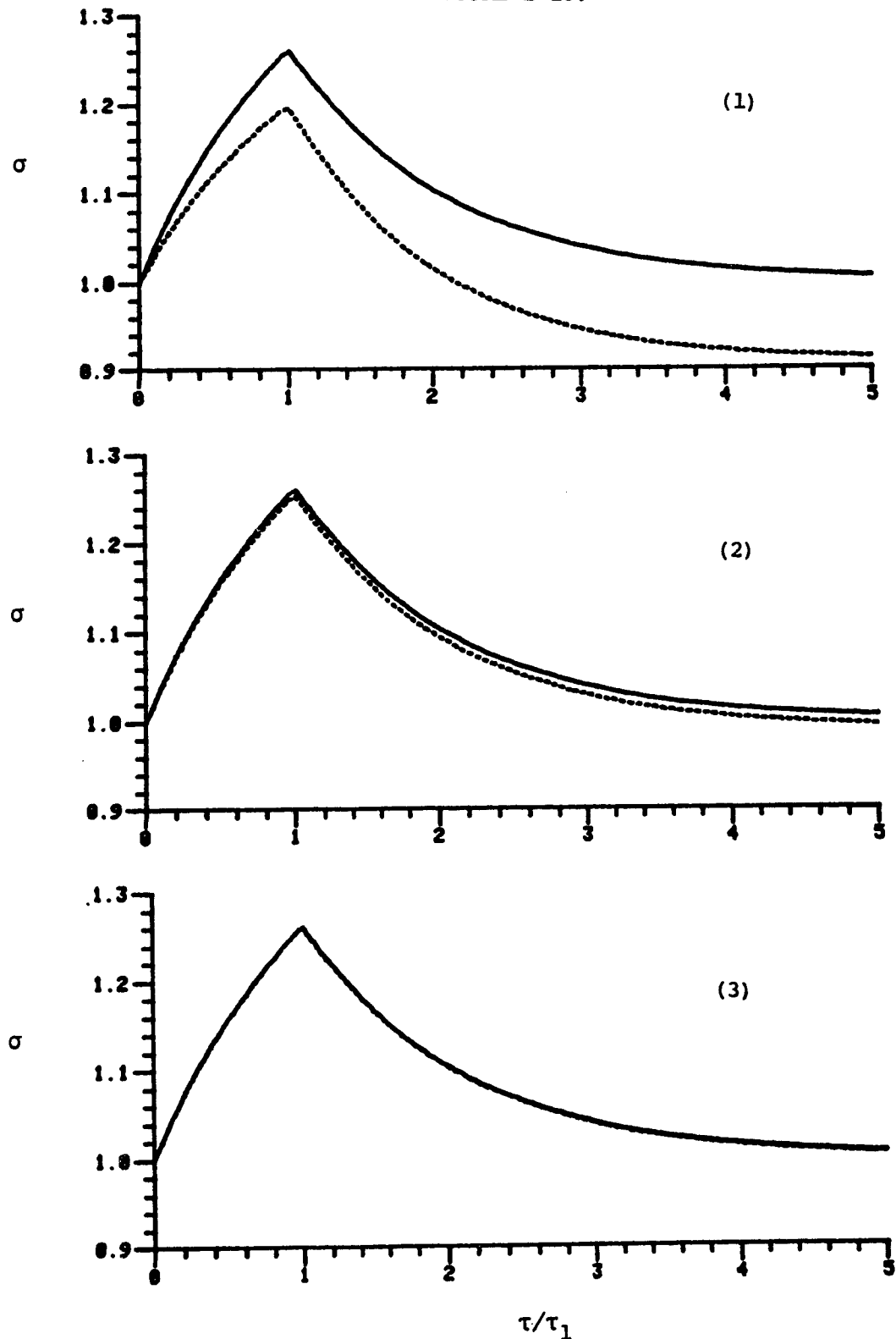
Figure 2-10.

The dynamic behavior of  $\sigma$  during the stationary phase for Michaelis-Menten kinetics with net mass exchange with the environment. The parameters are  $K_{eq} = 1000$ ,  $Q_s = .1$ ,  $\bar{\psi} = .5$  and  $\bar{\sigma} = 1$  and:

- (1)  $St = .1$ ,  $\tau_1 = 45$ ,
- (2)  $St = .01$ ,  $\tau_1 = 413$ ,
- (3)  $St = .001$ ,  $\tau_1 = 4096$ .

A square pulse in the input rate of magnitude .1 and duration  $\tau_1$  is given at time 0. Note that the time is scaled in terms of the slower time constant. The solid line represents the exact solution, the dotted line represents the quasi-equilibrium solution.

FIGURE 2-10.



steady state, the quasi-equilibrium assumption does not relax the dynamics of any particular variable. Rather it assumes that certain algebraic relationship holds, the equilibrium relationship of substrate binding, which does not lead to the correct steady state. However this problem becomes less pronounced as St drops and the quasi-equilibrium solution converges to the exact one.

### 2.6. Discussion and Conclusions.

This chapter discusses Michaelis-Menten kinetics, from a continuum viewpoint, with the particular goals of obtaining additional insight into transients governed by these familiar but intractable equations and finding optimum computational approximations for situations of dynamic importance. Yet another analysis of these much studied equations is justified by their intractability and the large number of parameters contained within them. A judicious combination of scaling and linearization has provided substantial progress towards both goals. The results are valuable both because the approximations represented by the Michaelis-Menten model are often justified in practice and because full numerical solutions are expensive and conceptually unsatisfying: the lack of closed form analytical solutions (Hommes, 1962a, Darvey et al., 1978) has lead enzyme kineticists to seek approximate solutions suitable for the specific conditions of interest to themselves. The success of quasi-stationary analysis of initial

velocity experiments is the prime example. We return to this problem in large part because we are interested in wider ranges of parameter values and process conditions than normally are studied to date.

The first step in our analysis is an improved scaling which not only clearly establishes the number of governing parameters but also collects them into dimensionless ratios of clear physical significance. The dimensionless groups are of two types:

a) kinetic properties,  $St$  and  $K_{eq}$ . The Stickiness number,  $St = k_2/k_{-1}$ , is a ratio of the two breakdown rate constants of the intermediate enzyme complex. This ratio gives us a quantitative measure of the notion of substrate stickiness; if  $St > 1$  the intermediate enzyme complex is more likely to break down to yield the product than the unaltered substrate and then the substrate is said to stick well to the enzyme. Conversely if  $St < 1$  the substrate is more likely to come off the enzyme than be released as product, and then the substrate does not stick well to the enzyme. The second kinetic parameter  $K_{eq}$  is the overall equilibrium constant, a familiar quantity.

b) Two ratios containing concentrations appear,  $Q_s$  and  $M_r$ . The quasi-steady state number,  $Q_s = e_t/K_m$ , is the total enzyme concentration relative to the Michaelis constant. The mass ratio,  $M_r = e_t/s_t$ , is the ratio between the total enzyme concentration and the total substrate concentration.

The second step is linearization about a characteristic steady

state. Even though the linearized model is only an approximation to the exact equations it gives several very important insights into the properties of the full model. In particular it leads to the establishment of two time scales, and a modal analysis that enables us to estimate the dynamic interactions between the concentration species on each time scale. Specifically this approach is useful for at least four purposes;

- a) exploration of dynamic characteristics and their parametric sensitivity,
- b) justification and deeper understanding of approximate solution procedures,
- c) approximation to the transient behavior,
- d) an estimate of the relative magnitudes of the time constants of reaction and diffusion (Appendix A), and
- e) characterization of overall kinetics in terms of temporal moments (see chapter 5).

The linear analysis reveals the fact that there are two quite distinct relaxation times inherent in the dynamic behavior of the reaction, and they are normally well separated for parameter values of physiological importance. Time scale separation effectively results in reduction in the dynamic dimensionality of the system and that is expected increase stability and the intermediary metabolism will have more flexibility in its operation. The extent of this separation seems limited by diffusional constraints, that is, it is

only feasible to have the faster time scale approach the time scale of diffusion, appendix A.

To complete the linear analysis we study the dynamically independent modes of the linearized model. This study reveals that in several limiting cases approximate analytical solutions are possible. If the St number is small, which appears to be the normal situation for metabolic enzymes, a fast mode emerges that represents rapid equilibration of the substrate binding step and the quasi-equilibrium assumption applies. Hence quasi-equilibrium behavior is a result of kinetic properties.

When the Qs number becomes small interactions are reduced; the intermediate complex does not disturb the motion of the substrate, and because of time scale separation  $\chi$  adjusts quickly to any movement of the substrate, hence the quasi-steady state solution is appropriate. The Qs number is condition dependent and the numerical value of this group for conditions for kinetic experiments is small and quasi-steady state analysis holds. However for in vivo situations the Qs number may very well be such that the quasi-steady state solution is highly incorrect.

When the substrate is in the saturation region one-way interactions are observed during the transient phase and one can safely assume that the substrate is stationary during this period. Although this situation is not expected to arise often under in vivo conditions this result is useful in explaining the commonly used  $M_r - e_t/s_t \ll 1$  criterion for the quasi-steady state assumption. The

ratio  $M_r$  is small if both  $Q_s$  small and  $\sigma$  large and then we have two-way decoupling guaranteeing success of both zeroth order singular perturbation solutions and quasi-steady state analysis. However  $M_r$  small is not sufficient we have to have  $e_t \ll K_m \ll s_t$  to produce these decoupling features. As discussed in sections 2.3.5 and 2.4, the criterion  $Q_s$  small is enough to justify the utility of the quasi-steady state solution and the zeroth order outer solution of singular perturbations.

In short the linear analysis presented herein provides new important results with respect to; a) quasi-stationary analysis:

- 1) it leads to a new interpretation of the quasi-steady state assumption (as outlined in section 2.3.5) and gives us the conditions under which it is expected to be applicable, and
- 2) it puts the extension of quasi-stationary analysis via singular perturbations into perspective (as described in section 2.4) and gives us the conditions under which the zeroth order terms in the inner and outer solution expansions are adequate.

and b) the quasi-equilibrium assumption:

it gives a clear understanding of the quasi-equilibrium and under which parameter combinations it is applicable.

For situations where the simplifications discussed above do not apply we propose that a linear solution may be a viable alternative. The applicability of the linear solution for dynamic description rests on two facts. The first one is that the system is weakly

non-linear and the second one is that typical in vivo conditions are such that the reaction operates close to the linear region and we are concerned with modest perturbations from this steady state. Both of these restrictions are independent of any particular dimensionless parameter.

In this chapter we have discussed in some detail the kinetics of the simple Michaelis-Menten reaction mechanism, using continuum approach. The mass action kinetic model discussed, as a representation of both in vivo and in vitro situations, rests on some important simplifying features. First is the important absence of diffusional effects. The fact that diffusion is a little faster than reaction has been discussed in the literature (e. g. Weisz, 1973, Careri, Fasella and Gratton, 1975, Albery and Knowles, 1976, 1977). Our short analysis of the relative time scales of diffusion and reaction, appendix A, indicates that the estimated diffusional distances for the occurrence of diffusional resistance are close to, but longer than, actual in vivo distances.

The second major simplification arises from lumping the reaction mechanism by considering only two reaction steps. A thermodynamic justification for this lumping is found in Albery and Knowles (1976, 1977). These authors basically conclude that the intermediate transformations have evolved to the point where they are faster than the substrate/product association/disassociation steps. This has further been supported by discussion of several enzyme systems by Orsi and Cleland (1972) and Cleland (1975) where the product release

step is found to be rate limiting.

### 2.7. Summary.

As a starting point for modelling of metabolic networks this chapter considers the simple Michaelis-Menten reaction mechanism. After the elimination of diffusional effects a mathematically intractable mass action kinetic model is obtained. The properties of this model are explored via scaling and linearization. The scaling is carried out such that kinetic properties, concentration parameters and external influences are clearly separated. We then try to obtain reasonable estimates for values of the dimensionless groups and examine the dynamic properties of the model over this part of the parameter space.

Linear analysis is found to give excellent insight into reaction dynamics and it also gives a forum for understanding and justifying the two commonly used quasi-stationary and quasi-equilibrium analyses. The first finding is that there are two separate time scales inherent in the model existing over most of the parameter space, and in particular over the regions of importance here. Full modal analysis gives a new interpretation of quasi-stationary analysis, and its extension via singular perturbation theory, and a rationalization of the quasi-equilibrium approximation. The new interpretation of the quasi-steady state assumption is that the applicability is intimately related to dynamic interactions between

the concentration variables rather than the traditional notion that a quasi-stationary state is reached, after a short transient period, where the rates of formation and decomposition of the enzyme intermediate are approximately equal. The modal analysis reveals that the generally used criterion for the applicability of quasi-stationary analysis that total enzyme concentration must be much less than total substrate concentration,  $e_t \ll s_t$ , is incomplete and that the criterion  $e_t \ll K_m \ll s_t$  is the appropriate one. The first inequality ( $e_t \ll K_m$ ) guarantees agreement over the longer time scale leading to quasi-stationary behavior or the applicability of the zeroth order outer singular perturbation solution but the second half of the criterion ( $K_m \ll s_t$ ) justifies zeroth order inner singular perturbation solution where the substrate concentration is assumed to be invariant. Furthermore linear analysis shows that when a fast mode representing the binding of substrate to the enzyme is fast it can be relaxed leading to the quasi-equilibrium assumption.

The influence of the dimensionless groups is ascertained by integrating the equations numerically, and the predictions made by the linear analysis are found to be accurate. Hence the dynamic properties and suitable approximations for a particular enzyme system may be predicted by simply examining the numerical values of the dimensionless groups. Finally it is found that under many in vivo conditions the linearized model can be successfully used to describe the dynamics of the reaction, and it frequently represents the exact behavior better than the widely used quasi-steady state solution.

## CHAPTER 3

## MICHAELIS-MENTEN KINETICS - A REVIEW

The most extensively studied enzymatic reaction model is the Michaelis-Menten mechanism discussed in the previous chapter. Vast amount of mathematical literature on it has accumulated since its formulation in the early 1900's and I shall review these developments in this chapter.

The dynamic description of the Michaelis-Menten kinetics take the form of non-linear differential equations derived from the law of mass action. This description is mathematically intractable (Hommes, 1962a, Darvey et al., 1978), and one is left with numerical techniques as the only alternative for obtaining exact solutions. Furthermore the distribution of relaxation times of these differential equations for typical physical parameters is often wide, resulting in highly stiff characteristics. One way to avoid both these difficulties is by using the quasi-steady state assumption to relax rapid, and hopefully unimportant, dynamics resulting in what is known as steady state kinetics. We begin the survey by discussing the application of the commonly used quasi-steady state assumption and also the quasi-equilibrium assumption in section 3.1.

The earliest experimental evidence concerning the applicability of the quasi-steady state assumption in enzyme kinetics came from a study by Chance (1943). He along with other investigators had developed experimental equipment capable of measuring transient behavior of certain enzymatic reactions. Furthermore Chance computed the entire time course of the concentration of the enzyme intermediate complex using an analog computer. His results, both experimental and computational, showed that in many cases the stationary phase of the reaction is very short and the validity of the stationary analysis is in question. Because of the widespread use of this simplification in data analyses these findings created a strong motivation and need to assess its validity. One cannot of course not obtain exact analytical error bounds, since that would require knowledge about the exact solution which can only be obtained numerically. Instead approximate error bounds can be obtained, or limits on the maximum error introduced. The available material on error analysis for the quasi-stationary treatment is covered in section 3.2.

In addition to the experimental evidence, such as that presented by Chance (1943), the possibility of evaluating the individual rate constants motivated the development of solutions for the transient phase. This is not possible utilizing only steady state kinetics because much of the kinetic information is lumped in constants like the well known Michaelis constant  $K_m$ . In section 3.3 we discuss the attempts made to obtain full or partial transient solutions and then

we discuss how these analyses have lead to improved solutions for the stationary phase in section 3.4.

### 3.1. Simple Approximations.

The Michaelis-Menten reaction mechanism, equation 1 in chapter 2, has the intractable mass action kinetic description, equations 7 and 8 in chapter 2. Simplification is attained by two commonly used approximations; the quasi-steady state and quasi-equilibrium assumption.

#### 3.1.1. The quasi-steady state assumption.

The quasi-steady state assumption (introduced by Bodenstein and Lutkemeyer, 1924) was first applied to the Michaelis-Menten mechanism by Briggs and Haldane (1925). The the quasi-steady state rate law is normally derived by equating the left side of equation 4 in chapter 2 to zero and solving it for  $x_{qss}$ . This gives for the reversible case

$$x_{qss} = \frac{o + \pi}{1 + o + \pi} \quad (1)$$

This expression for the quasi-steady state concentration of the intermediate complex is then substituted into the differential equation either for the substrate giving

$$-\frac{d\sigma}{d\tau} = \frac{d\pi}{d\tau} = \frac{St}{1+St} \frac{\sigma-\pi/St}{1+\sigma+\pi} \quad (2)$$

This equation was first derived by Haldane (1930).

It can immediately be seen that the quantity  $x_{qss}$  is not a truly stationary variable by differentiating equation 1 to get

$$\frac{dx_{qss}}{d\tau} = \frac{1-K_{eq}/St}{(1+\sigma+\pi)^2} \frac{d\sigma}{d\tau} \quad (3)$$

Clearly this derivative is not zero, except for the special case when  $K_{eq} = St$  as we saw in the last chapter. Whether  $x$  decays or builds up during the quasi-steady state phase is dependent on the relative magnitudes of  $K_{eq}$  and  $St$  as this ratio determines the sign of the derivative in equation 3.

For the much studied irreversible case we obtain in an analogous fashion

$$x_{qss} = \frac{\sigma}{1 + \sigma} \quad (4)$$

and

$$-\frac{d\pi}{d\tau} = \frac{d\sigma}{d\tau} = -\frac{St}{1+St} \frac{\sigma}{1+\sigma} \quad (5)$$

which in dimensioned form is

$$-\frac{dp}{dt} = \frac{ds}{dt} = \frac{V_m s}{K_m + s} \quad (6)$$

The two parameters describing the kinetics are; the Michaelis constant,  $K_m = (k_{-1} + k_2)/k_1$ , and the saturation velocity,  $V_m = k_2 e_t$ .

Integration of equation 5 gives

$$\frac{St}{1+St} \tau = s_0 - s + \ln(s_0/s) \quad (7)$$

which is known as the progress curve. Similar results are available for the reversible case Alberty (1959).

This simple mathematical treatment results in equation 5(6) which is the celebrated Michaelis-Menten equation. It has been used extensively to analyse initial rate experiments. Parameter estimation was first carried out by linear transformation of the Michaelis-Menten equation. However today parameter estimation is achieved via least squares techniques using digital computers (Garfinkel, Kohn and Garfinkel, 1977) but linear transformations of enzyme kinetics equations are used for analyzing the data. Parameter estimation for Michaelis-Menten kinetics has recently been reviewed by Atkins and Nimmo (1980).

### 3.1.2. The quasi-equilibrium approximation.

The Michaelis-Menten equation was originally derived using the quasi-equilibrium assumption (Henri, 1903, Michaelis and Menten, 1913). As discussed in chapter 2 by applying this assumption one converts, as for the quasi-steady state assumption, the two differential equations into one differential equation and an algebraic equation which is the equilibrium relationship for the substrate binding step. This results in

$$-\frac{dp}{dt} = \frac{V_m s}{K_s + s} \quad (8)$$

which is the original Michaelis-Menten equation.

This rate law has the exact same functional form as equation 6 but with some important differences.

- 1) The first difference lies in the definition of the lumped kinetic constant  $K_m$ , which under the quasi-equilibrium assumption becomes the equilibrium constant of dissociation for the first step  $K_s = k_{-1}/k_1$ . The ratio between  $K_m$  and  $K_s$  is related to the dimensionless group St by  $K_m/K_s = 1+St$ . Since St is normally small the two constants are essentially identical, Atkinson (1977). As shown in chapter 2 the quasi-equilibrium assumption is applicable if St is small.
- 2) Another important difference is that for in vivo situations the quasi-equilibrium assumption does not give the correct initial conditions which the quasi-steady state assumption does.
- 3) Equation 8 gives the rate of change in the product concentration, not the substrate, whereas under the quasi-steady state assumption the two are given by the same equation, equation 5.

### 3.2. Error Analysis.

The errors introduced by the quasi-steady state assumption are

basically two. The first one arises from the fact that the events during the transient phase are ignored. The criterion for estimating the magnitude of this error is usually that the length of duration of the faster relaxation time is short (Laidler, 1955, Wong, 1965, Schauer and Heinrich, 1979). The other error is the difference between the exact motion and the quasi-steady state motion during the stationary phase. This error is normally assessed by obtaining the maximum difference between these two motions (Wong, 1965, Walter, 1974b, Park, 1974, Heinrich et al., 1977, Schauer and Heinrich, 1979).

### 3.2.1. Analytical error estimation.

Laidler (1955) was the first to attempt quantification of the error introduced by the quasi-steady state assumption. His interesting approach is generalized below to finite values of  $K_{eq}$ .

The differential equation for the enzyme intermediate is factored as

$$\frac{dx}{d\tau} = (x-x_1)(x-x_2) \quad (9)$$

If the value of  $x$  is close to either root,  $x_1$  or  $x_2$  the derivative is expected to be small. Only the smaller root,  $x_2$ , is physically meaningful and by using the results of appendix A one can show that when  $Q_s$  is small

$$\chi_2 \approx \frac{\sigma + \pi}{1 + \sigma + \pi} \quad (10)$$

which is the quasi-steady state value of the enzyme intermediate, in equation 1. The conclusion then is that the quasi-steady state assumption is good when  $Q_s$  is small which is in agreement with the results obtained by linear analysis, chapter 2.

More systematic approaches to the assessment of the errors introduced by the quasi-steady state assumption have been developed by Wong (1965), and Schauer and Heinrich (1979). Wong developed an approximate unified solution to the entire time course of the reaction, see section 3.3, for the irreversible case. His development is really based on decoupling the substrate and the enzyme intermediate via an underlying assumption of time scale separation. In this development the two basic errors are described by the indices  $\delta_c$  and  $\delta_p$ . The first one,  $\delta_c$ , is intended to describe the consequence of omitting the transient phase. It is derived to be

$$\delta_c = e^{-(1+\sigma_0)\tau/Q_s} \quad (11)$$

The time constant is similar to the shorter time constant obtained from linear analysis and forcing  $\delta_c$  to be small is equivalent to forcing the transient phase to be short.

The distance between the quasi-steady state motion and the exact one during the stationary phase is described by the index  $\delta_p$ . Wong presents an estimate of the maximum anticipated magnitude of  $\delta_p$  as  $(\delta_p)_{max} = 4Mr/27$  and thus by keeping the ratio  $Mr (= Q_s/\sigma_0)$  low this

error stays small. This error originates from the assumption that the particular integral is assumed to be the quasi-steady state solution, section 3.3. This same error bound was also derived by Meiske (1978) by a more refined analysis.

The upper bound on  $\delta_p$  was extended to finite values of  $K_{eq}$  by Walter (1974). He concluded that the error is in fact strongly dependent on this parameter. Walter concludes that the error is minimal when  $K_{eq} = St$ . For  $K_{eq} > St$  the error is found to be maximal at  $K_{eq} \rightarrow \infty$  and here the error bound is found to be the same as that of Wong (1965). On the other hand when  $K_{eq} < St$  the bound on  $\delta_p$  is larger and is found to be  $(\delta_p)_{max} = 4MrSt/27K_{eq}$ .

A more detailed error analysis was developed by Schauer and Heinrich (1979). It consists of three error indices. The first two deal with the error associated with ignoring the transient phase, and the third deals with the quasi-steady state movement.

The first index is the relative relaxation deficit,  $\delta_s$  is intended to describe how much the substrate concentration has decreased during the transient phase. The reason for this index is that when enzyme kinetic data is analysed using the quasi-steady state assumption, one uses the initial concentration as an estimate for the substrate concentration at the beginning of the stationary phase. The index is defined as

$$\delta_s = \frac{\sigma_o - \sigma_{o,qss}}{\sigma_o - \sigma_{eq}} = \frac{\Delta\sigma}{\sigma_o - \sigma_{eq}} \quad (12)$$

where  $\Delta\sigma$  is the amount of substrate consumed during the transient

phase, and  $e_{eq}$  is the equilibrium concentration of the substrate. This index should be small so that the initial substrate concentration and that at the beginning of the stationary phase differ insignificantly, and one can be justified in using the initial substrate concentration in the stationary analysis.

The second index, the relative relaxation time  $\delta_t$ , is designed to represent the relative time spans of the transient phase and the stationary phase and it is defined as

$$\delta_t = \frac{\tau_{tr}}{\tau_{relax}} = \frac{\tau_{tr}}{\tau_{tr} + \tau_{qss}} \quad (13)$$

The importance of this index, probably first pointed out by Laidler (1955), has already been discussed during the linear analysis in chapter 2.

The third index, the relative relaxation error,  $\delta_r$ , describes the maximal deviation of the quasi-steady state solution from the exact one during the stationary phase, and it is analogous to the indices of Wong (1965) and Walter (1974). It is defined as

$$\delta_R = \epsilon_{max}/e_t \quad (14)$$

where  $\epsilon_{max}$  is the maximum deviation between the exact and the quasi-steady state trajectories during the stationary phase. The maximal deviation occurs at a point where the motion vector of the exact solution,  $f=(f_1, f_2)$ , is perpendicular to the normal vector  $n$  of the quasi-steady state line, see figure 3-1 for illustration. The estimates of Wong (1965), Walter (1974) and Park (1974), of this

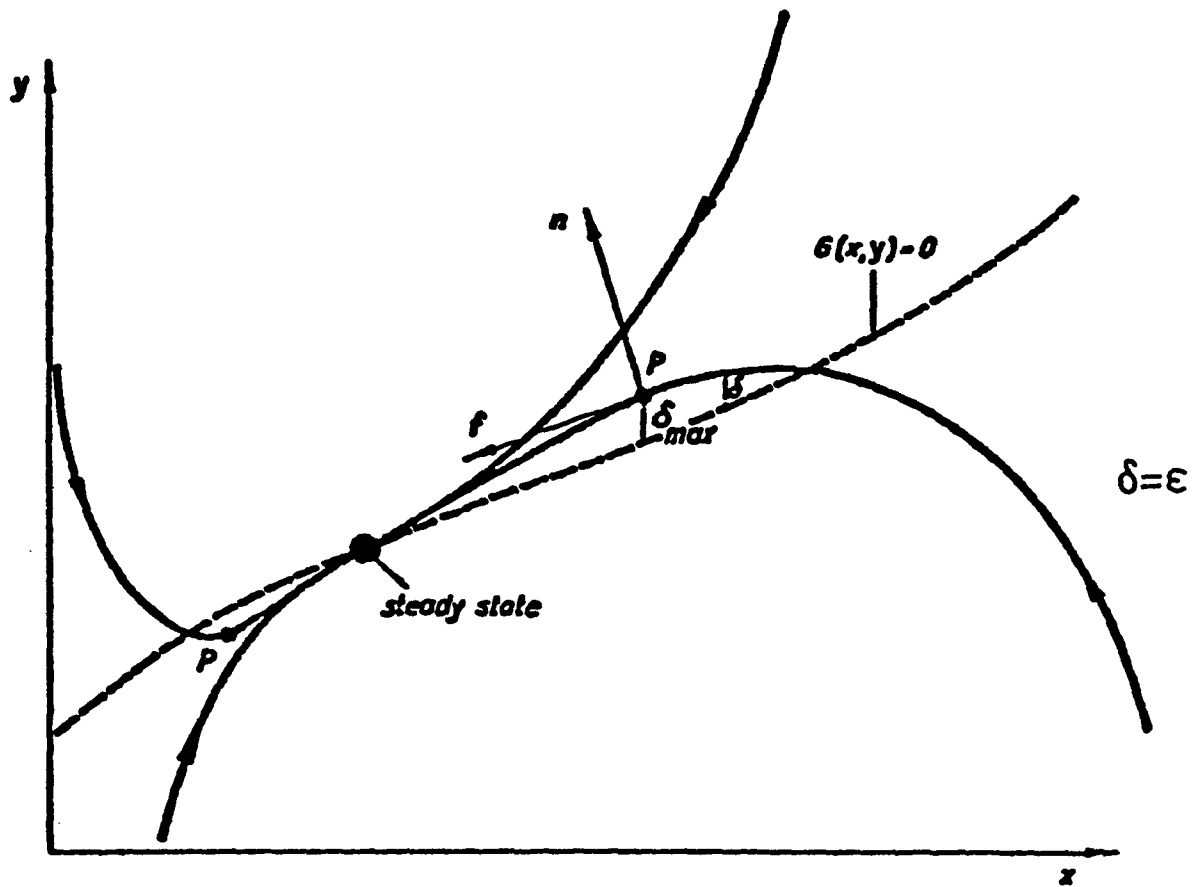


Figure 3-1. Quasi-steady state motion in the phase plane, taken from Heinrich et al. (1977). The vectors are:  $\underline{n}$  the normal vector of the quasi-steady state trajectory,  $\underline{f}$  the motion vector.  $\delta_{\max}$  ( $= \epsilon_{\max}$  of equation 14) is the maximum deviation of the quasi-steady state solution from the exact one during the quasi-stationary phase. Solid line - exact trajectory, broken line - quasi-steady state trajectory.

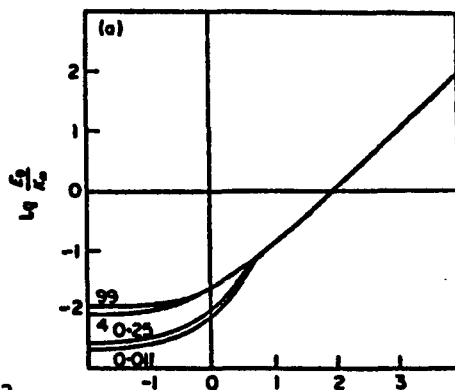
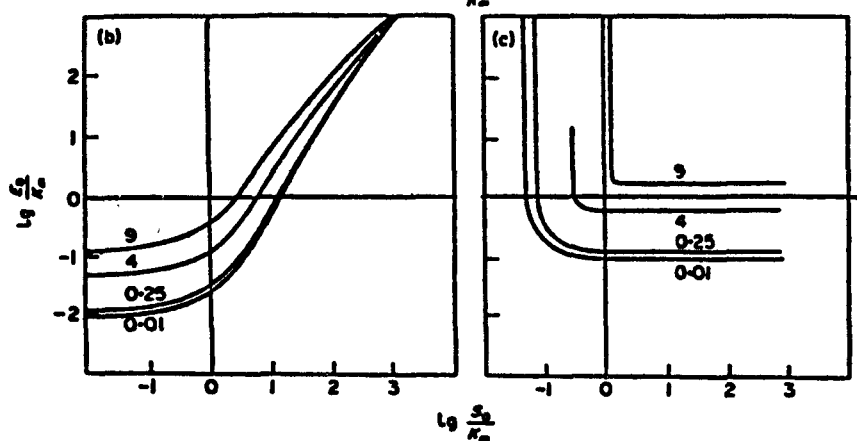
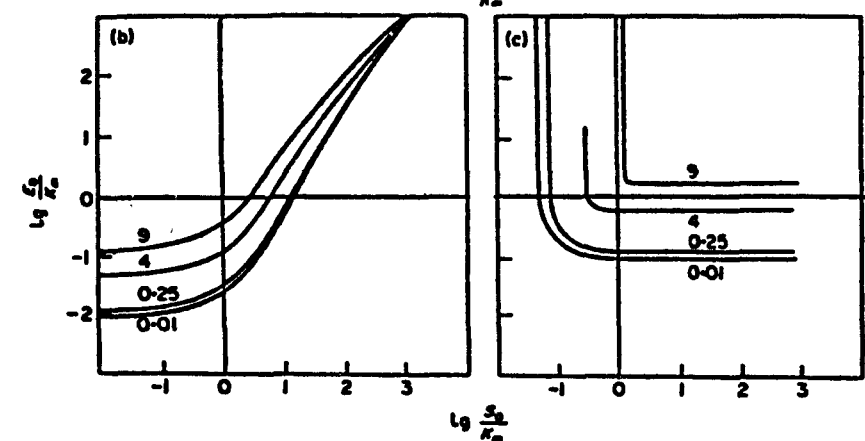
distance may be shown to be special cases of the above treatment (Schauer and Heinrich, 1979), which must be considered as the general case.

Schauer and Heinrich have computed their error indices for the irreversible case. By an approximate solution to the transient phase Schauer and Heinrich are able to estimate  $\tau_{tr}$  as the time at which the stationary solution intersects the approximate solution. This time can then be used as an upper limit in the integration necessary to compute the substrate concentration at the beginning of the stationary phase, and hence  $\delta_s$ . The other time quantity,  $\tau_{qss}$ , they evaluate by integrating the stationary solution between the start of the quasi-steady state phase and equilibrium point. They compute them for different values of St, figures 3-2,3,4,5. Figures 3-2,3,4 shows the three indices in the  $Q_s, \sigma_0$ -plane, and figure 3-5 shows them all simultaneously for St = 4. The hatched region in figure 3-5 is the region where all the indices are less than 1%. One should note that the value of  $k_1$  ( $-10 (\text{Ms})^{-1}$ ) used to compute these figures is low compared to common values (Hammes and Schimmel, 1970).

We note here that these results are in agreement with those obtained from linear analysis (chapter 2). The hatched region in figure 3-5 expands in the direction of  $e_t \ll K_m$  and  $K_m \ll s_t$  which is the same result as given in sections 2.3 and 2.4.

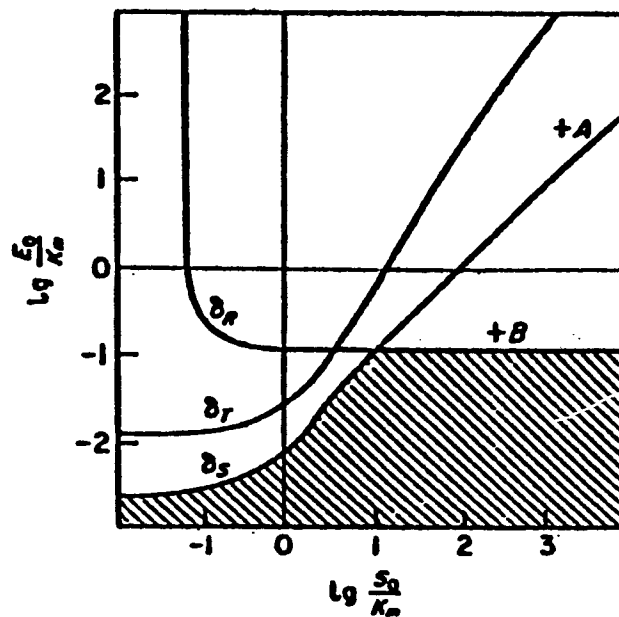
### 3.2.2. Numerical error analysis.

A few authors, Hommes (1962b), Walter and Morales (1964),

FIGURE 3-2.FIGURE 3-3.FIGURE 3-4.

Lines of constant relaxation deficit  $\delta_s = 0.01$  (a), constant relaxation time  $\delta_r = 0.01$  (b) and constant relaxation error  $\delta_r = 0.01$  (c) in the  $S_q, S_r$ -parameter plane. In all diagrams the lines differ by the values of the parameter  $k_{-1}/k_2$ . The other parameters are  $K_m = 1 \text{ mM}$ ,  $k_1 = 1 \text{ mM}^{-1} \text{s}^{-1}$ .

Figures 3-2, 3, 4. Loci of constant relaxation deficit,  $\delta_s$ , relaxation time,  $\delta_t$ , and relaxation error,  $\delta_r$  in the  $S_q, S_r$ -plane. From Schauer and Heinrich (1979).



Range of validity of the quasi-steady state approximation in the  $E_0S_0$ -parameter plane (hatched). The lines correspond to  $\delta_s = \delta_r = \delta_t = 0.01$ . Points  $A$  and  $B$  denote different experimental situations. Parameters:  $K_m = 1 \text{ mM}$ ,  $k_1 = 1 \text{ mM}^{-1} \text{s}^{-1}$ ,  $k_{-1}/k_2 = 0.25$ .

Figure 3-5. The three error criteria,  $\delta_s$ ,  $\delta_t$ , and  $\delta_r$ , in the  $Q_s, E_0$ -plane for  $St = 4$ . Taken From Schauer and Heinrich (1979).

Stayton and Fromm (1979), have addressed the question of the validity of the quasi-steady state assumption from a computational, rather than analytical point of view. The idea is to compute the exact as well as the quasi-steady state solutions under a variety of initial conditions and a wide range of parameter values and compare them. Then general rules, or heuristics, can be developed to assess where the quasi-steady state assumption is applicable. This methodology cannot provide general results as the mathematical approach does, but it offers the advantage of rigor for the cases considered.

Stayton and Fromm (1979) integrated the equations for the Michaelis-Menten mechanism for typical values of initial conditions found in kinetic experiments and for typical values of kinetic parameters. Their findings were that the quasi-steady state assumption is valid over a wide range of parameters, and particular for a set of parameters where the maximum error bounds of Wong (1965) and Walter (1974) predicted possible large errors. Hence they concluded that the error bounds developed to date are not tight enough.

### 3.3. Transient Solutions.

Several authors have developed full or partial transient solutions to the Michaelis-Menten equations. The main motivation, from a practical point of view, was the possibility of estimating the individual rate constants. Several approximate solutions to the

kinetic equations have been developed and we shall review them below.

A) through D) represent approximate solutions to the transient phase and E) through G) contain attempts to obtain full transient solutions.

A). Assuming the substrate to be constant during the transient phase (Roughton, 1954, Gutfreud, 1955, Swoboda, 1957b). One assumption is to consider the substrate concentration, and product concentration if non-zero, to be constant and equal to their initial values. This is the assumption used to obtain the zeroth order inner solution in the framework of singular perturbation theory, see section 2.4 and item F) below.

Under this assumption the differential equation for the enzyme complex becomes

$$\frac{dx}{d\tau} + \left(\frac{1+a_0}{Qs}\right)x = \frac{a_0}{Qs} \quad (15)$$

This is a linear first order differential equation which is immediately integrable yielding

$$x = \frac{a_0}{1+a_0} \left(1 - e^{-\left(\frac{1+a_0}{Qs}\right)\tau}\right) \quad (16)$$

for the intermediate and for the product one obtains

$$\pi - \pi_0 = \left(\frac{St}{1+St}\right) \left(\frac{a_0}{1+a_0}\right) \left(\tau + \frac{Qs}{1+a_0} \left(e^{-\left(\frac{1+a_0}{Qs}\right)\tau} - 1\right)\right) \quad (17)$$

The exponent contains only steady state parameters in addition to  $K_m$ .

Thus if the time constant can be estimated  $k_1$  can be evaluated, Guntfreund (1955). Swoboda (1957a) extended this discussion and shows how the pre-steady state phase can be used to estimate all the individual rate constants.

B). Ignoring the second order terms in the product (Morales and Goldman, 1955, Swoboda 1957b). The simplicity of the differential equations for the irreversible case allow for combination of the two into a non-linear second order differential equation

$$Qs \frac{d^2\theta}{d\tau^2} + (1+Qs+\theta) \frac{d\theta}{d\tau} + \left(\frac{St}{1+St}\right)\theta + Qs(1+1/St)\left(\frac{d\theta}{d\tau}\right)^2 = 0 \quad (18)$$

Where a new variable  $\theta = \sigma_0 - \pi$  has been defined for convenience. This equation was first presented by Swoboda (1955) and Morales and Goldman (1955). This particular equation was demonstrated to be mathematically intractable by Hommes (1962a).

Removing the second order terms in the product ( $\pi d\pi/d\tau = (d\pi/d\tau)^2 = 0$ ) in equation 18 gives

$$\frac{d^2\theta}{d\tau^2} + \left(1 + \frac{1+\sigma_0}{Qs}\right) \frac{d\theta}{d\tau} + \frac{1}{Qs} \left(\frac{St}{1+St}\right)\theta = 0 \quad (19)$$

This second order linear differential equation is readily integrated. Using the initial conditions  $\theta = \sigma_0$ ,  $d\theta/d\tau = 0$  at  $\tau = 0$  the solution is

$$x = \left(\frac{1+St}{St}\right) \left(\frac{\sigma_0}{m_2 - m_1}\right) (e^{m_2 \tau} - e^{m_1 \tau}) \quad (20)$$

$$\pi = \frac{\theta_0}{m_1 - m_2} (m_1(1 - e^{-m_2 \tau}) - m_2(1 - e^{-m_1 \tau})) \quad (22)$$

where

$$m_1, m_2 = -\frac{1+Qs+\theta_0}{2Qs} \pm \sqrt{\left(\frac{1+Qs+\theta_0}{2Qs}\right)^2 - \frac{1}{Qs} \left(\frac{St}{1+St}\right)} \quad (22)$$

C). Treating  $\bar{\theta} = \theta_0 - \pi$  as a constant during the transient phase (Laidler, 1955). This assumption implies that little product is formed during the transient phase, and the substrate being consumed binds to the enzyme. This can be seen by rewriting the substrate mass balance as

$$\bar{\theta} = \theta_0 - \pi = s + Qsx = \text{constant} \quad (23)$$

Under this assumption the equation for the enzyme complex becomes

$$\frac{dx}{d\tau} = x^2 - \left(1 + \frac{1+\bar{\theta}}{Qs}\right)x + \frac{\bar{\theta}}{Qs} \quad (24)$$

This equation is separable and can be integrated to give

$$\pi - \pi_0 = \frac{St}{1+St} \left( (m_1 + m_2)\tau + \frac{1}{m_2 - m_1} \ln \left( \frac{m_2 + m_1 e^{(m_2 - m_1)\tau}}{m_1 + m_2 e^{(m_1 - m_2)\tau}} \right) \right) \quad (25)$$

where

$$m_1, m_2 = -\frac{1+\bar{\theta}}{2Qs} \pm \sqrt{\left(\frac{1+\bar{\theta}}{2Qs}\right)^2 - \frac{1}{Qs} \left(\frac{St}{1+St}\right)} \quad (26)$$

D). Successive approximations, Schauer and Heinrich (1979). In search for a transient solution to compute their error indices,

discussed in the last section, these authors apply the method of successive substitutions, also known as Picard's method, to obtain a description of the transient phase. The first approximation gives the same solution as derived by Swoboda (1957a). An algebraic expression is obtainable for the second approximation, but beyond that the procedure becomes necessarily numerical.

E). Decoupling by assuming a form of a particular solution, Wong (1965). Wong's development was the first attempt to obtain an explicit integral description of the entire course of the reaction. His approach is basically based on time scale separation and really involves splicing together the transient solution, under item A above, and the quasi-stationary solution.

He writes the differential equation for the intermediate complex as

$$\left(\frac{Qs}{1+\sigma}\right) \frac{dx}{d\tau} + x = \frac{\sigma}{1+\sigma} \quad (27)$$

which can be viewed as a linear differential equation with non-constant coefficients. The solution to 27 can be written as a sum of the solution of 27 and its homogeneous equivalent as  $x = x_c + x_p$ , where  $x_c$  is the complimentary function and  $x_p$  is the particular integral. The homogeneous equation has a solution

$$x_c = A \exp\left(-\int_0^\tau \left(\frac{1+\sigma}{Qs}\right) d\tau\right) \quad (28)$$

If we assume that the complementary function has vanished when

the stationary phase is reached, leaving  $x = x_p$ , the particular solution can then be approximated as the steady state solution

$$x_p = \frac{\sigma}{1+\sigma} \quad (29)$$

and the solution becomes

$$x = \frac{\sigma}{1+\sigma} - \frac{\sigma_0}{1+\sigma_0} \exp\left(-\int_0^{\tau} \left(\frac{1+\sigma}{Qs}\right) d\tau\right) \quad (30)$$

using the initial conditions  $\sigma = \sigma_0$ .

Under condition such that the substrate concentration does not deviate substantially from its initial value the exponent may be approximated as

$$\int_0^{\tau} \frac{1+\sigma}{Qs} d\tau \approx \left(\frac{1+\sigma_0}{Qs}\right)\tau \quad (31)$$

Substituting this expression into equation 30 will yield a solution which is effectively a combination of the solution discussed under item A) above and the quasi-steady state solution. This development provided the first unified treatment of both the transient and stationary phases, and yields a solution that gives a continuous change from the transient phase into the stationary phase, figure 3-6.

F). Solution by singular perturbation theory Heineken et al., (1967). The concept of a quasi-steady state in kinetic reaction mechanism becomes particularly clear in the context of the mathematical technique of singular perturbations (Bowen et al., 1963). This technique involves an expansion of the solution into a

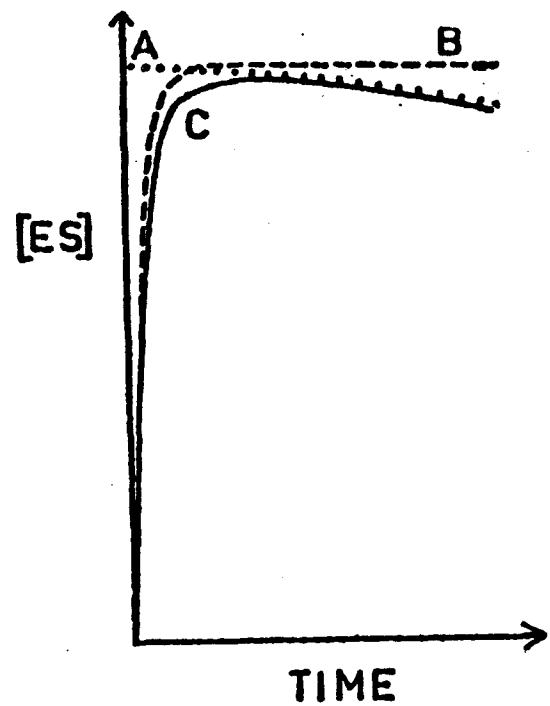


Figure 3-6. The unified solution, Wong (1965), to Michaelis-Menten kinetics. A the quasi-steady state solution, B the transient solution, and C the unified solution. Taken from Wong (1965).

series in a small parameter  $\eta$ , known as the perturbation parameter. For chemical kinetics the problem may be formulated such that the first term in the series, called the zeroth order outer solution, is in fact the quasi-steady state solution (Bowen et al., 1963, chapter 2). This technique has been applied to the Michaelis-Menten reaction scheme (Heineken et al., 1967, Lin and Segal, 1974 and Meikse 1978) giving valuable information about the stationary phase.

Heineken et al., (1967) derived solutions both for transient phase (the "inner" solution) and the stationary phase (the "outer" solution) using this method. They use  $\eta = Mr$  as their perturbation parameter. The mathematical details of this work are considerable, and they will not be belabored here. We note though that the solution derived for the transient phase is separate from the solution to the stationary phase. This separation is based on time scale separation. Their numerical results are shown in figures 3-7,8. Here they have chosen  $\sigma_0 = K_m$  so  $\eta = Qs$ . These results show the solution series converges rapidly to the exact solution. Even for  $Qs = 1$ , only two terms are needed to obtain adequate representation. Their zero order solution corresponds to Wong's (1965) unified treatment.

A more general perturbation solution was presented by Meiske (1978). He used  $\eta = Qs St/1+St$  as his perturbation parameter and could thus include the quasi-equilibrium condition. This development is very valuable since, as we shall see in the following section, it can be used to establish how stationary rate laws converge to the

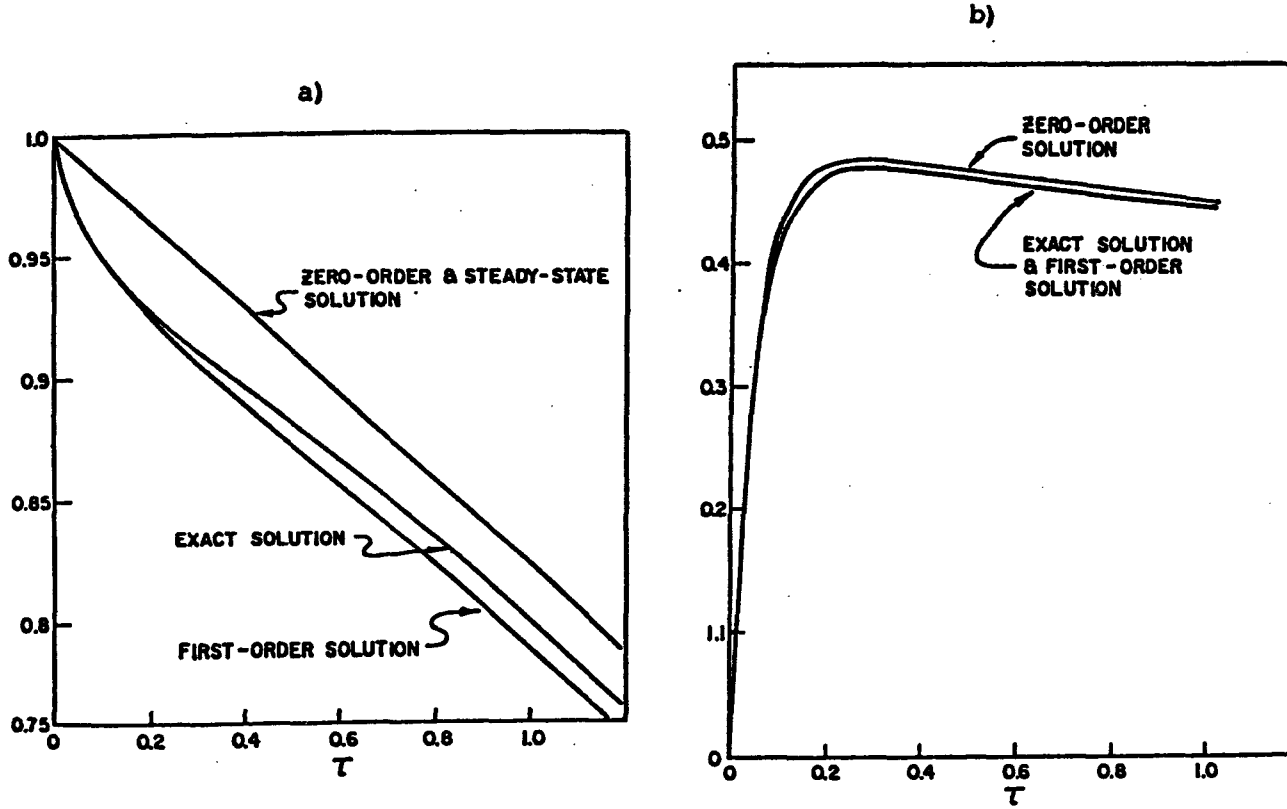


Figure 3-7. The singular perturbation solution for  $Q_s = .1$ , a) the substrate concentration profile, b) the intermediate enzyme concentration profile. Taken from Heineken et al. (1967).

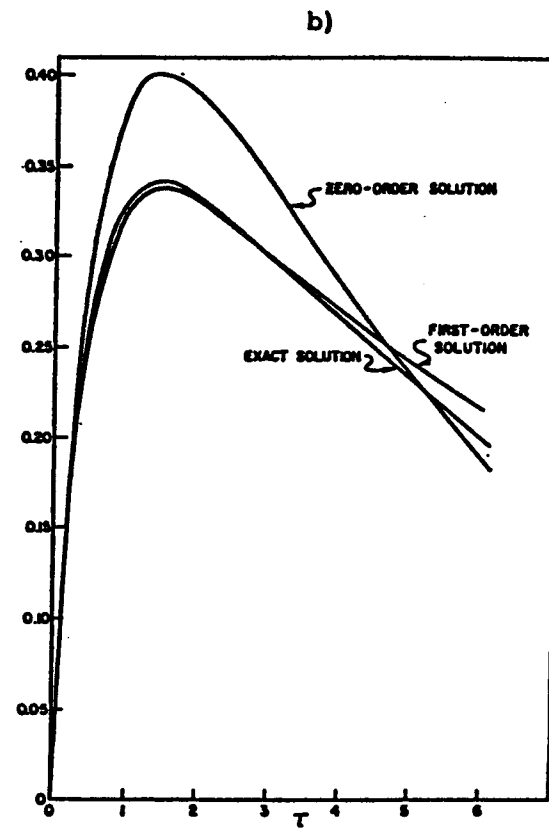
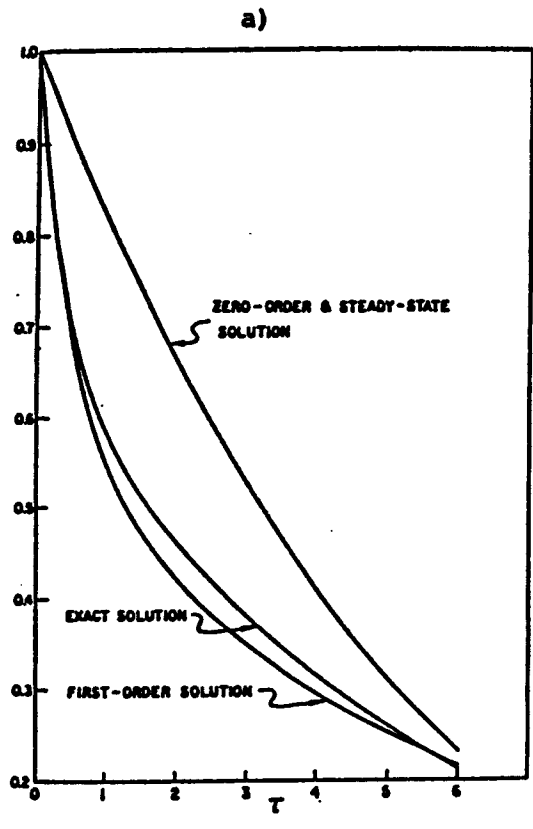


Figure 3-8. The singular perturbation solution for  $Q_s = 1$ , a) the substrate concentration profile, b) the intermediate enzyme concentration profile. Taken from Heineken et al. (1967).

exact solution under both the quasi-steady state assumption and the quasi-equilibrium assumption. Other asymptotic expansion type solutions have appeared, Yang (1953), Mathua (1971), Ingetik, Deakin and Fandry (1981), Ingetik and Deakin (1981), but a uniformly valid expansions have not been derived.

G). Assuming a two term solution (Otten, 1974). The idea of Wong to write the solution as a sum of two terms, a transient term and a term solely dependent on the concentration was further explored and refined by Otten (1974). He assumes a solution of the form  $a(\tau) + b(\sigma)$  and derives differential equations for each function. The equation for  $a(\tau)$  can be integrated, section 3.4. Otten proves that a function  $b(\sigma)$  exists that satisfies all the imposed conditions. However an explicit form for  $b(\sigma)$  is not presented.

Otten derives an asymptotic expansion of the solution when  $Q_s/(a_0 + 1)$  is small. This corresponds to the situation where the transient phase is short and an explicit form for  $b(\sigma)$  can be obtained. As we will see in the following section this results in a stationary solution that is an improvement over the Michaelis-Menten equation.

### 3.4. Improved stationary solutions.

As discussed earlier the quasi-steady state assumption provides a relief from the stiffness of the differential equations describing

the Michaelis-Menten reaction mechanism, and greatly improves computing efficiency. To correct the error introduced by the quasi-steady state assumption one can add correction terms to compensate for the error. Such correction terms arise from error analysis or from asymptotic expansions such as those discussed above. Several such error terms have been developed for the irreversible Michaelis-Menten mechanism, and we shall discuss them in chronological order below.

A). Perturbation solution of Heineken et al., (1967). In this development, the stationary solution, or the outer solution, is written as an expansion with  $M_r$  as the perturbation parameter. The zeroth order solution,  $\sigma_{MM}$ , is the solution obtained from the quasi-steady state treatment, or the progress curve of equation 7. The first order term is given explicitly in terms of  $\sigma_{MM}$  as

$$\sigma_1 = \frac{\sigma_0 \sigma_{MM}}{1 + \sigma_{MM}} \left( \frac{1}{1 + St} \ln \left( \frac{(1 + \sigma_{MM}) \sigma_0}{(1 + \sigma_0) \sigma_{MM}} \right) - \frac{1}{1 + St} + \sigma_0 \right) \quad (32)$$

which gives the improved solution  $\sigma(t) = \sigma_{MM} + \eta\sigma_1$ .

B). The error analysis of Vergonnet and Berendsen (1970). These authors obtain a first order correction term to the quasi-steady state solution by considering piecewise linear treatment. When it is applied to the Michaelis-Menten mechanism for the irreversible case in a closed system one obtains (Meiske, 1978),

$$-\frac{d\sigma}{d\tau} = \left(\frac{St}{1+St}\right)\left(\frac{\sigma}{1+\sigma}\right)\left(1 - \frac{Qs}{(1+\sigma)^2}\right) \quad (33)$$

clearly as  $Qs \rightarrow 0$  this equation converges to the original Michaelis-Menten equation.

C). The improved stationary solution of Otten and Duysens (1973). If the time derivative of the intermediate enzyme complex concentration is set to zero the stationary rate law is obtained. However that is not exact and the derivative is close to zero. Otten and Duysens postulate that by setting

$$\frac{dx}{d\tau} = \frac{dx_{QSS}}{d\tau} \quad (34)$$

rather than equating  $dx/d\tau$  to zero, a more accurate rate expression should result. By applying this postulate they obtain (Meiske, 1978)

$$-\frac{d\sigma}{d\tau} = \left(\frac{St}{1+St}\right)\left(\frac{\sigma}{1+\sigma}\right)\left(1 + \frac{Qs}{(1+\sigma)^2}\right)^{-1} \quad (35)$$

This expression reduces to the Michaelis-Menten if  $Qs \rightarrow 0$ . Otten and Duysens provide no justification for their postulate, but a justification may be found in the more general framework of Hirschfelder (1957).

D). The asymptotic solution of Otten (1974). Otten has developed a solution approach to the irreversible case as discussed in the next section. His solution is in terms of an asymptotic series and is hard to write out explicitly, except in special cases.

Otten considers the case when  $Qs/(a_0 + 1) \ll 1$ . For this special case he derives the following solution for the stationary phase

$$-\frac{da}{d\tau} = \left( \frac{St}{1+St} \right) \left( \frac{a}{1+a} \right) \left( 1 - \frac{Qs(1+St)a-1}{(1+St)(1+a)^2 a} \left( 1 - \sum_{n=1}^{\infty} \frac{1}{(1+a)^n} \right) \right) \quad (36)$$

The first term in the series is the Michaelis-Menten equation. The remaining terms make up an expression that must be considered an improvement over the Michaelis-Menten equation, under the limiting conditions where  $Qs/(a_0 + 1)$  is small.

E). Unified treatment of Meiske (1978). Meiske analyses the irreversible Michaelis-Menten mechanism in the context of singular perturbation theory. He chooses the perturbation parameter,  $\eta = QsSt/(1+St)$ , which allows him to treat quasi-steady state and quasi-equilibrium at the same time. This is due to the fact that if  $Qs \rightarrow 0$ , quasi-steady state is reached, but quasi-equilibrium if  $St \rightarrow 0$ . He uses his approach to derive two stationary laws. One is the same as the one of Otten and Duysens (1973) and the other does not have an explicit form.

Meiske's unified treatment enables him to compare the convergence of the various improved stationary rate laws to the exact solution. From his analysis Meiske concludes that

$$a_{MM} < a_{MI} < a < a_{OD} < a_{VB} \quad (37)$$

Where MI refers to Meiske's second improved solution,  $a$  is the exact solution, and OD and VB refer to the solution of Otten and Duysenes,

and Vergonet and Berendsen respectively. Furthermore Meiske shows that

$$\sigma_{MM}, \sigma_{VB} \rightarrow \sigma \text{ when } Q_s \rightarrow 0 \quad (38)$$

which corresponds to quasi-steady state, and

$$\sigma_{MI}, \sigma_{OD} \rightarrow \sigma \text{ when } n \rightarrow 0 \quad (39)$$

which corresponds to quasi-equilibrium or quasi-steady state. The solutions  $\sigma_{MI}$  and  $\sigma_{OD}$  must therefore be considered as more general solutions. This is an important development since one can compare the convergence to the exact behavior under both assumptions.

F). Applying a method by Hirschfelder (1957). Hirschfelder developed a technique to improve stationary solutions in chemical kinetics. It is based on a similar idea to the one of Otten and Duysens discussed under item C), but it has a more rigorous foundation. It involves higher and higher derivatives of the stationary solution in an infinite expansion of the exact solution during the quasi-steady state phase. I have applied this method to the Michaelis-Menten mechanism and obtained the first approximate solution

$$x_1 = \frac{\sigma}{1+\sigma} \left( 1 - \frac{St}{1+St} \frac{Q_s}{(1+\sigma)^3} \right) \quad (40)$$

-----

Examining the improved solutions above one can see that for all

of them, we have that

$$-(\frac{d\alpha}{d\tau})_{MM} > -(\frac{d\alpha}{d\tau})_{improved} \quad (41)$$

holds. This implies that the stationary treatment of the irreversible Michaelis-Menten reaction mechanism overestimates the derivative. This can be shown to be the case by differentiating the mass balance on the substrate species to give

$$-\frac{d\alpha}{d\tau} = \frac{d\pi}{d\tau} + Q_s \frac{dx}{d\tau} < \frac{d\pi}{d\tau} = -(\frac{d\alpha}{d\tau})_{MM} \quad (42)$$

The derivative  $dx/dt$  is assumed to be zero in the stationary treatment. However it is not identically zero, leading to overestimation of the substrate consumption since  $x$  is a decaying variable during the stationary phase and its derivative is less than zero. The fact that the improved solutions converge to the exact ones in the limit  $Q_s \rightarrow 0$  is in agreement with the results from the linear analysis in chapter 2.

## CHAPTER 4

## DYNAMIC BEHAVIOR OF SIMPLE HOMOTROPIC ENZYMES

A unique property of biochemical reactions is cooperative kinetic behavior. This feature arises from homotropic interactions between reaction sites on the enzyme molecule: the binding of a substrate molecule to one site induces a conformational change in the enzyme molecule that in turn alters the kinetic properties of the other sites. This interaction can be positive or negative, that is increasing or decreasing respectively the activity of other sites.

In this chapter we focus our attention on the dynamic properties of cooperativity. According to our modelling philosophy we exercise parsimony and we begin by considering the simplest situation possible in an attempt to extract the salient features: we consider the simplest homotropic cooperative enzyme. It is a dimeric enzyme with identical but interacting sites where each site follows a reaction mechanism identical to the irreversible Michaelis-Menten reaction scheme. This model, a simple extension of the two-site Adair model (Adair, 1925) to account for catalysis, is the simplest possible cooperative enzyme both to mathematically and conceptually. It has been the subject of steady state analysis (Volkenstein and Goldstein,

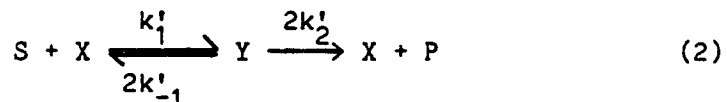
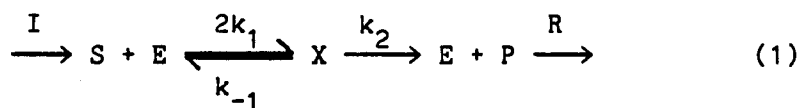
1966, Volkenshtein, 1969, Rubinow 1975, Rubinow and Segel, 1981 and Lane, 1982) and we shall expand on these studies to investigate dynamic behavior.

We proceed much as for the single-site Michaelis-Menten mechanism (chapter 2), and we start by developing a mass action kinetic model which we then scale to define essential parameters in the form of dimensionless property ratios. The characteristics of the model are then explored via linearization and full modal analysis. The dependence of the relaxation times and the modes of the linearized system on the dimensionless groups are given particular attention as they have been found to give excellent predictions of dynamic behavior for the Michaelis-Menten mechanism (chapter 2). The limit of independent sites, where the dimer is identical to a pair of independent Michaelis-Menten enzymes, forms the basis for our analysis. Then we extend the investigation from this well characterized base case into the regions of the parameter space where cooperativity exists to explore the effects of interactions between the sites.

#### 4.1. Development of a Kinetic Model.

##### 4.1.1. The reaction mechanism.

The system considered is a simple extension of the two-site Adair model accounting for chemical transformation as



which represent a simple dimeric enzyme, with identical but dependent reaction sites. This mechanism accounts for the reversible binding of a substrate (S) to the free enzyme (E) which forms the intermediate complex (X). This complex can break down to form the product (P) and regenerate the free enzyme (E), as in the Michaelis-Menten reaction mechanism; alternatively it can bind reversibly to a second substrate molecule to form another intermediate complex (Y) which carries two substrate molecules. The catalytic properties of the intermediate X are different than of the free enzyme E because the attached substrate molecule alters enzyme conformation. The exchange of mass with the surroundings is via the influx (I) of substrate to the reaction zone and removal (R) of product. The rate constants used here are intrinsic ones, that is they are properties of the individual sites, as supposed to the phenomenological rate constants used by some authors.

This dimeric model is the simplest scheme incorporating cooperativity. The next level of complexity is to make the two reaction sites non-identical which introduces several additional parameters (e. g. Rubinow and Segel, 1981), a complication we can do without since, as we shall see below, the number of parameters is already high and data justifying such complexity seems non-existent.

#### 4.1.2. Kinetic description.

The simple dimeric model has five chemical species (S,E,X,Y and P). We are interested in situations where the enzyme is contained within the boundaries of the system and hence a mass balance on the enzyme species holds

$$e_t = e + x + y \quad (3)$$

where  $e_t$  is the total enzyme concentration and the lower case letters denote the concentration of the species denoted by the corresponding upper case letter. A mass balance on the substrate species is

$$s_t = s + x + 2y + p \quad (4)$$

The total concentrations of substrate,  $s_t$ , may change with time because of imbalances in I and R, but since the breakdown step is irreversible such changes will not effect the dynamics of S, X and Y and this mass balance can be used to compute the product concentration. Hence the number of concentration variables we need to consider is three and the mass action kinetic model for the dimeric enzyme takes the form

$$\frac{ds}{dt} = -2k_1 e_t s + k_{-1} x + 2k'_{-1} y + (2k_1 - k'_1) sx + 2k_1 sy + I \quad (5)$$

$$\frac{dx}{dt} = 2k_1 e_t s - (k_{-1} + k_2)x + 2(k'_{-1} + k'_2)y - (k'_1 - 2k_1)sx - 2k_1 sy \quad (6)$$

$$\frac{dy}{dt} = -2(k'_{-1} + k'_2)y + k'_1 sx \quad (7)$$

on choosing S, X and Y as the three independent variables.

#### 4.1.3. Scaling.

We choose as scaled variables

$$\sigma = \frac{s}{K_m} \quad x = \frac{x}{2e_t} \quad \gamma = \frac{y}{2e_t} \quad \epsilon = \frac{e}{2e_t} \quad \pi = \frac{I}{K_m} \quad (8)$$

$$\psi = \frac{I}{2e_t k_2} \quad \tau = 2e_t k_1 t$$

where  $K_m = (k_{-1} + k_2)/k_1$  is the well known Michaelis constant. By introducing these dimensionless variables the model in scaled form is

$$\frac{d\sigma}{d\tau} = -\sigma + \frac{\chi + 2BiAf\gamma}{1+St} + (2-Bi)\sigma\chi + 2\sigma\gamma + \frac{St}{1+St}\psi \quad (9)$$

$$Qs \frac{d\chi}{d\tau} = \sigma - \chi + 2BiMi\gamma - (Bi+2)\sigma\chi - 2\sigma\gamma \quad (10)$$

$$Qs \frac{d\gamma}{d\tau} = -2BiMi\gamma + Bi\sigma\chi \quad (11)$$

with the mass balances

$$\sigma + Qs(\chi + 2\gamma) + \pi = \frac{Qs}{Mr} \quad (12)$$

$$\epsilon + \chi + \gamma = 1/2 \quad (13)$$

This scaling is closely related to that used for the Michaelis-Menten equations except we use twice the total enzyme concentration, or the concentration of reaction sites, whenever the enzyme concentration is introduced. In addition the variable Y ( $\gamma$ ) appears along with and two sets of kinetic constants, one set for each reaction site.

#### 4.1.4. The dimensionless groups.

Three dimensionless groups appearing, the "Stickiness number", the "Mass ratio" and the "Quasi-steady state number"

$$St = \frac{k_2}{k_{-1}} \quad Mr = \frac{2e_t}{s_t} \quad Qs = \frac{2e_t}{K_m} \quad (14)$$

are similar to those introduced for the Michaelis-Menten reaction mechanism (chapter 2). However, three additional groups are needed to express the cooperativity properties of the system. These are the "Binding number", the "Affinity ratio" and the "Acceleration number" defined as

$$Bi = \frac{k'_1}{k_1} \quad Af = \frac{K'_s}{K_s} = \frac{k'_{-1}/k'_1}{k_{-1}/k_1} \quad Ac = \frac{k'_2}{k_2} \quad (15)$$

respectively. These three numbers allow us to express in a compact format the different types of cooperativity that can occur.

- (1) The Binding number ( $Bi$ ) is a measure of the altered velocity at which the substrate binds to X. Positive cooperativity is observed if  $Bi$  is in excess of unity, and negative cooperativity for  $Bi < 1$ .

(2) The Affinity ratio (Af) is a measure of relative magnitudes of the disassociation constants  $K_s$  and hence it is a measure of the relative affinity of the substrate for the two binding sites. If the binding of substrate to X is thermodynamically more favorable than to the free enzyme E then Af is less than unity and positive cooperativity is observed.

(3) The Acceleration number (Ac) is a measure of how much faster the Y form catalyses chemical transformation, than the X form, that leads to the product formation. If it is in excess of unity the cooperativity is positive in this step.

Another, mathematically redundant, but useful dimensionless groups is

$$M_i = \frac{K'_m}{K_m} = \frac{Af + AcSt/Bi}{1 + St} \quad (16)$$

$M_i$  is the ratio between the  $K_m$  values for a reaction site on the free enzyme ( $K_m$ ) and for a altered site on X ( $K'_m$ ) and we call it the "Michaelis number". It is not independent of the other groups but is defined here for mathematical convenience. If no reaction takes place ( $k_2 = k'_2 = 0$ ) then  $M_i = Af$  which is the case for proteins that only associate with ligands, such as Hemoglobin and Calmodulin.

Numerical ranges for the dimensionless groups. The model has five concentration variables ( $\sigma$ ,  $\epsilon$ ,  $\chi$ ,  $\gamma$  and  $\pi$ ) and six dimensionless property ratios (St, Qs, Mr, Bi, Af and Ac): eleven quantities in all. Five equations (9) - (13) describe the model, and hence the model has six independent parameters which we choose to be ( $\sigma$ , St,

$Q_s$ ,  $B_i$ ,  $A_f$ ,  $A_c$ ). It is clearly necessary to restrict discussion to limited ranges of each! For the first three we can obtain reasonable estimates of probable in vivo values:  $\sigma \in [.1-1]$ ,  $S_t \in [10^{-4}, 10^{-2}]$ ,  $Q_s \in [10^{-2}, 1]$  (Srere, 1967, 1970, Hammes and Schimmel, 1971, Segel, 1975 and Atkinson, 1977).

For the rest,  $A_f$ ,  $A_c$  and  $B_i$ , the discussion is necessarily somewhat speculative. The affinity ratio for the binding of  $O_2$  to Hemoglobin in sheep can be estimated from the data of Roughton, Deland, Kernohan and Severinghaus (1972) and the calculation of the Adair equilibrium constants by Rubinow (1975). The affinity ratios for consecutive binding of  $O_2$  are .195 (site 1 to 2), 4.52 (site 2 to 3) and .0023 (site 3 to 4).

#### 4.1.5. The non-cooperative dimer.

In the absence of cooperative behavior the cooperativity numbers  $B_i$ ,  $A_f$  and  $A_c$  assume values of unity. The mass action kinetic model is then

$$\frac{d\sigma}{dt} = -\sigma + \frac{\chi+2Y}{1+St} + (\chi+2Y)\sigma + \frac{St}{1+St}\psi \quad (17)$$

$$Q_s \frac{dx}{dt} = \sigma - \chi + 2Y - 3\sigma\chi - 2\sigma Y \quad (18)$$

$$Q_s \frac{dY}{dt} = -2Y + \sigma\chi \quad (19)$$

Inspection of these equations reveals that a lumped variable  $\tilde{x} = x + 2Y$  appears naturally, and it arises because the kinetic behavior of

the two intermediates is identical. Introducing  $\tilde{x}$  into equations 17 to 19 reduces the kinetic description to

$$\frac{d\sigma}{dt} = -\sigma + \frac{\tilde{x}}{1+St} + \sigma\tilde{x} + \frac{St}{1+St}\psi \quad (20)$$

$$Qs \frac{d\tilde{x}}{dt} = \sigma - \tilde{x} - \sigma\tilde{x} \quad (21)$$

These equations are identical to those for a simple Michaelis-Menten enzyme. This familiar system thus represent the non-cooperative limit and forms a natural basis for discussion.

#### 4.1.6. Solution strategies.

This mass action kinetic model is unfortunately mathematically intractable, but its properties can be explored by approximate mathematical analysis and exact numerical solutions. Below we start out by discussing the stationary solution. Then we go on to explore the dynamic behavior of the dimeric enzyme. First we apply the commonly used quasi-stationary analysis in which the dynamics are simplified by considering only the motion of the substrate. This method is incomplete and of yet unknown validity, but it can be extended by the use of singular perturbations as has been done successfully for the Michaelis-Menten reaction (Heineken, Tsuchiya and Aris, 1967, Lin and Segel, 1974, and Meiske, 1978). Secondly we apply full linear analysis examining both relaxation times as well as the relationship between the modes of the linear description to species concentrations. As for the Michaelis-Menten mechanism this

analysis is useful for organizational and exploratory purposes and for instance tells us when the quasi-steady state and quasi-equilibrium approximations are expected to give good results.

#### 4.2. The Stationary Point.

The stationary state is obtained by equating the left-hand sides of equations 13 to 15 to zero. This leaves us with a set of non-linear algebraic equations which fortunately can be solved explicitly to give

$$\bar{x} = \frac{\bar{a}}{1 + 2\bar{a} + \bar{a}^2/M_i} \quad (22)$$

$$\bar{y} = \frac{\bar{a}^2/2M_i}{1 + 2\bar{a} + \bar{a}^2/M_i} \quad (23)$$

$$\bar{\psi} = \frac{(1 + A_{co}/M_i)\bar{a}}{1 + 2\bar{a} + \bar{a}^2/M_i} \quad (24)$$

where the overbar denotes steady state conditions. We note here that the steady state solution depends only on two dimensionless groups  $M_i$  and  $A_{co}$  and therefore the steady state analysis permits the magnitudes of these two. The  $M_i$  number represents a combination of dimensionless groups which can not be individually identified from steady state experiments only. This is a general limitation of steady state analysis.

The cooperative case. The steady state solution can display

sigmoidal dependence of flux on substrate concentration. The inflection point, found by equating the second derivative of  $\bar{\Psi}$  with respect to  $\bar{a}$  to zero, occurs at

$$(2Ac-1)\bar{a}_{infl}^3 + 3Ac\bar{a}_{infl}^2 + 3Mi\bar{a}_{infl} + Mi(2Mi - Ac) = 0 \quad (25)$$

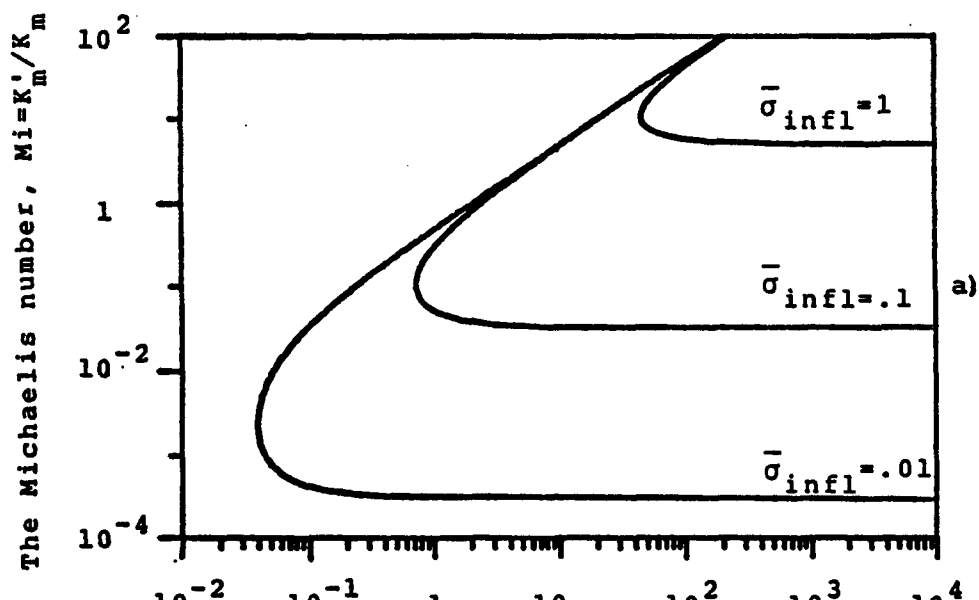
By setting  $\bar{a}_{infl} = 0$  in equation 25 we obtain a bound on the region in the  $Mi, Ac$ -plane, figure 4-1, for sigmoidal behavior which is observed when  $Ac \leq 2Mi$ . For the non-reactive case this condition translates to  $Af \leq 2$  for sigmoidal behavior, which is the same result as obtained by Rubinow and Segel (1981). Hence positive cooperativity does not necessarily lead to an S-shaped initial rate curve.

A maximum appears in equation 24 as negative cooperativity in the chemical transformation step, characterized by  $Ac < 1$ , increases. This maximum occurs for  $Ac < .5$  at a substrate concentration given by

$$\bar{a}_{max} = \frac{1}{1-2Ac}(Ac + \sqrt{Ac^2 - 2MiAc + Mi}) \quad (26)$$

The maximum, figure 4-2 zero  $Mi$  numbers for  $Ac = .5$  and moves rapidly to finite values as  $Ac$  decreases below .5. The appearance of this maximum corresponds to substrate inhibition at substrate concentrations above  $\bar{a}_{max}$ . The dynamic implications of a such maximum are discussed below.

The non-cooperative case. In this limit the steady state equations are the same as for the Michaelis-Menten mechanism.



The acceleration number,  $Ac = k_2'/k_2$

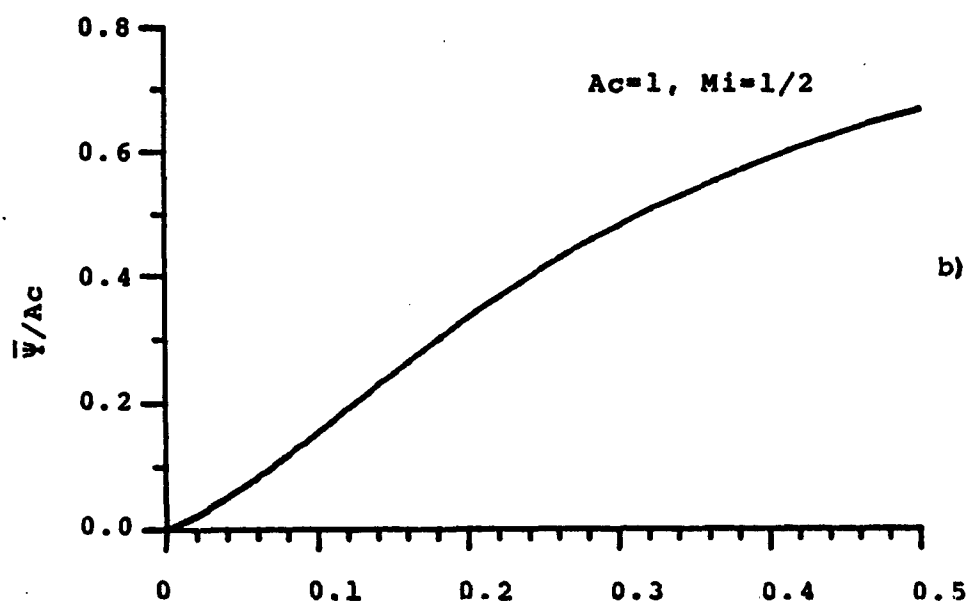


Figure 4-1. The stationary solution to the dimeric model and the location of the inflection point:  
 a) loci of inflection point for initial rate curves in the  $Ac, Mi$ -plane,  
 b) example of a sigmoidal initial rate curve for  $Ac = 1$  and  $Mi = .5$ .

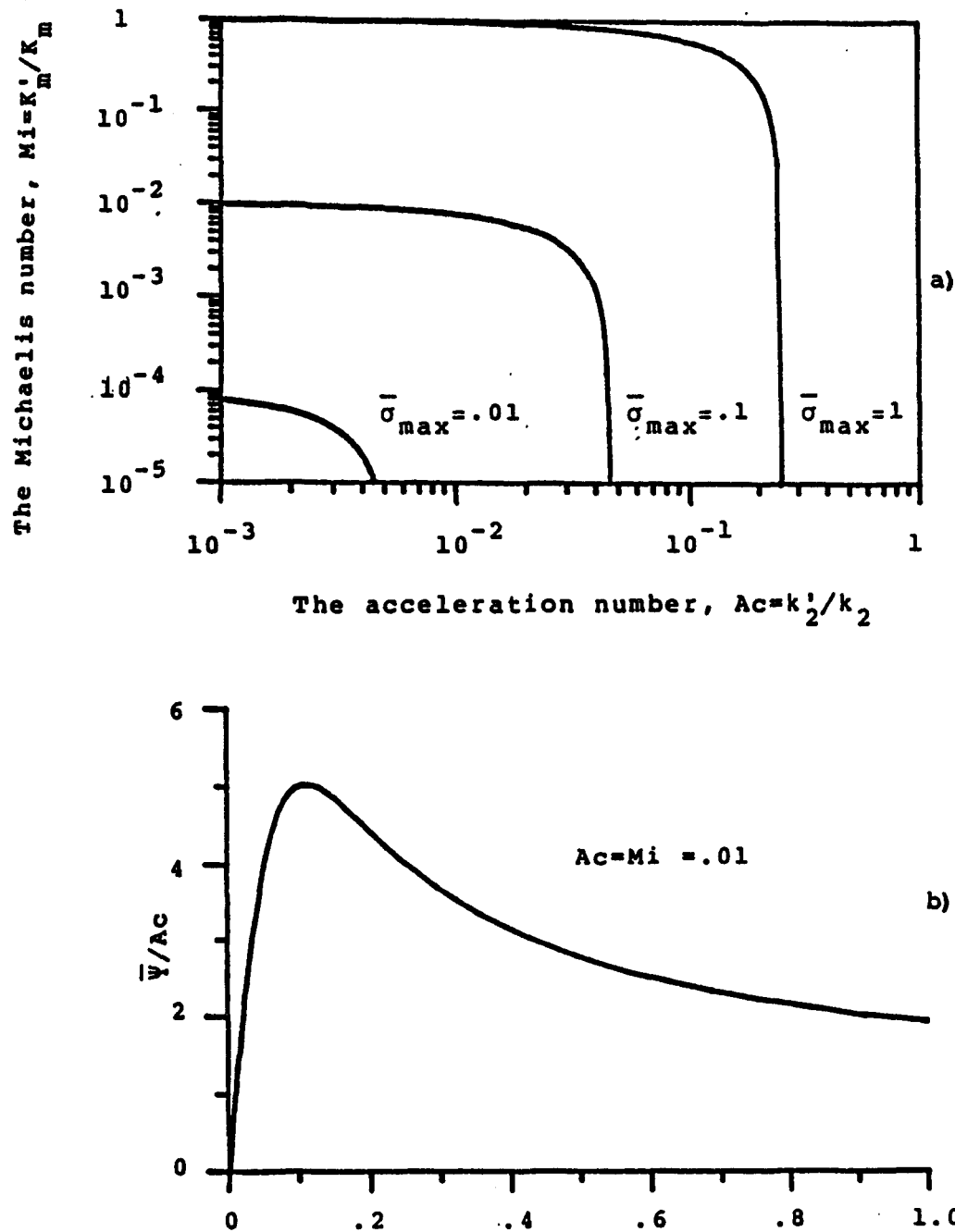


Figure 4-2. The stationary solution for the dimeric model and maximum flux rates:

a) loci of maximum values for the initial rate curves in the  $Ac, Mi$ -plane,  
 b) example of an initial rate curve with a maximum rate,  $Ac = Mi = .01$ .

#### 4.3. Quasi-steady State Analysis.

The most commonly used simplification of enzyme kinetic descriptions is the quasi-stationary analysis which is based on the assumption that rates of formation and decomposition of the intermediates become effectively equal after a short transient period. The transients of the intermediates are then relaxed; that is their rates of change can be neglected.

The cooperative case. For the dimeric reaction mechanism under study equations 10 and 11 are converted to algebraic equations and solved explicitly for the quasi-stationary concentrations of the intermediates as

$$x_{qss} = \frac{\sigma}{1 + 2\sigma + \sigma^2/M_i} \quad (27)$$

$$y_{qss} = \frac{\sigma^2/2M_i}{1 + 2\sigma + \sigma^2/M_i} \quad (28)$$

These equations are then substituted into equation 9 to give a single differential equation that describes the motion of the substrate as

$$\frac{d\sigma}{d\tau} = - \frac{St}{1+St} \left( \frac{(1+A\sigma/M_i)\sigma}{1+2\sigma+\sigma^2/M_i} - \psi \right) \quad (29)$$

One must then integrate this equation for a given forcing function  $\psi$ . In general this must be done numerically but for closed systems,  $\psi = 0$ , the integration can be achieved analytically yielding the so-called progress curve:

$$\frac{St}{St+1}(\tau_0 - \tau) = \frac{\sigma_0 - \sigma}{Ac} + \ln\left(\frac{\sigma}{\sigma_0}\right) + \left(\frac{Mi(2-1/Ac)-Mi}{Ac}\right)\ln\left(\frac{Aco/Mi+1}{Aco_0/Mi+1}\right) \quad (30)$$

Quasi-stationary analysis is thus capable, where applicable, of yielding an extra parameter, St, for a total of three, compared with two obtainable from steady state analysis.

The non-cooperative dimer. Equations 29 and 30 reduce to the hyperbolic rate law and the progress curve for Michaelis-Menten kinetics if  $Mi = Ac = 1$ .

-----

The quasi-stationary analysis gives a simplified one-dimensional dynamic description of the intractable mass action kinetic model. It is not, however, immediately clear where in the parameter space and why the quasi-stationary analysis gives an accurate solution. Furthermore its physical meaning is somewhat ambiguous. It has, however, been extensively utilized in the analysis of kinetic experiments and to simulate metabolic networks. The linear analysis introduced below will be seen to resolve these ambiguities.

#### 4.4. Linear Analysis.

As found earlier for single-site Michaelis-Menten enzymes (chapter 2) full linear analysis has been shown to give a useful complete description of system dynamics as well as means for

determining the parameter ranges over which the quasi-stationary approach is appropriate. More particularly it enables us to identify where in the parameter space the following features are found:

- 1) Well separated eigenvalues. This separation implies the existence of multiple time scales, and it also means that the differential equations are stiff and difficult to treat numerically.
- 2) Limited species interaction. This condition is met when the modal matrix has a row containing one element much larger than all the other elements in that row, and a mode of the linear system approximates a species concentration.
- 3) Complex eigenvalues. If complex eigenvalues exist the reaction can exhibit damped oscillatory behavior.

We will be particularly interested in the regions where 1) and 2) occur simultaneously since then the approximate quasi-stationary analysis is applicable (section 2.3).

#### 4.4.1. Linearization of the dimeric model.

We begin as in chapter 2 by linearizing equations 9 to 11 to obtain

$$\frac{dx'}{dt} = J_3 \underline{x}' + \underline{\psi} \quad (31)$$

with a Jacobian matrix

$$J_3 = \begin{bmatrix} \frac{-(1+Bi\bar{\sigma})}{1+2\bar{\sigma}+\bar{\sigma}^2/Mi} & \frac{1}{1+St} + (2-Bi)\bar{\sigma} & 2\left(\frac{BiAf}{1+St} + \bar{\sigma}\right) \\ \frac{(1-Bi\bar{\sigma})}{Qs(1+2\bar{\sigma}+\bar{\sigma}^2/Mi)} & -\frac{1 + (Bi+2)\bar{\sigma}}{Qs} & \frac{2(BiMi-\bar{\sigma})}{Qs} \\ \frac{Bi\bar{\sigma}}{Qs(1+2\bar{\sigma}+\bar{\sigma}^2/Mi)} & \frac{Bi\bar{\sigma}}{Qs} & -\frac{2BiMi}{Qs} \end{bmatrix} \quad (32)$$

and the state,  $\underline{x}' = \underline{x} - \bar{\underline{x}}$  ( $\underline{x} = (\sigma, x, \gamma)^T$ ), and flux,  $\underline{\psi}' = \underline{\psi} - \bar{\underline{\psi}}$  ( $\underline{\psi} = (St\Psi/(1+St), 0, 0)^T$ ), vectors, which are in terms of deviation variables from steady state,  $\bar{\underline{x}}, \bar{\underline{\psi}}$ , about which the equations have been linearized. We now examine the dynamic behavior of the simple dimeric model by examining the properties of the Jacobian matrix.

#### 4.4.2. The eigenvalues.

The eigenvalues of the 3x3 Jacobian are given as the roots of the characteristic equation

$$\lambda^3 - S_1\lambda^2 + S_2\lambda - S_3 = 0 \quad (33)$$

where the  $S_i$ 's are the sums of the determinants of the principal minors. One can show, for  $Ac > .5$ , that all the coefficients in equation 33 are positive and hence the real parts of the eigenvalues are negative. The implications are that no dynamic instabilities can arise under these conditions. The principal eigenvalue can become real positive when  $Ac$  is less than one-half and this means that the system is unstable and runs away from the stationary point. This happens when the steady state is chosen to the right of the maximum

in figure 4-2b. One can intuitively visualize such behavior because, if the substrate concentration is higher than  $\bar{o}_{\max}$ , then the reaction rate decreases with increasing substrate concentration. This will lead to a buildup of substrate, unless the reaction is regulated by some other means.

We will now look at the effects of the cooperativity parameters and in particular at the ways in which they change the behavior of the base case of independent sites.

The non-cooperative dimer. Here the description reduces to two independent variables, equations 20 and 21. The linearized form of this 2x2 system has a Jacobian matrix

$$J_2 = \begin{bmatrix} -\frac{1}{1+\bar{o}} & \frac{1}{1+St} + \frac{\bar{o}}{\bar{o}} \\ \frac{1}{Qs(1+\bar{o})} & -\frac{1+\bar{o}}{Qs} \end{bmatrix} \quad (34)$$

with eigenvalues

$$\lambda_1, \lambda_2 = \frac{\text{tr}(J_2)}{2} \left( 1 \pm \sqrt{1 - \frac{4\det(J_2)}{\text{tr}^2(J_2)}} \right) \quad (35)$$

where

$$\text{tr}(J_2) = -\left(\frac{1}{1+\bar{o}} + \frac{1+\bar{o}}{Qs}\right) \quad (36)$$

$$\det(J_2) = \left(\frac{1}{Qs}\right)\left(\frac{1}{1+\bar{o}}\right)\left(\frac{St}{1+St}\right) \quad (37)$$

All the properties of this 2x2 system are identical to the linearized version of the Michaelis-Menten mechanism, see chapter 2.

The cooperative dimer. General expressions for the roots of third order polynomials are available (e. g. Spiegel 1968) but the complexity of the algebra involved in the case under study here discourages a general analytical treatment. The eigenvalues are of course readily obtained numerically.

We have found a region of complex eigenvalues, figure 4-3, which shows a qualitative departure from the properties of the Michaelis-Menten mechanism. In this region of complex eigenvalues the possibility of damped oscillatory behavior arises. To assess the seriousness of these damped oscillations we rewrite the characteristic equation as

$$(\lambda - \lambda_2)(\lambda^2 + 2(\xi\sqrt{\lambda_1\lambda_3})\lambda + \lambda_1\lambda_3) = 0 \quad (38)$$

This factoring is possible since the equation has always one real root. In our case the principal eigenvalues can become complex and the real root always represents a fast motion. The damping factor  $\xi$  is a measure of the relative size of the real and imaginary part of the complex root. If  $\xi$  is less than unity the roots are complex and as it approaches zero the roots become purely imaginary (a detailed discussion on the effects of  $\xi$  on dynamic behavior is found in e. g. Coughanowr and Koppel (1965)). We have found that this parameter is never less than about .7, which means that serious damped oscillations will not appear.

#### 4.4.3. The normal modes.

The modes of a linear system move independently of each other

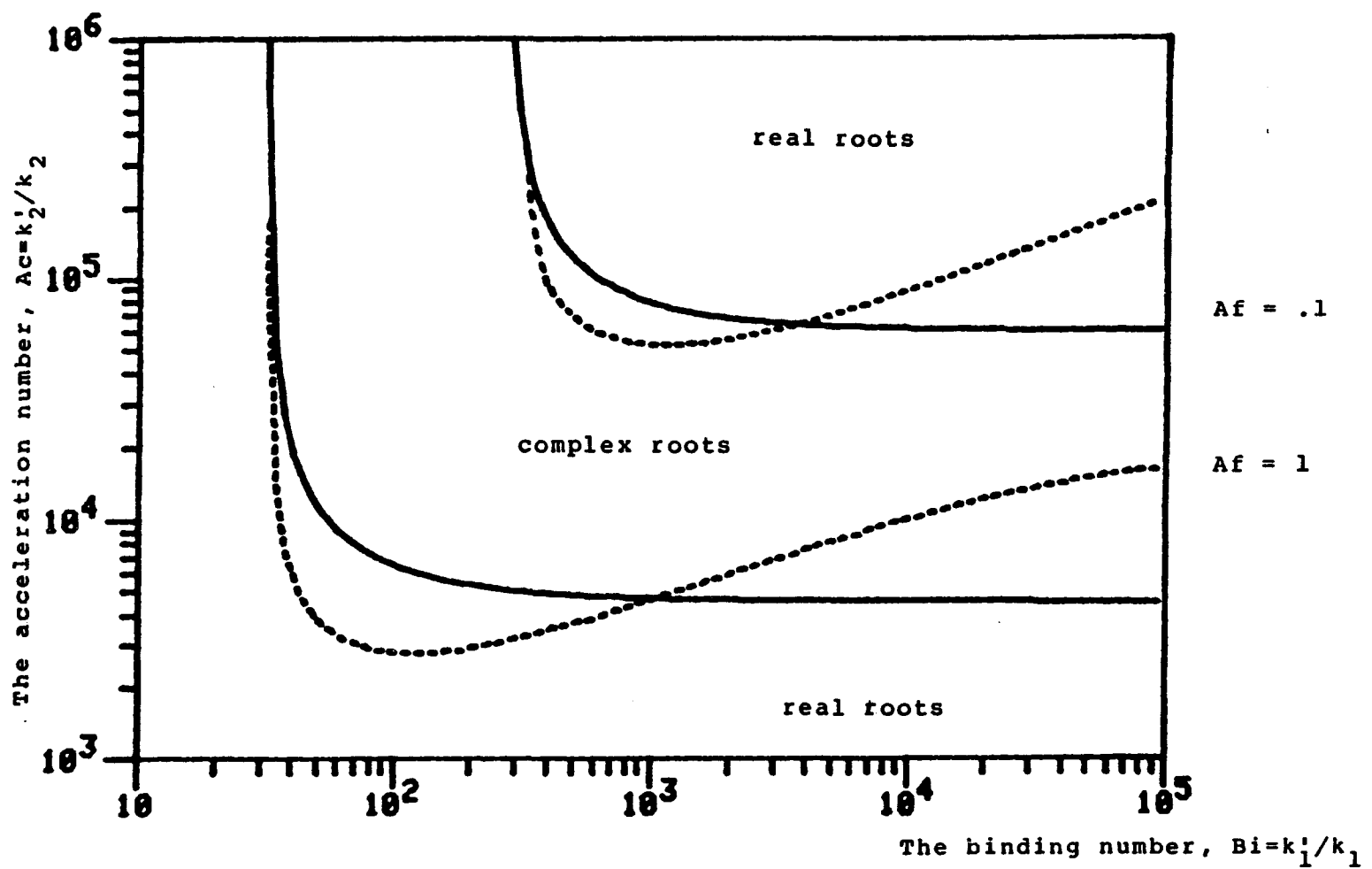


Figure 4-3. Regions of complex eigenvalues in the  $Bi, Ac$ -plane. Complex eigenvalues exist between the curves shown, 1) solid curve  $Af = 1$ , and 2) dotted curve  $Af = .01$ . The other parameters are  $St = .01$ ,  $Qs = .1$ ,  $\bar{\sigma} = 1$ .

and on time scales defined by the eigenvalues. They are related to the original variables by a matrix  $M^{-1}$  as  $\underline{m} = M^{-1}\underline{x}'$  where the vector  $\underline{m}$  contains the modes. The matrix  $M^{-1}$  is comprised of the eigenrows as  $M^{-1} = (\underline{u}_1, \underline{u}_2, \underline{u}_3)^t$  where  $\underline{u}_i$  are the eigenrows. The eigenrows are defined by  $\underline{u}_i(J - \lambda_i I) = \underline{0}$  or

$$(u_{i1}, u_{i2}, u_{i3}) \begin{pmatrix} j_{11} - \lambda_i & j_{12} & j_{13} \\ j_{21} & j_{22} - \lambda_i & j_{23} \\ j_{31} & j_{32} & j_{33} - \lambda_i \end{pmatrix} = \underline{0} \quad (39)$$

Only two of these three equations are independent, and if we choose the first two

$$\begin{aligned} u_{i1}(j_{11} - \lambda_i) + u_{i2}j_{21} + u_{i3}j_{31} &= 0 \\ u_{i1}j_{12} + u_{i2}(j_{22} - \lambda_i) + u_{i3}j_{32} &= 0 \end{aligned} \quad (40)$$

we can obtain  $u_{i2}$  and  $u_{i3}$  in terms of  $u_{i1}$  as

$$u_{i2} = \frac{(\lambda_i - j_{11})j_{32} + j_{31}j_{12}}{\lambda_i j_{31} + j_{21}j_{32} - j_{22}j_{31}} u_{i1} \quad (41)$$

$$u_{i3} = \frac{\lambda_i^2 - (j_{11} + j_{22})\lambda_i + j_{11}j_{22} - j_{12}j_{21}}{\lambda_i j_{31} + j_{21}j_{32} - j_{22}j_{31}} u_{i1} \quad (42)$$

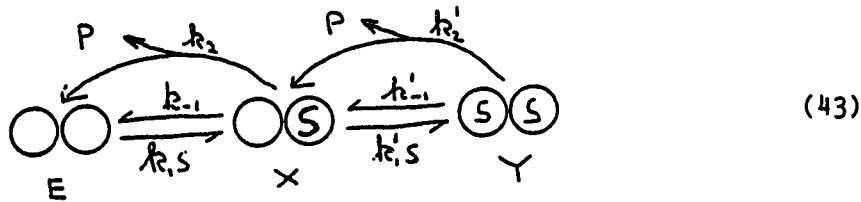
Only the direction of  $\underline{u}_i$  is defined, but the length is arbitrary.

Here we scale an eigenrow to the maximum element in each row,

i. e.  $u_{ij} \rightarrow u_{ij}/(u_i)_{\max}$  where  $(u_i)_{\max} = \max_j(u_{ij})$ , since that will give a coefficient of unity for the dominant variable in each mode and smaller coefficients for the variables contributing less.

The non-cooperative dimer. Again this limit is analytically manageable and it was found (chapter 2) that at low St numbers a slow mode appears which physically represents a quasi-equilibrium behavior for the binding step of the reaction. If the Q<sub>S</sub> number is lowered the intermediate substrate complex becomes a fast decoupled variable and this corresponds to a quasi-steady state behavior for the intermediate.

The cooperative dimer. We are now in a position to examine the three kinds of cooperativity on the dynamics of the reaction. The simultaneous consideration of the modes and the time constants provides an excellent way to interpret the dynamic behavior of the homotropic dimer. Figures 4-4, 4-6, 4-7 and 4-8 show how the elements of the modal matrix  $M^{-1}$  and the time constants  $\tau_i$ 's change with the cooperativity numbers. To facilitate interpretation of these graphs we write the reaction mechanism in the useful form



We now examine the effects of the departure of the three cooperativity groups from unity.

(a) Effects of Bi. The modal matrix and the time constants are shown in figure 4-4 as a function of Bi. During this calculation we keep Af constant so that the net result is that the ratio between  $k_1'$  and  $k_{-1}'$  is a constant but they both grow large (small) if Bi grows large

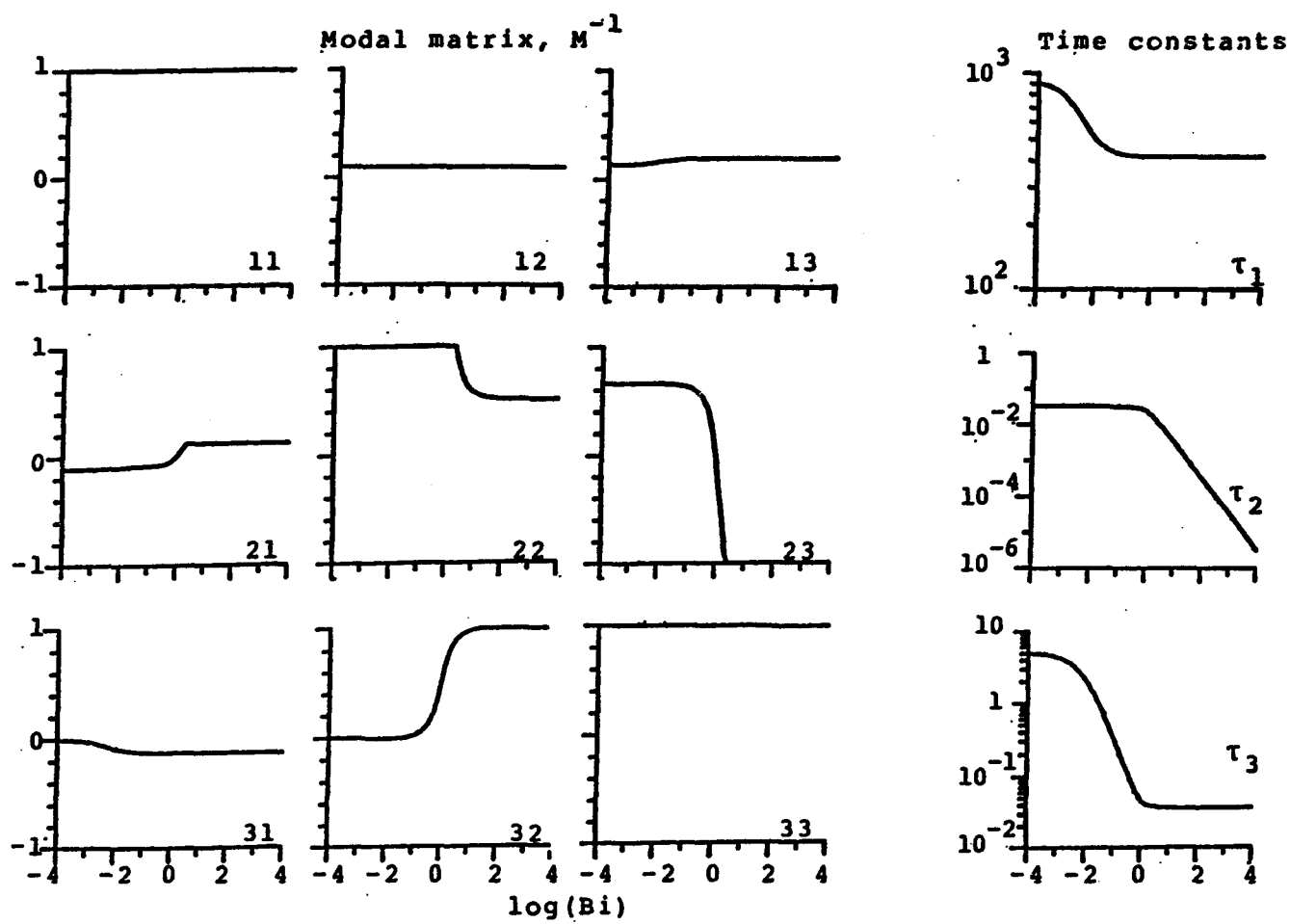
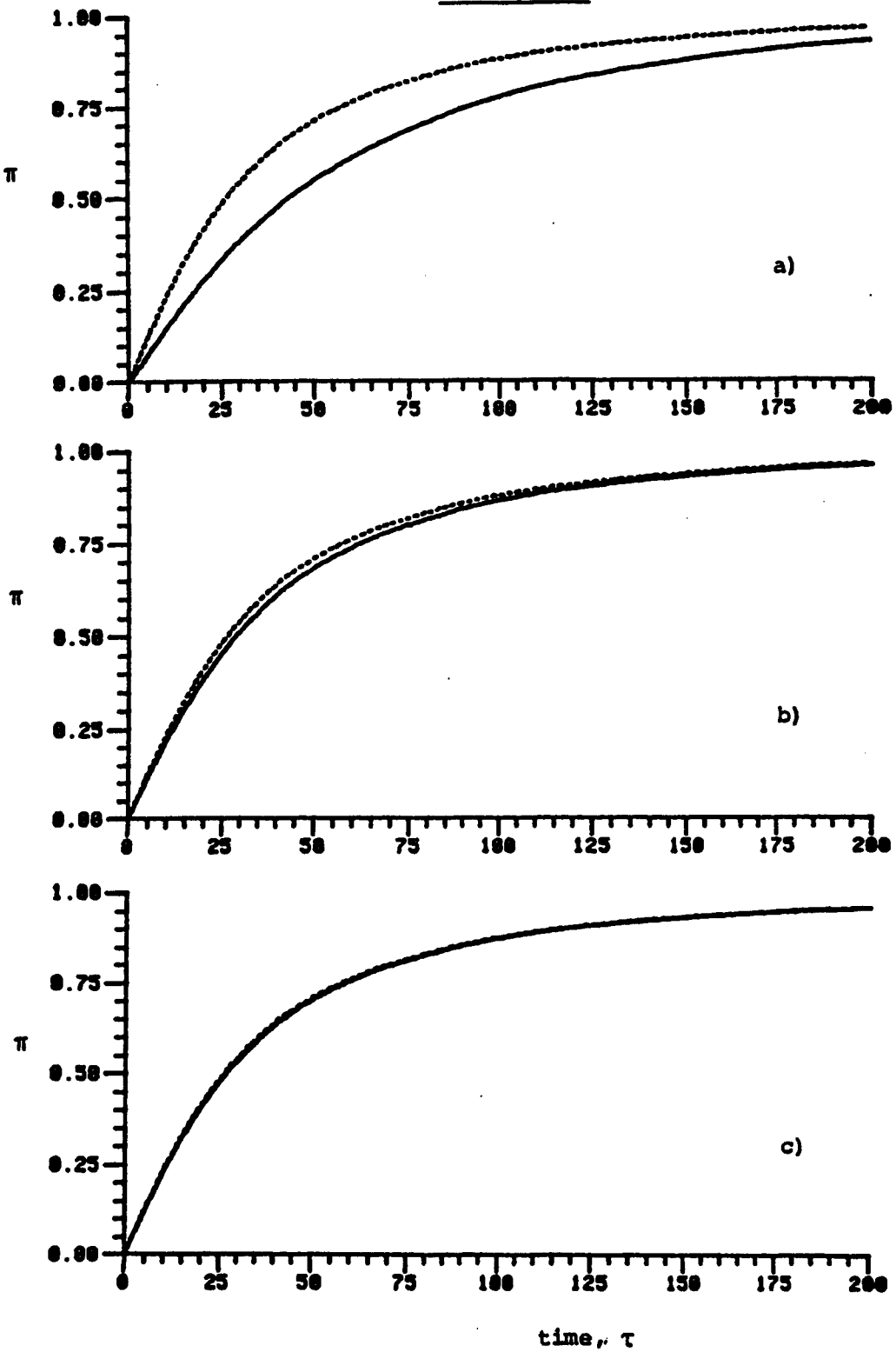


Figure 4-4. Modal matrix and time constants as they vary with the binding number,  $B_i$ , the other groups are  $St = .01$ ,  $Q_s = .1$ ,  $\sigma = 1$ .

**Figure 4-5.** The applicability of the quasi-equilibrium solution to the simple dimeric model. The solid line shows the exact solution for the product ( $\pi$ ) concentration profile and the dotted line shows the solution obtained by applying the quasi-equilibrium assumption. The parameters are:  $A_f = 1$ ,  $A_c = 10$ ,  $St = .01$ ,  $Q_s = .1$ ,  $\sigma_o = 1$ ,  $X_o = Y_o = 0$ , and  $B_i$  as follows, = .1 in part a), = 1 in b) and = 10 in c).

FIGURE 4-5.

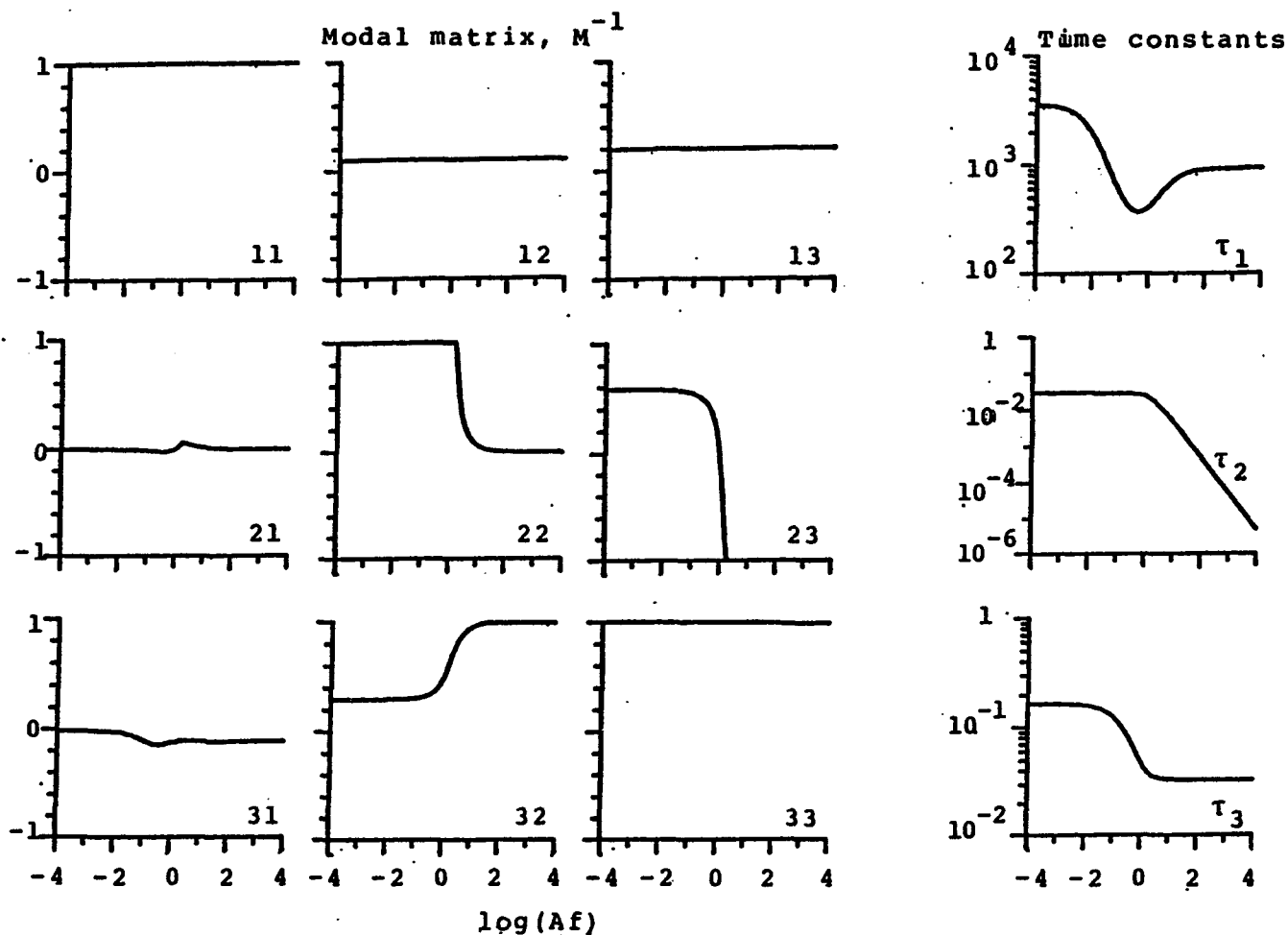


Figure 4-6. Modal matrix and time constants as they vary with the affinity ratio,  $Af$ ,  $St = .01$ ,  $Qs = .1$ ,  $\sigma = 1$ .

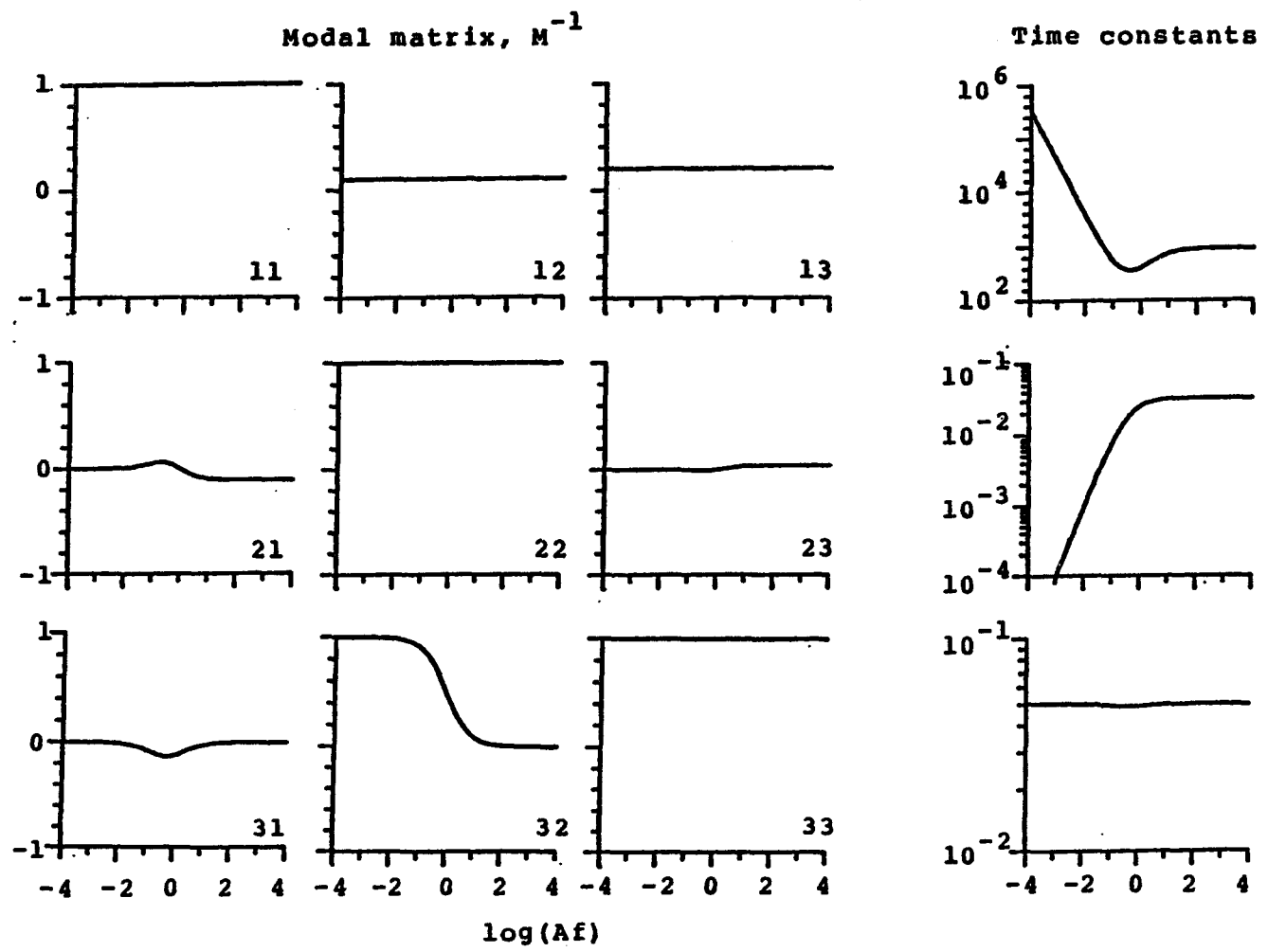


Figure 4-7. Modal matrix and time constants as they vary with the affinity ratio,  $Af$ , while  $Biaf$  (=1) is kept constant,  $St = .01$ ,  $Qs = .1$ ,  $\sigma = 1$ .

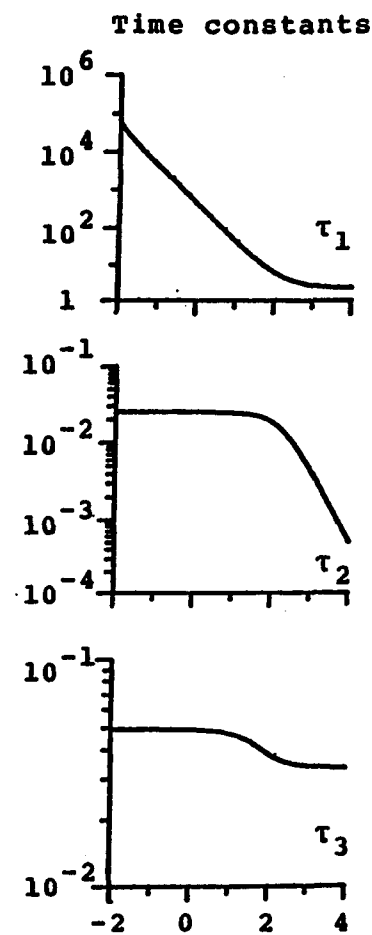
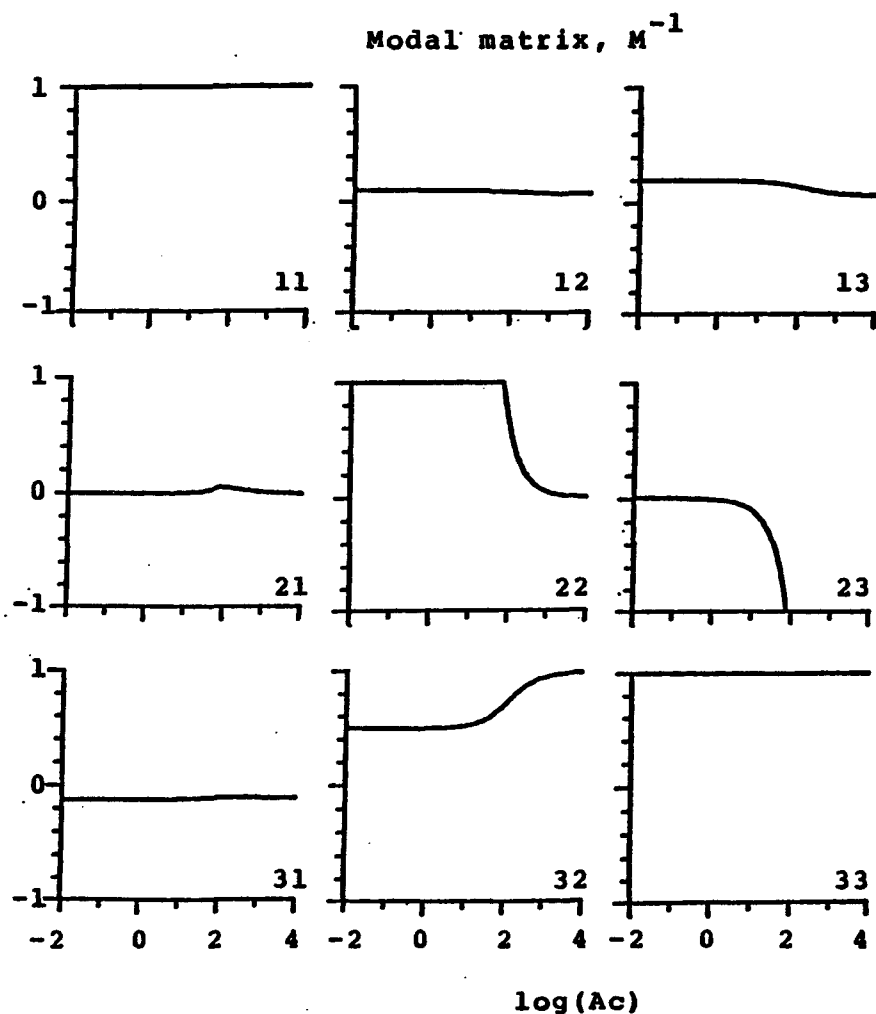


Figure 4-8. Modal matrix and time constants as they vary with the acceleration number,  $Ac$ ,  $St = .01$ ,  $Qs = .1$ ,  $\sigma = 1$ .

(small). At large Bi numbers a very fast mode

$$\omega_2 = \alpha/8 + \chi/2 - \gamma \quad (44)$$

appears. Adding equations (9) - (11) in these proportions gives

$$8Qs \frac{dm_2}{d\tau} = Bi(Qs+12) \left( \frac{2Af}{1+St} \gamma - \alpha \chi \right) \quad (45)$$

This mode will relax much faster than the other two and its steady state equation is

$$\frac{\alpha \chi}{\gamma} = \frac{2Af}{1+St}, \quad \text{or} \quad 2K'_s = \frac{sx}{y} \quad (46)$$

Hence all the fast transients are associated with the equilibration of the second substrate binding step. Then if one chooses to ignore all the fast transients the dynamic description can be reduced to two differential equations and an algebraic equation which is the equilibrium relationship for the second binding step. This is equivalent to introduction of the quasi-equilibrium assumption. This is a remarkable result: through modal analysis we are able to justify a quasi-equilibrium assumption for substrate binding to X. This prediction is ascertained by numerical integration as shown in figure 4-5.

As seen from equation 43 reducing Bi eliminates the only step leading to the formation of Y and Y becomes decoupled from the other variables, figure 4-4.

(2) Effects of Af. In figure 4-6 we show the modal matrix as a function of Af. Since Bi is kept constant varying Af will result in varying the relative magnitudes of  $k'_{-1}$  and  $k_{-1}$ . At high Af values

where the binding of substrate to the X form becomes thermodynamically unfavorable the Y complex breaks down very fast to give S and X and Y becomes a fast independent variable suggesting that its dynamics can be relaxed leading to the quasi-steady state assumption. At low Af values the Y form becomes thermodynamically favored but no simplifications in the dynamic description appear.

(3) Effects of Af when BiAf is kept constant. Varying the parameters according to this scenario leads to changes in the relative magnitude of  $k'_1$  and  $k_1$ . When  $k'_1 \gg k_1$ , X becomes a fast decoupled variable suggesting that the quasi-steady state assumption could be applied to relax its dynamics. Conversely when  $k_1 \gg k'_1$  Y becomes decoupled but no simplification is suggested since its motion is not fast.

(4) Effects of Ac. The principal time constant drops, figure 4-8 when Ac increases, resulting in a faster response of the reaction until Ac is greater than St or when  $k'_{-1} > k'_2$  and hence Y preferentially degrades towards product formation, equation 43. Beyond that stage the effects are to speed up the motion of Y, and the second mode becomes dominated by Y, figure 4-8. Hence Y becomes a fast decoupled variable and mathematical analysis can be simplified. If Ac becomes small the principal time constant grows to infinity and eventually becomes negative. This happens when the maximum in figure 4-2 moves across  $\sigma$  of unity. Beyond that point the principal eigenvalue is positive and the stationary point is unstable.

#### 4.5. Discussion and Conclusions.

In this chapter we have successfully extended the approach of scaling and linearization from the Michaelis-Menten mechanism to a simple homotropic dimeric enzyme. This simple dimer has two identical, but dependent, reaction sites each following irreversible Michaelis-Menten kinetics. Scaling the equations gives three new dimensionless groups, two of which describe cooperativity in the binding step and one that describes cooperativity in the chemical transformation. In the limit where cooperativity effects vanish the dimer is identical to a Michaelis-Menten enzyme and possesses the same properties, which are thoroughly discussed in chapter 2.

Our exploration over the parameter space where cooperativity exists reveals behavior that is qualitatively different from the Michaelis-Menten reaction. First we have the possibility of complex eigenvalues which lead to damped oscillatory behavior. These damped oscillations are never very prominent for the dimeric enzyme, but one would expect them to become more significant for an enzyme that has a higher number of reaction sites. For instance commonly found tetrameric enzymes are expected to exhibit more prominent oscillatory behavior. Second, negative cooperativity in the chemical transformation can lead to unstable stationary states. Instability occurs because of the maximum that appears in the steady state equations beyond which the flux decreases with increasing substrate concentration leading to infinite buildup of substrate.

The computation of the time constants indicates that the

influence of cooperativity in the binding step is not effective to speed up the reaction, figures 4-4 and 4-6. More significant acceleration of reaction velocities is achieved by cooperativity in the chemical transformation step. However it is precisely at high reaction acceleration where the complex eigenvalues arise. This is in agreement with the general observation that open reacting systems are more likely to exhibit oscillatory behavior the more non-linear their kinetics are.

The modal analysis leads to important information regarding two commonly used approximations to simplify dynamic description of enzyme kinetics, as discussed in chapter 2; the quasi-steady state assumption and the quasi-equilibrium assumption.

The computation of the modal matrix indicates that no additional conditions, to  $Q_s \rightarrow 0$  previously demonstrated for simple Michaelis-Menten kinetics, lead to the justification of a full quasi-stationary analysis. However  $x$  or  $y$  become fast and decoupled variables under some circumstances leading partial quasi-stationary analysis. Another limitation of full quasi-steady state analysis arises here which is that it cannot represent oscillatory behavior since it is a one-dimensional dynamic description. The non-linear quasi-steady state analysis can be extended by the use of singular perturbation theory as discussed in chapters 2 and 3.

Quasi-equilibrium behavior is expected when a fast mode of the reaction system describes only a single reversible reaction step. This mode will relax quickly leading to rapid equilibration of this

reaction step which can then be assumed to be at quasi-equilibrium at all times greater than the time constant of that fast mode.

#### 4.6. Summary.

The dynamics of enzyme cooperativity are examined by studying a homotropic dimeric enzyme with identical reaction sites, both of which follow irreversible Michaelis-Menten kinetics. The problem is approached via scaling and linearization of the governing mass action kinetic equations. Homotropic interaction between the two sites are found to depend on three dimensionless groups, two for the substrate binding step and one for the chemical transformation.

The interaction between the two reaction sites is shown capable of producing dynamic behavior qualitatively different from that of a simple Michaelis-Menten system; (a) when the two sites interact to increase enzymatic activity over that of two independent monomeric enzymes (positive cooperativity) damped oscillatory behavior is possible, and (b) for negative cooperativity in the chemical transformation step a multiplicity of steady states can occur, with one state unstable and leading to runaway behavior.

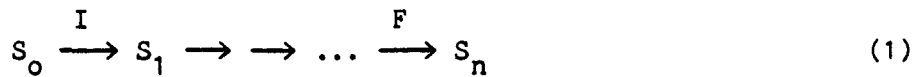
Linear analysis gives; (1) significant insight into system dynamics, and their parametric sensitivity, and (2) a way to identify regions of the parameter space where the approximate quasi-stationary and quasi-equilibrium analyses are appropriate.

## CHAPTER 5

## LINEAR REACTION SEQUENCES

In this chapter we study the dynamics of linear chains of enzymatic reactions connecting pools of key intermediates. This is a natural extension of previous chapters which dealt with the dynamics of individual enzymatic reactions. We build upon these earlier results to seek realistic dynamic models for reaction sequences which are sufficiently tractable to permit incorporation into global descriptions of metabolic networks.

More specifically we are interested in the dynamic relations between the influx ( $I$ ) of initial substrate ( $S_0$ ) into a reaction sequence and the formation rate ( $F$ ) of the end product ( $S_n$ ) of the reaction sequence. The reaction scheme we consider is



The formation flux is normally a product of a rate constant and the concentration of the last substrate-enzyme complex.

The analysis is carried out for a sequence of enzymes exhibiting irreversible Michaelis-Menten kinetics, the simplest realistic enzymatic reaction mechanism and one which frequently provides a good

approximation to observed behavior. Our problem is to find a tractable but realistic dynamic approximation for this system, since the mass action kinetic model of the Michaelis-Menten mechanism is mathematically intractable (Hommes 1962a, Darvey, Klotz and Ritter, 1978).

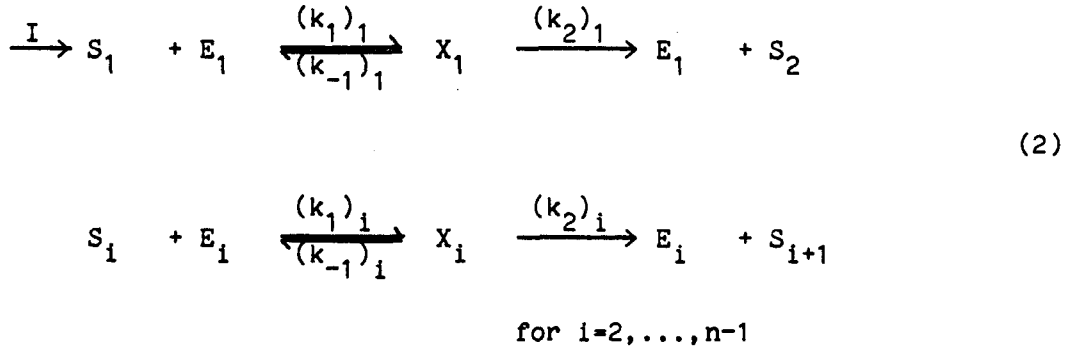
The approach that we adopt is one of scaling and full linear analysis, which has proven successful for single enzymes (chapters 2 and 4). This is an attractive procedure from several standpoints, in addition to mathematical simplicity. The primary value of the relaxation times and modes of the linear description is in the assessment of the validity of the quasi-steady state approximation and how it depends on system parameters. In addition the linear analysis permits use of the moments to relate global system dynamics to the kinetic behavior of the individual reactions. This use of the moments provides the important link between kinetic properties of individual reactions and overall dynamic behavior as well as forming a basis for model reduction via the method of moments.

### 5.1. Linear Analysis.

In this section we develop a linear approximation to a sequence of reactions exhibiting irreversible Michaelis-Menten kinetics in an analogous fashion to chapters 2 and 4.

### 5.1.1. Kinetic description.

The kinetic behavior of such systems is defined by



where each substrate,  $S_i$ , binds reversibly to the corresponding free enzyme,  $E_i$ , to form an intermediate substrate-enzyme complex,  $X_i$ , which breaks down irreversibly to give the product,  $S_{i+1}$ , and to regenerate the free enzyme. The  $(k)_i$  are rate constants. The rate of formation of  $S_n$  is given by  $F = (k_2)_{n-1} x_{n-1}$  (where lower case letters denote the concentration of the corresponding upper case chemical species).

### 5.1.2. Scaling.

To facilitate the identification of important parameters we now scale the mass action kinetic model of this reaction scheme much as chapters 2 and 4 to produce the dimensionless equations for:  
the substrates,  $\sigma_i$

$$(B\sigma_i) \frac{d\sigma_i}{d\tau} = \frac{S_{t_i} S_{a_{i-1,i}} X_{i-1}}{1+S_{t_i}} - \sigma_i + \frac{X_i}{1+S_{t_i}} + \sigma_i X_i,$$

the enzyme complexes,  $x_i$  (3)

$$(B_{i-1} Qs_i) \frac{dx_i}{d\tau} = o_i - x_i - o_i x_i, \quad i=1, \dots, n-1$$

where  $Sa_{i-1,1} x_{i-1} = \psi$  for  $i = 1$ . Here we have scaled the substrate concentrations  $s_i$  relative to the corresponding Michaelis constant  $K_m$

$K_m$  as,  $o_i = s_i/K_m$ . Normally substrate concentrations,  $s_i$ , under in vivo conditions are close to or somewhat less than their  $K_m$  values (Srere 1967, 1970, Hammes and Schimmel, 1971 and Segel 1975). In fact Atkinson (1977) suggests that the expected in vivo values for  $s_i$  are 20-100% of the  $K_m$  value so that we expect  $\sigma$  to fall in the range .2-1. This range has been argued to be optimum Reich (1984). The intermediate enzyme-substrate concentrations,  $x_i$ , are scaled relative to the total amount of enzyme,  $(e_t)_i$ , as  $x_i = x_i/(e_t)_i$ , where  $(e_t)_i = e_i + x_i$ , so that they vary from zero to unity. The concentration of the free enzyme,  $e_i$ , is not an independent variable since we will consider the total enzyme concentration to be constant over time. Time is scaled relative to the slowest substrate-enzyme binding step in the chain as  $\tau = (k_1 e_t)_{\text{min}} t$ .

The dimensionless groups appearing in equation 3 represent our choice of system parameters, and they deserve some attention. The "Quasi-steady state" numbers  $Qs_i$  and the "Stickyness" numbers  $St_i$  are defined for all the individual reactions as

$$Qs_i = \left(\frac{e_t}{K_m}\right)_i, \quad St_i = \left(\frac{k_2}{k_{-1}}\right)_i \quad (4)$$

These two numbers were previously described in chapters 2 and 4 and

they have well defined physical significance.

For our reaction sequence we get in addition to the above familiar ratios two sets of dimensionless numbers with no counterparts for single reactions; these describe interactions of chain elements. One set of these numbers describes relative saturation velocities

$$Sa_{i,j} = \frac{v_{\max_i}}{v_{\max_j}} = \frac{(k_2 e_t)_i}{(k_2 e_t)_j} \quad (5)$$

between two reactions in the sequence. We call these the "Saturation numbers". It has been suggested (Atkinson, 1977 pg 118) that in order to minimize the chances of substrate buildup while maintaining catalytic efficiency the saturation velocities in the chain should be approximately equal and perhaps increase slightly as we move down the chain, i. e.  $Sa_{i,j} < 1$  if  $i > j$ .

The other dimensionless groups expressing chain characteristics are measures of the rates of individual substrate-enzyme binding scaled to the slowest binding reaction in the chain

$$Bi_i = \frac{(k_1 e_t)_{\min}}{(k_1 e_t)_i} \quad (6)$$

We call these the "Binding numbers" and note that they must range between zero and unity. The distribution of Bi numbers in a chain is expected to be wide. The mass flux across the system boundary is scaled relative to the saturation velocity of the first reaction as  $\Psi = I/(k_2 e_t)_1$ , and Atkinson (1977, pg 118) suggests that  $\Psi$  should

typically fall in the range .15-.5.

Mathematical description of our system is now complete, except for the specification of the initial conditions which will be taken to be those defining the steady state.

### 5.1.3. The steady state equations.

The steady state solution, obtained by setting the time derivatives in equation 3 to zero, takes a particularly simple form. It is

$$\bar{x}_i = S_{a_{1,i}} \bar{\psi}, \quad \bar{o}_i = \frac{S_{a_{1,i}} \bar{\psi}}{1 - S_{a_{1,i}} \bar{\psi}} \quad (7)$$

Note that  $S_{a_{1,i}} \bar{\psi} > 1$  implies that the steady state flux exceeds the saturation flux of reaction  $i$ , and hence no physically realistic solution exists for this situation.

### 5.1.4. Linearization.

We now proceed as before by expanding the bi-linear terms into a Taylor series as

$$\underline{o_x} = \bar{o_x} + \bar{o}(\underline{x} - \bar{x}) + \bar{x}(\underline{o} - \bar{o}) + \underline{(x - \bar{x})(o - \bar{o})} \quad (8)$$

and substituting these into equation 3. We then omit those terms quadratic in the deviation variables (the underlined term), to obtain

$$\frac{d\underline{x}'}{d\tau} = J\underline{x}' + \underline{\psi}' \quad (9)$$

where the state and input vectors are

$$\underline{x}' = (\sigma'_1, x'_1, \dots, \sigma'_{n-1}, x'_{n-1})^t \quad (10)$$

$$\underline{\psi}' = \left( \frac{St_1 \Psi'}{B_{11}(1+St_1)}, 0, \dots, 0 \right)^t \quad (11)$$

and where the deviation variables are

$$\sigma'_i = \sigma_i - \bar{\sigma}_i, \quad x'_i = x_i - \bar{x}_i, \quad \Psi' = \Psi - \bar{\Psi} \quad (12)$$

and the Jacobian matrix is

$$J = \begin{bmatrix} A_1 & & & \\ B_2 & A_2 & & \\ & B_3 & A_3 & \\ & & \ddots & \\ & & & \ddots & \\ & & & & B_{n-1} & A_{n-1} \end{bmatrix} \quad (13)$$

where  $A_i$  and  $B_i$  are  $2 \times 2$  matrices given by

$$A_i = \frac{1}{B_{11}} \begin{bmatrix} -(1-Sa_{1,i}\bar{\Psi}) & \frac{1}{1+St_i} + \frac{Sa_{1,i}\bar{\Psi}}{1-Sa_{1,i}\bar{\Psi}} \\ \frac{1-Sa_{1,i}\bar{\Psi}}{Qs_i} & \frac{-1}{Qs_i(1-Sa_{1,i}\bar{\Psi})} \end{bmatrix} \quad (14)$$

$$B_i = \begin{bmatrix} & & \\ & 0 & \frac{Sa_{i-1,i}St_i}{1+St_i} \\ \frac{1}{B_{11}} & 0 & 0 \end{bmatrix} \quad (15)$$

The matrix  $A_i$  is equal to the Jacobian matrix for the individual

reactions scaled to  $B_i$ , or  $A_i = J_i/B_i$ , where  $J_i$  is the  $2 \times 2$  Jacobian matrix for reaction  $i$  discussed in chapter 2.

### 5.1.5. Modal analysis.

We now use the linearized description to perform a modal analysis of our system. The modes are defined as the linear combinations of the original variables which move on time scales corresponding to the reciprocals of the eigenvalues of the Jacobian matrix. The modes are linearly independent.

The eigenvalues. The eigenvalues are the roots to the familiar characteristic equation,  $\det(J - \lambda I) = 0$ , which in our case can be simplified as

$$\begin{aligned} \det(J - \lambda I) &= \prod_{i=1}^{n-1} \det(A_i - \lambda I) \\ &= \prod_{i=1}^{n-1} (\lambda^2 - \text{tr}(A_i)\lambda + \det(A_i)) \\ &= \prod_{i=1}^{n-1} (\lambda - \lambda_{i,1})(\lambda - \lambda_{i,2}) \end{aligned} \quad (16)$$

where

$$\text{tr}(A_i) = \lambda_{i,1} + \lambda_{i,2} = -\frac{1}{B_i} \left( 1 - S_{a_{1,i}} \bar{\Psi} + \frac{1}{Qs_i (1 - S_{a_{1,i}} \bar{\Psi})} \right) \quad (17)$$

$$\det(A_i) = \lambda_{i,1} \lambda_{i,2} = \frac{St_i}{1+St_i} \left( \frac{1 - S_{a_{1,i}} \bar{\Psi}}{B_i^2 Qs_i} \right) \quad (18)$$

The individual roots can be obtained analytically as

$$\lambda_{i,1}, \lambda_{i,2} = \frac{1}{2} (\text{tr}(A_i) \pm \sqrt{\text{tr}(A_i)^2 - 4\det(A_i)}) \quad (19)$$

$$= \frac{1}{2B_{i,i}} (\text{tr}(J_i) \pm \sqrt{\text{tr}(J_i)^2 - 4\det(J_i)})$$

The time constants are simply the negative reciprocals of the eigenvalues for the individual reactions

$$\tau_{2i-1} = -1/\lambda_{i,1}, \quad \tau_{2i} = -1/\lambda_{i,2} \quad (20)$$

where  $\tau_{2i-1}$  and  $\tau_{2i}$  are the two time constants associated with reaction  $i$ .

As discussed in chapter 2 and appendix B analytical approximations can be obtained for the time constants when a parameter  $\delta_i$  ( $= \det(A_i)/\text{tr}(A_i)^2$ ), is small as  $\tau_{2i-1} = -\text{tr}(A_i)/\det(A_i)$ , and  $\tau_{2i} = -1/\text{tr}(A_i)$ . For the individual reactions letting  $Qs_i$  or  $St_i$  tend to zero leads to a separation of the two time constants for each reaction. The relative magnitude of time constants between the reactions can be altered by letting the  $B_{i,i}$  numbers become small.

The normal modes. The dynamically independent modes of the linearized description are defined as  $\underline{m} = M^{-1}\underline{x}$  where  $M^{-1}$  is a matrix comprised of the eigenrows  $\underline{u}_i$  as  $M^{-1} = (\underline{u}_1, \underline{u}_2, \dots, \underline{u}_n)^t$ . The eigenrows are defined by  $\underline{u}_i(J - \lambda_i I) = 0$ .

Due to the simple block bi-diagonal structure of  $J$  the eigenrows are readily obtained as

$$u_{i,j}(a_{11}^j - \lambda_i) + u_{i,j+1}a_{21}^j = 0, \quad j = 1, \dots, n-1 \quad (21)$$

$$u_{i,j}a_{12}^j + u_{i,j+1}(a_{22}^j - \lambda_i) + u_{i,i+2}b^{j+1} = 0, \quad j = 1, \dots, n-2$$

where  $a_{ij}^k$  denotes the  $ij^{\text{th}}$  element of  $A_k$ ,  $b^k$  denotes the non-zero element of  $B_k$ . Since the  $m (=2(n-1))$  elements of  $\underline{u}_i$  are linearly dependent we omit the last equation. These equations can be solved to give

$$u_{i,j+1} = \frac{\lambda_i - a_{11}^j}{a_{21}^j} u_{i,j} \quad (22)$$

$$u_{i,j+2} = \frac{1}{b^{j+1} a_{21}^j} ((\lambda_i - a_{11}^j)(\lambda_i - a_{22}^j) - a_{12}^j a_{21}^j) u_{i,j}$$

The eigenrow is only specified up to a constant and we scale it relative to its largest element as  $u_{i,j} \rightarrow u_{i,j}/(u_i)_{\max}$  where  $(u_i)_{\max} = \max_j(u_{i,j})$ .

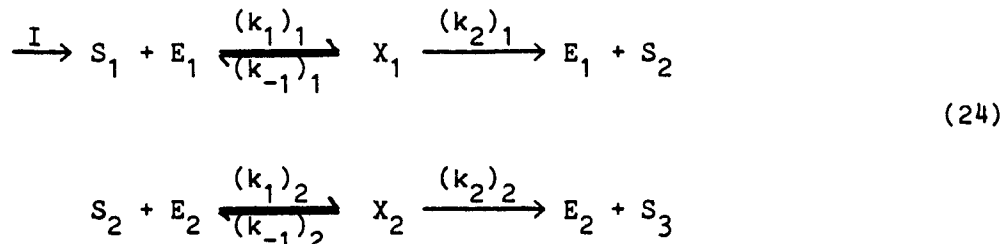
The simple structure of  $J$  allows an easy derivation of the form of  $M^{-1}$  as

$$M^{-1} = \begin{bmatrix} M_{11}^{-1} & 0 & 0 & \dots & 0 \\ M_{21}^{-1} & M_{22}^{-1} & 0 & \dots & 0 \\ M_{31}^{-1} & M_{32}^{-1} & M_{33}^{-1} & & \\ \vdots & \ddots & \ddots & & \\ \vdots & \ddots & \ddots & & \\ \vdots & \ddots & \ddots & & \\ M_{n-1,1}^{-1} & M_{n-1,2}^{-1} & M_{n-1,3}^{-1} & \dots & M_{n-1,n-1}^{-1} \end{bmatrix} \quad (23)$$

where  $M_{ij}^{-1}$  are  $2 \times 2$  matrices which give the influence of reaction  $j$  on

reaction  $i$ . The  $M_{ii}^{-1}$ 's are equal to the modal matrices for the individual reactions divided by  $B_{i,i}$ . The properties of these are thoroughly discussed in chapter 2. If  $i < j$  then  $M_{ij}^{-1} = 0$  since the reactions are irreversible. However if  $i > j$  the interactions can be significant.

An example - two reaction chain. We now examine the reaction scheme:



where we will consider the case where  $B_{i,2}$  is unity or  $(k_1 e_t)_2 < (k_1 e_t)_1$ . The dimensionless numbers that we have are

$$\begin{aligned} St_1 &= (k_2/k_{-1})_1, & Qs_1 &= (e_t/K_m)_1 \\ St_2 &= (k_2/k_{-1})_2, & Qs_2 &= (e_t/K_m)_2 \\ Bi = Bi_1 &= (k_1 e_t)_2 / (k_1 e_t)_1, & Sa = Sa_{1,2} &= (k_2 e_t)_1 / (k_2 e_t)_2 \end{aligned} \quad (25)$$

The numerical values chosen for these groups will dictate the dynamic behavior. The effects of  $Qs_i$  and  $St_i$  on the dynamics of the individual reactions is discussed at length in chapter 2, but here we concentrate on how the two reactions interact dynamically with each other.

The elements of the modal matrix and the time constants are

shown in figure 5-1 as functions of Bi. The figure shows all the non-zero elements of  $M^{-1}$  and the time constants for values of Bi ranging from one-thousandth to unity. The numerical values used for  $St_i$  and  $Qs_i$ , .01 and .1 respectively, fall into the range believed to be physiologically meaningful (see chapter 2). The effects of lowering Bi are basically that  $M_{21}^{-1} \rightarrow 0$  and  $\tau_1$  and  $\tau_2$  become smaller which suggests that quasi-stationary analysis is applicable. The reason is that the dynamic interactions between the two reactions are reduced and furthermore the first reaction becomes fast relative to the second one: hence the two differential equations describing the first reaction become a fast dynamically independent sub-set and hence unimportant when considering the motion of the second reaction.

The transient behavior of the same two reaction chain as in figure 5-1 for various values of Bi are shown in figure 5-2. As Bi is lowered we see that the transient behavior of the reaction chain becomes dominated by the second reaction and the quasi-steady state assumption gives good results for low Bi numbers as predicted by the modal matrix. This can also be rationalized by noticing that the transient behavior of  $x_1$  and  $\Psi$  become essentially identical at low Bi values implying that the flux into reaction 2 is essentially the same as into reaction 1.

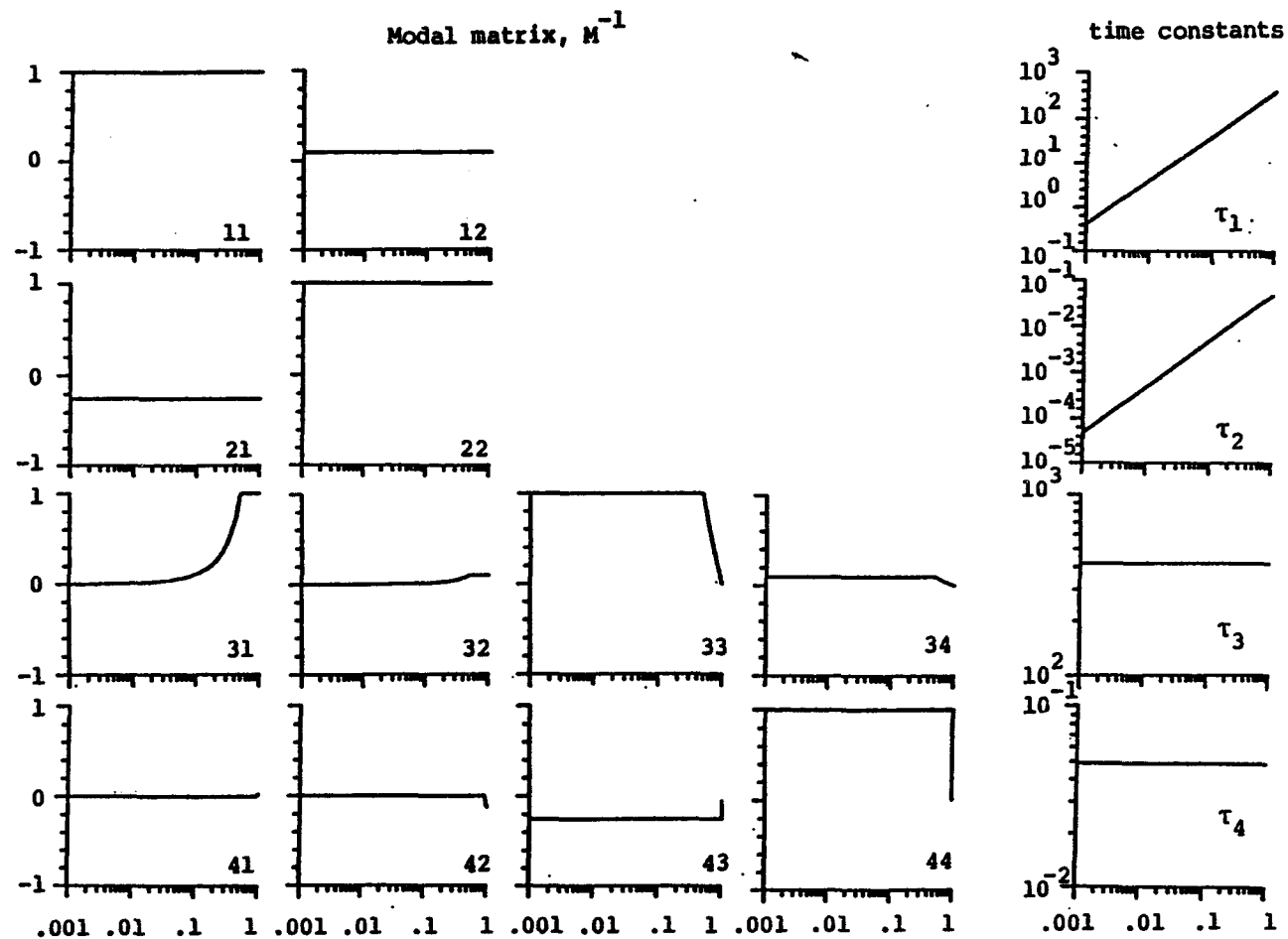
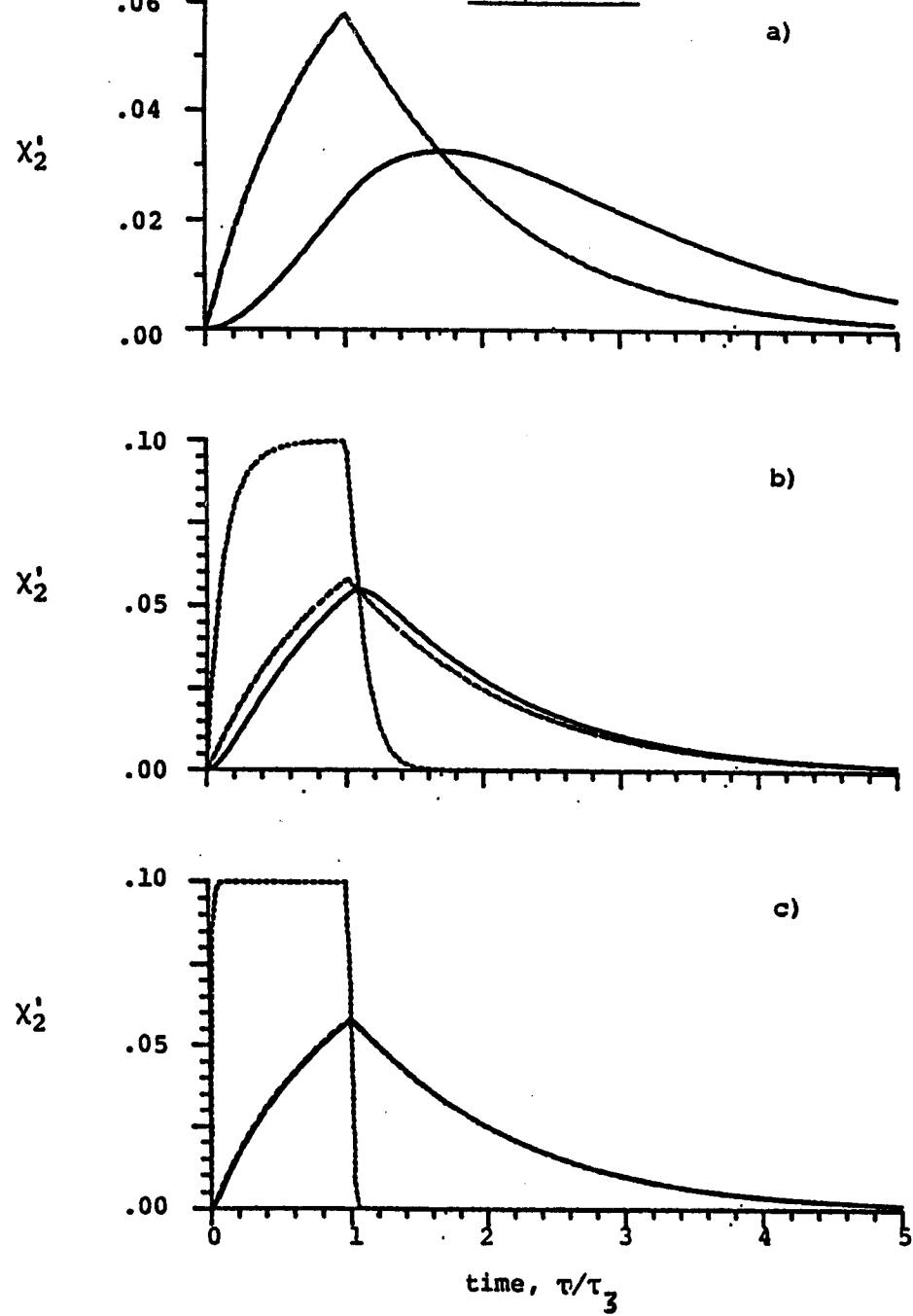


Figure 5-1. The modal matrix and the time constants as a function of the Binding number  $B_i$ , for a two reaction chain.  $Qs_1 = Qs_2 = .1$ ,  $St_1 = St_2 = .01$ ,  $Bi_1 = 1$ ,  $Sa_{1,2} = 1$  and  $\bar{Y} = .5$ .

Figure 5-2.

Transient solutions for the two reaction chain at different Binding numbers, a)  $Bi_1 = 1$ , b)  $Bi_1 = .1$  and c)  $Bi_1 = .01$ . The solid curve represents the exact solution for  $x_1$ , the dotted curve shows the transient behavior of  $x_2$  when the quasi-steady state assumption has been applied to reaction 1 and the dashed curve shows the exact solution for  $x_2$ . The dimensionless groups have the numerical values,  $Qs_1 = Qs_2 = .1$ ,  $St_1 = St_2 = .01$ ,  $Bi_2 = 1$ ,  $Sa_{1,2} = 1$  and  $\bar{\Psi} = .5$ , and the pulse in the input rate used is a square pulse on duration  $\tau_3$  and height .1 ( 20% of  $\bar{\Psi}$ ).

FIGURE 5-2.

### 5.2. Moments and Model Reduction.

Metabolic models frequently contain a larger number of parameters than can be reasonably determined, and it is therefore desirable to see if this number can be reduced to manageable proportions without significant loss of insight. More specifically we wish here to see if we can provide a useful overall description of chain dynamics which is related to the behavior of the individual elements in a well defined way and which at the same time permits suppression of un-necessary detail. The temporal moments turn out to be particularly useful for this purpose.

#### 5.2.1. Definition and meaning of temporal moments.

The normalized temporal moments of a function of time  $h(t)$  are defined as

$$M_n = \frac{\int_0^\infty t^n h(t) dt}{\int_0^\infty h(t) dt} \quad (26)$$

They are useful for primarily two reasons. First, the moments provide means of parameter estimation: if one has a model characterizing  $h(t)$  in terms of  $N$  parameters, one can determine these  $N$  parameters by equating the  $N$  first moments of the data and the model. Second the lower moments have simple physical significance, and their evaluation often provides useful physical insight.

The function that we are concerned with is the transfer function that which gives the dynamic relationship between changes in the

influx rate,  $I$ , and the formation rate,  $F$ , of the last intermediate  $S_n$  in the reaction chain of equation 1. It generally has the form of a single peak in the time domain. We shall find that this peak, like many other biological response functions, can be adequately described by the first three moments which are measures of mean response time, variance and skewness respectively. The mean response time  $\bar{t}$ , which in our case is the average processing time, is in fact identical to the first temporal moment  $M_1$ . This quantity turns out to be simply the sum of the mean processing times for each element of the reaction chain and its use to characterize system performance is a formal way of recognizing the importance of time lags in the system.

The variance,  $T_2$ , of the processing time is simply the second moment taken around  $\bar{t}$ ,

$$T_2 = M_2 - M_1^2 \quad (27)$$

and the skewness,  $T_3$ , is the corresponding third moment

$$T_3 = M_3 - 3M_2M_1 + 2M_1^3 \quad (28)$$

These are the most important measures of the shape of the response curve, which in our case is the distribution of processing times. Moreover we will find that each successive moment puts increasing emphasis on the slowest elements of the chain. Physically this means that the details of the shape of the response curve of a high order model where the contributing time constants well distributed can be adequately approximated by a model of lower dynamic dimensionality.

The fourth moment relative to  $\bar{t}$  describes curtosis and it is normally found to be of little value. Experience suggests that fourth moments contribute little of importance to the description of response functions, and that they are all but impossible to determine from experimental data: their computation tends to be dominated by noise at long times.

### 5.2.2. Evaluation of the moments.

The evaluation of the moments from the integrals of equation 26 is not always convenient, and for our case the moments are more easily obtained from a transfer function description. The transfer functions are obtained once the dynamic description has been transformed into the Laplace domain. The Laplace transform,  $L[\cdot]$ , of a function  $h(t)$  is defined as

$$h(s) = L[h(t)] = \int_{-\infty}^{+\infty} h(t)e^{-st} dt \quad (29)$$

where time has been replaced by  $s$ , the Laplace variable. Once our dynamic description of the reaction has been transformed into the Laplace domain it takes the form

$$F(s) = g(s)I(s) \quad (30)$$

where  $g(s)$  is the transfer function giving the dynamic relationship between the input flux,  $I$ , and the formation flux,  $F$ . The moments of the transfer function are obtained by computing

$$\left( \frac{d^n g}{ds^n} \right)_{s=0} = (-1)^n \alpha_n, \quad M_n = \frac{\alpha_n}{\alpha_0} \quad (31)$$

We now proceed to derive the appropriate transfer functions.

The transfer functions. Equation 11 can be transformed into the frequency domain and solved as

$$x'(s) = (sI - J)^{-1} \underline{\psi}'(s) = G(s) \underline{\psi}'(s) \quad (32)$$

where  $G(s)$  is a matrix of transfer functions. The elements of the transfer function matrix,  $G(s) = (sI - J)^{-1}$ , that give the dynamic relationships between  $\sigma_{n-1}$  and the input rate are  $g_{\sigma_{n-1}}(s) = ((sI - J)^{-1})_{1,m-1}$  and between  $x_{n-1}$  and the input rate are  $g_{x_{n-1}}(s) = ((sI - J)^{-1})_{1,m}$  (again  $m=2(n-1)$ ).

The general formula for the elements of the inverse of an arbitrary matrix  $A$  is

$$(A^{-1})_{ij} = \frac{\text{cof}(A)_{ji}}{\det(A)} \quad (33)$$

where  $\text{cof}(A)_{ji}$  is the  $ji^{\text{th}}$  cofactor of  $A$ . The cofactor is the determinant of the sub-matrix formed by deleting the  $j^{\text{th}}$  column and  $i^{\text{th}}$  row of  $A$  and multiplied by  $-1$  to the  $i+j^{\text{th}}$  power. Since both the minors under consideration have no elements below the diagonal their determinants are simply the product of their diagonal elements and the cofactors become

$$\text{cof}(sI-J)_{m-1,1} = \left( \frac{1-\bar{\Psi}}{B_{11}Qs_1} \right) \left( \frac{S_{1,n-2,n-1} S_{n-1}}{B_{1,n-1} (1+S_{n-1})} \right) \left( s + \frac{1}{B_{1,n-1} Qs_{n-1} (1-S_{1,n-1} \bar{\Psi})} \right) \\ (34)$$

$$x \left( \prod_{i=2}^{n-2} \left( \frac{1-S_{1,i} \bar{\Psi}}{B_{1,i} Qs_i} \right) \left( \frac{S_{1-i,i} S_{i}}{B_{1,i} (1+S_{i})} \right) \right)$$

$$\text{cof}(sI-J)_{m,1} = \left( \frac{1-\bar{\Psi}}{B_{11}Qs_1} \right) \left( \prod_{i=2}^{n-1} \left( \frac{1-S_{1,i} \bar{\Psi}}{B_{1,i} Qs_i} \right) \left( \frac{S_{1-i,i} S_{i}}{B_{1,i} (1+S_{i})} \right) \right) \\ (35)$$

The expression for the determinant may be written as

$$\det(sI-J) = \left( \prod_{i=1}^{n-1} \lambda_{i,1} \lambda_{i,2} \right) \left( \prod_{j=1}^m (\tau_j s+1) \right) \\ (36)$$

using equation 18. Now the desired transfer functions may be obtained by substituting equations 34-36 into equation 33 as

$$g_{\chi_{n-1}}(s) = \frac{x_{n-1}}{\bar{\Psi}} = \frac{S_{11} \text{cof}(sI-J)_{m,1}}{B_{11} (1+S_{11}) \det(sI-J)} \\ (37)$$

$$= \frac{S_{1,n-1}}{\prod_{i=1}^m (\tau_i s+1)}$$

for the enzyme intermediates and

$$g_{o_{n-1}}(s) = \frac{o_{n-1}}{\bar{\Psi}} = \frac{S_{11} \text{cof}(sI-J)_{m-1,1}}{B_{11} (1+S_{11}) \det(sI-J)}$$

(38)

$$= \frac{S_{a_{1,n-1}}}{(1-S_{a_{1,n-1}}\bar{\Psi})^2} \left( \frac{\tau_z^{s+1}}{\prod_{j=1}^m (\tau_j^{s+1})} \right)$$

for the substrates where the time constant for the zero is

$$\tau_z = B_{n-1} Q_{n-1} (1-S_{a_{1,n-1}}\bar{\Psi}) \quad (39)$$

Equations 37 and 38 give us the desired dynamic relationship between the  $n-1^{st}$  intermediate and substrate concentrations and the influx  $\bar{\Psi}$ , respectively. The formation flux of metabolite  $S_n$  is given by concentration the  $n-1^{st}$  intermediate as discussed above so equation 37 becomes our focus of attention.

Evaluation of the moments from transfer functions. The transfer functions of equation 37, and the low order approximations discussed below, contain only poles and are of the general form

$$g(s) = \frac{1}{p(s)} \quad (40)$$

where  $p(s)$  is the pole polynomial. For a three parameter approximation we need only the three first derivatives of the transfer function evaluated at  $s = 0$  and these are

$$g_0 = \alpha_0 = 1 \quad (41)$$

$$g'_0 = \alpha_1 = -p'_0 \quad (42)$$

$$g''_0 = \alpha_2 = 2(p'_0)^2 - p''_0 \quad (43)$$

$$g'''_0 = \alpha_3 = 6p'_0 p''_0 - 6(p'_0)^3 - p'''_0 \quad (44)$$

where the prime denotes the derivative with respect to  $s$ , and the

subscript o indicates that the quantity with the subscript is evaluated at  $s = 0$ . The three moments of interest then become

$$M_1 = p'_o \quad (45)$$

$$T_2 = (p'_o)^2 - p''_o \quad (46)$$

$$T_3 = p'''_o + 2(p'_o)^3 - 3p'_o p''_o \quad (47)$$

In this way one can evaluate the moments of equation 37, and analogously for equation 38. The derivation is quite laborious and is omitted here, but the final results are shown in table 5-1.

### 5.2.3. The moments of $g_x$ .

Using equation 45 the first moment of  $g_x$  is found to be simply the sum of all the time constants in the chain, table 5-1. The time constants for each reaction can be obtained from equations 17-20 as

$$\begin{aligned} \tau_{2i-1} + \tau_{2i} &= \frac{-\text{tr}(A_i)}{\det(A_i)} = (B_{1i}) \left( \frac{Qs_i(1+St_i)}{St_i} \left( 1 + \frac{1}{Qs_i(1-Sa_{1,1}\bar{\Psi})^2} \right) \right) \\ &= B_{1i} \beta_i \end{aligned} \quad (48)$$

and the first moment becomes

$$M_1 = \sum_{i=1}^{n-1} \frac{-\text{tr}(A_i)}{\det(A_i)} = \sum_{i=1}^{n-1} B_{1i} \beta_i \quad (49)$$

Normally  $\tau_{2i}$  is much smaller than  $\tau_{2i-1}$ , as discussed above, and hence  $\tau_{2i-1} \approx -\text{tr}(A_i)/\det(A_i)$ . Under those circumstances the second and third moments around the mean can be approximated as

Table 5-1.

Moments for the transfer functions of a sequence of irreversible  
Michaelis-Menten reactions

<u>Moments</u>	<u><math>g_{X_i}</math></u>	<u><math>g_{\sigma_i}</math></u>
$M_1$	$\sum_{\ell=1}^{2i} \tau_\ell$	$\left( \sum_{\ell=1}^{2i} \tau_\ell \right) - \tau_z$
$T_2$	$\sum_{\ell=1}^{2i} \tau_\ell^2$	$\left( \sum_{\ell=1}^{2i} \tau_\ell^2 \right) - \tau_z^2$
$T_3$	$2 \sum_{\ell=1}^{2i} \tau_\ell^3$	$2 \left[ \left( \sum_{\ell=1}^{2i} \tau_\ell^3 \right) - \tau_z^3 \right]$

$$T_2 = \sum_{i=1}^{n-1} (B_i)^2 (\beta_i)^2, \quad T_3 = \sum_{i=1}^{n-1} 2(B_i)^3 (\beta_i)^3 \quad (50)$$

These results deserve closer attention: the distribution of the  $B_i$  numbers would dictate how each reaction contributes to the overall properties of the chain. For instance in a two reaction chain a reaction chain where all the  $\beta_i$  are equal ( $=\beta$ ) and where one  $B_i$  number is one-tenth then the corresponding reaction contributes only about 10% to the first moment, 1% to the second and only .1% to the third. Hence most of the dynamic behavior of the chain is determined by the reaction with  $B_i$  of unity.

This prediction can be seen in figure 5-2 at  $B_i = .1$  where the quasi-steady state solution is similar to the exact one except it is shifted in time by about .1 time unit (10% of the largest time constant). This is exactly what the moments predict since only the first moment, or the average processing or transit time, is noticeably influenced by reaction 1 at these parameter values, but the variance and skewness characteristics are essentially determined by the second reaction. The quasi-steady state assumption ignores all the transients associated with the first reaction, and hence the mean processing time is in error by about 10%, but in other aspects the curves look similar.

Similar results can be obtained by distributing the  $\beta_i$  or equivalently the  $Q_i$ 's and the  $S_i$ 's. Hence it is clear that any distribution of kinetic properties in the chain will lead to dynamic behavior that resembles a lower order model, and the dynamic

description can be simplified.

#### 5.2.4. Frequency response.

Transfer functions  $g_{x_n}(s)$  are not directly accessible from transient behavior of  $x'_{n-1}$  obtained either from computations or experimental data. This is seen from the relationship  $x'_{n-1}(s) = g_{x_{n-1}}(s)\psi'(s)$ . The only way that  $x'_{n-1}$  is the same as the transfer function is if  $\psi'(t) = \delta(t)$  ( $\delta(s) = 1$ ), the delta Dirac function, then  $x_{n-1} = g_{x_{n-1}}$ : hence the transient response of  $x_{n-1}$  contains all the information embedded in the transfer function. Since it is not possible to implement the impulse pulse other types of pulses in the input rate are used and the frequency response of the transfer functions is evaluated by computing the quotient

$$g_{x_{n-1}}(i\omega) = \frac{\int_0^\infty x'_{n-1}(t)e^{-i\omega t} dt}{\int_0^\infty \psi'(t)e^{-i\omega t} dt} \quad (51)$$

where the denominator represents the Fourier integral transform of the input pulse  $\psi'(t)$  and the numerator for the  $n-1$  intermediate  $x_{n-1}(t)$  over all frequencies,  $\omega$ , of interest.

Our interest here is only computational, and one can introduce various pulses in the influx rate, whose Fourier integral transforms can be evaluated analytically (see appendix A). The transient response of the last enzyme intermediate,  $x'_{n-1}(t)$ , of the chain is obtained by numerically solving equation 5 in response to such a pulse in the input rate. The numerator is evaluated using Filon's

quadrature (Filon, 1926).

The effects of distributing the Bi numbers on the transient and frequency response for the two reaction chain is shown in figure 5-3. The frequency response, here presented as a Nyquist plot, indicates a rapid convergence to an effectively lower dynamic order as Bi drops. This means that the second order character in the transfer function diminishes, figure 5-3a, because of time scale separation, and the dynamic behavior should resemble a lower order response. This prediction is confirmed by numerically integrating the full model, figure 5-3b. The figure shows how the transient response of the two reaction chain approaches that of the one reaction chain as Bi drops. At Bi = .01 the response of the two chains is essentially indistinguishable.

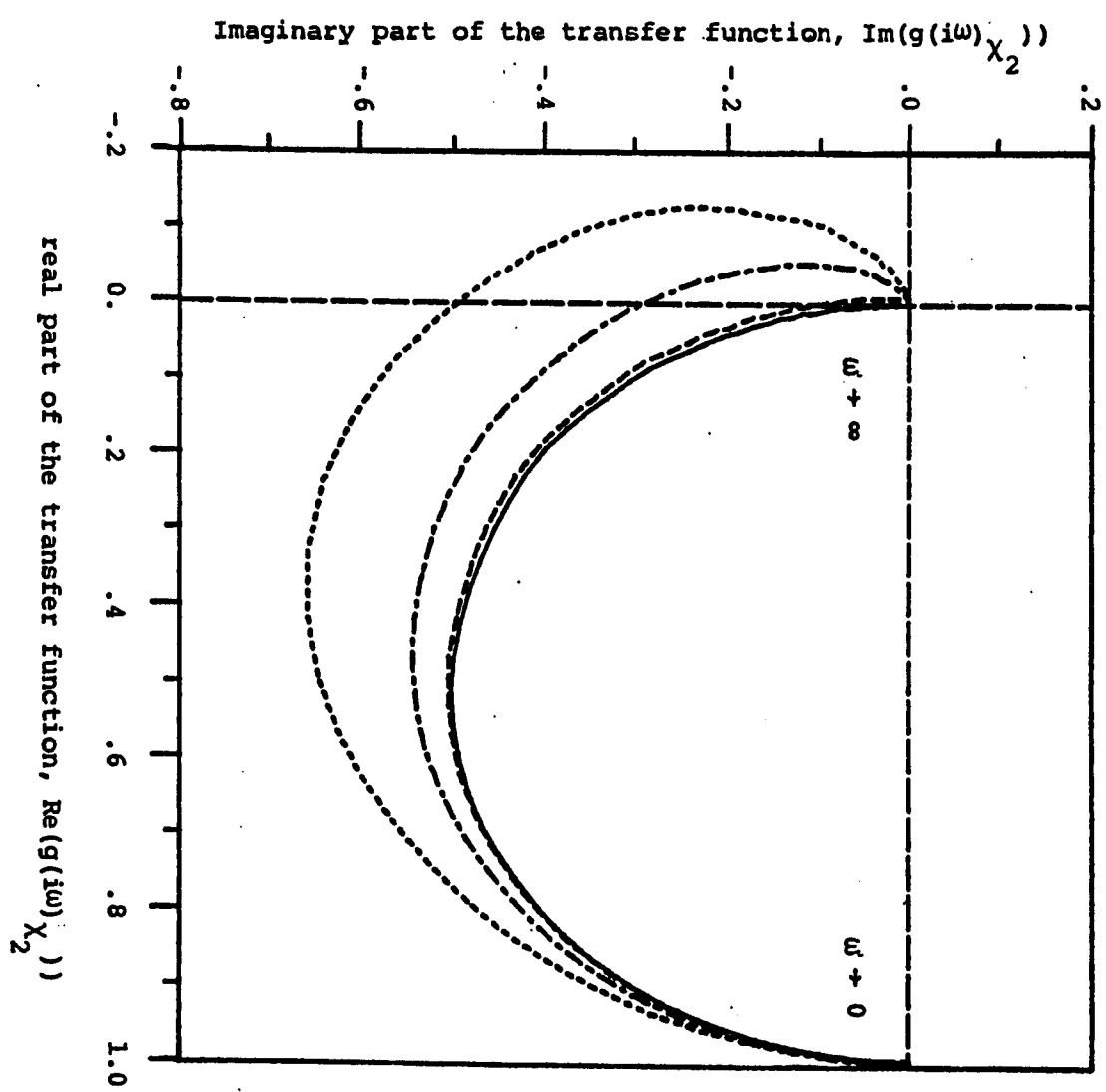
#### 5.2.5. Model reduction - The method of moments.

We are now in a position to reduce the order of the dynamic description of the reaction chain. As we have seen in the preceding discussion the essential dynamic characteristics are expressed through the moments and they are, under many important circumstances, mostly specified by relatively few kinetic parameters. We now use this property as the basis for model reduction and our goal is to preserve the dynamic properties expressed by the moments. This procedure is known as the method of moments and one simply equates the moments of a higher order description to those of a lower order approximate model. Then the parameters of the approximate model can

Figure 5-3.

- a) The influence of the Binding number  $Bi_1$  on the Nyquist plot for the same two reaction chain as in figures 5-1 and 5-2. The Nyquist plot shows the real part of  $g(i\omega)$  on the X-axis and the imaginary part of  $g(i\omega)$  on the Y-axis for frequencies over the range from zero to infinity. The curves start out at (1,0) for  $\omega = 0$  and end in the origin when  $\omega \rightarrow \infty$ . Dotted curve -  $Bi_1 = 1$ , dashed/dotted curve -  $Bi_1 = .1$ , dashed curve -  $Bi_1 = .01$ . The other parameters are:  $Qs_1 = Qs_2 = .1$ ,  $St_1 = St_2 = .01$ ,  $Bi_2 = 1$ ,  $Sa_{1,2} = 1$  and  $\bar{\Psi} = .2$ .
- b) the transient response corresponding to part a), using a square pulse in the input flux,  $\Psi'$ , of duration  $\tau_3$  (=167.87) and height .1.

FIGURE 5-3a.



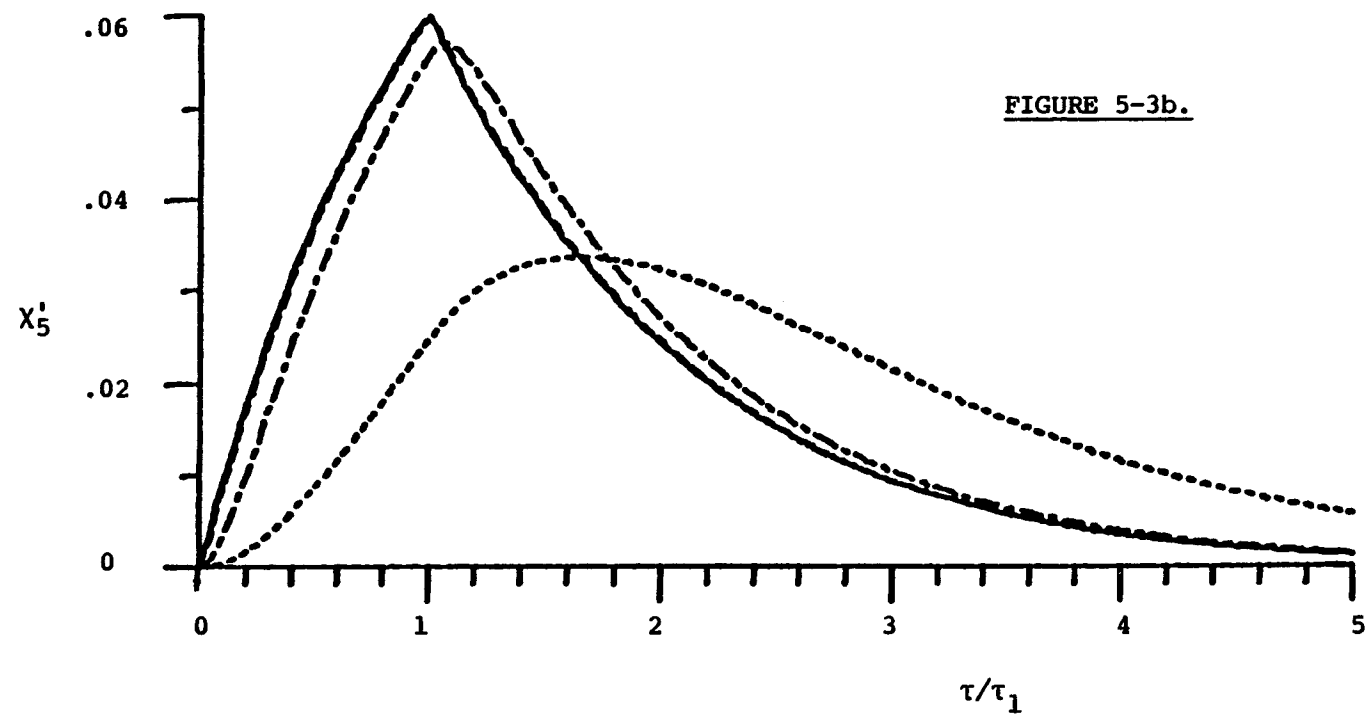


FIGURE 5-3b.

be computed knowing the moments of the higher order description. As many moments are equated as parameters needed to be determined (for a discussion of this technique see for example Gibilaro and Lees, 1969), and here we aim for at most three parameter descriptions.

Adequate dynamic representation can be obtained in the form of low order transfer functions. These are shown in table 5-2 and are of the general form of equation 40 so that their moments can be evaluated from equations 45-47, see appendix B. Then by substituting the moments of the higher order description into the expressions in table 5-2 one can obtain the parameters for the reduced description. This is readily done (appendix B) and the results are shown in the table. The moments for an arbitrary reaction chain may not be analytically attainable. They can be obtained numerically, however, and the parameters of the reduced description are readily evaluated.

We have found that the reduced linear descriptions represent the transient response of the exact model well at low flux values, or in the so-called "linear" region ( $\bar{\sigma} \leq 1$ ) of Michaelis-Menten kinetics. In figure 5-4 we have fitted a five reaction chain in which the Bi numbers are successively reduced by a factor of one half, but all other properties are the same. The Nyquist plot of figure 5-4a shows that as the order of the fitted transfer function increases the frequency content of the reduced approximation approaches that of the full description. Transient response of the low order transfer functions and the exact description is shown in figure 5-4b; as the order of the approximate model increases better representation is

Table 5-2.

Low order transfer functions and  
their parameters given in  
terms of their moments\*

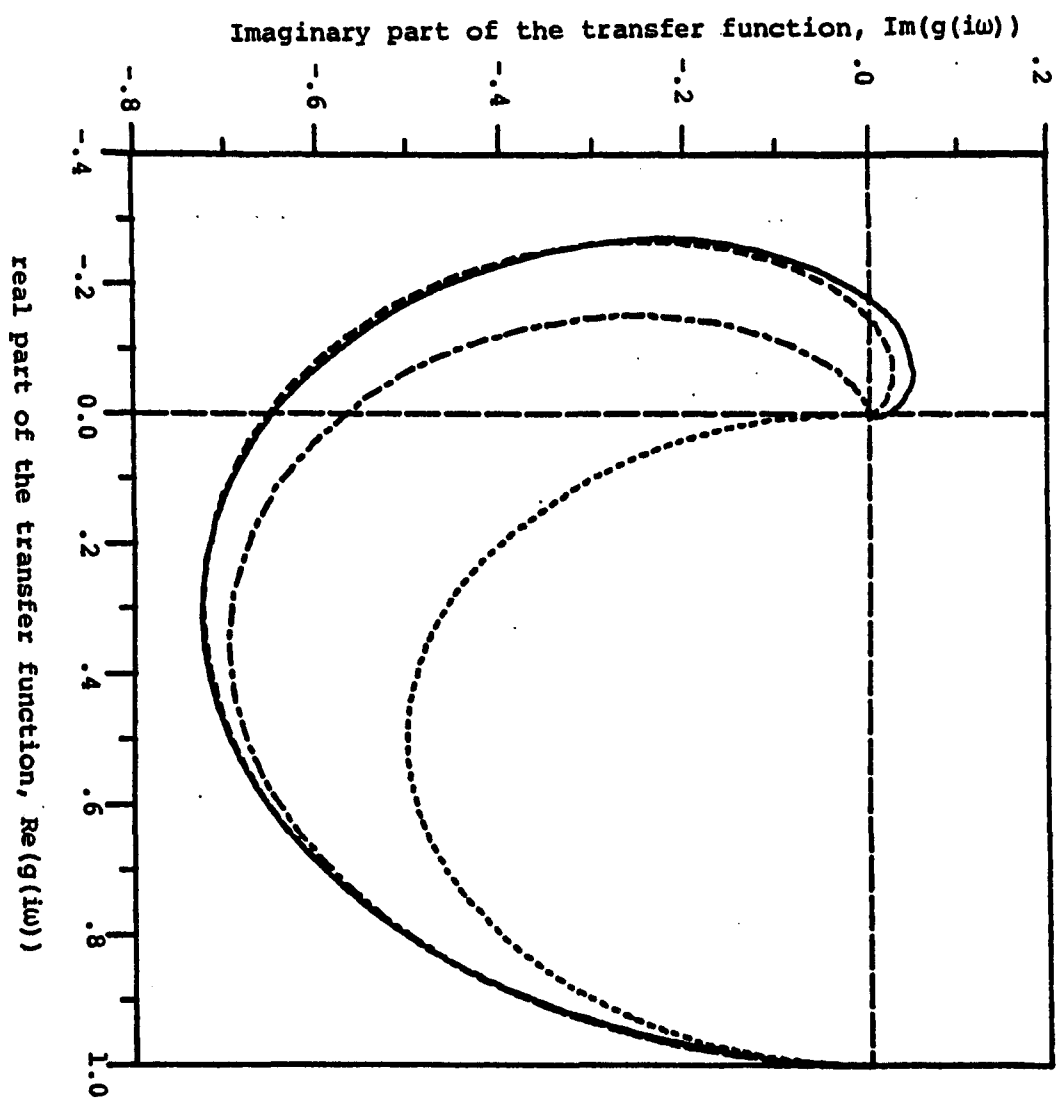
<u>Transfer function</u>	<u>Parameters</u>
1st order	
$\frac{1}{\tau s + 1}$	$\tau = M_1$
2nd order	
$\frac{1}{\tau^2 s^2 + 2\tau\xi + 1}$	$\tau^2 = \frac{1}{2} (M_1^2 - T_2)$
or	$\xi = M_1 / 2\tau$
$\frac{1}{(\tau_1 s + 1)(\tau_2 s + 1)}$	$\tau_1, \tau_2 = \tau \left[ \xi \pm \sqrt{\xi^2 - 1} \right]$
3rd order	
$\frac{1}{(\tau_a s + 1)(\tau_b s^2 + 2\tau_b\xi s + 1)}$	$\tau_a^3 - M_1 \tau_a^2 + \frac{1}{2} [M_1^2 - T_2] \tau_a - \frac{1}{6} [T_3 + M_1^3 - 3T_2 M_1] = 0$ $\tau_b^2 = [T_3 + M_1^3 - 3T_2 M_1] / 6\tau_a$
or	$\xi = (M_1 - \tau_a) / 2\tau_b$ $\tau_1 = \tau_a$
$\frac{1}{(\tau_1 s + 1)(\tau_2 s + 1)(\tau_3 s + 1)}$	$\tau_2, \tau_3 = \tau_b \left[ \xi \pm \sqrt{\xi^2 - 1} \right]$

\*  $M_1$ : First moment $T_2, T_3$ : Second and third moment around the mean

Figure 5-4.

Illustration of model reduction. The full model is a reaction chain with five identical reactions ( $St_i = .01$ ,  $Qs_i = .1$  and  $Sa_{i-1,i} = 1$ ) except the binding numbers decrease successively by a factor of one half,  $Bi_1 = 1$ ,  $Bi_2 = 1/2$ ,  $Bi_3 = 1/4$ ,  $Bi_4 = 1/8$  and  $Bi_5 = 1/16$ . The fitted low order transfer functions are as follows: Dotted curve - first order with  $\tau_1 = 325.33$ , dashed/dotted curve - second order with  $\tau_1 = 184.8$  and  $\xi = .88$ . dashed curve - third order with  $\tau_a = 179.75$ ,  $\tau_b = 89.39$  and  $\xi = .815$  (the moments are  $M_1 = 325.33$ ,  $T_2 = 3.752 \times 10^4$  and  $T_3 = 1.08 \times 10^7$ ) a) Nyquist plot, and b) transient response to a square pulse of duration 10 and height .1.

FIGURE 5-4a.



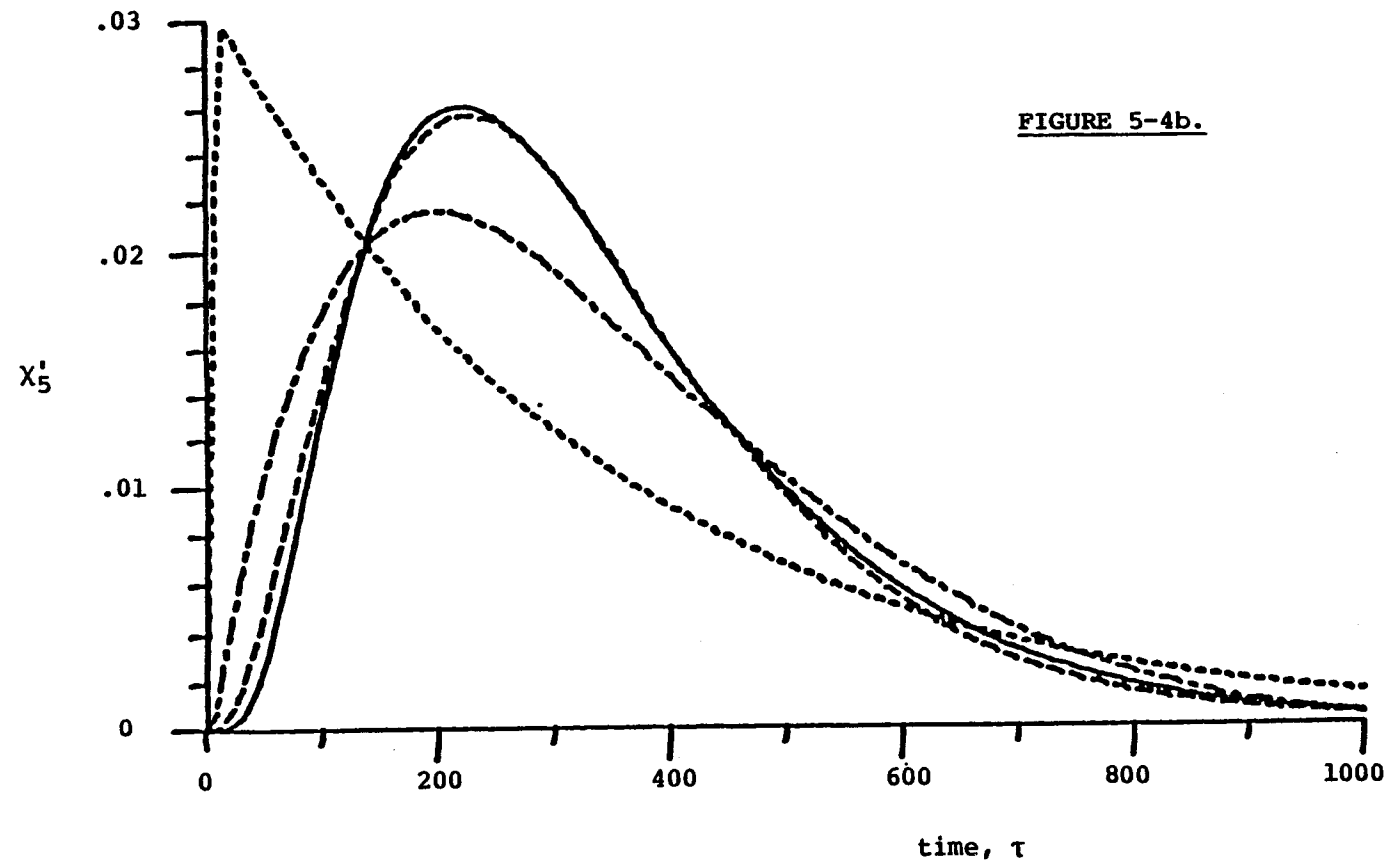


FIGURE 5-4b.

obtained.

What we have achieved here is to develop a three parameter third order dynamic description of a tenth order nonlinear model that contains eighteen independent parameters. The third order transfer function seems to represent the transient response of the five reaction chain adequately for moderate perturbations from steady state. Clearly there are limitations to the reduced description. The most serious problem that we have found is that the reduced model breaks down as the perturbations from steady state become large and in particular if the saturation region, where the non-linear effects show up, is approached. This is shown in figure 5-5. As the deviation from steady state becomes large, meaning more than approximately 20% deviation from steady state, significant non-linear characteristics show up and the linear model fails to give good representation.

### 5.3. Discussion and Conclusions.

#### 5.3.1. Trials and tribulations of metabolic modellers.

The development of mathematical models for metabolic networks and concomitant parameter estimation is hampered by several intrinsic, and seemingly insurmountable, difficulties. These difficulties arise from basically three sources:

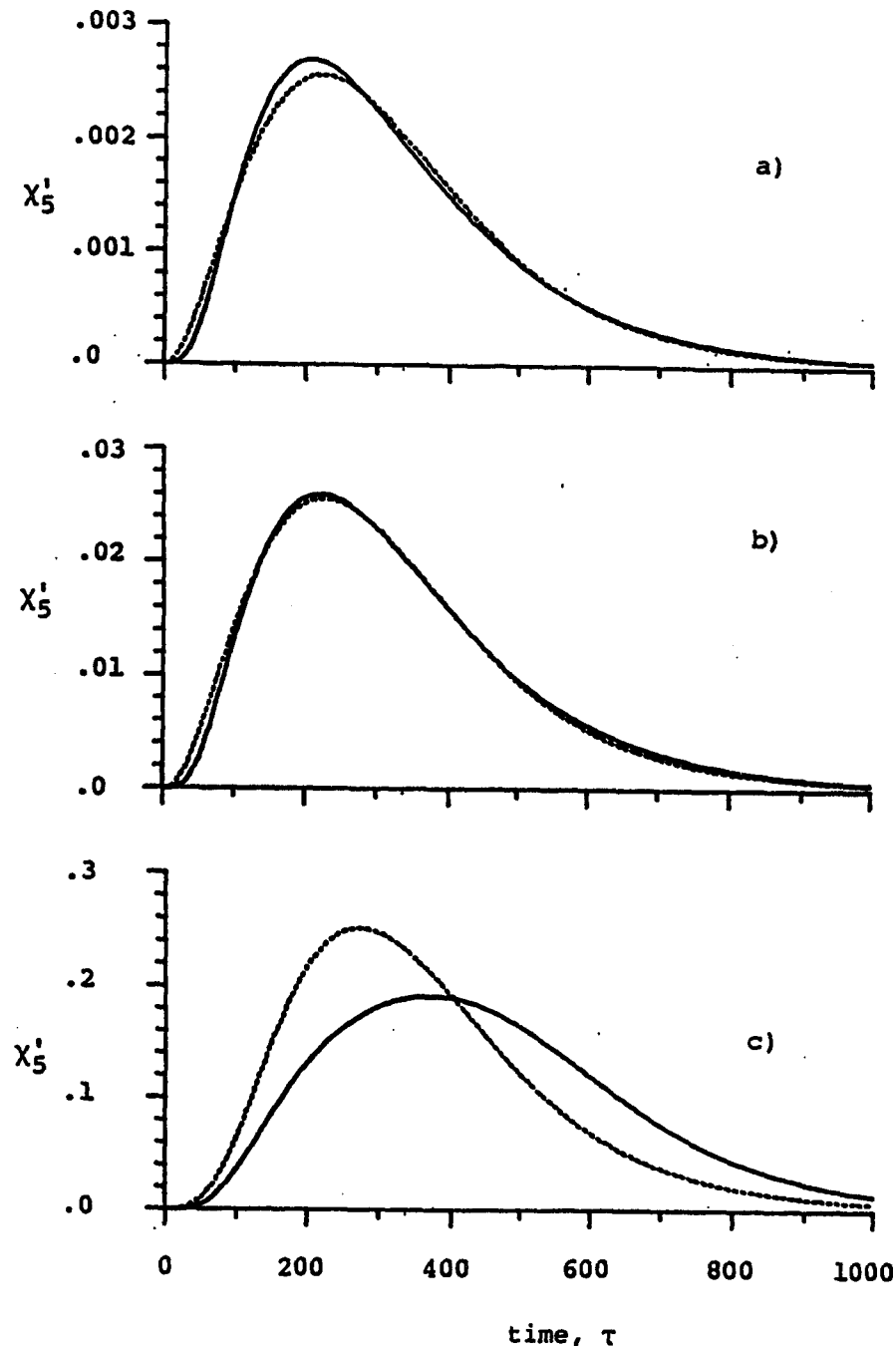


Figure 5-5. Illustration of how the linear reduced model fails to represent chain dynamics as deviation from the steady state increases, a) 1% deviation, b) 10% deviation, and c) 100% deviation. Parameters the same as in figure 4, except the square pulse used is; a)  $h = 1$ ,  $t_1 = 1$ , b)  $h = 1$ ,  $t_1 = 10$ , and c)  $h = 1$ ,  $t_1 = 100$ .

- 1) Mathematical models based on mass action kinetics are very large even for the simplest networks. In addition they are plagued by mathematical intractability, which has been demonstrated rigorously for the simple Michaelis-Menten mechanism (Hommes, 1962a, Darvey et al., 1978). These features limit both analytical work, and the concomitant conceptual progress, as well as making full numerical integration notoriously difficult (e. g. Garfinkel, Garfinkel, Pring, Green and Chance, 1970, Park, 1974, Heinrich, Rapoport and Rapoport, 1977)
- 2) Until now it has been very difficult to obtain extensive and reliable data on in vivo metabolism as it takes place in the intact cell. However the presently available NMR techniques provide a hope for a remedy to this problem.
- 3) The detailed kinetic models contain a large number of parameters. Since it is difficult to estimate all of these from available experimental data this calls for an assessment of the relative importance of the various kinetic and concentration parameters. Such an assessment will give us a basis for reducing the dynamic description to approximate ones with fewer, hopefully identifiable, parameters and also to determine if such reduction is feasible.

In the first part of this thesis we have tried to develop approximate dynamic descriptions of simple biochemical transformations with the goal of resolving the mathematical aspects of the above listed problems. Inspite of the mathematical

intractability of enzyme kinetic models we have succeeded in examining key dynamic features and their parametric sensitivity through judicious scaling and full linear analysis. The investigation becomes naturally focused on two key properties: the relaxation times and dynamic interactions between constituent species.

### 5.3.2. The time constants.

The numerical values for the kinetic constants tend to be such that the distribution of relaxation times is wide. This feature leads to a reduction in effective dynamic order, e. g. figure 5-3, and naturally forms a basis for model reduction. The demonstrated success in this respect is particularly important as this wide distribution of time constants is the source of the numerical stiffness of the differential equations (e. g. Park, 1974).

In the present paper we carried out the model reduction via the method of moments. This technique ignores the structure of the underlying model and yields effectively a phenomenological description in terms of the lower temporal moments which all are physically meaningful. The result is simple enough to offer hope for parameter estimation from data such as obtained from in vivo NMR. The moments also provide the important link between the overall kinetic properties and those of the individual elements of the chain. Hence we develop some capability to assess the relative importance of system parameters.

However the resulting reduced description is limited to a range around the steady state about which the equations have been linearized. Preliminary indications are that the approximations to transient behavior presented herein are reasonable under physiological conditions, where the substrate concentrations are 20-100% of their  $K_m$  values, and hence is hopefully sufficient for our purposes.

Since a wide distribution of kinetic properties seems to be the rule in metabolic systems, it is pertinent to speculate on the reasons for such a design. Perhaps the most obvious reason has to do with stability considerations. In general as the order of a process to be controlled increases instability is more likely. Systems of such complexity as metabolic networks are expected to become easily destabilized unless some special precautions in design and parameter selection are taken. One way to achieve this goal is to distribute the kinetic properties in the reaction chains and thereby lower the effective order of the system. The resulting time scale separation would enable a complicated network of interacting reaction sequences to tolerate larger and a wider variety of disturbances and hence will improve overall robustness. This is clearly advantageous and one really should not be surprised to find that the dynamic behavior of linear reaction sequences in metabolic networks will resemble low order dynamic systems.

### 5.3.3. Species interactions.

Another commonly used reduction technique for biochemical kinetics is the quasi-stationary assumption, which is used herein to one reaction relative to another. Conversely to the method of moments it assumes an underlying model structure. Due to the requirement of model structure preservation the conditions for the applicability of the quasi-steady state assumption are stringent: it not only requires well separated time scales but it also requires limited species interactions (chapter 2). These interactions are assessed through modal analysis. The quasi-steady state assumption, when applicable, offers the advantage of yielding a reduced non-linear description whose applicability is independent of deviations from any particular steady state: it gives a globally valid description.

### 5.4. Summary.

Kinetics of linear sequences of enzymatic reactions converting a single substrate into a single product are examined with emphasis on obtaining the relationship between the individual kinetic parameters and overall dynamic behavior. Chains of reactions exhibiting irreversible Michaelis-Menten kinetics are examined via scaling, linearization and modal analysis. The modal analysis gives the conditions under which the quasi-steady state assumption is

applicable for one reaction relative to another in such a reaction sequence. The linearized description permits characterization of the transient response in terms of temporal moments. The moments provide useful physical insight and also provide a basis for systematic model reduction.

PART II

BIOCHEMICAL REGULATION

## CHAPTER 6

## SINGLE BIOCHEMICAL CONTROL LOOPS:

## LOCAL STABILITY ANALYSIS

The intermediary metabolism is a complex network of interacting enzyme catalyzed reactions which transform substrate molecules, such as sugars and fats, into energy and a variety of products, most importantly monomers such as amino and nucleic acids that are used to synthesize macromolecules. The large number of products and wide variability of demand and environmental conditions imply a multi-objective operation and to achieve all objectives simultaneously requires an elaborate regulatory structure. Self-regulatory ability is a key feature which allows cells to make internally their own decisions on how to allocate available energy and material resources.

The regulatory structure is in essence a complex hierarchy of interacting control loops, ranging from control by hormones and cofactors to the metabolites themselves. In this second part of the thesis I begin analysis of the control structure, and, in accord with the hierarchical modelling approach, I start by considering the simplest of the constituent control loops. These are regulated

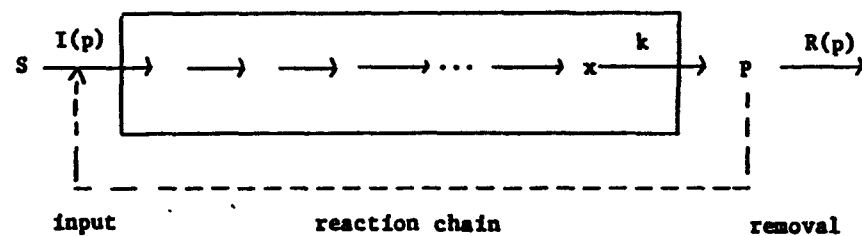
reaction chains consisting of three elements: a regulatory enzyme, or control element, controlling mass flux into the unit, a passive reaction sequence, or process element, completing the chemical transformations required of the chain, and a mechanism for removal of the reaction product to the next compartment of the metabolic network. The product of the reaction sequence can combine with the regulatory enzyme to control input flux and thus provides a feedback loop. Such a structure is indicated schematically in figure 6-1.

Simple feedback of this kind was the first type of metabolic regulation to be extensively investigated, starting with the studies of Umbarger (1956) and of Yates and Pardee (1956). Although a variety of regulatory mechanisms of enzyme activity have been observed (Stadtman, 1966, 1970), the regulatory action is most often through an allosteric mechanism (Sols 1981).

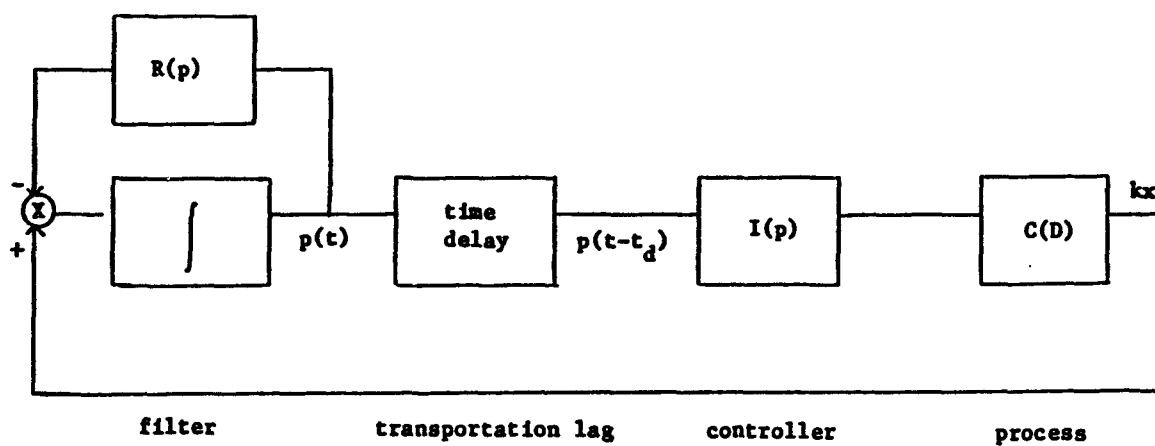
Initially we seek domains of qualitatively different dynamic behavior. This goal is attained via bifurcation analysis which is performed by examining the properties of the linearized model at the stationary point and it gives us the desired information about the qualitative nature of global dynamics. We start our analysis from as general a standpoint as possible and try to see how much of system behavior is independent of kinetic detail. The eigenvalues of the characteristic equation associated with the linearized model are found to give criteria for static and dynamic bifurcations, without having to specify the dependence of input and removal rates on product concentration in detail. When the functional dependence of

a) Kinetic scheme:

Figure 6-1. The single biochemical control loop.



b) Block diagram:



input and removal rate on product concentration are specified, the general result presented herein can be projected into the parameter spaces formed by the parameters of the chosen rate laws.

The local analysis suggests that static bifurcations, leading to multiple steady states, only appear with positive feedback and that dynamic bifurcations, leading to oscillatory behavior, only occur with negative feedback. This feature decomposes the problem down into two parts and in chapters 7 and 8 we introduce physiologically significant rate laws for input and removal rates and map out the general bifurcation criteria into relevant parameter spaces.

### 6.1. Objectives and Approach.

Our primary goal is to characterize the dynamic response of the control loop to perturbations in both genetically determined kinetic properties and process dependent concentrations. We are particularly concerned with identifying conditions leading to static and dynamic bifurcations, multiple steady states and sustained oscillations respectively, since such behavior is an essential characteristic of biological function. The technique we shall employ is local stability analysis based on linearization of the defining equations about appropriate steady states. We are moreover interested in determining how much information can be obtained without detailed knowledge of system kinetics.

### 6.1.1. System definition.

Our system is defined in both chemical and process control terminology in figure 6-1. It is a reaction sequence into which a substrate S is introduced through a regulatory enzyme whose kinetics are determined by the function  $I(s, p, \dots)$ , where the incomplete argument list of I represents concentrations of chemical species affecting the flux and a number of kinetic parameters. After the initial reaction the metabolite undergoes a series of chemical transformations through a sequence of enzymatic reactions whose dynamics are collectively described by a dynamic operator  $C(D)$ , where D represents the time derivative ( $D = d/dt$ ). This dynamic operator relates the input flux (I) to the rate of formation ( $kx$ ) of P, where k is a first order rate constant, and x is the concentration of the last enzyme-substrate complex in the reaction chain. The final product P regulates the input flux via binding to the regulated enzyme and thus closes the control loop. At the same time the product is removed from the system according to the rate law  $R(p, \dots)$ .

The reaction rates of the regulated reaction and removal reaction can depend on a variety of factors. For instance the total concentrations of the enzymes catalysing these steps typically determine the saturation velocities. The input and removal rates may also be influenced by other factors such as the levels of other metabolites and cofactors such as the adenyl nucleotides; the input rate is certainly influenced by the availability of the initial

substrate. Herein we take these factors to be constant, and investigate the dynamic behavior for any constant set of these factors, and we shall confine our attention here to the end product concentration  $p$ , but we can expect additional influences on the loop when it is integrated into a larger reaction network.

#### 6.1.2. Kinetic description.

By assuming the binding of the product  $P$  to the regulatory enzyme to be fast the kinetic description of this loop reduces to a pair of differential equations. The first provides a dynamic description of the reaction chain:

$$C(D)[kx] = I(p(t-t_d)) \quad (1)$$

where the steady state gain of the dynamic operator is unity ( $C(D) \rightarrow 1$  as  $t \rightarrow \infty$ ). If the final product has to be transported, e. g. by diffusion from the formation site to the regulatory site, a time lag  $t_d$  occurs.

The second differential equation is a dynamic mass balance on the final product

$$\frac{dp}{dt} + R(p) = Dp + R(p) = kx \quad (2)$$

We are particularly interested in the steady state condition which is simply that all the fluxes, the production rate of product, the input rate and the removal rate, are equal

$$I(\bar{p}) = k\bar{x} = R(\bar{p}) \quad (3)$$

Here the overbar denotes steady state conditions.

### 6.1.3. Interpretation.

In attempting to elucidate the control strategy inherent in the construction of the loop it is useful to interpret kinetic behavior in the terminology of process control. In doing so we define the following:

- 1) The process to be regulated is the reaction chain leading to the formation of the product P; it is described by the dynamic operator  $C(D)$ .
- 2) The regulated variable is taken to be the rate of product formation by the reaction chain,  $k_x$ . This choice is arbitrary during the discussion of the isolated loop, but will prove convenient when the demand for P is added at a later stage in our series. By the same token we define the setpoint as the "desired" rate of product formation as determined by the steady state equation. This definition can only be completed when a larger system is considered.
- 3) A low-pass filter is provided by the product pool which tends to buffer rapid perturbations in the flux and it is mathematically expressed through the dynamic mass balance on the end product, equation 2. Physically it means that rapid fluctuations in the fluxes dampen out and the concentration of P does not move as radically.
- 4) The feedback signal is provided by concentration level of P, which must diffuse to the regulated enzyme, and this transport process can introduce a time lag. As discussed below such a time

delay imposes serious limitations on the achievable control performance. It appears that in general diffusion paths are sufficiently short that such time delays are negligible, chapter 2 and appendix A.

- 5) The regulatory element is clearly the regulatory enzyme. This controller is really comprised of two elements: a) Detection. The level of end product is detected by its association with the regulatory enzyme. This sensor mechanism is assumed to be fast compared to other time constants in the loop and in the above model we have not associated any dynamics with this process. b) Implementation. Once the level of the product has been detected control action is implemented via a conformational change in the enzyme molecule. The time constants of conformational changes in protein are typically much faster than the time constants of interest here (Careri, Fasella and Gratton, 1975), and hence we ignore all dynamics associated with this process. The two processes a) and b) are combined in the input rate I. This is reasonable in view of control theory since it is desirable to have the time constants of detection and implementation faster than those of the process to be regulated to facilitate good control performance. The gain of the controller is defined as the sensitivity of the input variable to the feedback signal which is simply the partial derivative of I with respect to p.
- 6) The manipulated variable is the influx I of substrate into the reaction chain via the regulatory enzyme.

The control system can be viewed as comprised of two parts. First we have a non-linear first order filter, characterized by R, and a non-linear static element I. These two elements are not independent since I and R are related through the steady state equation 3. The gain can thus not be increased without changing the response characteristics of the filter and that imposes some constraints on the design of the control system.

#### 6.1.4. Scaling.

We are now ready to start a parametric study, and since there are many important parameters our first task is dimensional analysis via appropriate scaling. Scaling is not a unique procedure, but we present a particularly convenient choice here which puts us in the happy situation of being able to separate genetically and process determined parameters. This feature becomes explicit when the functional forms of I and R are specified and will be thoroughly discussed in chapters 7 and 8.

We now introduce our scaled variables:

$$\Psi(\pi) = \frac{I(p)}{I_{\text{sat}}} , \quad \theta = \frac{kx}{I_{\text{sat}}} , \quad \Omega(\pi) = \frac{R(p)}{I_{\text{sat}}} \quad (4)$$

Here all the flux variables are scaled to the saturation flux,  $I_{\text{sat}}$  through the regulated reaction. This forces all the flux variables to vary from zero to unity. Time is scaled to the characteristic time constant of the reaction chain,  $t_c$ , as  $\tau = t/t_c$ , and the product as  $\pi = p/I_{\text{sat}}t_c$ .

Our description now takes the form

$$C(\mathcal{D})[\theta] = \Psi(\pi) \quad (5)$$

for the process and

$$F(\mathcal{D})[\pi] = \pi + \Omega(\pi) = \theta \quad (6)$$

for the filter. Here  $\mathcal{D}$  denotes the derivative with respect to  $\tau$  ( $\mathcal{D} = d/d\tau = t_c d/dt = t_c D$ ), and  $F$  is the filter operator. The steady state equation is now

$$\Psi(\bar{\pi}) = \bar{\theta} = \Omega(\bar{\pi}) \quad (7)$$

## 6.2. The Dynamic Operator $C(\mathcal{D})$ .

### 6.2.1. General operators.

The dynamic operator  $C(\mathcal{D})$ , based on mass action kinetics, can be written as a set of  $n$  first order non-linear ordinary differential equations, where  $n$  is the order of the operator

$$\underline{d\theta}/d\tau = f(\underline{\theta}) + \underline{\beta}(\Psi(\pi) - \theta) \quad (8)$$

Here

$$\underline{\theta} = (\theta_1, \theta_2, \dots, \theta_n)^T, \quad \theta = \theta_1 \quad (9)$$

$$\underline{\beta} = (0, 0, \dots, 1)^T \quad (10)$$

are  $n$ -dimensional vectors. The  $n$ -dimensional function  $f(\bar{\theta})$  vanishes at steady state so that

$$f(\bar{\theta}) = \underline{0}, \quad \Psi(\bar{\pi}) = \bar{\theta} = \Omega(\bar{\pi}) \quad (11)$$

are the steady state conditions. Local description of the dynamic

operator can be obtained through linearization and represented as a transfer function. Such description can be used for the local stability analysis to follow but it has also been found to give reasonable representation of the dynamics under typical in vivo situations, chapter 5.

#### 6.2.2. Linear operators - Transfer functions.

As discussed in chapter 5 a local description of a reaction chain consisting of  $m$  irreversible Michaelis-Menten reactions can be obtained through linearization as

$$\left( \prod_{i=1}^{2m} (\tau_i \mathcal{D} + 1) \right) \theta = \psi(\pi) \quad (12)$$

This description can be transferred into the Laplace domain as

$$\frac{\theta}{\psi(\pi)} = \frac{1}{\prod_{i=1}^{2m} (\tau_i s + 1)} = \frac{1}{p(s)} \quad (13)$$

Here  $s$  is the Laplace variable which has replaced  $\mathcal{D}$ . These transfer functions contain only poles, the negative reciprocals of the time constants  $\tau_i$ , and the dynamic operator can be expressed through the pole polynomial  $p(s)$ . If the distribution of time constants is wide the order of the above linear operator is effectively reduced as described in chapter 5, and simpler low-order descriptions can be obtained as shown in table 6-1.

Frequently the saturation velocities of regulated reactions are much lower than those of other enzymes. This would force unregulated

Table 6-1.

## Linear operators used to represent the reaction chain

<u>Order</u>	<u>Pole polynomial p(s)</u>	<u>Reference time <math>t_c</math></u>	<u>Remarks</u>
1	$(s+1)$	$t_1$	$t_1$ : time constant for the first order system
2	$(s^2 + 2\xi s + 1)$	$t_2$	$t_2$ : time constant for the second order system
3	$(s^2 + 2\xi s + 1)(\phi^{-1} s + 1)$	$t_2$	$t_2$ : time constant for the second order system $\phi = t_2/t_1$ and is normally assumed to be larger than unity
n	$\prod_{i=1}^n (\tau_i s + 1)$	$\min_i \{t_i\}$	The largest time constant is unity
time delay	$p'(s) = p(s) e^{-\tau_d s}$	$\min_i \{t_i\}$	$p(s)$ : pole polynomial containing no time delays $\tau_d$ : time delay $= t_d/t_c$

reactions described by Michaelis-Menten kinetics to operate in the pseudo-first order region. Under such circumstances a linearized description is a close approximation to the exact behavior for a wide range around the stationary point. An alternative treatment, incorporating non-linear effects, is to apply the quasi-steady state assumption (Briggs and Haldane, 1925) and extend it by the use of singular perturbations as described in Heineken, Tsuchiya and Aris (1967) and Meiske (1978). This approach is algebraically cumbersome and should only be considered if linear descriptions prove inadequate to describe experimental data.

### 6.3. Local Stability Analysis.

The normal starting point for assessing behavior of a dynamic system is through local stability analysis, in which the equations describing the system are linearized around a stationary point. The eigenvalues of the associated characteristic equation provide a basis for predicting the occurrence of static and dynamic bifurcations.

#### 6.3.1. Linearization.

The equations that describe the single biochemical control loop contain two non-linear elements, assuming that the reaction chain can be described by a transfer function. They are the rate laws that describe the input rate,  $\Psi(\pi)$ , and removal rate,  $\Omega(\pi)$ . These

functions may be expanded into Taylor series around the stationary point as

$$\Psi(\pi) = \Psi(\bar{\pi}) + \bar{\Psi}_{\pi}(\pi - \bar{\pi}) + \frac{1}{2}\bar{\Psi}_{\pi\pi}(\pi - \bar{\pi})^2 + \dots \quad (14)$$

$$\Omega(\pi) = \Omega(\bar{\pi}) + \bar{\Omega}_{\pi}(\pi - \bar{\pi}) + \frac{1}{2}\bar{\Omega}_{\pi\pi}(\pi - \bar{\pi})^2 + \dots \quad (15)$$

where the subscript  $\pi$  denotes a partial derivative with respect to  $\pi$ . These series are then truncated after the linear term and substituted into the differential equations. This yields the linear system of equations which in the Laplace domain take the form

$$p(s)\theta' = \bar{\Psi}_{\pi} e^{\tau_d s} \pi' \quad (16)$$

$$F_{\pi}(s)\pi' = (s + \bar{\Omega}_{\pi})\pi' = \theta' \quad (17)$$

see section 5.2 for a description of the Laplace transforms. The prime denotes deviation variables from the steady state, denoted by the overbar,

$$\pi' = \pi - \bar{\pi}, \theta' = \theta - \bar{\theta} \quad (18)$$

The signs on the slopes at the stationary point are expected to be as follows: the sign on  $\bar{\Psi}_{\pi}$  is positive if the feedback regulation is one of activation (i. e. positive gain), and it is negative if the feedback interaction is inhibitory (i. e. negative gain). On the other hand the parameter  $\bar{\Omega}_{\pi}$  is expected to take positive values only.

### 6.3.2. The Eigenvalues.

The eigenvalues are the roots of the characteristic equation associated with the linearized model. One can combine equations 16

and 17 to get

$$(p(s)F_\pi(s)e^{-\tau_d s})\pi' = \bar{\Psi}_\pi \pi' \quad (19)$$

and the associated closed loop characteristic polynomial is

$$p(\lambda)F_\pi(\lambda)e^{-\tau_d \lambda} - \bar{\Psi}_\pi = 0 \quad (20)$$

The open loop poles (the roots of equation 20 when the gain  $\bar{\Psi}_\pi$  is zero) are simply the roots of  $p(s)$  and  $F_\pi(s)$ . The roots of  $p(s)$  are expected to be real negative. The root of  $F_\pi(s)$  is  $-\bar{\Omega}_\pi$  and as mentioned above  $\bar{\Omega}_\pi$  is expected to be positive. If  $\bar{\Omega}_\pi$  is negative the loop is open loop unstable which is expected to be undesirable, see chapter 4. These roots then move around in the complex plane as the feedback gain  $\bar{\Psi}_\pi$  varies from zero and trace out loci in the complex plane known as root loci.

Two different sets of eigenvalue loci are of interest:

1) The first set surrounds the region where static bifurcations occur, or where multiple steady state solutions exist. This locus is at the point where a root of equation 20 goes through the origin in the complex plane and the Jacobian matrix becomes singular. Zero root occurs when  $\bar{\Omega}_\pi = \bar{\Psi}_\pi$  and multiplicity of steady state solutions is possible when

$$\bar{\Psi}_\pi > \bar{\Omega}_\pi \quad (21)$$

or when the slope of the input rate in the stationary state exceeds that of the removal rate. This simple criterion is necessary and sufficient to determine the existence of multiple steady states (Tyson and Othmer, 1978), and it shows that the dynamic properties of

the reaction chain do not influence the occurrence of multiple steady state solutions.

2) The second set of loci of interest is when a pair of complex conjugate roots crosses the imaginary axis,  $\text{Re}(\lambda_i) = 0$ . These loci define the onset of dynamic bifurcations which define a region where the steady state point is dynamically unstable and periodic solutions may be found. These loci are readily obtained for delay free systems from the Routh criterion (see Coughanowr and Koppel, 1965) but are, in contrast to the case of static bifurcations, strongly dependent on the characteristics of the reaction chain operator. This leads to algebraic complications, but the intricacy of the algebra is not always overwhelming, and we shall now describe this condition for systems of particular interest here.

a) First-order reaction chains. The characteristic closed-loop polynomial is

$$(\lambda+1)(\lambda+\bar{\Omega}_\pi) - \bar{\Psi}_\pi = 0 \quad (22)$$

No purely imaginary roots exist for positive  $\bar{\Omega}_\pi$  and hence dynamic bifurcations do not exist in systems with a first order reaction chain.

b) Second-order reaction chains. The closed loop characteristic polynomial is now a cubic

$$\begin{aligned} & (\lambda^2 + 2\xi\lambda + 1)(\lambda + \bar{\Omega}_\pi) - \bar{\Psi}_\pi = 0 \\ & \lambda^3 - s_1\lambda^2 + s_2\lambda - s_3 = 0 \end{aligned} \quad (23)$$

where

$$S_1 = -(2\xi + \bar{\Omega}_\pi), \quad S_2 = 1 + 2\xi \bar{\Omega}_\pi, \quad S_3 = \bar{\Psi}_\pi - \bar{\Omega}_\pi \quad (24)$$

For a third order polynomial the criteria for imaginary roots can be obtained from the Routh array (Hamer, Akramov and Ray, 1981) as

$$S_3 - S_1 S_2 = 0, \quad S_3 < 0, \quad S_2 > 0, \quad S_1 < 0 \quad (25)$$

Using equation 24 these conditions translate into

$$\frac{\bar{\Psi}}{\pi} = -2\xi(\bar{\Omega}_\pi^2 + 2\xi \bar{\Omega}_\pi + 1) \quad (26)$$

which is the locus for purely imaginary roots for positive  $\bar{\Omega}_\pi$ .

The loci defining the regions of instability are shown in figure 6-2a For negative feedback the principal roots move towards each other on the real axis and join and then branch off and head towards the imaginary axis and eventually cross it, figure 6-2b. This crossing marks the onset of dynamic instability. The third root moves down the real axis. For positive feedback the opposite behavior is observed, figure 6-2c. The principal root moves up the real axis and crosses the origin where static bifurcations appear.

c) Third-order reaction chains. The closed loop characteristic polynomial is

$$\begin{aligned} (\phi^{-1}s+1)(s^2 + 2\xi s + 1)(s + \bar{\Omega}_\pi) - \frac{\bar{\Psi}}{\pi} &= 0 \\ \lambda^4 - S_1 \lambda^3 + S_2 \lambda^2 - S_3 \lambda + S_4 &= 0 \end{aligned} \quad (27)$$

where

$$\begin{aligned} S_1 &= -(\phi + 2\xi + \bar{\Omega}_\pi) & S_3 &= -(\phi + (1 + 2\xi\phi)\bar{\Omega}_\pi) \\ S_2 &= 1 + 2\xi\phi + (\phi + 2\xi)\bar{\Omega}_\pi & S_4 &= \phi(\bar{\Omega}_\pi - \bar{\Psi}_\pi) \end{aligned} \quad (28)$$

The criteria for purely imaginary roots of equation 27 are obtained

from the Routh array as (Hamer et al., 1981)

$$\begin{aligned} s_1 s_2 s_3 - s_3^2 - s_1^2 s_4 &= 0 \\ s_1 < 0, s_2 > 0, s_3 < 0, s_4 > 0 \end{aligned} \quad (29)$$

Substituting the expressions for the coefficients in these constraints does not give a particularly simple algebraic expression. For the special case when  $\phi = \xi = 1$ , i. e. when all three of the time constants are identical, the expression reduces to

$$\bar{\psi}_{\pi} = \frac{-8(\bar{\Omega}_{\pi} + 1)^3}{(\bar{\Omega}_{\pi} + 3)^2} \quad (30)$$

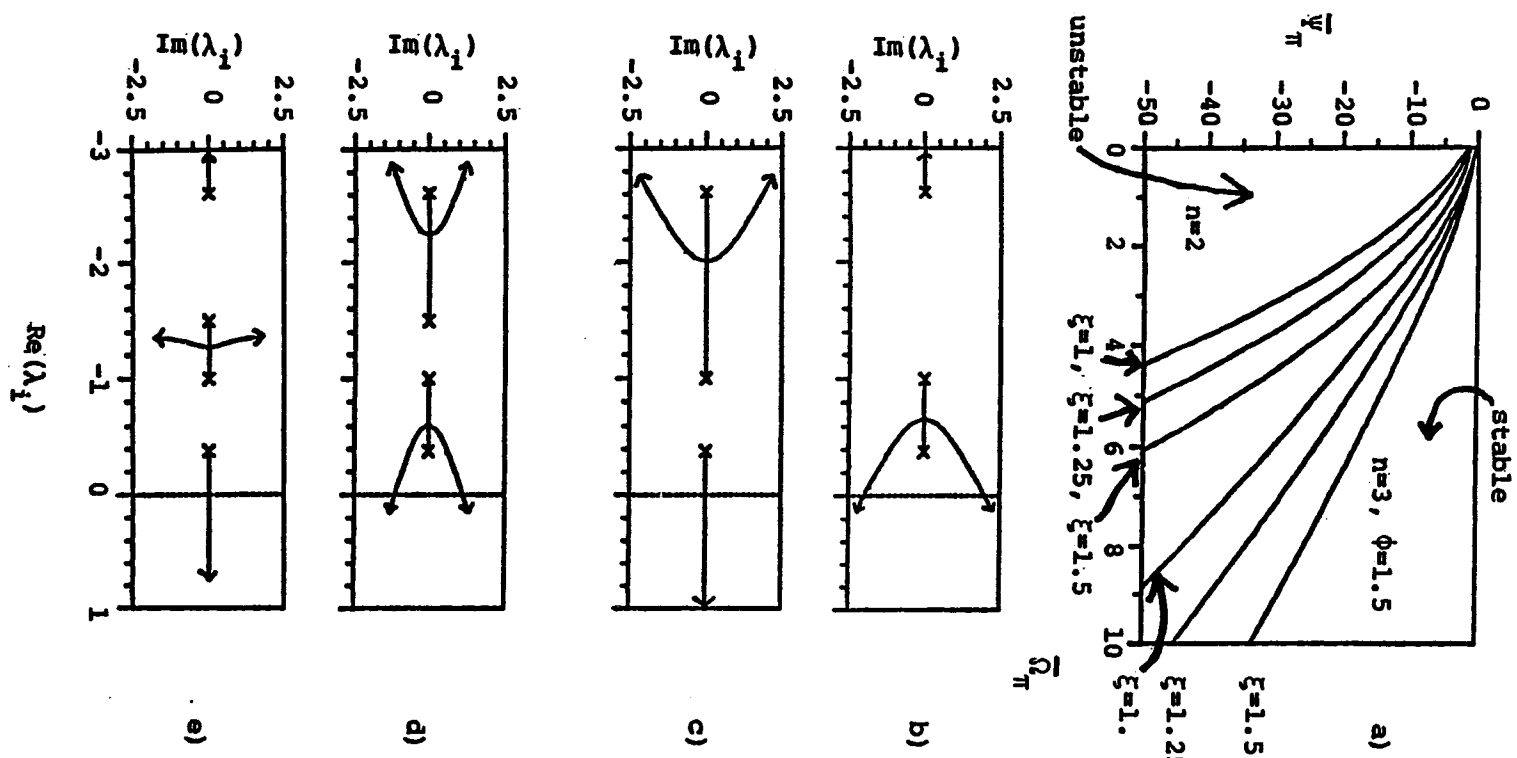
The loci marking the onset of dynamic instability are shown in figure 6-2a. The results are similar to those for the second order reaction chain except that now the principal roots move faster towards the imaginary axis. Another difference is that we also get a pair of secondary roots branching off the real axis, figure 6-2d. These roots are of minor significance since they move away from the imaginary axis and their real part is always much smaller than that of the principal roots.

d) Higher order reaction chains. For a loop with an  $n^{th}$  order reaction chain the closed loop characteristic polynomial is

$$\left( \prod_{i=1}^n (\tau_i \lambda + 1) \right) (\lambda + \bar{\Omega}_{\pi}) - \bar{\psi}_{\pi} = 0 \quad (31)$$

The locus for dynamic bifurcations can be located numerically by using the Nyquist criterion (Coughanowr and Koppel 1965). Results from such calculations are shown in figure 6-3a. As the order of the

Figure 6-2. Instability in the single biochemical control loop. a) Location of the loci marking the onset of dynamic bifurcations for  $n = 2, 3$ . b) Root locus for  $n = 2$ ,  $\xi = 1.5$  and  $\bar{\Psi} < 0$  or negative feedback ( $\bar{\Psi} = -15$  at the crossover point). c) Same as b) except  $\bar{\Psi} > 0$  or positive feedback. d) Root locus for  $n = 3$ ,  $\xi = 1.5$ ,  $\phi = 1.5$  and  $\bar{\Psi} > 0$  or negative feedback ( $\bar{\Psi} = -6.4$  at the crossover point). e) Same as c) except  $\bar{\Psi} > 0$  or positive feedback.



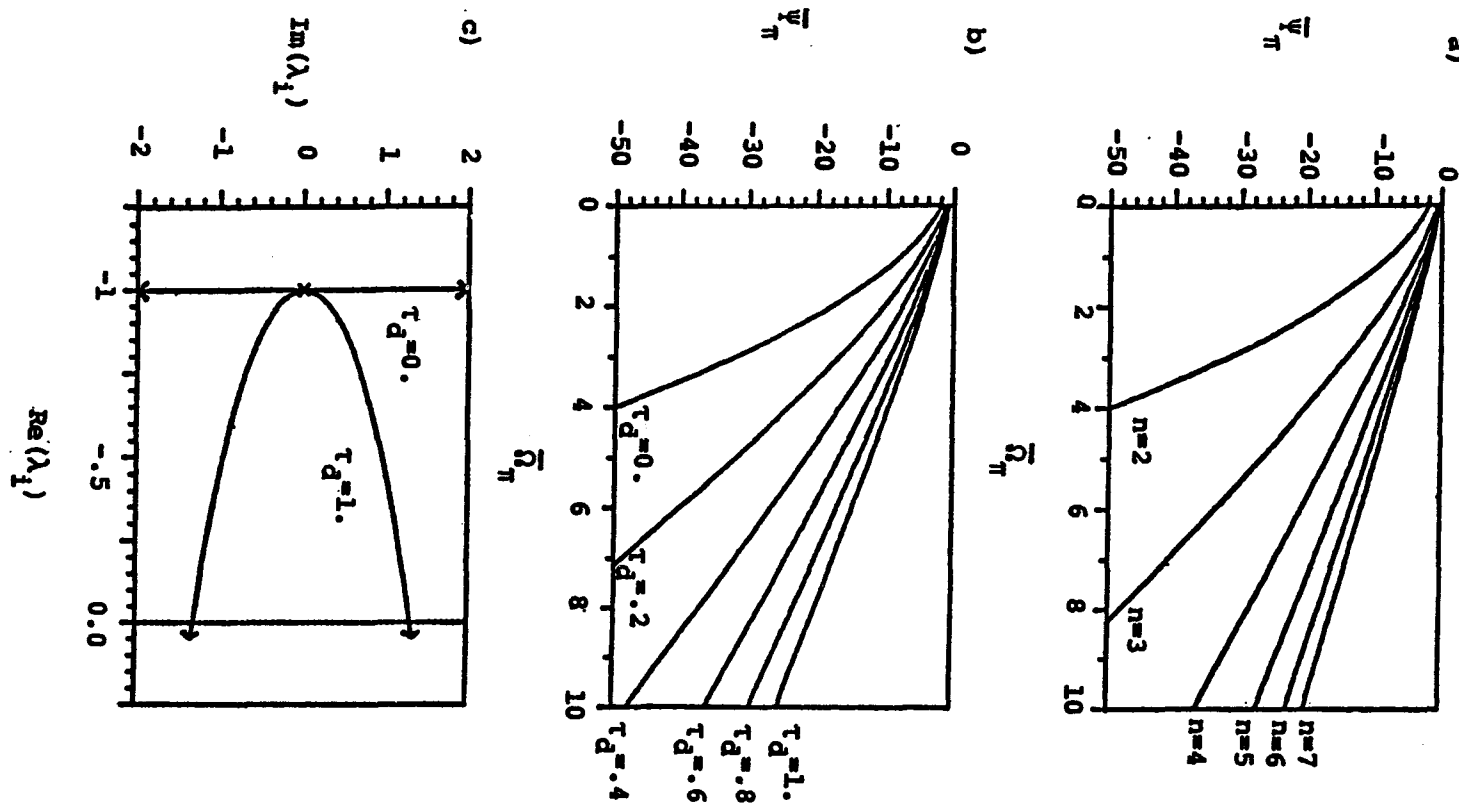


**Figure 6-3.** Instability in the single biochemical control loop. a) Influence of transfer function order on the occurrence of dynamic bifurcations. b) Influence of time delays on the occurrence of dynamic bifurcations. c) Influence of time delay ( $\tau_d = 1$ ) on the root locus plot for a first order transfer function (only the principal roots are shown  $\Psi_\pi = -2.72$  at the crossover point).

reaction chain increases more complicated patterns are observed on the root locus plot. But the important feature is that the principal roots cross the imaginary axis for lower gain values and the region of stable steady states shrinks significantly with increasing order.

A special case occurs for the restrictions  $\bar{\Omega}_\pi = 1$  and all time constants equal. Then the roots of equation 31 can be written as

$$\lambda_i = \sqrt[n+1]{\frac{\Psi}{\pi}} - 1, \quad i = 1, \dots, n+1 \quad (32)$$

The real part of the principal pair of roots vanishes when

$$\frac{\Psi}{\pi} = \frac{1}{\cos^{n+1}\left(\frac{\pi}{n+1}\right)} \quad (33)$$

and dynamic bifurcations arise.

We note here that this limit is similar to the widely discussed case of the Goodwin equations (Goodwin, 1963, 1965, Morales and McKay, 1967). For an excellent survey on these equations see Tyson and Othmer (1978). In the Goodwin equations  $\Psi(\pi)$  is assumed to obey Hill type kinetics and the removal rate is considered to be linear. We shall discuss these equations in more detail in chapters 8 and 9.

e) Time delays. Time delays significantly influence the size of the regions of stable steady states as the example in figure 6-3b,c shows. As shown in the figure time delays tend to accelerate the movement of the principal roots towards the imaginary axis and even for loops with first order reaction chains instability can be observed, figure 6-3c. Any significant time delay thus significantly limits the domain of stable operation and it is not surprising that

diffusional limitations appear to be absent for typical cellular dimensions (Weissz, 1973, Appendix A).

#### 6.4. Discussion.

Perhaps the most significant advance in the area of theoretical biology over the past couple of decades is the highly non-trivial and surprising demonstration that the origin of the highly ordered state of living matter can be explained from macroscopic physics. These remarkable developments, arising from non-linear non-equilibrium thermodynamics, provide an explanation for the appearance and evolution of structure and for the coherent behavior of living systems. These developments originated in the so-called Brussels School and are best summarized in Nicolis and Prigogine (1977), also see a more qualitative discussion in Prigogine and Stengers (1983). Several studies of this type suggest the existence of multiple steady states as well as temporal organization through sustained oscillations in living systems, both of which may be regarded as essential features of biological activity. Herein and in the two following chapters we examine a single biochemical control loop for both these characteristics.

The local stability analysis of the single biochemical control loop, applicable to a very wide range of detailed kinetic behavior, is surprisingly powerful for providing insight into the dynamic behavior of metabolic systems. From a qualitative standpoint it is

important for demonstrating that the regions of static and dynamic bifurcations are disparate and for providing a simple criteria for the existence of each.

Multiple steady states can only occur in loops with positive feedback, and these systems are incapable of exhibiting oscillatory instabilities. This is at least true in a local sense and probably also holds globally as conjectured in Tyson and Othmer (1978) for the Goodwin equations. The necessary and sufficient condition for the existence of multiple steady states is provided by equation 21. It is a surprisingly simple but powerful result obtained without defining the details of the input and removal rates and is furthermore independent of the kinetic properties of the reaction chain.

Conversely oscillatory behavior can occur only in loops with negative feedback, and these systems cannot exhibit multiple steady states. Oscillatory instabilities are also more complex in their origins, and they are influenced in an important way by system kinetic and transport properties. The main features of the dynamic operator that make the loop more prone to go unstable are high order and time delays. Since it is difficult to keep large interacting dynamic systems, like the metabolic network, stable it is expected that these single loops are designed such that they are far removed from the regions of instability. Apparently evolution has dealt with both these destabilizing trends. The dynamic operator is of high order if many of the reactions in the sequence have similar time

scales. If the kinetic constants in the chain are well distributed it leads to dynamic behavior that is of effectively lower order (chapter 5) and this appears to be the case for metabolic networks (see e. g. Savageau, 1975, Rapoport, Rapoport and Heinrich, 1977). Time delays arise if the system has diffusional limitations. However it is believed that the dimensions of the cell are such that diffusional processes are faster than those of reaction and hence time delays are not expected to appear under most in vivo conditions (Weisz, 1973, Appendix A). This discussion provides initial insight into the apparently contradictory behavior of biological systems in the way that stability seems to increase with increasing complexity. Normally these two trends move oppositely but evolutionary design seems to have selected the few possible situations where these two trends go hand in hand.

The qualitative differences between systems of positive and negative feedback are of biological interest and warrant further discussion. Positive feedback regulation seems to be more common in the catabolic part of the metabolic network. Here the possibility of more than one stable operating state arises. This means that the cell can (Tyson and Othmer, 1978, Rapp, 1983, chapter 7) shift between operating states depending on the concentration of the initial substrate and the various enzymes involved. From a philosophical standpoint it suggests that the decision making capability, which is perhaps the chief distinguishing characteristic of living systems, is exhibited to a rudimentary degree even at the

level of simple biochemical control loops. The appearance of such servo type control in the catabolic part seems very reasonable in that the operation can be shifted between suitable operating states depending on what substrates are available and at what quantities.

Negative feedback is by far the more common mode of regulation, occurring throughout the metabolic network, and its control function seems to be mostly regulatory in nature. It appears from the above analysis that oscillatory instabilities are an inherent characteristic of such regulatory processes, and the problem faced by the organism is minimize their occurrence. The degree of achievable performance, here indicated by the allowable gain without inducing oscillatory behavior, is limited by two factors, high dynamic order and diffusional delays as discussed above. This represents a tradeoff between metabolic rates and controllability. The tradeoff seems to favor robustness over performance, that is slower response is tolerated in order to allow for the capability to handle a wider variety of unexpected situations. This is reasonable in view of the unpredictable environments with which the cell must cope. One would, though, expect that the degree of tradeoff varies from organism to organism. For instance the red blood cell lives in a relatively constant environment, and one would expect to find less robust control here than in, say, a yeast or a bacterial cell in their highly variable natural environment.

The two bifurcation criteria derived herein are obtained without specifying the functional form of the input and removal rates, and

also without imposing the restrictions set by the steady state equation. In the two following chapters we shall specify these rate laws and translate the bifurcation criteria along with the steady state equation into the relevant parameter spaces.

### 6.5. Summary.

The objective of this chapter is to describe the dynamic behavior of a single biochemical control loop, a simple system but an important element of metabolic networks. This loop is a self-regulated sequence of reactions that converts an initial substrate (S) into a final product (P). It consists of three basic elements: 1) a regulated reaction, where the concentration of P controls the flux (I) into the system. This element serves as the control element in the feedback circuit. 2) a sequence of unregulated reactions that leads to the formation of P. This process is to be regulated so that the production rate of P meets a desired target. 3) a process (R) that removes P from the loop to another part of the metabolic network.

A mathematical description is formulated that consists of two differential equations and two unspecified functions that represent the reaction rates of I and R. This description is scaled to clarify functional dependence and to attempt a separation of genetic and process determined parameters.

The global dynamic behavior of the model is assessed

qualitatively by examining the occurrence of static and dynamic bifurcations, multiple steady states or persistent oscillations respectively, via local stability analysis. General criteria for both types of bifurcations are developed without specifying the functional form of I and R, but explicitly accounting for the kinetic properties of the reaction chain. A particularly simple criterion is found for static bifurcations which can appear only for loops with positive feedback, i. e. when the regulated reaction is activated by P. This criterion only contains the properties of I and R. The criteria for dynamic bifurcations, which can occur only when the feedback interaction is inhibitory, are more complex. These depend strongly on the properties of the reaction chain, and oscillations are favored if the dynamic operator describing the reaction sequence is of high order or if it contains time delays.

## CHAPTER 7

## SINGLE BIOCHEMICAL CONTROL LOOPS:

## POSITIVE FEEDBACK

The basic impetus for the analysis presented herein is the success of non-linear non-equilibrium thermodynamics (Nicolis and Prigogine, 1977) in describing the formation of coherent structures of which living systems are perhaps the most important example. Central to these developments is the notion of bifurcations that bring about qualitative changes in the dynamic behavior and which normally lead to some form of coherent patterns. Here we begin by looking at the simplest kind of bifurcations, static bifurcations (or bifurcation from a simple eigenvalue, Crandall and Rabinowitz (1979)), which lead to the possibility of multiple stable steady states. Such a feature provides the obvious and teleologically feasible possibility of on-off control by switching between stable operating states (see for instance discussion in Tyson and Othmer, 1978, and Rapp 1983), thereby offering a basis for elementary decision making capabilities such as substrate selection at the metabolic level.

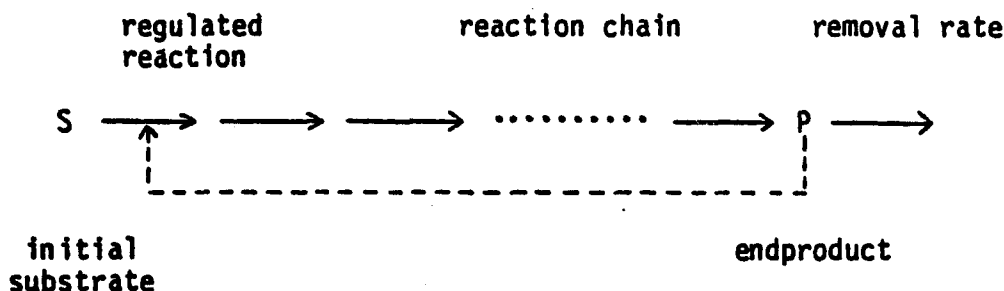
The earlier analysis in chapter 6 revealed that activation of the first step in a reaction sequence by the end product can lead to multiple steady states. Perhaps the best known example is induction of enzyme synthesis, advantageous for activating a process in the presence of a suitable substrate, or shutting it down when the substrate is absent. In particular the mechanism of induction of the Lac operon in E. coli, is well known and multiplicities in transcription rates have been observed (Norwick and Weiner, 1957, 1959, Cohn and Horibata, 1959). Analogous positive regulation of enzyme activity is frequently found in amphibolic pathways, where it provides advantages similar to those in the epigenic system: flux through a reaction sequence can be "geared" up or down in response to substrate availability or current needs of the cell. Furthermore if the pathway is reversible, as is the case with amphibolic pathways, one steady state may lead to operation of the pathway in one direction whereas the other steady state can lead a situation where the pathway is operated in the opposite direction. Hess, Boiteux and Sel'kov (1980), and Tornheim (1980) have recently discussed this possibility for glycolysis.

A particularly noteworthy aspect of our earlier analysis is that criteria for the existence of multiple steady states, in the control loop of figure 7-1, involve only the kinetics of the regulated reaction and of product removal. The behavior of the intermediate, unregulated, reactions need not be specified. We wish to build here on this finding by considering specific rate laws of widespread

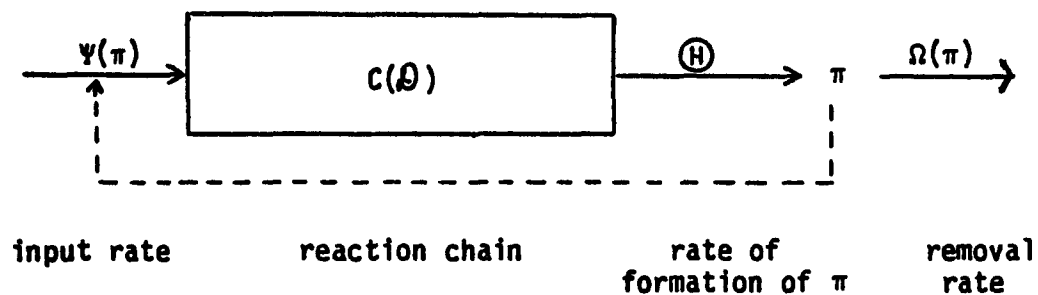
FIGURE 7-1.

A schematic illustration of the single biochemical control loop.

Reaction scheme:



Mathematical description (dimensionless form):



biological importance and exploring the parametric sensitivity of the regions of multiple solutions.

The control action is normally exerted through enzymes which have binding sites for the effector molecules, distinct from the catalytic site on the enzyme molecule. The binding of the regulator induces a conformational change in the enzyme molecule and alters the properties of the catalytic sites. This phenomenon is called allosterism following the suggestions of Monod, Changeux and Jacob (1963). Although a variety of regulatory mechanisms for enzyme modulation exist (Stadtman, 1966, 1970), allosteric regulation seems to be, by far, the most common way by which control is achieved in metabolic networks (Sols, 1981).

The kinetic behavior of allosteric enzymes is, fortunately, well characterized. In particular, the symmetry model of Monod, Wyman and Changeux (1965) and the sequential model of Koshland, Nemethy and Filmer (1966) appear to describe many allosteric enzymes adequately. One can also postulate simpler reaction mechanisms for the regulation such as the mechanism for oxygen binding to hemoglobin postulated by Hill (1910). Kinetics of allosteric enzymes are reviewed in Whitehead (1970) and Hammes and Wu (1974). Here we shall discuss and compare the response of a "lumped" controller, based on Hill-type kinetics, with that of the mathematically elegant, but physically realistic, symmetry model. Our purpose, in part, is to determine the level of complexity needed to represent the important features of feedback activation in single biochemical control loops. For the

removal rate we use Michaelis-Menten kinetics.

We begin our analysis in section 7.1 by defining the single biochemical control loop (described in detail in chapter 6) which we use as a vehicle for probing enzyme behavior, and by presenting the necessary and sufficient criteria for the appearance of static bifurcations, or multiple steady state solutions. Then in section 7.2 we briefly review and discuss the properties of the two kinetic models of regulatory enzymes that we wish to introduce into the loop: the lumped controller and the symmetry model. In sections 7.3 and 7.4, respectively, we examine the steady state solutions for the two models of regulatory enzymes for the occurrence of multiple stationary states.

### 7.1. The Single Biochemical Control Loop.

In chapter 6 the following kinetic model was developed for the single biochemical control loop, see figure 7-1

$$C(\mathbb{D})\theta = \Psi(\pi) \quad (1)$$

$$\frac{d\pi}{d\tau} + \Omega(\pi) = \theta \quad (2)$$

Here  $C(\mathbb{D})$  is a dynamic operator describing the reaction chain ( $\mathbb{D} = d/d\tau$ ), whose properties are discussed in the first part of this thesis.  $\Psi(\pi)$  is the reaction rate through the regulated reaction,  $\theta$  is the rate of formation of the final product  $\pi$ , and  $\Omega(\pi)$  is the

removal rate of the final product. This model is presented here in a dimensionless form, and the scaling of the equations, described in detail by chapter 6 is not repeated here.

Local stability analysis shows (chapter 6) that

$$\overline{\psi}_\pi \geq \overline{\Omega}_\pi \quad (3)$$

is a necessary and sufficient condition for multiple stationary solutions to appear (see also Othmer, 1976, Tyson and Othmer, 1978). Here the subscript  $\pi$  denotes a partial derivative with respect to  $\pi$  and the overbar denotes the steady state conditions. This equation then simply states that the slope of the input rate at steady state must exceed that of the removal rate in order for multiple solutions to occur. In addition to considering these derivatives the steady state requirement

$$\psi(\overline{\pi}) = \overline{\theta} = \overline{\Omega}(\overline{\pi}) \quad (4)$$

has to satisfied.

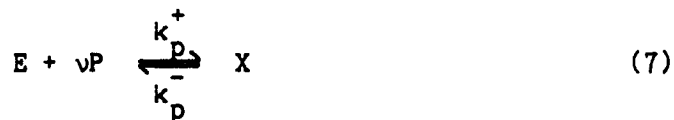
### 7.2. Kinetic Descriptions of Regulatory Enzymes.

In this section we briefly review two rate laws that can be used to describe kinetic behavior of regulatory enzymes: the simple lumped controller and the more realistic, but also more complex, symmetry model.

### 7.2.1. The Lumped Controller.

Very simple reaction mechanisms may be postulated for enzymatic reactions which are regulated by a metabolite, normally called an effector, modulator or modifier, that does not participate in the reaction itself. For the single biochemical control loop the modifier is the final product in the reaction sequence.

Reaction Mechanism. One of the simplest schemes possible is based on three reactions



This mechanism assumes that the controlled reaction is an irreversible bi-molecular reaction between the substrate (S) and the enzyme (E) to form the product ( $S_1$ ) and the free enzyme in a single elementary reaction. The enzyme in turn can be put into a catalytically altered state (X), catalyzing the same reaction but at a different rate, through binding simultaneously and reversibly to  $v$  molecules of the end product (P). The regulatory action of P is then lumped in the simple E to X transformation.

If we assume that the binding of the inhibitor is fast, so that a quasi-equilibrium forms for reaction 7, we have

$$x = \left(\frac{k_p^+}{k_p^-}\right)p^v e = (L_p p)^v e \quad (8)$$

where  $L_p$  is a "per-site" equilibrium constant for reaction 7. Here the lower case letters denote concentrations of the chemical species of the corresponding upper case letter. The enzyme is assumed to be contained within the system and lies in one of the two states so that we have the mass balance

$$e_t = e + x = (1 + (L_p)^v)e \quad (9)$$

where  $e_t$  is the total concentration of the enzyme. Using the mass balance and the quasi-equilibrium assumption gives the flux through the regulated reaction as

$$I(p) = (k_I e + k'_I x)s = \left( \frac{k_I + k'_I (L_p)^v}{1 + (L_p)^v} \right) s e_t \quad (10)$$

Scaling. To use this rate law for the input rate into the reaction chain we must scale it relative to its saturation velocity (see chapter 6) as

$$\Psi(\pi) = \frac{I(p)}{I_{sat}} = \frac{1 + Ac(\Lambda_\pi^\pi)^v}{1 + (\Lambda_\pi^\pi)^v} \quad (11)$$

where

$$\pi = \frac{p}{I_{sat} t_c} \quad Ac = \frac{k'_I}{k_I} \quad \Lambda_\pi = L_p I_{sat} t_c \quad I_{sat} = k_I e_t s \quad (12)$$

$I_{sat}$  is the saturation velocity,  $\pi$  is the scaled product concentration and  $t_c$  is the characteristic time constant for the reaction chain. The parameter  $Ac$  is the ratio between the two second-order rate constants, and we call this dimensionless quantity the "Acceleration number" since it is a measure of how much the

modifier accelerates the regulated reaction. If  $A_c$  is in excess of unity the reaction is accelerated in the presence of the modifier, which is the case considered herein. On the other hand if  $A_c$  is less than unity the reaction is slowed down and the modulation is inhibitory. If  $A_c$  assumes a value of unity the influence of the modifier disappears. The parameter  $A_{\pi}$  is a dimensionless binding constant of the product to the enzyme, and  $v$  is called the degree of cooperativity or the Hill coefficient.

At this point it is conceptually useful to define two types of dimensionless groups:

a) Genetically determined parameters. Here we are referring to the kinetic and thermodynamic properties of the enzymes, which may be divided into two sub-groups: (1) kinetic parameters, i.e. dimensionless groups containing rate constants, such as  $A_c$  defined above (also  $S_t$  in chapter 2) and (2) thermodynamic parameters, i.e. dimensionless groups containing equilibrium and binding constants (such as  $K_{eq}$  and  $A_f$  from chapters 2 and 4). For a constant intra-cellular environment, i.e. constant temperature, pressure, etc. This group dimensionless parameters may be assumed to be invariant.

b) Process determined parameters. Here we are referring to parameters that explicitly contain concentrations of metabolites and enzymes (such as  $Q_s$  of chapter 2). These parameters will vary from one physiological state to another.

For the lumped controller  $v$  and  $A_c$  are kinetic parameters

whereas  $\Lambda_{\pi}$  is process dependent.

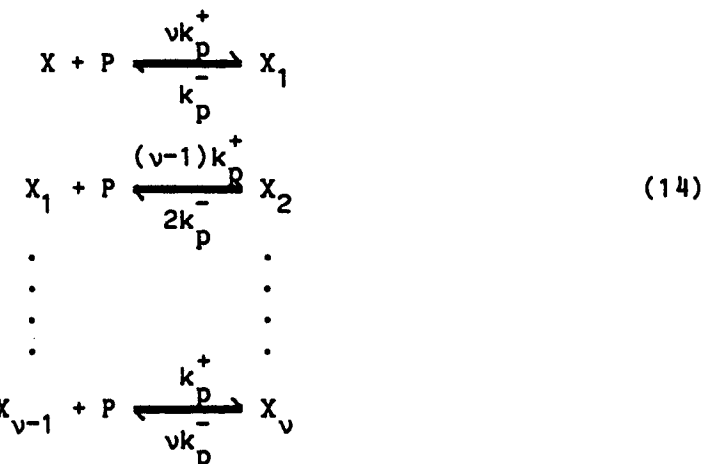
### 7.2.2. The Symmetry Model.

One of the earliest kinetic models that accounted for allosterism was the model of Monod et al (1965), called the symmetry model after certain assumed symmetry properties of the subunits of the enzyme. This model is very well known (e. g. Newsholme and Start, 1973, Ferdinand, 1977, Cornish-Bowden, 1979) and will only be briefly discussed here. It is a more realistic description of the allosteric mechanism than the lumped controller.

Reaction Mechanism. The symmetry model postulates that the regulatory enzyme lies naturally in two forms E and X and is converted between the two states simply as



Then  $v$  molecules of the modifier can bind sequentially to the X form as



Assuming that all the  $X_i$  forms catalyze reaction 6 with a rate

constant  $k_I'$ , and that the product binding steps are at quasi-equilibrium, one can derive the rate law

$$I(p) = \left( \frac{k_I + k_I' L (1+L_p)^v}{1 + L (1+L_p)^v} \right) s e_t \quad (15)$$

through a similar procedure as for the lumped controller. Here  $L = k^+/k^-$  is the equilibrium constant for reaction 13 and has a special name, the allosteric constant. If  $L_p$  is large relative to unity the symmetry model becomes analogous to the lumped controller with  $L_p$  for the lumped controller being equivalent to  $L_p^{1/v}$  for the symmetry model. We shall discuss this feature more closely in section 7.4 below.

Scaling. Scaling this rate law as above one obtains

$$\psi(\pi) = \frac{1 + A c L (1 + \Lambda_{\pi})^v}{1 + L (1 + \Lambda_{\pi})^v} \quad (16)$$

with all parameters defined as above. The two models yield similar rate laws and the price we pay for the more sophisticated binding mechanism is the additional thermodynamic parameter  $L$ .

### 7.3. Loops with Lumped Controllers.

We now use the lumped controller to describe the input rate and we call the resulting circuit Loop 1. To evaluate the criterion for multiplicity we need  $\psi_{\pi}$  which is

$$\psi_{\pi} = \frac{v(Ac-1)}{\pi} \frac{(\Lambda_{\pi})^v}{(1+(\Lambda_{\pi})^v)^2} \quad (17)$$

and when combined with the steady state equation

$$\Omega(\bar{\pi}) = \frac{1 + Ac(\Lambda_{\bar{\pi}})^v}{1 + (\Lambda_{\bar{\pi}})^v} \Rightarrow (\Lambda_{\bar{\pi}})^v = \frac{\Omega(\bar{\pi}) - 1}{Ac - \Omega(\bar{\pi})} \quad (18)$$

gives the multiplicity criterion as

$$\Omega^2(\bar{\pi}) + \left(\frac{Ac-1}{v}\right)\Omega(\bar{\pi}) - (Ac+1)\Omega(\bar{\pi}) + Ac \leq 0 \quad (19)$$

It remains only to find an explicit expression for the removal rate  $\Omega(\bar{\pi})$ . A common feature of biological rate laws is saturation kinetics at high substrate concentrations, and the simplest of these rate laws is the Michaelis-Menten equation

$$\Omega(\bar{\pi}) = \frac{\kappa\bar{\pi}}{1+\kappa\bar{\pi}/\Omega_m}, \quad \kappa = \frac{V_m}{K_m}t_c, \quad \Omega_m = \frac{V_m}{I_{sat}} \quad (20)$$

where  $\Omega_m$  is the dimensionless form of the saturation velocity  $V_m$ , and where  $\kappa$  is the dimensionless form of the pseudo-first order rate constant  $V_m/K_m$  ( $K_m$  is the well known Michaelis constant). This rate law changes from first order to zeroth order kinetics depending on reaction conditions and the numerical values of the rate constants. We first examine the simple linear limit where  $\Omega(\bar{\pi}) = \kappa\bar{\pi}$ .

### 7.3.1. Linear removal rate.

Using the linear removal rate in equation 19 transforms it into

$$z^2 - ((1-1/v)Ac + (1+1/v))z + Ac \leq 0, \quad z = \kappa\bar{\pi} \quad (21)$$

If this inequality holds for real positive values of  $z$  multiplicities arise. The problem then is to find real positive roots,  $z_1$  and  $z_2$ , to the corresponding equality which are

$$z_1, z_2 = \frac{1-1/v}{2} (Ac + \frac{v+1}{v-1} \pm \sqrt{(Ac-1)(Ac - (\frac{v+1}{v-1})^2)}) \quad (22)$$

Both these roots can be shown to be real and positive if

$$Ac \geq Ac_{\min} = \left(\frac{v+1}{v-1}\right)^2 \quad (23)$$

A double root

$$z_{\min} = \frac{v+1}{v-1} \quad (24)$$

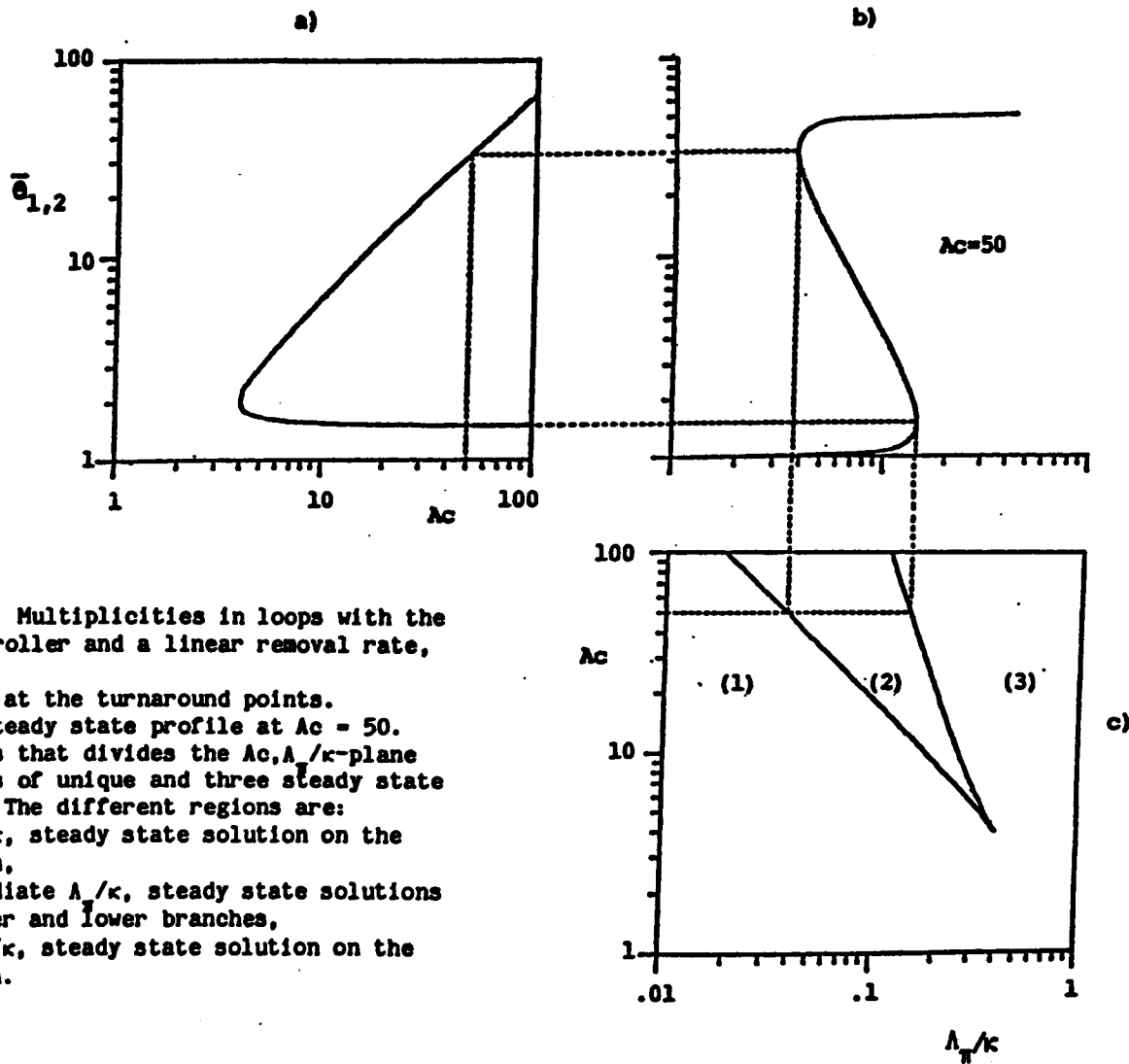
occurs at  $Ac = Ac_{\min}$ . The loci surrounding the region of multiple stationary solutions may be obtained from the steady state equation as

$$\left(\frac{\Lambda_{\pi}}{\kappa}\right) = \frac{1}{z} \left(\frac{z-1}{Ac-z}\right)^{1/v} \quad (25)$$

using  $z = z_1$  or  $z_2$ . An upper bound on  $\Lambda_{\pi}/\kappa$  may be obtained by substituting  $z_{\min}$  and  $Ac_{\min}$  into equation 25 as

$$\left(\frac{\Lambda_{\pi}}{\kappa}\right)_{\max} = \left(\frac{v-1}{v+1}\right)^{1+1/v} \quad (26)$$

As illustrated in figure 7-2 multiple steady state solutions arise if the groups  $Ac$  and  $\Lambda_{\pi}/\kappa$  exceed their critical values given by equations 23 and 26 and then equation 25 is used to trace out the loci. Also figure 7-2 shows that the flux at the lower turnaround point is virtually invariant with increased acceleration. However the turnaround point on the upper branch changes profoundly with  $Ac$  and it is located at high fluxes, which ensures that the catalytic capacities of the enzymes in the reaction chain are as well utilized



as possible.

In the region of three solutions the middle steady state is unstable, but the upper and lower branches are stable. A similar result to equation 23, for an activation mechanism at the genetic level of Yagil and Yagil (1971), has been obtained by Othmer (1976) and Tyson and Othmer (1978).

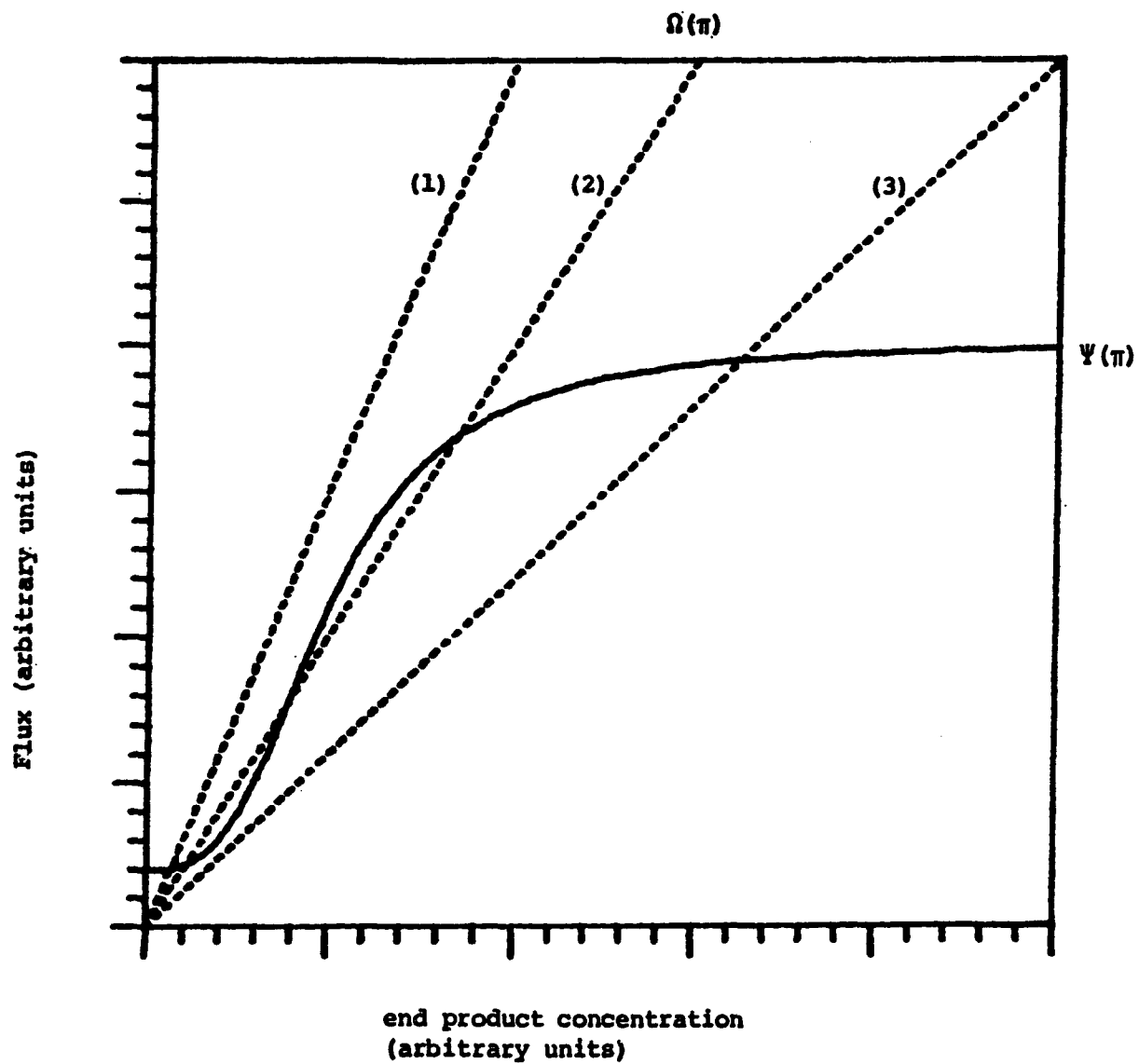
The relationship between the parameters  $A_c$  and  $v$ , equation 23, gives a necessary condition for multiplicities to appear. Since most regulatory enzymes have Hill coefficients ( $v$ ) roughly in the range 2-3, equation 23 indicates that an approximately ten-fold acceleration of the regulated reaction is necessary to produce multiple solutions. For  $A_c > A_{c_{\min}}$  the appearance of multiplicities is determined by the relative strength of end product association to the regulatory enzyme and the rate of removal, or the ratio  $\Lambda_{\pi}/\kappa$ , figure 7-3. When the ratio  $\Lambda_{\pi}/\kappa$  is small only one steady state solution, on the lower branch, is observed. Under these circumstances the product-enzyme interactions are weak relative to the rate of product removal. This means that the feedback regulation is not very significant, and the system behaves much like an uncontrolled system. In the opposite limit, where the product significantly stimulates its production, or when the removal rate is relatively low, the loop is tuned to ensure high product concentrations. For the proper weighting of these two opposing effects both of the stable solutions can be observed. The approximate ratio between the steady state conditions on the upper

Figure 7-3.

Illustration of steady state conditions for loop 1 with linear removal rate and how they are influenced by the ratio  $\Lambda_{\pi}/\kappa$ ;

- (1) low  $\Lambda_{\pi}/\kappa$ , steady state solution on the lower branch,
- (2) intermediate  $\Lambda_{\pi}/\kappa$ , steady state solutions on both upper and lower branches,
- (3) high  $\Lambda_{\pi}/\kappa$ , steady state solution on the upper branch. Solid line -  $\Psi(\pi)$ , dotted lines -  $\Omega(\pi)$ .

FIGURE 7-3.



and lower branch is approximately  $A_c$ , hence if the acceleration is strong the two steady states could represent quite distinct physiological states.

### 7.3.2. Michaelis-Menten removal rate.

Using the Michaelis-Menten form for  $\Omega(\pi)$  transforms the criterion for multiplicity into

$$z^2 - \frac{(1-1/v-2/\Omega_m)A_c + (1+1/v)}{(1-1/\Omega_m)(1-A_c/\Omega_m)}z + \frac{A_c}{(1-1/\Omega_m)(1-A_c/\Omega_m)} \leq 0 \quad (27)$$

As before we look for real positive roots to the quadratic equation which are

$$z_1, z_2 = \frac{(1-1/v-2/\Omega_m)A_c + (1+1/v) \pm \sqrt{(A_c-1)((1-1/v)^2 + 4/v\Omega_m)A_c - (1+1/v)^2}}{(1-1/\Omega_m)(1-A_c/\Omega_m)} \quad (28)$$

These roots can only be positive if  $\Omega_m$  is greater than unity. Two positive real roots appear if

$$A_c \geq A_{c_{\min}} = \frac{(v+1)^2}{(v-1)^2 + 4v/\Omega_m} \quad (29)$$

A double root appears

$$z_{\min} = \frac{v+1}{(1-1/\Omega_m)(v-1)} \quad (30)$$

if  $A_c = A_{c_{\min}}$ . Here the boundaries on the region of multiplicities are given by

$$\frac{\Lambda_\pi}{\kappa} = \frac{1}{z} \left( \frac{(1-1/\Omega_m)z - 1}{A_c - (1-A_c/\Omega_m)z} \right)^{1/v} \quad (31)$$

Using  $z_{\min}$  and  $A_{c_{\min}}$  in equation 31 gives a maximum value for  $\Lambda_\pi/\kappa$  as

$$\left(\frac{\Lambda_{\pi}}{\kappa}\right)_{\max} = \left(\frac{v-1}{v+1}\right)^{1+1/v} \left(1 + \frac{4v}{(v-1)^2 \Omega_m}\right)^{1/v} (1-1/\Omega_m) \quad (32)$$

One of the real roots becomes zero at  $A_c = \Omega_m$  while the other is

$$z_{\min} = \left(\frac{1}{1-1/v}\right) \left(\frac{1}{1-1/\Omega_m}\right) \quad (33)$$

$$\left(\frac{\Lambda_{\pi}}{\kappa}\right)_{\min} = \frac{(v-1)^{1-1/v} (1-1/\Omega_m)}{v \Omega_m^{1/v}} \quad (34)$$

Here the upper turnaround point disappears and the steady state equation can have none or two solutions. The second root crosses the origin and becomes negative at  $\Omega_m = 1$  and beyond which no steady state solutions exist. The regions of the various types of multiplicities are shown in figure 7-4.

The stability of the solutions is such that in the region of three solutions the middle steady state is unstable and the other two are stable, and in the region of two solutions the upper solution is unstable, but the lower one is stable.

The ratio  $\Lambda_{\pi}/\kappa$  contains both kinetic and concentration determined parameters and can be conveniently split into two parts as a product of two ratios:

$$\frac{\Lambda_{\pi}}{\kappa} = \left(\frac{L}{1/K_m}\right) \left(\frac{I_{\max}}{V_m}\right) = Af \frac{1}{\Omega_m} \quad (35)$$

The parameter  $Af$  is the ratio between the binding constant of the end product to the regulatory enzyme and the removal enzyme: it is thus a measure of the end product's relative affinity for the two enzymes. If  $Af$  is less than unity the product has greater affinity for the

Figure 7-4.

Multiplicities in Loop 1 with Michaelis-Menten removal.

a) regions of multiple steady states in the  $(1/Ac), (1/\Omega_m)$ -plane.

Four possibilities arise:

Region (1): below the line  $1/Ac = 1$  and above the solid line

(which is given by equation 29 and depends on  $\nu$ ) - unique steady states,

Region (2): below the solid line and above the dashed line,  $1/Ac = 1/\Omega_m$  - one or three steady states,

Region (3): below the dashed line and to the left of the line  $1/\Omega_m = 1$  - two or no steady state,

Region (4): right of the line  $1/\Omega_m = 1$  - no steady states.

b) Illustration of steady state conditions, (1) unique steady state, (2) three steady states, (3) two steady states, and (4) no steady state. Solid line -  $\Psi(\pi)$ , dotted lines -  $\Omega(\pi)$ .

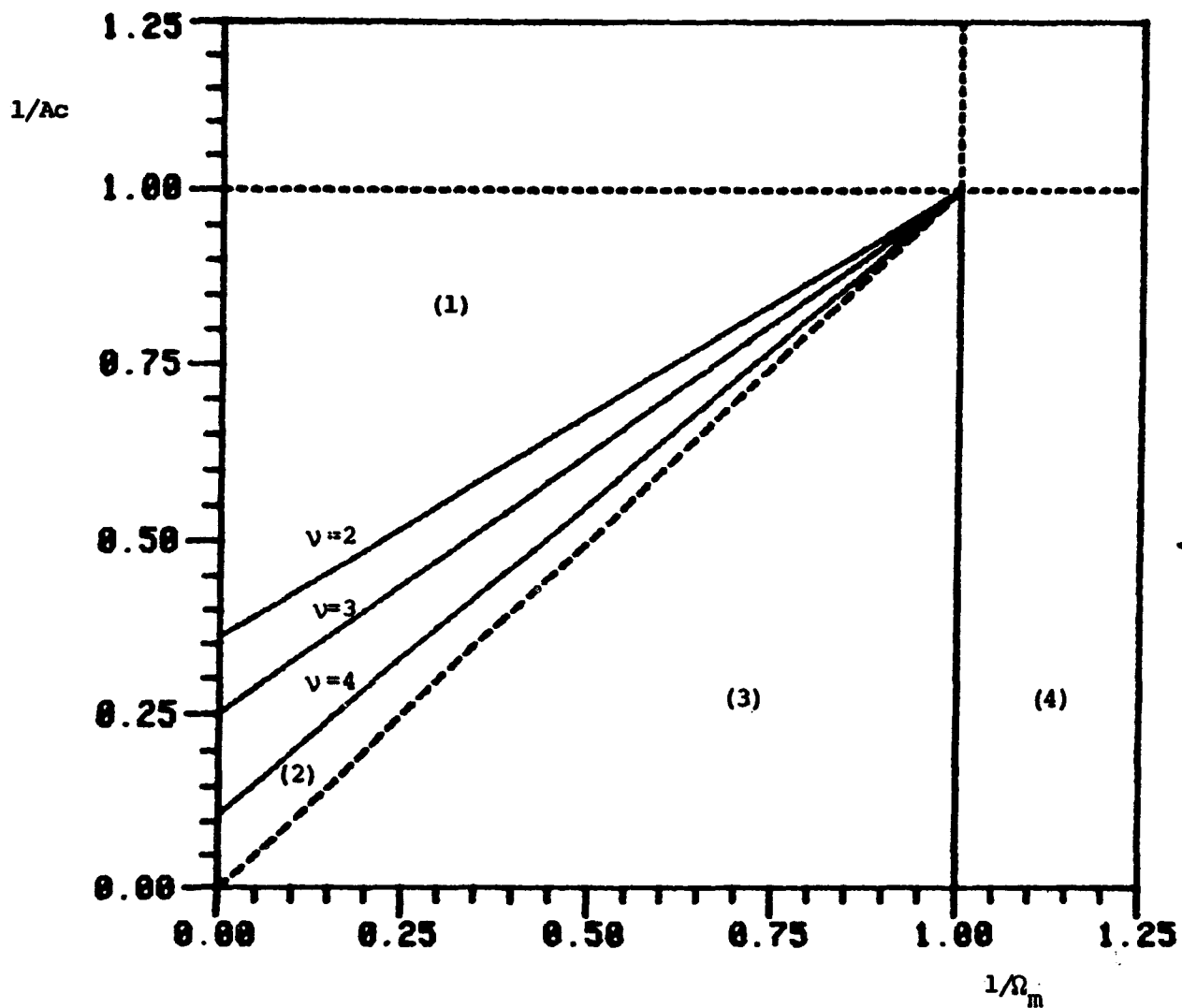
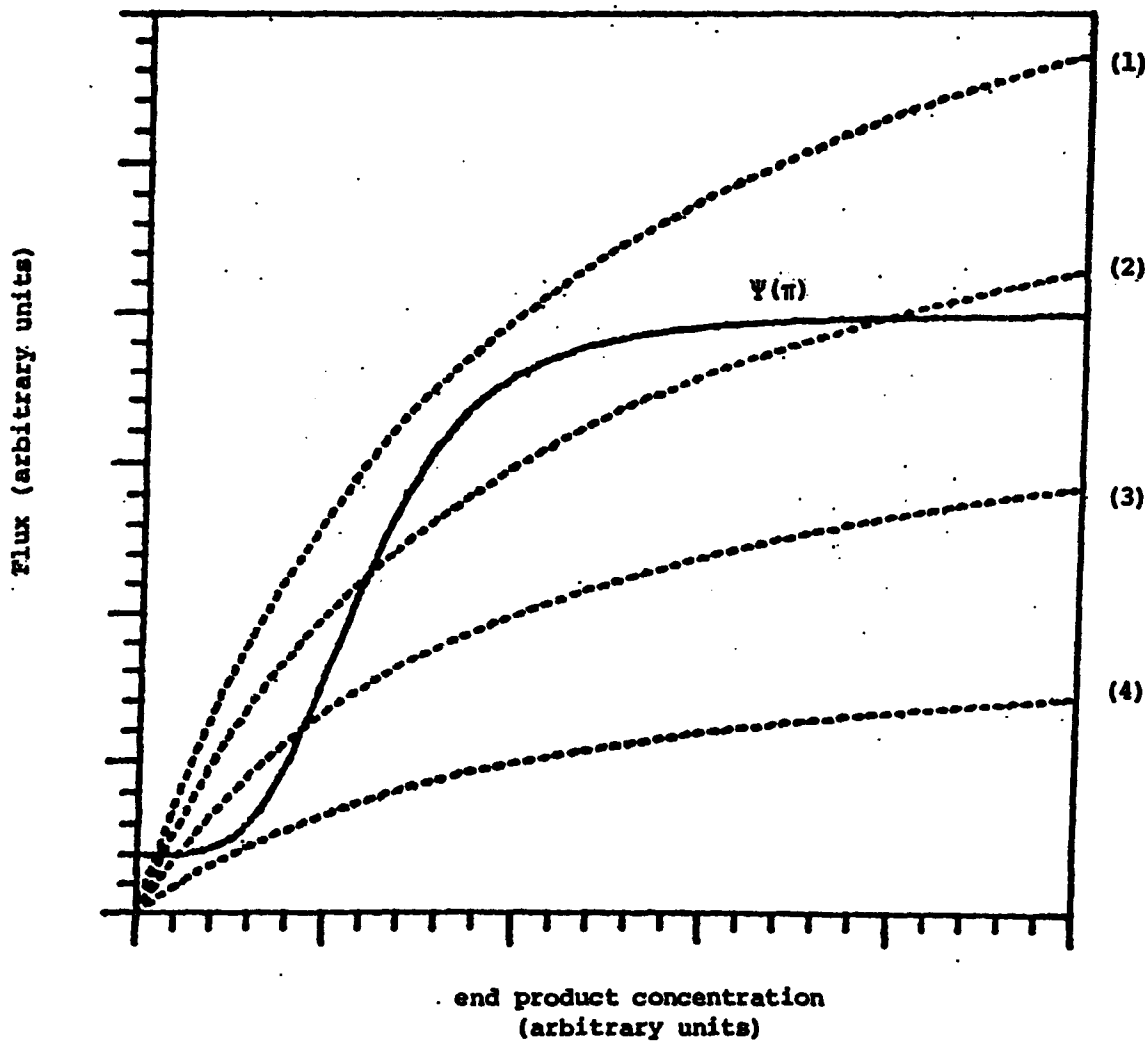


FIGURE 7-4a.

FIGURE 7-4b.



removal enzyme than the regulatory enzyme and vice versa when Af is in excess of unity. Hence an appropriate name for this parameter is "the Affinity ratio" and since the binding constants are thermodynamic quantities so is Af. On the other hand the ratio between the saturation velocities is directly dependent on the concentrations of the two enzymes and the initial substrate as well hence  $\Omega_m$  is a concentration dependent group and will vary with the physiological state of the cell.

As shown in figures 7-4 and 7-5 the effects of a change in saturation velocity for the removal rate are dramatic. There is a major difference in the behavior of the turnaround point for the upper branch, from that of the linear limit, since it depends significantly on  $\Omega_m$ . As  $\Omega_m$  drops from infinity the upper turnaround point moves to lower Af values, and eventually the upper branch disappears as  $\Omega_m$  crosses Ac. The lower branch also disappears when  $\Omega_m$  crosses unity and then no steady state solution exists.

As seen in figure 7-6 this leads to the possibility of moving the region of multiplicities around by varying  $\Omega_m$ . For a fixed set of genetically determined parameters v, Ac, and Af, one can in this way shift the steady state from one branch to the other. This feature allows the loop to make decisions on the steady state flux depending on substrate availability or the enzyme concentrations, since both influence  $\Omega_m$ , where the information that the decision is based on is embedded in the genetically determined parameters.

In the region of three steady states the ratio between the

Figure 7-5.

Multiplicities in the  $A_c, \Lambda_{\pi}/\kappa$ -plane for loop 1 with Michaelis-Menten removal rate,  $v = 3$ ,  $\Omega_m = 100$ . The number of steady states are:

region (1) unique steady state,

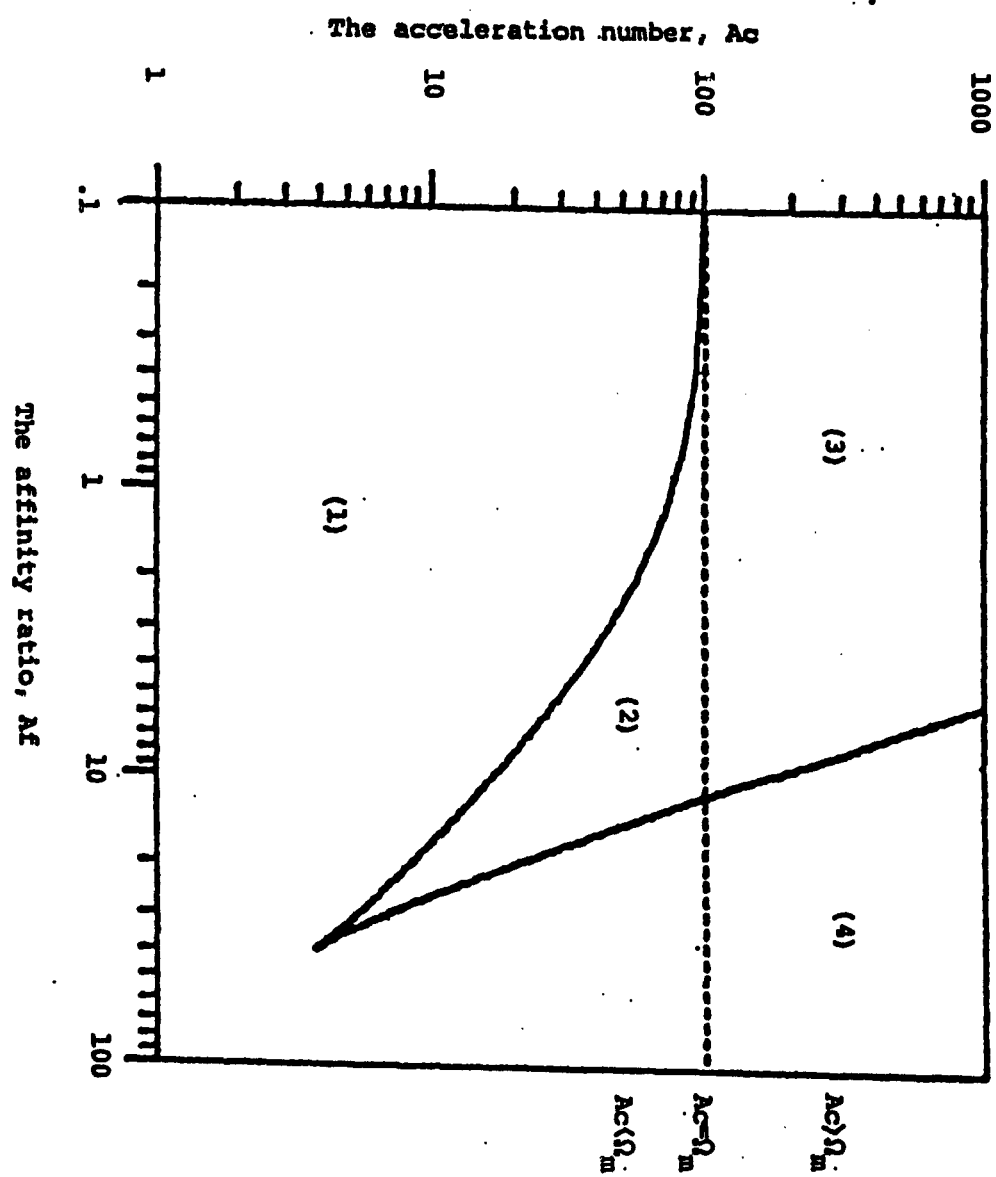
region (2) three steady states,

region (3) two steady states, and

region (4) no steady state.

Note that at the line  $A_c = \Omega_m$  the upper steady state disappears.

FIGURE 7-5.



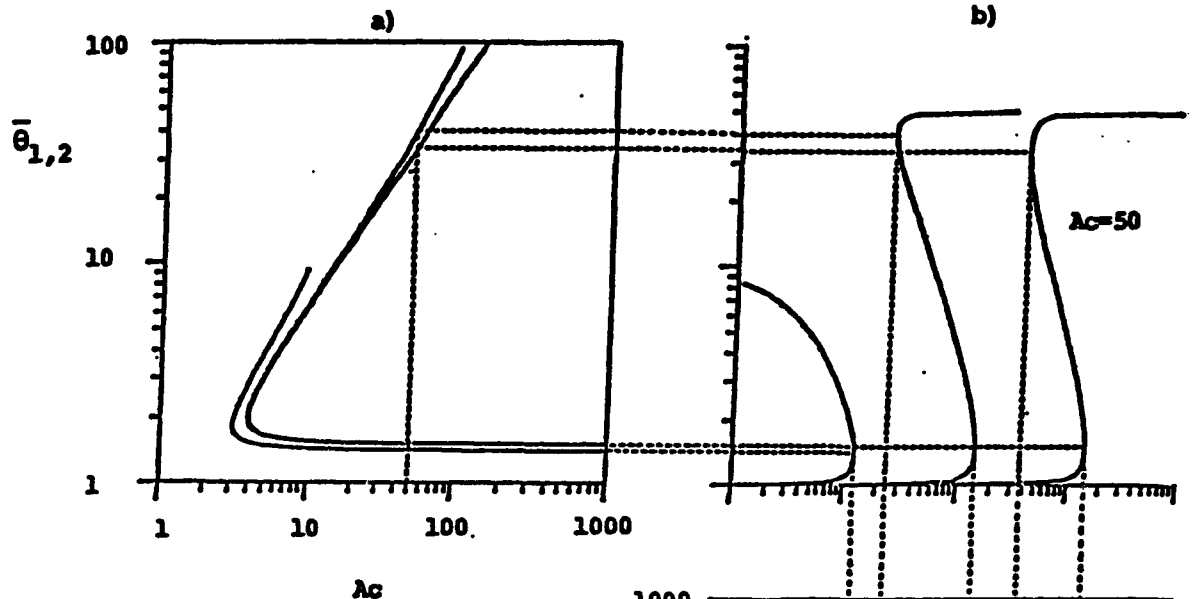
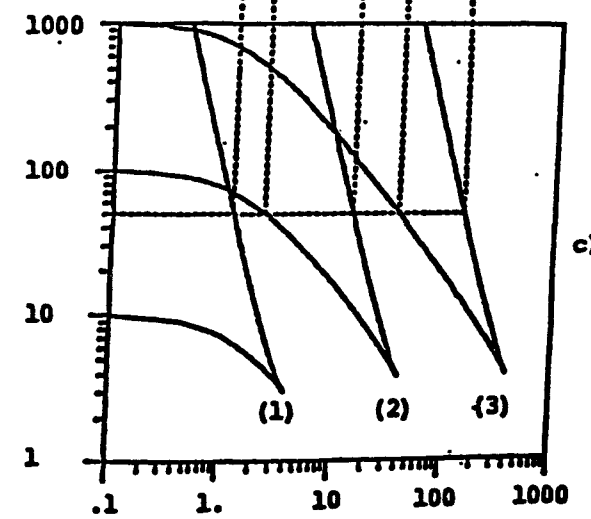


Figure 7-6. Multiplicities in loops with the lumped controller and a Michaelis-Menten removal rate,  $v = 3$ .  
 a) The flux at the turnaround points.  
 b) Sample steady state profile at  $Ac = 50$ .  
 c) The loci that divide the  $Ac, Af$ -plane into regions of unique and multiple steady state solutions. The curves are (1)  $\theta_m = 10$ , (2)  $\theta_m = 100$ , (3)  $\theta_m = 1000$ .



steady state fluxes in the two states is approximately  $A_c$ , as for the linear limit, but the ratio between the steady state end product concentrations is

$$\frac{\bar{\pi}_{\text{upper}}}{\bar{\pi}_{\text{lower}}} \approx \frac{1 - 1/\Omega_m}{1/A_c - 1/\Omega_m} \quad (36)$$

since the upper steady state is pushed into the saturation region of  $\Omega(\bar{\pi})$ .

#### 7.4. Loops with the Symmetry Model.

We now look at a circuit that has an input flux described by the symmetry model which we call Loop 2. To evaluate the criterion for multiplicity we need  $\Psi_{\bar{\pi}}$  which is

$$\Psi_{\bar{\pi}} = \frac{v(Ac-1)}{\bar{\pi}} \frac{L(1+\Lambda_{\bar{\pi}})^v}{(1+L(1+\Lambda_{\bar{\pi}})^v)^2} \quad (37)$$

and when combined with the steady state equation

$$\Omega(\bar{\pi}) = \frac{1 + AcL(1+\Lambda_{\bar{\pi}})^v}{1 + L(1+\Lambda_{\bar{\pi}})^v} \Rightarrow L(1+\Lambda_{\bar{\pi}})^v = \frac{\Omega(\bar{\pi}) - 1}{Ac - \Omega(\bar{\pi})} \quad (38)$$

gives the multiplicity criterion as

$$\Omega^2(\bar{\pi}) + \left(\frac{Ac-1}{v\Lambda_{\bar{\pi}}}\right)(1+\Lambda_{\bar{\pi}})\bar{\Omega}_{\bar{\pi}} - (Ac+1)\Omega(\bar{\pi}) + Ac \leq 0 \quad (39)$$

### 7.4.1. Linear removal rate.

Substituting  $\Omega(\pi) = \kappa\pi$  into equation 39 we find the criterion for multiplicity to be

$$z^2 - ((1-1/v)Ac + (1+1/v))z + Ac + \frac{Ac-1}{v(\Lambda_\pi/\kappa)} \leq 0 \quad (40)$$

The corresponding equality has real positive roots if

$$z_1, z_2 = \frac{1-1/v}{2}(Ac + \frac{v+1}{v-1}) \pm \sqrt{(Ac-1)(Ac - (\frac{(v+1)^2 + 4v/(\Lambda_\pi/\kappa)}{(v-1)^2}))} \quad (41)$$

These roots can be shown to be real and positive if

$$Ac \geq Ac_{\min} = \frac{(v+1)^2 + 4v/(\Lambda_\pi/\kappa)}{(v-1)^2} \quad (42)$$

A double root

$$z_{\min} = \frac{v+1+2/(\Lambda_\pi/\kappa)}{v-1} \quad (43)$$

occurs at  $Ac = Ac_{\min}$ . The loci surrounding the region of multiple stationary solutions may be obtained from the steady state equation as

$$L = \left(\frac{z-1}{Ac-z}\right)\left(\frac{1}{1+(\Lambda_\pi/\kappa)z}\right)^v \quad (44)$$

An upper bound on L may be obtained by substituting  $z_{\min}$  and  $Ac_{\min}$  into equation 44 as

$$L_{\max} = \left(\frac{v-1}{v+1}\right)^{1+v}\left(\frac{1}{1+\Lambda_\pi/\kappa}\right)^v \quad (45)$$

When  $Ac > Ac_{\min}$  and  $L < L_{\max}$  the steady state equation can have three solutions, with the middle one being unstable.

Here in contrast to loop 1 the region of multiple steady-state solutions is not only determined by  $A_c$  but also by the ratio  $\Lambda_{\pi}/\kappa$  for any given  $v$ , figure 7-7. Loop 1 is the limit where  $\Lambda_{\pi}$  of loop 2 becomes infinite, as expected from the discussion in section 3, and all the results in this section reduce to those of the previous one in this limit simply by changing  $\Lambda_{\pi}$  to  $\Lambda_{\pi} L^{1/v}$ . As the ratio  $\Lambda_{\pi}/\kappa$  drops below about 1 to 10 the region of multiplicities starts to shrink. An example of how the region of multiplicity converges to the same region as for loop 1 is shown in figure 7-8. This implies that loops with the symmetry model are less likely to exhibit multiplicities than loops containing the lumped controller when  $\Lambda_{\pi}/\kappa$  is less than about 1-10. Hence the differences between the lumped controller and the symmetry model become noticeable when  $\Lambda_{\pi}/\kappa$  drops below approximately unity, but above this range one can safely assume lumped behavior. Note in figure 7-8 that the symmetry model influences mostly the lower branch as expected from the discussion in section 3.

Loop 2 is more complex than loop 1 since there are two binding parameters describing the tightness of end product association to the regulatory enzyme. However, as for loop 1, a single lower steady state prevails if the binding of the end product to the regulatory enzyme is weak. On the other hand if the feedback interaction is strong the higher branch of steady state solutions is favored. For intermediate values of the binding constants both stable steady states can appear simultaneously with the approximate ratio between

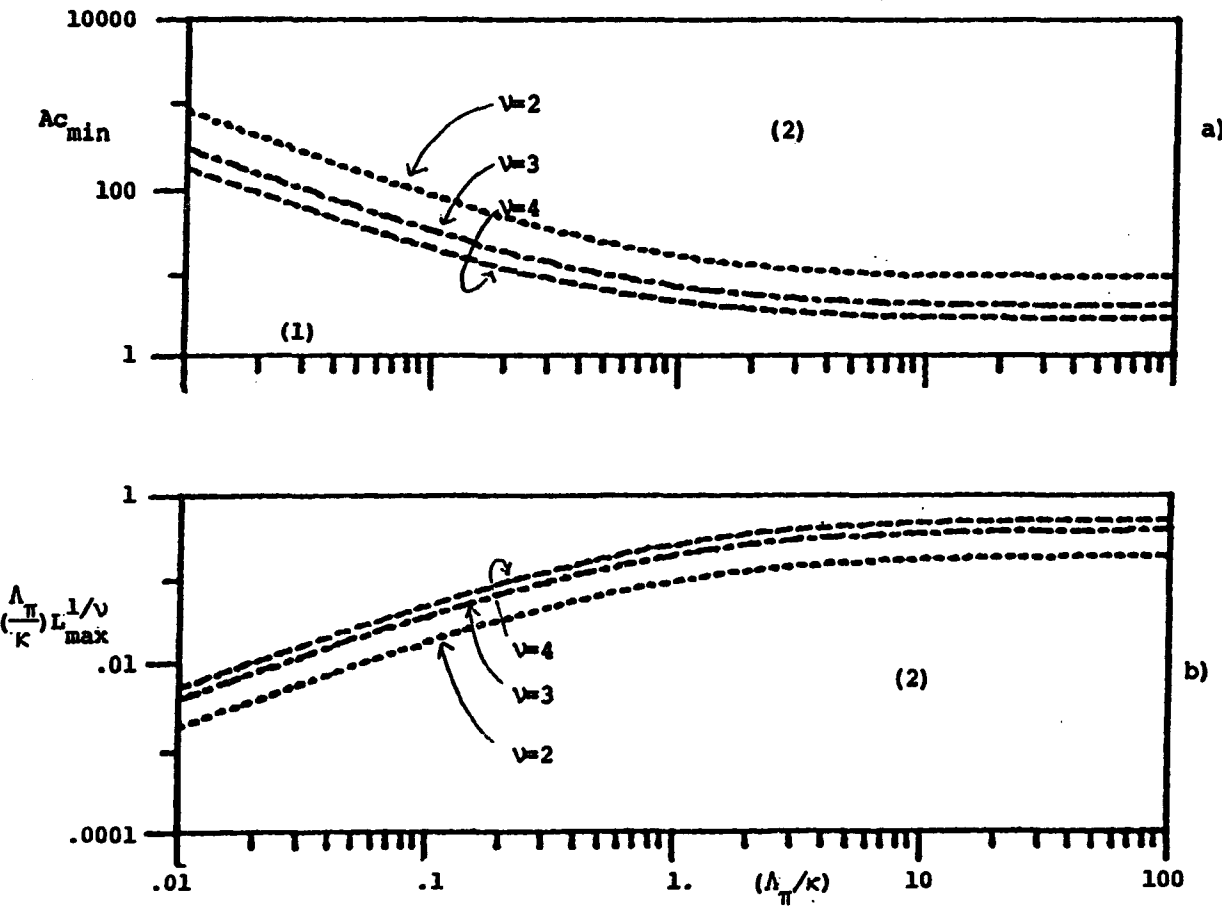


Figure 7-7. Critical values, a) of  $Ac$  (equation 42) and, b) of  $L$  (equation 45) for the appearance of multiple steady state solutions for a loop with the symmetry model and linear removal. (1)  $v = 2$ , (2)  $v = 3$ , (3)  $v = 4$ . Region (1) unique solution, and region (2) multiple solutions possible. Limiting values at high  $\Lambda_{\pi}/\kappa$  values are given by equations 23 and 26 (with  $L^{1/v}\Lambda_{\pi}/\kappa$  exchanged with  $\Lambda_{\pi}/\kappa$ ).

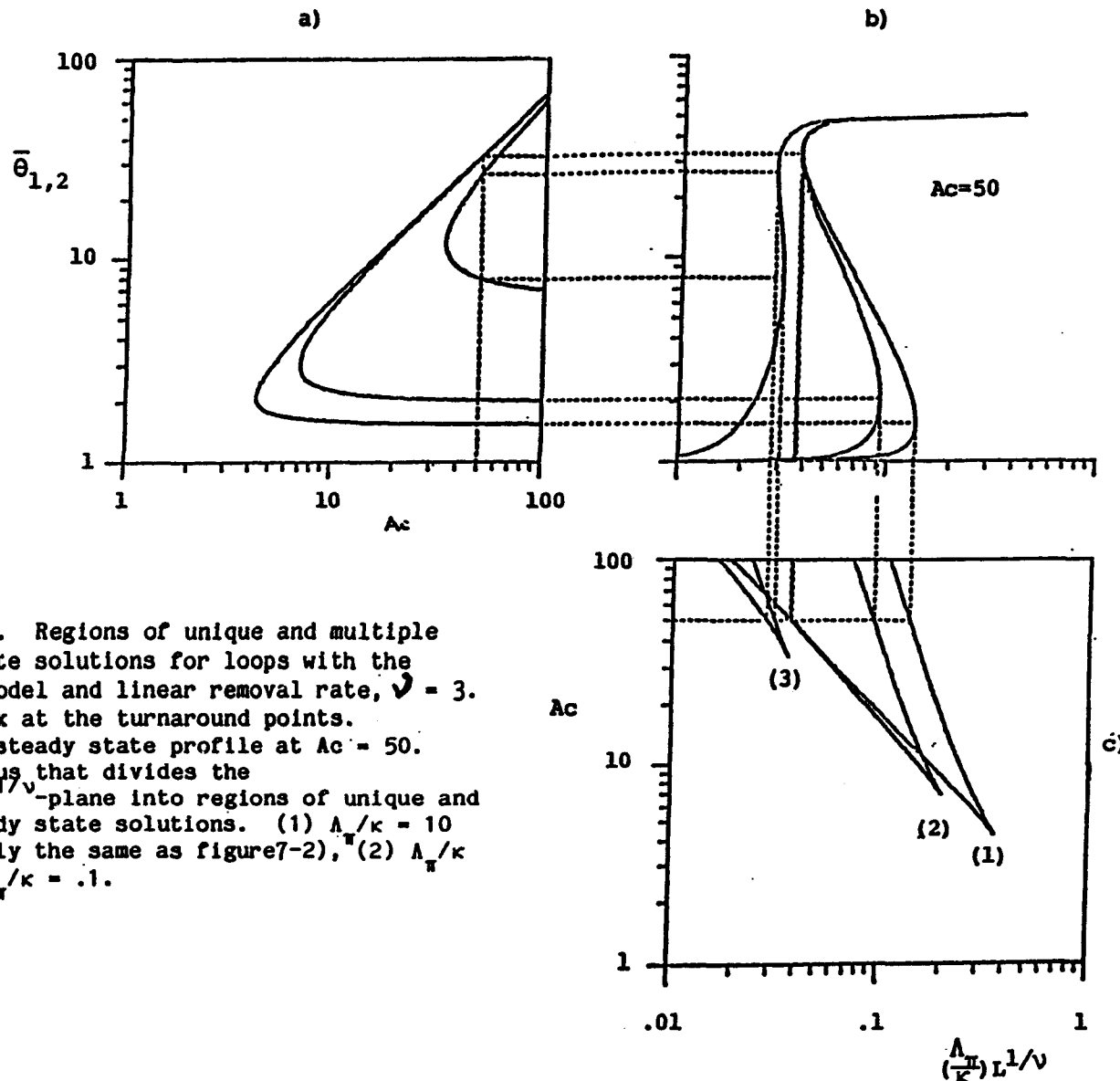


Figure 7-8. Regions of unique and multiple steady state solutions for loops with the symmetry model and linear removal rate,  $v = 3$ .

a) The flux at the turnaround points.

b) Sample steady state profile at  $A_c = 50$ .

c) The locus that divides the  $A_c, (\Lambda_\pi / k)L^{1/v}$ -plane into regions of unique and three steady state solutions. (1)  $\Lambda_\pi / k = 10$  (essentially the same as figure 7-2), (2)  $\Lambda_\pi / k = 1$ , (3)  $\Lambda_\pi / k = .1$ .

the end product concentrations in the two states being  
 $Ac(1+L)/(1+AcL)$ .

#### 7.4.2. Michaelis-Menten removal rate.

Substituting the rate law for Michaelis-Menten kinetics, equation 20, into the criteria for multiplicity we get

$$z^2 - \frac{(1-1/v-2/\Omega_m)Ac + (1+1/v)}{(1-1/\Omega_m)(1-Ac/\Omega_m)}z + \frac{Ac + (Ac-1)/v(\Lambda_\pi/\kappa)}{(1-1/\Omega_m)(1-Ac/\Omega_m)} \leq 0 \quad (46)$$

As before we look for real positive roots to the quadratic equation which are real positive only if  $\Omega_m$  is greater than unity. Two positive real roots appear if

$$Ac \geq Ac_{\min} = \frac{(v+1)^2 + 4v(1-1/\Omega_m)/(\Lambda_\pi/\kappa)}{(v-1)^2 + 4v(1+(1-1/\Omega_m)/(\Lambda_\pi/\kappa))/\Omega_m} \quad (47)$$

A double root appears

$$z_{\min} = \frac{v+1 + 2(1-1/\Omega_m)/(\Lambda_\pi/\kappa)}{(v-1)(1-1/\Omega_m)} \quad (48)$$

if  $Ac = Ac_{\min}$ . Here the boundaries on the region of multiplicities are given by

$$L = \left( \frac{(1-1/\Omega_m)z-1}{Ac-(1-Ac/\Omega_m)z} \right) \left( \frac{1}{1+(\Lambda_\pi/\kappa)z} \right)^v \quad (49)$$

Using  $z_{\min}$  and  $Ac_{\min}$  in equation 49 gives a maximum value for L as

$$L_{\max} = \left( \frac{v-1}{v+1} \right)^{v+1} \frac{1 + \frac{4v/\Omega_m}{(v-1)^2} \left( 1 + \frac{1-1/\Omega_m}{\Lambda_\pi/\kappa} \right)}{\left( 1 + \frac{\Lambda_\pi/\kappa}{1-1/\Omega_m} \right)^v} \quad (50)$$

One of the real roots becomes zero at  $A_c = \Omega_m$  while the other is positive

$$z_0 = \left(\frac{1}{1-1/v}\right)\left(\frac{1}{1-1/\Omega_m} + \frac{1}{v\Lambda_\pi/\kappa}\right) \quad (51)$$

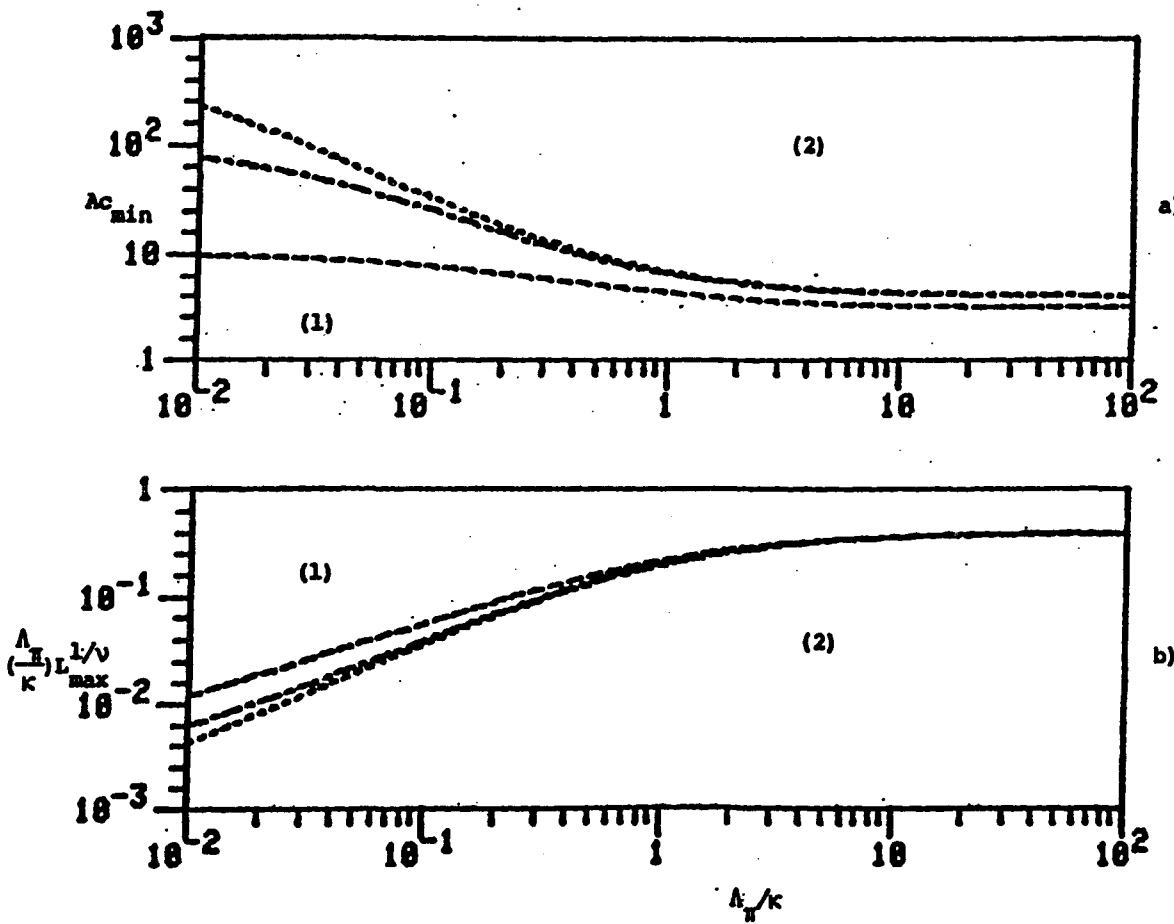
$$L_0 = (v-1)^{v-1} \left(\frac{1+(1-1/\Omega_m)/(\Lambda_\pi/\kappa)}{\Omega_m}\right) \left(\frac{1}{v(1+(\Lambda_\pi/\kappa)/(1-1/\Omega_m))}\right)^v \quad (52)$$

Here the upper turnaround point disappears and the steady state equation can have none or two solutions. The second root crosses the origin and becomes negative at  $\Omega_m = 1$ , and then no steady state solutions exist. Again in the limit  $\Lambda_\pi/\kappa \rightarrow \infty$  this is the same result as for loop 1. By making the saturation velocity finite the region of multiple solutions grows larger, as for loop 1, figure 7-9, and again the main effects of the symmetry mechanism start to appear when  $\Lambda_\pi/\kappa$  is less than about unity. In the region of three solutions the ratio between the two stable steady state fluxes is approximately  $A_c$ , but the ratio between the concentrations in the two states depends on  $\Omega_m$ .

### 7.5. Discussion.

In the above analysis we have examined feedback regulation via enzyme activation in a linear metabolic reaction sequence. Using the general criterion for multiple steady state solutions, derived in chapter 6, we search the parameter space of biologically relevant

Figure 7-9. Critical values, a) of  $A_c$  (equation 47) and, b) of  $L$  (equation 50) for the appearance of multiple steady state solutions for a loop with the symmetry model and Michaelis-Menten removal.  $\cdots \cdots \cdots \quad Q = 10$ ,  $- - - - \quad Q = 100$ ,  $\cdot \cdot \cdot \cdot \cdot \cdot \quad Q = 1000$ . Region (1) unique solution, and region (2) multiple solutions possible. Limiting values at high  $A_x/k$  values are given by equations 29 and 32 (with  $(A_x/k)L^{1/\nu}$  exchanged with  $A_x/k$ ).



rate laws for the regions of multiplicities. By scaling the equations we are able to attain separation of kinetic quantities from process dependent parameters. This separation is important conceptually since the kinetic parameters can be assumed to be genetically determined and invariant for normal in vivo conditions: such factors as ionic concentrations, temperature or pressure can be assumed to define an invariant intra-cellular environment in which the reactions take place. By process dependent parameters we mean dimensionless ratios that explicitly contain metabolite and enzyme concentrations. Substrate and enzyme concentrations will vary with the activity of the cell at a particular time and hence the concentration parameters will vary with the physiological state of the cell.

The kinetic parameters reflect the intrinsic properties of the metabolic machinery and have been chosen by the evolutionary process. They will in part reflect physical constraints imposed on the design of metabolic networks, such as through thermodynamic limitations on achievable equilibrium constants, attainable kinetic performance of enzymes, etc. In this respect it is pertinent to point out that Albery and Knowles (1976, 1977) have argued on thermodynamic grounds that enzymes have evolved essentially to perfection as catalysts. Cleland (1975) has also put this view forward and presents several case studies.

On the other hand the concentration related parameters are quantities which the cell can influence directly, but they are also

in part determined by the external environment, for instance through substrate availability. The concentration parameters will reflect the cell's efforts to specify the physiological state, for instance through genetic regulation of the enzyme concentrations. Let us elaborate these points by discussing the simple system under study herein.

The dimensionless kinetic parameters in the model discussed above are:  $v$ ,  $A_c$ ,  $L$  and  $A_f$ . The first three are strictly properties of the regulatory enzyme and the fourth is a measure of the end product's relative affinity for the regulatory enzyme and the removal enzyme. There are some limitations on the selection of numerical values for these kinetic constants. Measured values for the degree of cooperativity, the Hill coefficient, fall in a range between values above unity to about three. In the symmetry model  $v$  is the number of inhibitor binding sites which most commonly is 2 or 4, for the frequently occurring dimeric and tetrameric forms respectively.

The kinetic parameters can be modified by changing the structure of the proteins involved. For instance a regulatory protein following the symmetry model lies in two configurations in equilibrium with each other as described by  $L$ . If a higher value for  $L$  is more feasible then one can visualize a change in the amino acid composition of the enzyme, through an evolutionary process, that leads to a more stable  $X$  form. That will shift the  $E \leftrightarrow X$  equilibrium towards  $X$  leading to a higher value for  $L$ . Hence the kinetic properties can be modified by evolution if the design of the

metabolic machinery is unsatisfactory, but it appears that an "optimal" design of metabolic enzymes has been reached after billions of years of evolution (Cleland, 1975, Albery and Knowles, 1976, 1977).

The selection of the kinetic properties specifies the intrinsic properties of the loop, and its behavior is determined by the concentration parameter,  $1/\Omega_m$ . This parameter is a ratio between two saturation velocities, and for biological reactions saturation velocities are typically proportional to the total concentration of the enzyme catalysing the reaction and a rate constant, which may be a function of the reactant concentrations. Here we can write

$$\Omega_m = \frac{V_m}{I_{max}} = \frac{k_2(e_R)_t}{k'_I se_t} \quad (53)$$

by writing the saturation velocity for the Michaelis-Menten rate law in its standard form,  $V_m = k_2(e_R)_t$ , where  $k_2$  is the turnover rate constant and  $(e_R)_t$  is the total concentration of the removal enzyme. For  $I_{max}$  we have used equation 12. (The quantity multiplying the total enzyme concentration often has a complex dependence on the substrate, but those details are not important to this discussion). The ratio of equation 53 tells us explicitly how the availability of substrate and the concentrations of the two enzymes affect the behavior of the controlled reaction chain. By varying this ratio the loop can be forced to operate at two different steady states for the proper combination of the kinetic parameters.

Let us for instance examine figure 7-6. If  $A_f = 20-30$ ,  $A_c = 50$ ,

and  $v = 3$  the loop is operating at the lower steady state for  $\Omega_m = 1000$ . Now if an increase in the substrate occurs so that  $\Omega_m$  changes to 100 the loop will be "geared up" to the upper steady state leading to a higher flux and a more rapid rate of substrate utilization. Similar remarks apply to the other combination of rate laws discussed above. Another possible situation is where the cell has an intra-cellular substrate pool available but is not actively utilizing it. Then if the utilization of this substrate is desired the cell can, by simply changing the ratios of the enzyme concentrations, through some form of genetic regulation, shift the flux to the upper steady state.

It is most likely undesirable to have  $\Omega_m$  less than Ac. The reason is that when two steady state solutions exist the upper one is unstable. Then for sufficiently large perturbations from the lower steady state the removal rate will drop so far below the increasing input rate that an infinite buildup of product occurs. This is perhaps the reason why key regulatory enzymes frequently have relatively low saturation velocities. In the next chapter we shall see similar results for negative feedback. Also one can visualize a pathological situation developing from these considerations. Enzyme deficiency, in this case in the removal enzyme, can lead to the disappearance of the upper steady state which may be a state that is physiologically important. Then if the cell tries to shift its operation to that state a disaster results.

In short positive feedback regulation is well suited for servo

type regulation where the decision on operating conditions is imbedded in the kinetic properties of the enzymes involved and a decision is made depending on the concentrations at which key metabolites are present. The location of the turnaround points thus becomes a central issue since they tell us how and why the organism makes a decision. This issue is not discussed further herein since it requires further investigation.

Finally we note that although our development is aimed at metabolic systems they apply equally well to epigenic systems since such systems have analogous descriptions. Also, although perhaps not of major physiological importance, the above development applies directly to feedforward control. This is easy to see since the reaction chain does not influence the results; the results are only dependent on the two rate laws, and no information is required about their relative location in the reaction chain.

#### 7.6. Summary.

Here we expand the results from chapter 6 by searching the parameter space of biologically realistic rate laws for multiple stable steady states. The impetus for this work is to seek the origin of decision making strategies at the metabolic level, with particular emphasis on the switching between the operating conditions needed to meet changing substrate availability and organism requirements.

The control loop considered herein is a linear reaction chain in which the end product of the reaction sequence feedback activates the first reaction in the sequence to produce feedback control. It has been found that the criteria for the existence of multiple steady state solutions in such loops involve only the kinetics of the regulatory enzyme controlling the first reaction and that of end product removal. The effects of these kinetics are examined here using two representative models for the regulatory enzyme: the lumped controller, based on Hill-type kinetics, and the symmetry model. The removal rate is assumed to be of the Michaelis-Menten type.

The behavior of these two models is qualitatively similar, and both show the characteristics needed for switching between next-to-none and high substrate utilization. Moreover, judicious scaling of the governing equations permits separation of genetically determined kinetic parameters from process dependent ones. This allows us to conclude that, for a fixed set of kinetic parameters, the steady state flux through the loop can be switched between stable steady states by merely varying the process dependent numbers. In particular, when the initial substrate exceeds a certain critical level, the loop can be switched on, and similarly, when it falls below a critical level, the pathway is shut down. Similar effects can be realized by varying the ratios of enzyme concentrations. It is proposed that by identifying these critical points one can gain significant insight into the objectives of decision making at the metabolic level.

## CHAPTER 8

## SINGLE BIOCHEMICAL CONTROL LOOPS:

## NEGATIVE FEEDBACK

Metabolic oscillations have been known for some time now and the best studied examples are; glycolytic oscillations in yeast and muscle, mitochondrial oscillations, and the cAMP-oscillator in Dictyostelium discoideum, see reviews in Higgins (1967), Hess and Boiteux (1971), Chance, Pye, Ghosh and Hess (1973), Hess, Boiteux and Busse (1975), Goldbeter and Nicolis (1976), Goldbeter and Caplan (1976). Although some investigators have postulated a physiological role for metabolic oscillation it is not always clear whether they serve any purpose or whether this phenomena is simply a manifestation of the regulatory structure employed. For instance instabilities in yeast glycolysis are only observed over a narrow range of throughput fluxes, above and below which the oscillations disappear. It is conceivable that the organism is simply not "designed" to operate under these conditions and the "installed" control structure simply cannot achieve stable operation under the imposed circumstances. On the other hand cAMP driven oscillations in D. discoideum appear to have a well defined physiological role associated with the process of

differentiation.

Periodic synthesis of enzymes in exponentially growing cell populations has been known to occur for about 20 years. The period of these oscillations were found to be close to the cell cycle time, and that led to the notion of cell cycle dependent metabolism. This implies that the enzyme composition would change throughout the cell cycle in perfect harmony with the needs of the cell. However Tyson (1983), in an elegant analysis, has argued that the closeness of the two periods may just be a coincidence since both periods, those of cell cycling and protein synthesis, are found to be intimately related to the mass doubling time.

Modelling of metabolic/genetic regulation goes back about 20 years. The first studies appear to be due to Goodwin (1963, 1965, 1966) where he formulated a simple dynamic model, consisting of three differential equations, to describe repression of enzyme synthesis. This basic model was then extended to fit metabolic regulation by Morales and McKay (1967). Following these model formulations came a period of extensive analytical and numerical analysis of the properties of these equations, most often called the Goodwin equations even in their general form, during the late sixties and throughout the seventies. This extensive material is reviewed at some length in Tyson and Othmer (1978) and in more qualitative terms in chapter 9. Very similar feedback models have been used to describe feedback regulation on other levels of biology, see May (1974, 1976), Mckay and Glass (1977), and Nazarenko and Sel'kov

(1978).

We began our study in chapter 6 by formulating a structural model of the single biochemical control loop, which, as discussed above, appears to be of quite general occurrence at many levels of biology. In particular one limit of our model represents the well studied Goodwin oscillator and we shall among other things include extensive numerical results for this well known model. Biochemical control loops have been shown to display several qualitatively different types of dynamic behavior, including a stable monotonic approach to the steady state point, multiplicity of stable steady states, and sustained oscillations around an unstable steady state. Our first objective was to try to locate the onset of transition from one behavior regime to another. The loci separating these regions can be obtained through local stability and bifurcation analysis. We tried to carry out this analysis without specifying all details since in that way we can accommodate the wide range of situations of interest.

The local stability analysis (chapter 6) revealed that inhibition of the first step in a reaction sequence by the end product can lead to sustained oscillatory behavior. The bifurcation criteria were obtained without specifying all the details of the model, in particular the kinetics of the regulated input rate into the sequence and the removal rate of the end product. The purpose of the present chapter is to specify these details and map the bifurcation loci into parameter spaces of interest.

The control action is normally exerted through allosteric enzymes (Sols, 1981) whose the kinetic behavior, fortunately, well characterized. Here we shall discuss and compare the response of a "lumped" controller, based on Hill-type kinetics (Hill, 1910), with that of the mathematically elegant, but physically realistic, symmetry model of Monod, Wyman and Changeux (1965). The Goodwin equations have regulatory kinetic of the Hill type. For the removal rate we use Michaelis-Menten kinetics. Our purpose is to determine the level of complexity needed to represent the important features of feedback inhibition in single biochemical control loops, to examine the parametric sensitivity of the region of unstable steady states, and to compute the stability of the bifurcated solutions using Poore's magic number (Poore, 1975, 1976).

We begin our analysis in section 8.1 by defining the single biochemical control loop (described in detail in section 6.1) which we use as a vehicle for probing enzyme behavior, and by presenting criteria for the appearance of Hopf bifurcations. We also discuss how to assess the stability of the bifurcated solutions and the necessary kinetic rate laws for subsequent analysis. In sections 8.2 and 8.3, respectively, we examine the stability of steady state and oscillatory solutions for the two models of regulatory enzymes.

### 8.1. The Single Biochemical Control Loop.

#### 8.1.1. The mathematical model.

In chapter 6 the following kinetic model was developed for the single biochemical control loop, see figures 6-1 and 7-1

$$C(\mathcal{D})\theta = \Psi(\pi) \quad (1)$$

$$\frac{d\pi}{d\tau} + \Omega(\pi) = \theta \quad (2)$$

Here  $C(\mathcal{D})$  is a dynamic operator describing the reaction chain ( $\mathcal{D} = d/d\tau$ ), whose properties are discussed in the first part of this thesis.  $\Psi(\pi)$  is the reaction rate through the regulated reaction,  $\theta$  is the rate of formation of the final product  $\pi$ , and  $\Omega(\pi)$  is the removal rate of the final product. This model is presented here in a dimensionless form, and the scaling of the equations, described in detail in chapters 6 and 7, is not repeated here.

#### 8.1.2. Local stability analysis.

The famous Hopf bifurcation theorem (Hopf, 1942, also see Marsden and McCracken, 1976), loosely speaking, states that when the Jacobian matrix for a system of non-linear differential equations has a purely imaginary pair of eigenvalues then the solution bifurcates to a oscillatory orbit, called a limit cycle. The condition for purely imaginary eigenvalues in the above model has been found to be (chapter 6) a complicated condition that can in general represented by

$$\bar{\Psi}_{\pi} \leq \ell(\bar{\Omega}_{\pi}, n, \tau_d, (\tau_i)_{i=1,n}) \quad (3)$$

where  $\ell$  is a locus that is not always available explicitly. The locus depends on:  $\bar{\Omega}_{\pi}$ , the partial derivative of the removal rate with respect to the end product concentration  $\pi$  evaluated at the steady state (denoted by the overbar),  $n$ , the order of the dynamic operator  $C(t)$ ,  $\tau_d$ , a diffusional time lag (which we shall consider negligible herein) and  $\tau_i$ , the time constants of  $C(t)$ . The locus  $\ell$  is negative forcing  $\bar{\Psi}_{\pi}$  to be negative in order for Hopf bifurcations to occur, which implies that the feedback interaction must be inhibitory. To obtain the stationary conditions the steady state equation

$$\Psi(\bar{\pi}) = \bar{\theta} = \Omega(\bar{\pi}) \quad (4)$$

must be solved simultaneously with equation 3. It simply states that all the fluxes must be equal in the steady state.

The purpose of this chapter is to introduce physiologically meaningful rate laws for  $\Psi(\pi)$  and  $\Omega(\pi)$  into equations 3 and 4 and thereby project the dynamic stability criterion into the relevant parameter spaces.

#### 8.1.3. Kinetic description of regulatory enzymes.

In section 7.2 two kinds of regulatory kinetics, the lumped controller based on Hill-type kinetics and the symmetry model we examined. Here we shall use the same rate laws.

The Lumped Controller. One of the oldest reaction mechanisms for ligand binding to oligomeric enzymes is due to Hill (1910). By simple extension of it (section 7.2) one can derive

$$\Psi(\pi) = \frac{1}{1 + (\Lambda_{\pi}\pi)^v} \quad (5)$$

by assuming a transformation of the free enzyme (E) through simultaneous and reversible binding of  $v$  molecules of the end product P into a catalytically inactive state (X). The regulatory action of P is then lumped in the simple E to X transformation. The parameter  $\Lambda_{\pi}$  appearing is a dimensionless binding constant of the product ( $\pi$ ) to the enzyme, and  $v$  is called the degree of cooperativity or the Hill coefficient. Equation 5 is equation 11 in chapter 7 with  $Ac = 0$ .

The Symmetry Model. One of the earliest kinetic models that accounted for allosterism was the model of Monod et al., (1965), called the symmetry model after certain assumed symmetry properties of the subunits of the enzyme. It is a more realistic description of the allosteric mechanism than the lumped controller. Instead of simultaneous binding, as for the lumped controller, the symmetry model assumes a sequential binding of  $v$  molecules of the modifier the X form, which naturally exists in equilibrium with E. The rate law is

$$\Psi(\pi) = \frac{1}{1 + L(1+\Lambda_{\pi}\pi)^v} \quad (6)$$

which is the same as equation 16 in section 7.2 with  $Ac = 0$ . Here L

is the equilibrium constant for the conversion of E to X, the so-called allosteric constant, and the other parameters are defined as above. If  $\Lambda_{\pi}$  is large the symmetry model becomes analogous to the lumped controller with  $\Lambda_{\pi}$  for the lumped controller being equivalent to  $\Lambda_{\pi} L^{1/\nu}$  for the symmetry model. The two models yield similar rate laws and the price we pay for the more sophisticated binding mechanism is the additional thermodynamic parameter L.

#### 8.1.4. Kinetic description of the removal rate.

It remains only to find an explicit expression for the removal rate  $\Omega(\pi)$ . A common feature of biological rate laws is saturation kinetics at high substrate concentrations, and the simplest of these rate laws is the Michaelis-Menten equation

$$\Omega(\pi) = \frac{\kappa\pi}{1+\kappa\pi/\Omega_m}, \quad \kappa = \frac{V_m}{K_m} t_c, \quad \Omega_m = \frac{V_m}{I_{sat}} \quad (7)$$

where  $\Omega_m$  is the dimensionless form of the saturation velocity  $V_m$ , and where  $\kappa$  is the dimensionless form of the pseudo-first order rate constant  $V_m/K_m$  ( $K_m$  is the well known Michaelis constant). This rate law changes from first order ( $\Omega(\pi) = \kappa\pi$ ) to zeroth order ( $\Omega(\pi) = \Omega_m$ ) kinetics depending on reaction conditions and the numerical values of the rate constants.

#### 8.1.5. Stability of bifurcated solutions.

To assess the stability of the bifurcated solutions we need to

compute a complex quantity given by Poore (1975, 1976)

$$\begin{aligned} M_n = & -u_1 f_{ijk}^1 v_i v_j v_k^* + 2u_1 f_{ik}^1 v_j [J^{-1}]_{k,r} f_{pq}^r v_p v_q \\ & + u_1 f_{jk}^1 [(J - 2i\omega I)^{-1}]_{k,r} f_{pq}^r v_p v_q \end{aligned} \quad (8)$$

where (Tyson and Othmer, 1978):

(a)  $u_i$  and  $v_i$  are the elements of the eigenrows and eigenvectors, respectively, of the Jacobian matrix  $J$  corresponding to the purely imaginary eigenvalue,  $i\omega$ , and where  $v_i^*$  is the complex conjugate of  $v_i$ . The eigenrows and eigenvectors are normalized so that the inner product  $\underline{u} \cdot \underline{v}$  is real positive, normally chosen to be unity.

(b)  $f_{ijk}^l$ ;  $f^l$  is the  $l^{\text{th}}$  component of  $\underline{f}$ ,  $d\underline{x}/dt = \underline{f}(x)$ , and the subscripts on  $f$  denote partial derivatives, in this case with respect to  $x_i$ ,  $x_j$  and  $x_k$ .

(c) The expression is in the Einstein notation where the repeated indices,  $i,j,k,l,p,q$  and  $r$ , imply sums.

$M_n$  has been given the descriptive name the "Magic Number" by Mees and Rapp (1978).

To check for stability of the bifurcated solutions one examines the sign on the real part of  $M_n$ . If the real part is positive then the bifurcated solutions are stable, and conversely if it is negative the oscillatory solution is unstable.

For the equations under investigation here an explicit analytical expression for  $M_n$  is attainable. If the dynamic operator  $C(\mathbb{D})$  is described by an  $n^{\text{th}}$  order linear differential equation it can be written as a set of  $n$  first order differential equations and the

model of the loop becomes

$$\frac{d}{d\tau} \begin{bmatrix} \theta_1 \\ \theta_2 \\ \theta_3 \\ \vdots \\ \theta_n \\ \pi \end{bmatrix} = \begin{bmatrix} -1/\tau_1 & & & & & \cdot & \theta_1 \\ 1/\tau_2 & -1/\tau_2 & & & & \cdot & \theta_2 \\ & 1/\tau_3 & -1/\tau_3 & & & \cdot & \theta_3 \\ & & \ddots & \ddots & & \cdot & \vdots \\ & & & 1/\tau_n & -1/\tau_n & \cdot & \theta_n \\ \dots & \dots & \dots & \dots & \dots & 1 & 0 \end{bmatrix} \begin{bmatrix} \theta_1 \\ \theta_2 \\ \theta_3 \\ \vdots \\ \theta_n \\ \pi \end{bmatrix} + \begin{bmatrix} \Psi/\tau_1 \\ \vdots \\ -\Omega \end{bmatrix} \quad (9)$$

where the argument list of  $\Psi$  and  $\Omega$  has been dropped for convenience.

Here  $\theta_1, \dots, \theta_{n-1}$  are dummy variables and  $\theta = \theta_n$ . The non-linearities are confined to  $\Psi$  and  $\Omega$ . Linearizing this model gives a  $(n+1) \times (n+1)$  Jacobian matrix

$$J = \begin{bmatrix} -1/\tau_1 & & & & & \cdot & \bar{\Psi}/\tau_1 \\ 1/\tau_2 & -1/\tau_2 & & & & \cdot & \bar{\pi} \\ & 1/\tau_3 & -1/\tau_3 & & & \cdot & \vdots \\ & & \ddots & \ddots & & \cdot & \vdots \\ & & & 1/\tau_n & -1/\tau_n & \cdot & \vdots \\ \dots & \dots & \dots & \dots & \dots & 1 & -\bar{\Omega}/\bar{\pi} \end{bmatrix} \quad (10)$$

Our system is particularly simple since we have only two non-linear terms  $\Psi$  and  $\Omega$ , hence  $l$  and  $r$  take only two values 1 and  $n+1$ , and the only state variable appearing in these functions is  $\pi$ , hence  $i, j, k, p$  and  $q$  only take the value  $n+1$  corresponding to  $\pi$ . Introducing  $i = j = k = p = q = n+1$  into equation 8 yields

$$M_n = \|v_{n+1}\|^2 v_{n+1} u_1 \left( -f_{\pi\pi\pi}^1 + f_{\pi\pi}^1 f_{\pi\pi}^r N_r \right) \quad l, r = 1 \text{ and } n+1 \quad (11)$$

where

$$N_r = 2[J^{-1}]_{n+1,r} + [(J - 2i\omega I)^{-1}]_{n+1,r} \quad (12)$$

Now we are in a position to evaluate the necessary quantities for  $M_n$ .

(1) the eigenvectors can be obtained from  $(J - i\omega I)\underline{v} = \underline{0}$  as

$$v_k = \left( \prod_{j=k+1}^n (1 + i\tau_j \omega) (\Omega_\pi + i\omega) \right) v_{n+1}, \quad k=1, \dots, n \quad (13)$$

(2) the eigenrows can be obtained from  $\underline{u}(J - i\omega I) = \underline{0}$  as

$$u_k = \frac{\tau_k}{\prod_{j=k}^n (i\omega\tau_j + 1)} u_{n+1}, \quad k=1, \dots, n \quad (14)$$

(3) the inner product  $\underline{u} \cdot \underline{v}$  as

$$\underline{u} \cdot \underline{v} = \bar{\Psi}_\pi \left( \frac{u_1 v_{n+1}}{\tau_1} \right) \left( \sum_{k=1}^{n+1} \frac{\tau_k}{1 + i\omega\tau_k} \right) \quad (15)$$

(4) the function  $N_r$  as

$$N_1 = \tau_1 \left( \frac{2}{\bar{\Psi}_\pi - \bar{\Omega}_\pi} + \frac{1}{\bar{\Psi}_\pi - g_+^{-1}(2i\omega)} \right) \quad (16)$$

and

$$N_{n+1} = \frac{2}{\bar{\Psi}_\pi - \bar{\Omega}_\pi} + \frac{g_+^{-1}(2i\omega)}{\bar{\Psi}_\pi - g_+^{-1}(2i\omega)} \quad (17)$$

where

$$g^{-1}(i\omega) = \prod_{k=1}^n (1 + i\omega\tau_k) \quad (18)$$

$$g_+^{-1}(i\omega) = g^{-1}(i\omega)(\bar{\Omega}_\pi + i\omega) \quad (19)$$

Substituting expressions (12) - (19) into equation 11 and choosing  $|v_{n+1}|^2 = 1$ , and putting  $\underline{v} \cdot \underline{u} = 1$  one finally obtains

$$M_n = \frac{-\left(\Psi_{\pi\pi\pi} - \frac{\Omega_{\pi\pi\pi}}{g(i\omega)}\right) + \left(\Psi_{\pi\pi} - \frac{\Omega_{\pi\pi}}{g(i\omega)}\right)\left(2\frac{\Psi_{\pi\pi} - \bar{\Omega}_{\pi\pi}}{\bar{\Psi}_\pi - \bar{\Omega}_\pi} + \frac{\Psi_{\pi\pi} - \bar{\Omega}_{\pi\pi} g_+^{-1}(2i\omega)}{\bar{\Psi}_\pi - g_+^{-1}(2i\omega)}\right)}{\sum_{k=1}^{n+1} \frac{\tau_k}{1 + i\omega\tau_k}} \quad (20)$$

To complete the development we need the derivatives of the input and

removal rates which are easily obtained from equations 5,6 and 7 as,  
for the lumped controller

$$\Psi_{\pi} = \frac{-v}{\pi} \frac{(\Lambda_{\pi})^v}{(1+(\Lambda_{\pi})^v)^2} = \frac{v}{\pi} (\Psi-1)\Psi \quad (21)$$

$$\Psi_{\pi\pi} = \frac{v}{\pi} \left( \frac{1}{\pi} (1-\Psi)\Psi + (2\Psi-1)\Psi_{\pi} \right) \quad (22)$$

$$\Psi_{\pi\pi\pi} = \frac{v}{\pi^2} \left( \frac{2}{\pi} (\Psi-1)\Psi - 2\Psi_{\pi} (2\Psi-\pi\Psi_{\pi}-1) + (2\Psi-1)\pi\Psi_{\pi\pi} \right) \quad (23)$$

for the symmetry model

$$\Psi_{\pi} = \frac{-v\Lambda_{\pi}}{(1+\Lambda_{\pi})} \frac{(\Lambda_{\pi})^v}{(1+(\Lambda_{\pi})^v)^2} = \frac{v\Lambda_{\pi}}{(1+\Lambda_{\pi})} (\Psi-1)\Psi \quad (24)$$

$$\Psi_{\pi\pi} = \frac{v\Lambda_{\pi}}{(1+\Lambda_{\pi})} \left( \frac{\Lambda_{\pi}}{(1+\Lambda_{\pi})} (1-\Psi)\Psi + (2\Psi-1)\Psi_{\pi} \right) \quad (25)$$

$$\Psi_{\pi\pi\pi} = \frac{v\Lambda_{\pi}^2}{(1+\Lambda_{\pi})^2} \left( \frac{2\Lambda_{\pi}}{1+\Lambda_{\pi}} (\Psi-1)\Psi - 2\Psi_{\pi} \left( 2\Psi - \frac{1+\Lambda_{\pi}}{\Lambda_{\pi}} \pi\Psi_{\pi}-1 \right) + \frac{1+\Lambda_{\pi}}{\Lambda_{\pi}} (2\Psi-1)\pi\Psi_{\pi\pi} \right) \quad (26)$$

and for the removal rate

$$\Omega_{\pi} = \frac{1}{\kappa} \left( \frac{\Omega}{\pi} \right)^2 \quad (27)$$

$$\Omega_{\pi\pi} = \frac{2\Omega}{\kappa\pi^3} (\pi\Omega_{\pi} - \Omega) \quad (28)$$

$$\Omega_{\pi\pi\pi} = \frac{2}{\kappa} \left( \left( \frac{\pi\Omega_{\pi}}{\pi^4} - \frac{3\Omega}{\pi} \right) (\pi\Omega_{\pi} - \Omega) + \frac{\Omega\Omega_{\pi\pi}}{\pi^2} \right) \quad (29)$$

### 8.2. Loops with Lumped Controllers.

We now use the lumped controller to describe the input rate and we call the resulting circuit Loop 1. To evaluate the stability criterion we substitute  $\Psi_{\pi}$ , given by equation 21, into equation 3 and when combined with the steady state equation which gives

$$-\frac{v}{\pi}(1-\Omega(\bar{\pi}))\Omega(\bar{\pi}) \leq \lambda \quad (30)$$

Now it remains only to define  $\Omega(\pi)$  and we find it useful to consider limiting cases of Michaelis-Menten kinetics first.

#### 8.2.1. Linear removal rate.

The linear limit of equation 7 is when  $\Omega(\pi) = \kappa\pi$  and substitution into equation 30 gives the stability criterion

$$\bar{\pi} \leq \frac{1}{\kappa}(1 + \frac{\lambda}{vk}) \quad (31)$$

The steady state equation

$$\frac{1}{1+(\Lambda_{\pi}\bar{\pi})^v} = \bar{\pi}\kappa \quad (32)$$

cannot be solved explicitly for  $\bar{\pi}$  and hence expressions for the boundaries on the instability regions cannot be obtained explicitly. However in the limit  $\Lambda_{\pi} \rightarrow \infty$  the analysis simplifies since  $\bar{\pi} \rightarrow 0$ . Here equation 31 becomes

$$0 \leq \frac{1}{\kappa}(1 + \frac{\lambda}{vk}) \quad \text{or} \quad -\lambda \leq vk \quad (33)$$

Finding the roots of equation 33 gives us the boundaries on the

region of instability since equation 31 can only be satisfied for positive  $\bar{\pi}$  if  $(1+\lambda/v\kappa)/\kappa$  is greater than zero. Let us illustrate these results with a simple example.

Example. An explicit expression for  $\lambda$  is available for a second order reaction chain ( $n=2$ ) equation 26 in chapter 6 as

$$\lambda = -2\xi(\kappa^2 + 2\xi\kappa + 1) \quad (34)$$

where  $\xi$  is the well known damping factor. Combining equations 33 and 34 gives

$$\kappa^2 + (2\xi - \frac{v}{2\xi})\kappa + 1 \leq 0 \quad (35)$$

which has roots

$$\kappa_{1,2} = \frac{1}{2}(\frac{v}{2\xi} - 2\xi \pm \sqrt{(\frac{v}{2\xi} - 2\xi)^2 - 4}) \quad (36)$$

If these roots are real positive then the stability criterion, equation 35, can be violated and dynamic bifurcations arise for  $\kappa$  values between the roots  $\kappa_1$  and  $\kappa_2$ . The region of unstable steady states appears when equation 35 has a double real root which happens when

$$v_{\min} = 4\xi(1+\xi) \quad (37)$$

and  $v$  has to exceed  $v_{\min}$  in order for instabilities to occur. If the reaction chain is critically damped ( $\xi = 1$ ) then the minimum value of  $v$  is eight. This value of  $v$  is considerably higher than expected physiological values of  $v$  and hence instabilities are not expected to appear for this case  $n=2$ . The only way to observe instability for reasonable values of  $v$  is if the reaction chain is underdamped

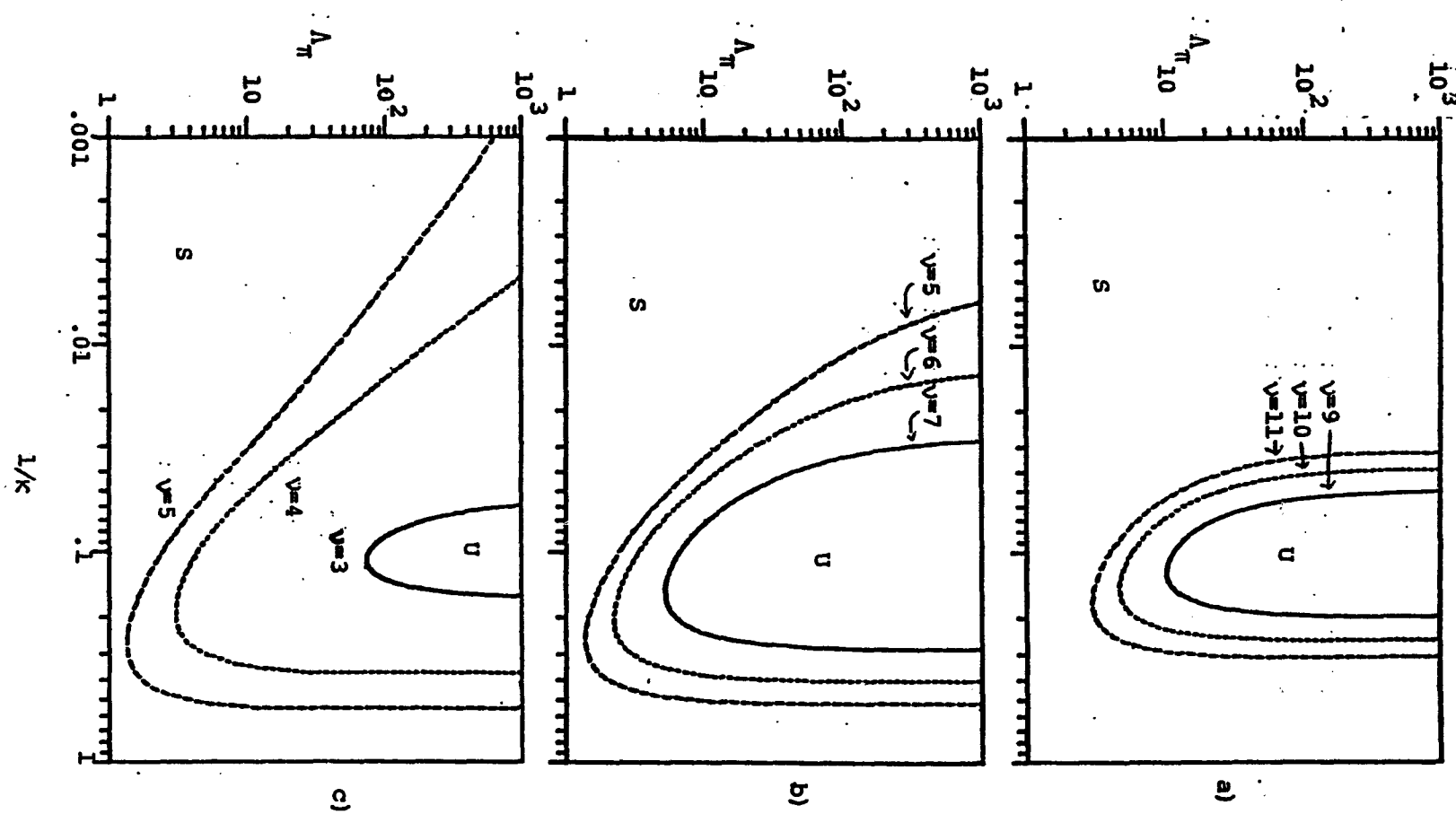
(e. g. if  $\xi = 1/2$  then  $v = 3$ ). Such underdamping is not expected unless the enzymes in the reaction chain show strong homotropic cooperativity (chapter 4). On the other hand if the reaction becomes overdamped,  $\xi > 1$ , the minimum value of  $v$  grows rapidly, e. g.  $v_{\min} = 15$  if  $\xi = 3/2$ .

-----

For higher order reaction chains this procedure is essentially numerical and results from computations are shown in figure 8-1. As the order of C( $\xi$ ),  $n$ , increases the non-linearity needed to produce instability needs to be less severe (reflected in lower values of  $v_{\min}$ ). Hence there is an inverse relationship between the order  $n$  and the degree of cooperativity  $v$ . From figure 8-1 it may be seen that in order for instability to be observed for reasonable values of  $v$  ( $\sim 3-4$ ) the order of the reaction chain has to be four or higher. An interesting observation is that the region of instability grows rapidly to higher values of  $\kappa$  but does not spread to lower values of  $\kappa$ .

The regions of instability shrink considerably if the reactions are not identical, i. e. if the damping factor  $\xi$  are greater than unity, figure 8-2. Here we show how the region of unstable steady states for  $n=4$  and  $v=5$  changes as one of the time constants is lowered (or equivalently when a damping factor is raised) to the same region as for  $n=3$ ,  $v=5$ . Hence distributing the time constants results in an effective reduction in the dynamic order, see also

Figure 8-1. Regions of instability in the  $\Lambda_\pi$ ,  $(1/\kappa)$ -plane for the linear limit of loop 1, ( $U$  = unstable region,  $S$  = stable region). a)  $n=2$ ,  $v = 9, 10, 11$ , b)  $n=3$ ,  $v = 5, 6, 7$ , and c)  $n=4$ ,  $v = 3, 4, 5$ . The values chosen for  $v$  are the three lowest values equal to or above  $v_{\min}$  ( $v_{\min}$  is the lowest value of  $v$  for which instability can be observed)



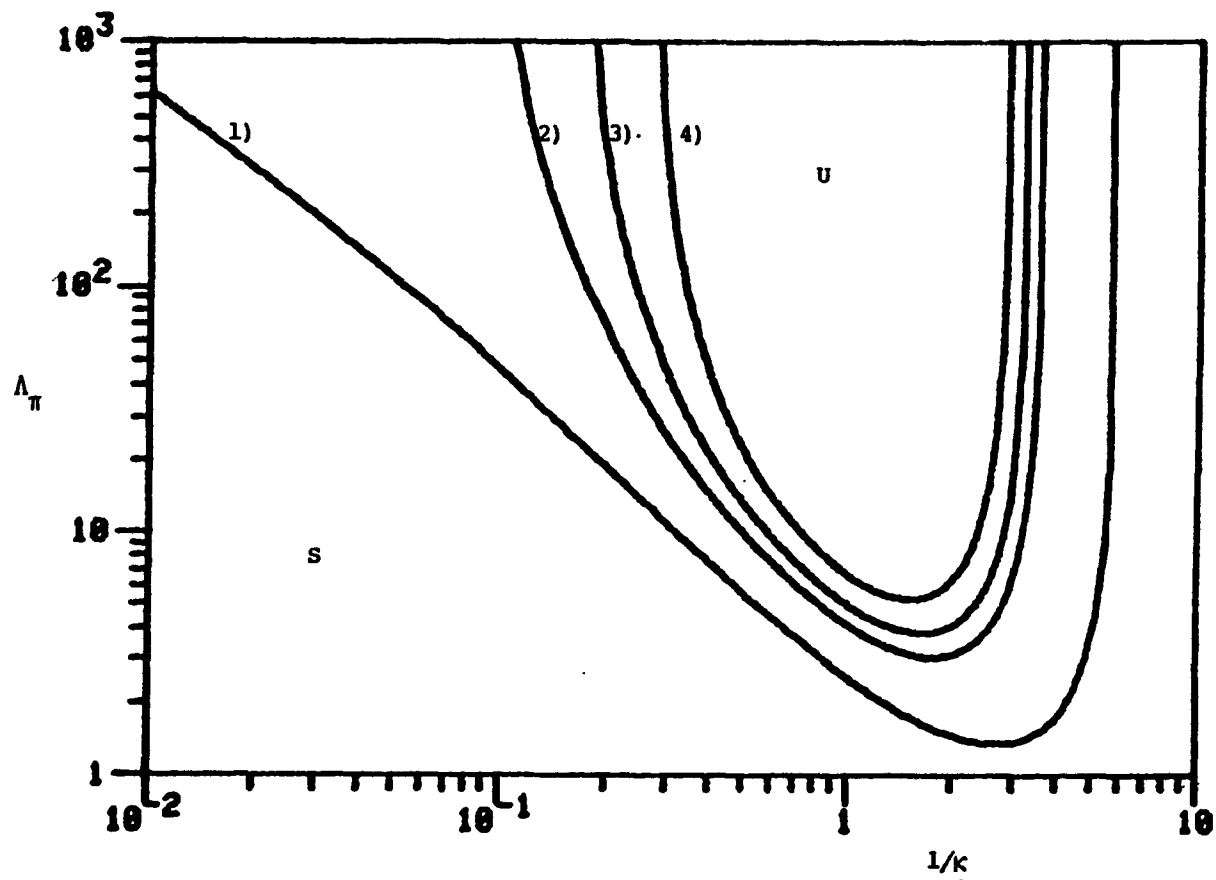


Figure 8-2. The effects of the damping factor  $\xi$  on the shape on the instability region for  $n=4$ ,  $v = 5$ , ( $U$  = unstable region,  $S$  = stable region). For all the curves  $\tau_1 = \tau_2 = \tau_3 = 1$  and  $\tau_4$  varies as follows; curve 1  $\tau_4 = 1$  (the same curve as in figure 8-1c), curve 2  $\tau_4 = .146$ , curve 3  $\tau_4 = .071$ , and curve 4  $\tau_4 = 0$  (the same curve as in figure 8-1b). Equivalent values of  $\phi$  and  $\xi$  for subsystem 2 are: curve 1,  $\phi = 1$ ,  $\xi = 1$ , curve 2,  $\phi = .382$ ,  $\xi = 1.5$ , curve 3,  $\phi = .268$ ,  $\xi = 2$ , and for curve 4,  $\phi = 1$ ,  $\xi$  meaningless.

chapter 5. This is the case when the kinetic properties of the reaction chain are well distributed, which appears to be the normal situation (Savageau, 1975, Rapoport et al., 1976 and Heinrich, Rapoport and Rapoport, 1977).

The Goodwin equations. In the 1960's Goodwin (Goodwin, 1963, 1965) proposed a model for repressive regulation of gene transcription which has become a well known model which is called the Goodwin Oscillator or the Goodwin equations. This model was later generalized to its most popular version by Morales and McKay (1967) in order to make it suitable for description of metabolic regulation. This common version of the Goodwin equations corresponds to the linear limit of our model and has been most extensively studied for the manageable limit of a critically damped reaction chain (i. e. when all the time constants and the removal rate constant are equal to unity). The available material on the Goodwin equations is reviewed and discussed in dept in the excellent paper of Tyson and Othmer (1978) (also a more qualitative discussion is found in chapter 9) and will not be repeated here.

The main result is an inverse relationship between  $n$  and  $v$  as discussed above. This led to the conclusion (e. g. Savageau, 1975) that making  $n$  low, which can be made by making the distribution of the relaxation times of the reaction chain wide (chapter 5), ensures stability for observed values of  $v$  ( $\approx 2-3$ ).

The computation of the magic number for the Goodwin equations has been discussed in MacDonald (1977a), Tyson and Othmer (1978) and

Mees and Rapp (1978) and these authors have argued, but not proven, that  $M_n$  is always positive and hence all bifurcated oscillatory solutions will be stable. Our extensive numerical work suggest that no sign changes in  $M_n$  exist in the linear limit and hence is in agreement with these investigators.

The original Goodwin equations also contained a zeroth order removal term in addition to the linear one. Recently Tyson (1983) has pointed out that the presence of such zeroth order term vastly changes the stability picture and we next examine the saturation limit.

### 8.2.2. Constant removal rate.

Substituting  $\Omega(\pi) = \Omega_m$  into equation 30 and the steady state equation gives

$$\bar{\pi} + \left(\frac{v}{\lambda_0}\right)(1-\Omega_m)\Omega_m \leq 0 \quad (38)$$

and

$$\bar{\pi} = (v\sqrt{1/\Omega_m - 1})/\Lambda_\pi \quad (39)$$

where  $\lambda_0 = \lambda$  at  $\bar{\Omega}_\pi = 0$ . Here we can eliminate  $\bar{\pi}$  between the two equations to obtain explicit bounds on  $\Lambda_\pi$  as

$$\Lambda_\pi \geq \left(\frac{-\lambda_0}{v\Omega_m^2}\right)\left(\frac{1-\Omega_m}{\Omega_m}\right)^{1/v-1} \quad (40)$$

This locus separating the stable steady states from unstable ones is shown in figure 8-3. The region of instability exists only for

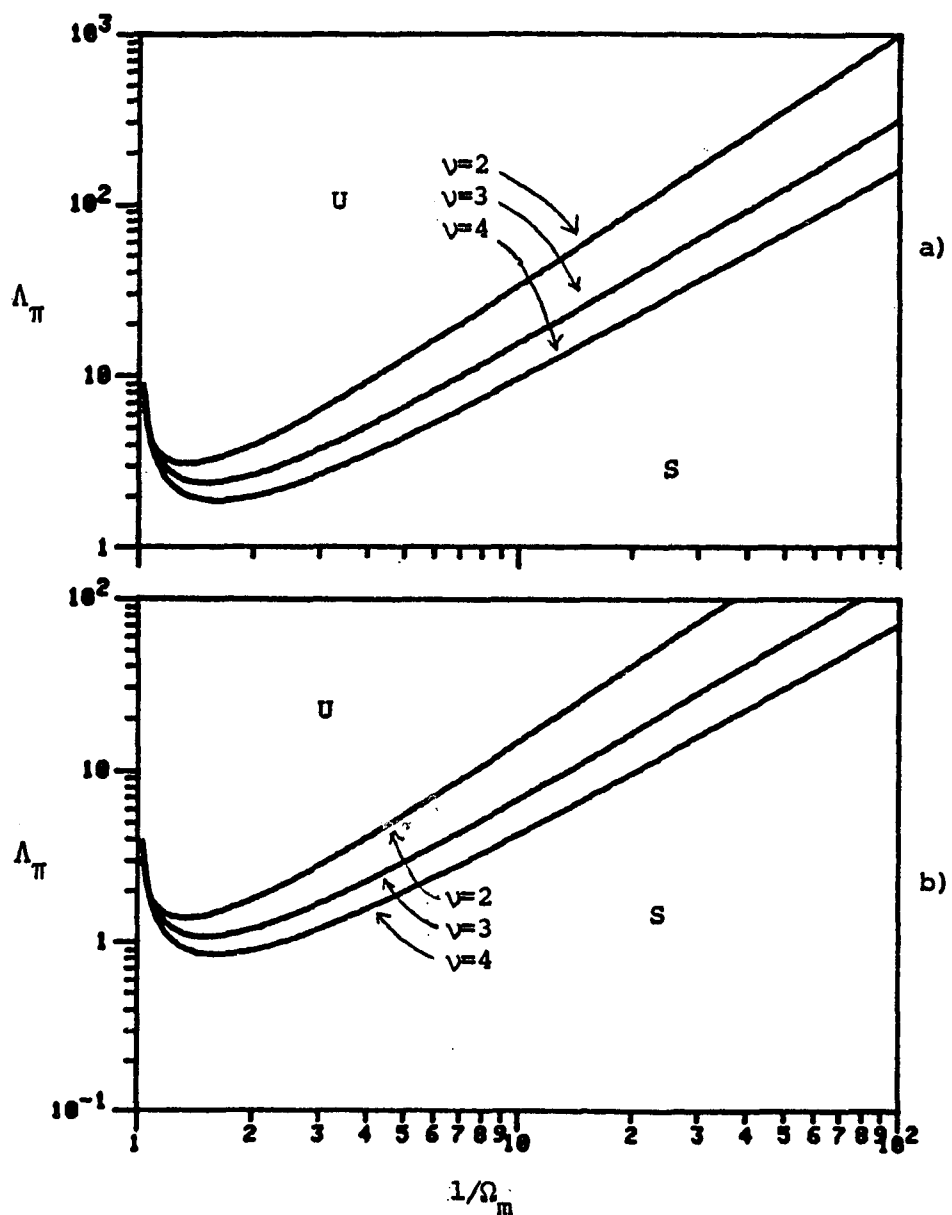


Figure 8-3. Instability regions for the saturation limit for loop 1 in the  $\Lambda_\pi, (1/\Omega_m)$ -plane, ( $U$  = unstable region,  $S$  = stable region). a)  $n=2$ ,  $v = 2, 3, 4$ , and b)  $n=3$ ,  $v = 2, 3, 4$ .

values of  $\Omega_m$  greater than unity since no steady state solutions exist for  $\Omega_m > 1$ , or  $V_m > I_{sat}$ . The region appears for physiologically meaningful values of  $v > 1$ . This is an important result since the extensive studies on the Goodwin equations, as discussed above, suggest that by keeping the effective order  $n$  low stability is ensured because larger than physiologically meaningful values of  $v$  are required to cause instabilities. Here, however, we observe instabilities for  $v$  values as low as 2 even for  $n=2$ .

As shown in figure 8-3 a minimum value of  $\Lambda_\pi$  occurs which corresponds to the inflection point of  $\Psi$  at  $(\bar{\Psi}_\pi)_{min} = (v+1)/2v$  and which is given by

$$(\Lambda_\pi)_{min} = \left(\frac{-4\lambda v}{v^2-1}\right) \left(\frac{v-1}{v+1}\right)^{1/v} \quad (41)$$

We have computed the magic number along the loci separating the regions and we have found the real part always to be positive and hence the bifurcated orbits are stable.

### 8.2.3. Michaelis-Menten removal rate.

Using the Michaelis-Menten form for  $\Omega(\pi)$  transforms the criterion for instability into

$$\bar{\pi}^2 + \frac{\Omega_m}{\kappa} \left(2 + \left(\frac{v\kappa}{\lambda}\right)(1-\Omega_m)\right) \bar{\pi} + \left(\frac{\Omega_m}{\kappa}\right)^2 \left(1 + \frac{v\kappa}{\lambda}\right) \leq 0 \quad (42)$$

This complicated criterion must be solved numerically.

Figure 8-4 shows the instability regions defined by equation 42.

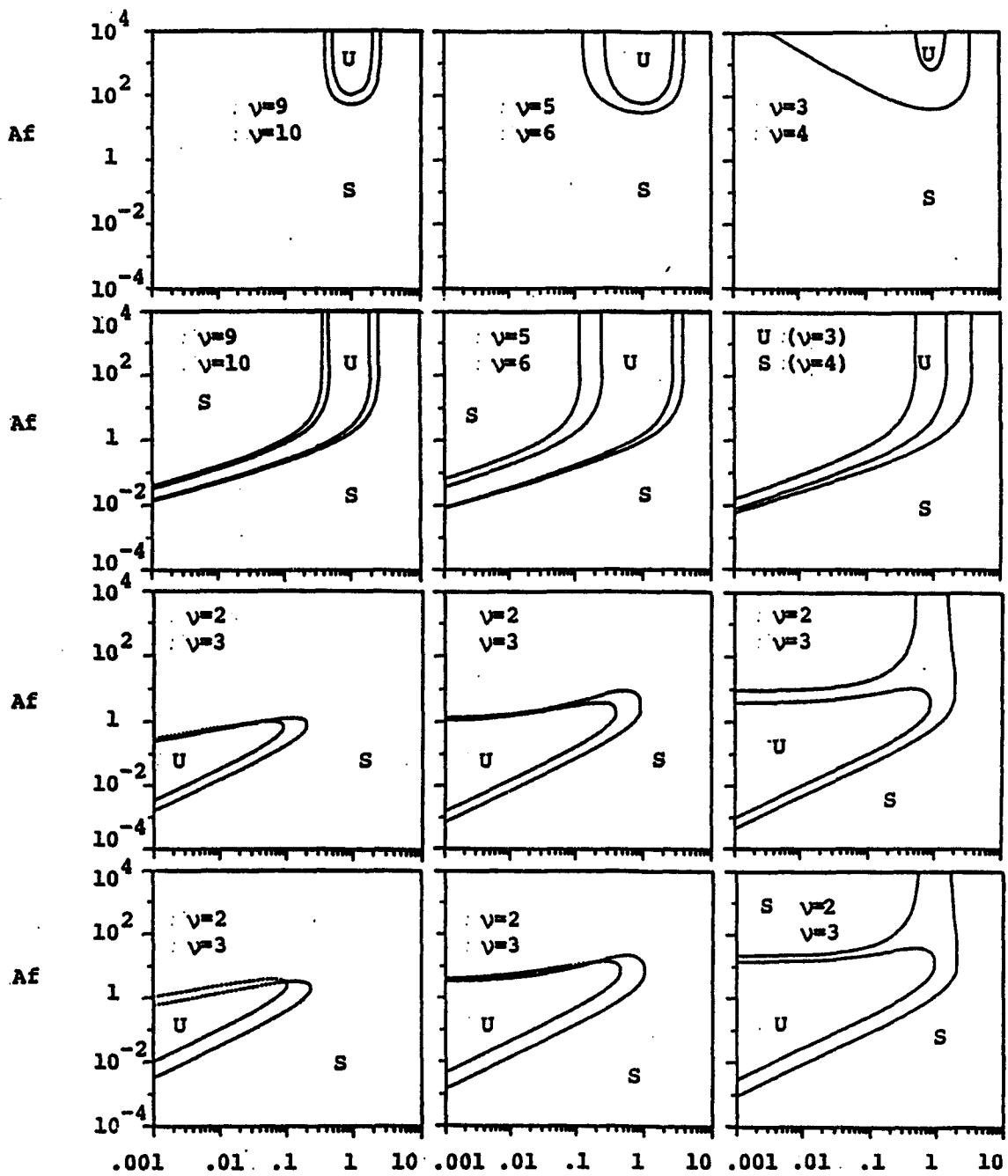
Figure 8-4.

Instability regions for loop 1 with Michaelis-Menten removal rate, ( $U = \text{unstable region}$ ,  $S = \text{stable region}$ ). The three columns represent  $n=2,3,4$  in increasing order from left to right. The four rows represent  $1/\Omega_m = .1, 1, 10, 100$  in increasing order from top to bottom. The instability regions shown are those for the two lowest values of  $v$  in each case. The parameter space in which the loci are traced is formed by the affinity ratio,  $Af$ , and the reciprocal of the dimensionless first order rate constant,  $1/\kappa$ . Solid curves indicate stable Hopf bifurcations, and dotted curves indicate unstable Hopf bifurcations. The reaction chain is critically damped.

Notes:

The roots of equation 33 are observed at  $1/\Omega_m = .1, 1$  and will also be seen at  $1/\Omega_m > 1$  for the appropriate values of  $v$  as can be seen for  $n=4$ .

For  $n=4$ ,  $1/\Omega_m = 1$  and  $v = 4$  only one root of equation 33 exists and all the region to the left of the loci is unstable.

FIGURE 8-4.

Here we have used the kinetic parameter  $Af$  (see equation 45 below) on the Y-axis and  $1/k$  on the X-axis and traced out the boundary between the stable and unstable region for several values of  $n$ ,  $v$  and  $\Omega_m$ . We now examine the influence of the dimensionless groups on the stability properties of the stationary point.

First we note the enormous influence of  $\Omega_m$  which can be written as

$$\Omega_m = \frac{V_m}{I_{sat}} = \left( \frac{k_R}{k_I s} \right) \left( \frac{(e_t)_R}{(e_t)_I} \right) \quad (43)$$

where the subscripts I and R refer to the regulatory (input) and removal enzymes respectively. Hence  $\Omega_m$  is a product of two ratios, the ratio of turnover numbers and enzyme concentrations for the removal and regulatory enzymes. If  $\Omega_m$  is greater than unity then the results of the linear limit do not change significantly, as can be seen from comparing the top row of figure 8-4 to figure 8-3. At  $\Omega_m = 10$  the instability regions have not changed much from figure 8-3 and instability is only observed for relatively high values of  $v$ . However when  $\Omega_m$  approaches and drops below unity significant changes occur both in the shape and size of the instability regions and they also appear at low values of  $v$ , even for the case  $n = v = 2$ . Hence instabilities can occur for realistic combinations of  $n$  and  $v$  which does not happen in the linear limit !

The value of  $\Omega_m$  depends on the relative concentration of the regulatory and removal enzymes, which is under epigenetic control, and the availability of the initial substrate: higher substrate supply

will tend to destabilize the loop. Here we see design considerations arise once again, the loop must be designed so that it is stable for the expected range of substrate concentrations or else modify the relative amounts of the enzymes.

The first order rate constant  $\kappa$  can be rewritten as

$$\kappa = \frac{V_m t_c}{K_m} = \left(\frac{k_R}{1/t_c}\right) \left(\frac{(e_t)_R}{K_m}\right) = \left(\frac{t_c}{t_R}\right) Qs_R \quad (44)$$

as a product of two ratios, a ratio between two time constants  $t_c$  and  $t_R$  ( $=1/k_R$ ) and of the total concentration of the removal enzyme to the Michaelis constant which is the quasi-steady state number,  $Qs_R$ , introduced in chapter 2. There is a minimum value of  $\kappa$  below which the loop is stable regardless of the value of  $Q_m$  which corresponds to the smaller root of equation 33. The value of  $\kappa$  is increased if the response time of the reaction chain becomes slow relative to  $t_R$ . This then suggests that the product of the turnover number of the removal enzyme and the reaction chain time constant should be kept of the order of  $1/Qs_R$ , since the smaller root is in the order of unity. Also  $\kappa$  increases with  $Qs_R$  which means, assuming that the kinetics have been chosen, that there is a concentration level of the removal enzyme above which instabilities can appear, implying that epigenic regulation of the loop is important.

In chapter 7 we defined the kinetic parameter  $Af$ ,

$$Af = \frac{L_p}{1/K_m} = \frac{\Lambda \pi Q_m}{\kappa} \quad (45)$$

the "Affinity ratio". It is a measure of the relative affinity of

the end product for the regulatory and removal enzymes; if  $A_f$  is less than unity then the end product binds more tightly to the removal enzyme, and vice versa. Instability occurs for high end product affinity for the regulatory enzyme, if  $\Omega_m$  is large, as expected since this situation represents tight control. However it is interesting to note that when  $\Omega_m$  is less than unity the opposite occurs; instability is observed when the end product has low affinity for the regulatory enzyme relative to the removal enzyme.

In contrast to the zeroth and first order limits a sign change is observed in the Magic number which occurs at low  $n$ ,  $v$  and  $\Omega_m$  values. This means that just short of the critical conditions three solutions coexist; a) a stable equilibrium point, b) an unstable limit cycle and c) a stable limit cycle. However much more detailed analysis is necessary to obtain the global properties of the solutions.

#### 8.2.4. Computations of bifurcated solution branches.

To examine the global character of the solutions to the kinetic equations one needs to undertake a major computational task. Fortunately these is now available computer software (a versatile generalized bifurcation pakage called AUTO) capable of carrying out these computations (see Doedel, 1984, Doedel and Heinemann, 1983 and Doedel, Jepson and Keller, 1984).

In figure 8-5a we show the bifurcated branch of periodic solutions as we let  $A_f$  range over the region of unstable steady

Figure 8-5.

Bifurcated solutions for a loop with the lumped controller and the Michaelis-Menten removal rate,  $\lambda = 100$ ,  $\Omega_m = 10$ ,  $v = 2$ ,  $n = 2$ , and  $Af$  varies.

- a) the graphs show the steady state solution (solid line where they are stable and dashed line where they are unstable) and the bifurcated periodic solution (the dots represent the maximum amplitude of the periodic solution).
- b) the graphs show the limit cycles for various values of  $Af$ , 1 -  $Af = 188$ , 2 -  $Af = 288$ , 3 -  $Af = 411$  and 4 -  $Af = 610$ .

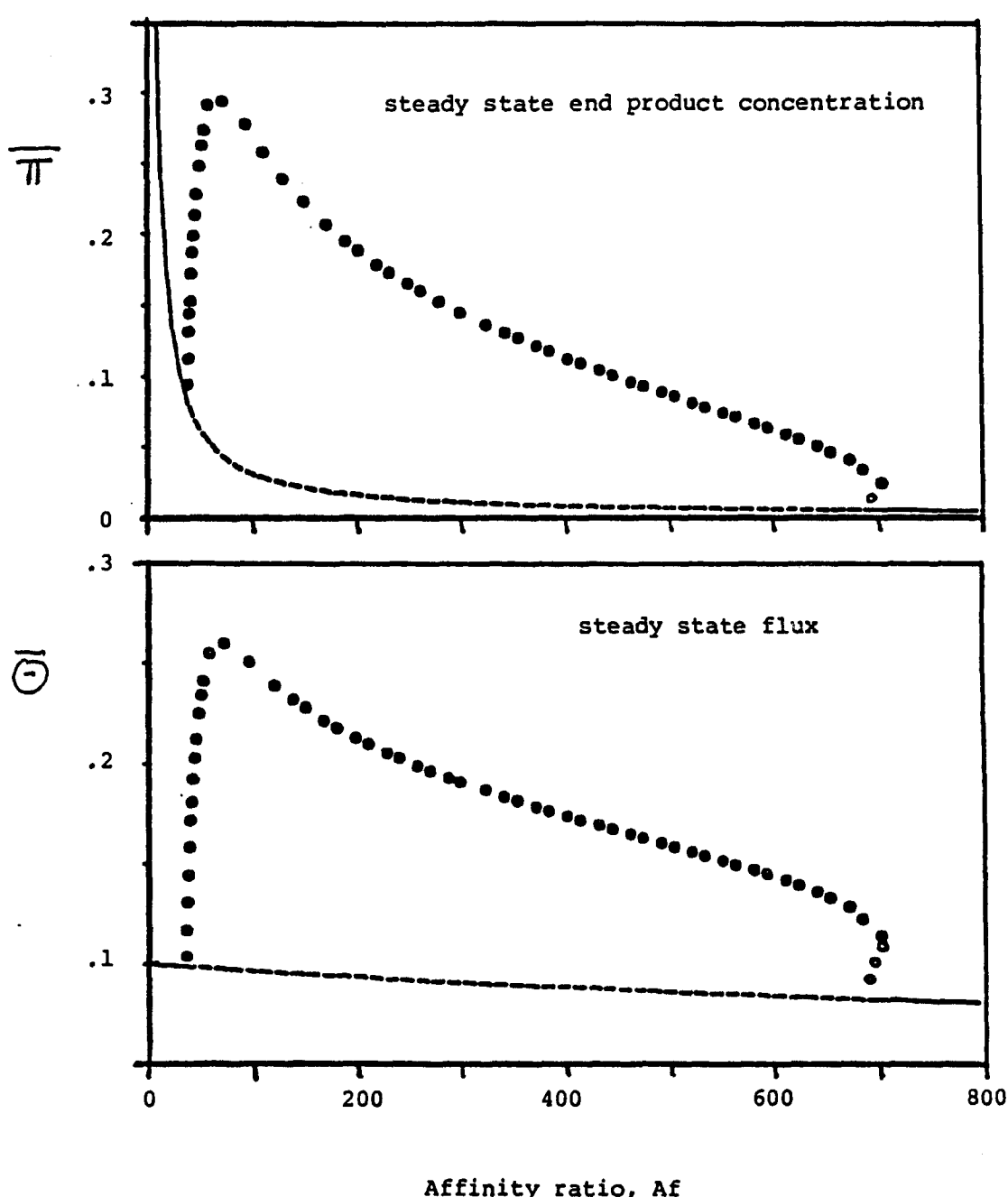
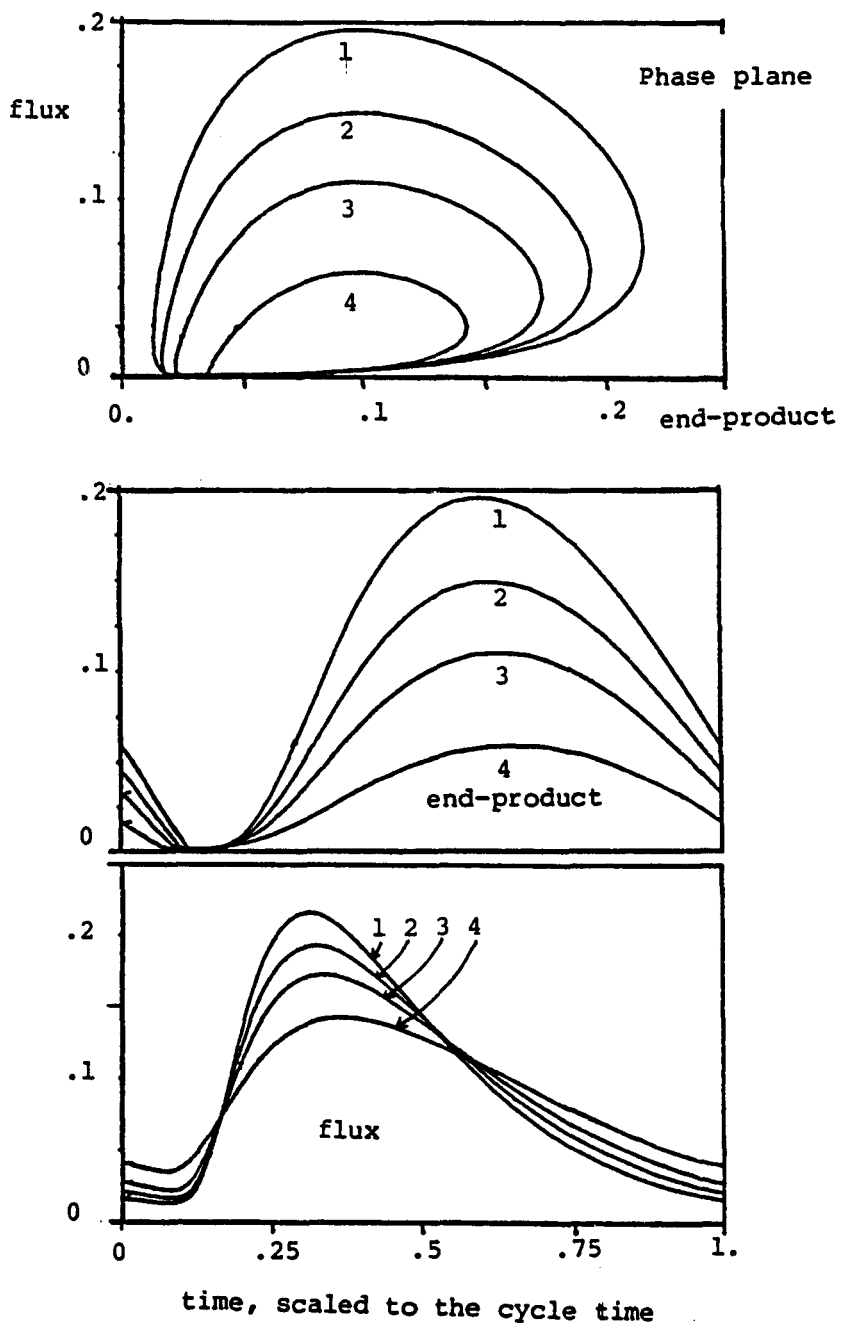
FIGURE 8-5a.

FIGURE 8-5b.

states (this region is shown in figure 8-4 where  $\Omega_m = .1$  and  $n=2$ , here in addition we fix  $\kappa$  at 100). At the lower Hopf bifurcation point the solution bifurcates onto a stable limit cycle but at the upper Hopf bifurcation point it bifurcates to an unstable limit cycle as predicted by the sign of the real part of  $M_n$ . The dots represent the maximum amplitude of the limit cycles. A few limit cycles computed for various values of  $A_f$  are shown in figure 8-5b.

The bifurcation onto unstable limit cycles gives rise to some interesting phenomena. Figure 8-6a shows a closeup of the region of coexisting stable steady, stable and periodic solutions (here we have used  $\kappa$  as the free parameter). Let us speculate on possible teleonomical advantages that this feature offers. Suppose that the value of  $\kappa$  is below the coexistence region and we are at the stable steady state. If  $\kappa$  is then increased beyond the Hopf bifurcation point the loop will start to oscillate spontaneously. Now if  $\kappa$  is again reduced, below the limit (turnaround) point on the bifurcation branch, the oscillations abruptly disappear. Hence bifurcations to unstable limit cycles offer a trigger mechanism to generate temporal signals!

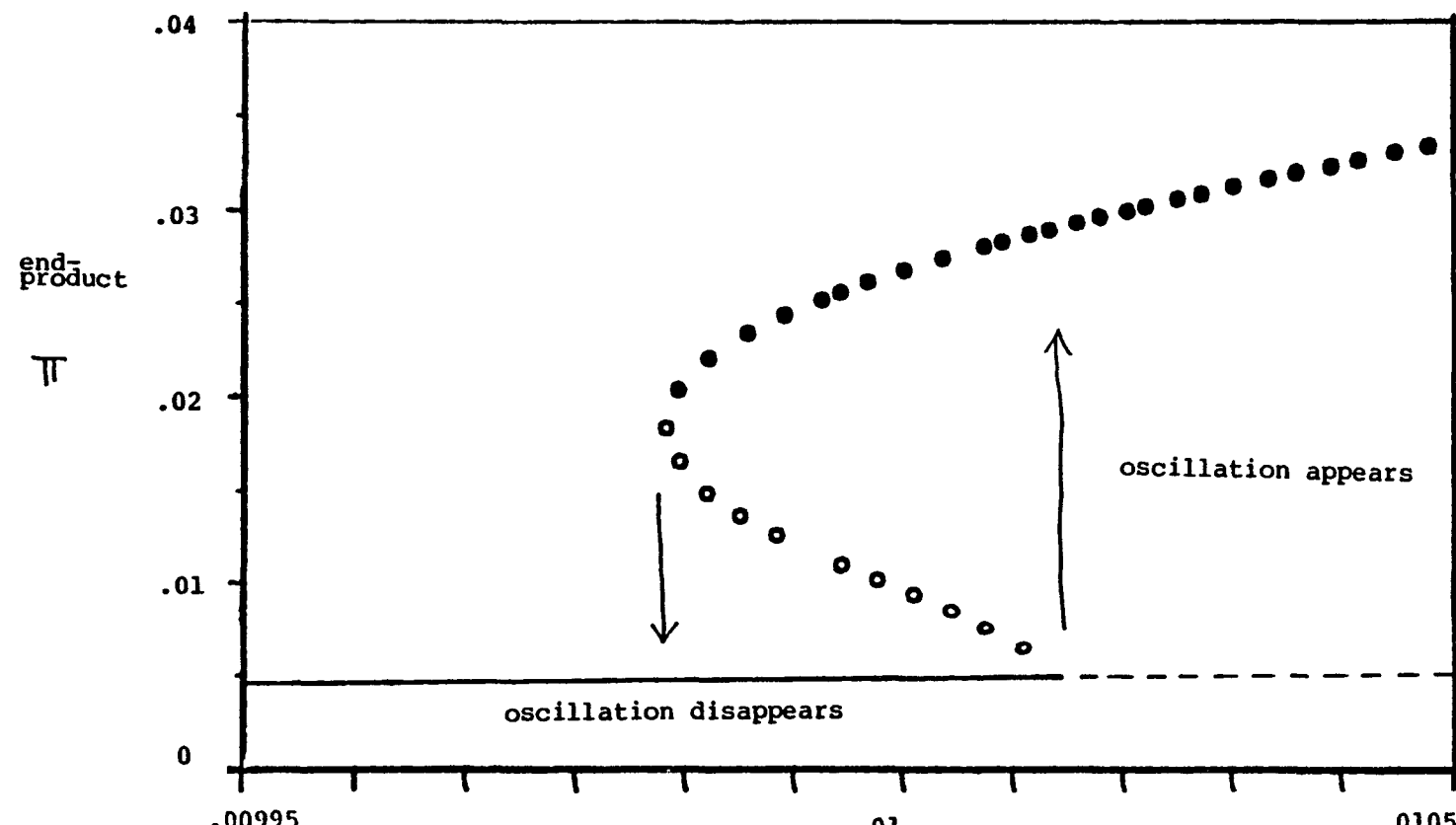
### 8.3. Loops with the Symmetry Model.

We now look at a circuit that has an input flux described by the symmetry model which we call Loop 2. To evaluate the stability criterion we substitute  $\Psi_{\pi}$ , given by equation 24, into the stability

Figure 8-6.

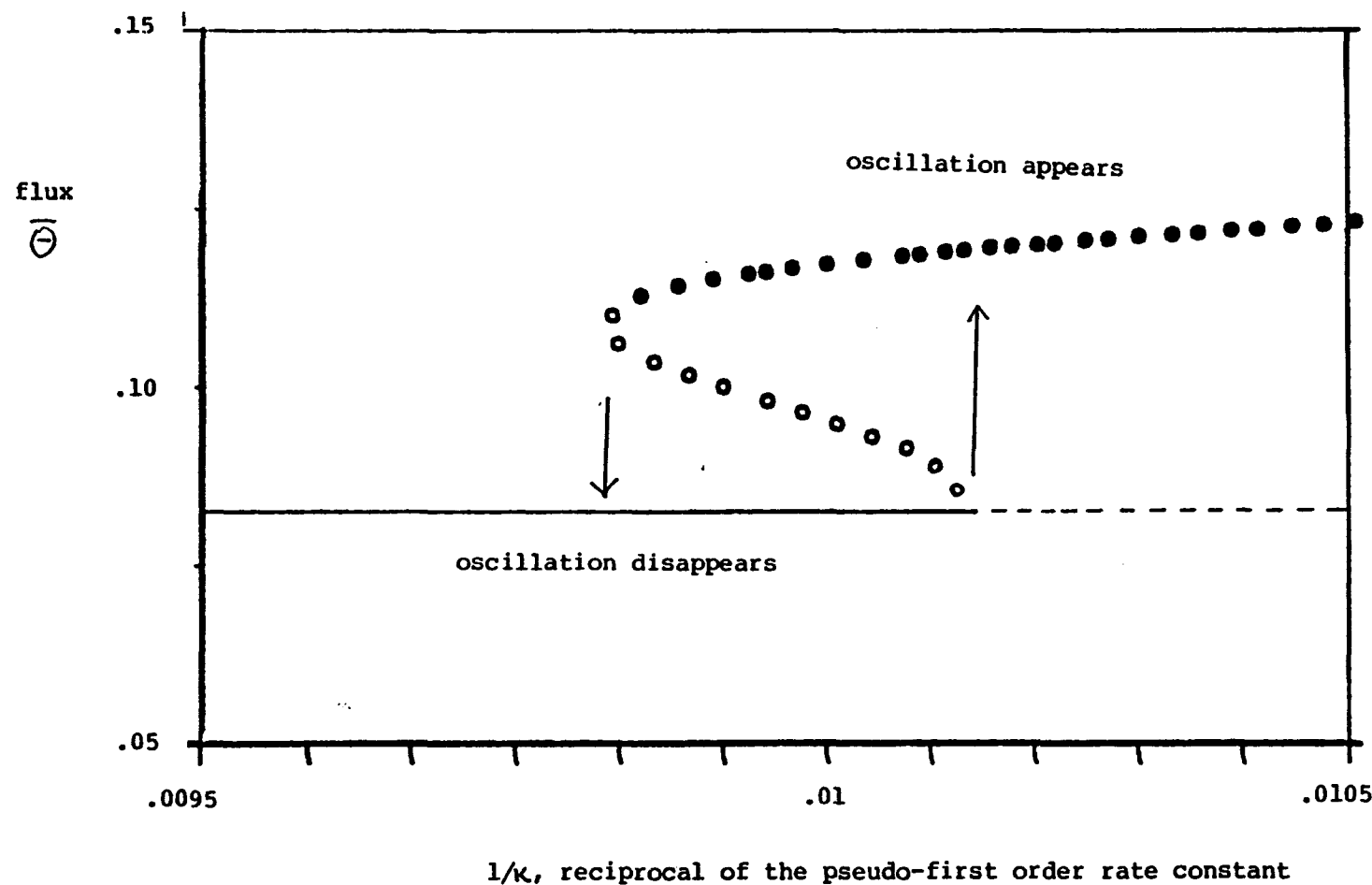
Bifurcated solutions for a loop with the lumped controller and the Michaelis-Menten removal rate,  $A_f = .695$ ,  $\Omega_m = 10$ ,  $v = 2$ ,  $n = 2$ , and  $\kappa$  varies. For description of figure symbols see caption of figure 8-5. a) Steady state flux through the chain, and b) steady state concentration of the end product. As indicated on the figures limit cycle behavior can spontaneously appear and disappear.

FIGURE 8-6a.



1/R, reciprocal of the pseudo-first order rate constant

FIGURE 8-6b.



criterion and when it is combined with the steady state equation gives

$$-\frac{v}{\pi} \left( \frac{\Lambda_{\pi}}{1+\Lambda_{\pi}} \right) (1-\Omega(\bar{\pi})) \Omega(\bar{\pi}) \leq l \quad (46)$$

Now it remains only to define  $\Omega(\pi)$  and as before we find useful to consider limiting cases of Michaelis-Menten kinetics first.

### 8.3.1. Linear removal rate.

Substitution of  $\Omega(\pi) = \kappa\pi$  into equation 46 yields

$$\bar{\pi}^2 - \frac{1}{\kappa} \left( 1 + \frac{l}{v\kappa} \right) \bar{\pi} - \frac{l}{v\kappa^2 \Lambda_{\pi}} \leq 0 \quad (47)$$

as the stability criterion. Again the steady state equation

$$\frac{1}{1+L(1+\Lambda_{\pi})^v} = \kappa\bar{\pi} \quad (48)$$

cannot be solved explicitly for  $\pi$ . As for loop 1 a closer look at allows the extraction of important information. If we rewrite equation 47 as

$$X^2 + a(b-1)X + ab \leq 0 \quad (49)$$

where  $X = \Lambda_{\pi}\pi$ ,  $a = \Lambda_{\pi}/\kappa$  and  $b = -l/v\kappa$ , then by looking for real roots by examining the discriminant

$$dis = a^2(b^2 - 2(1+2/a)b + 1) = a^2(b - b^*)(b - 1/b^*) \quad (50)$$

where  $b^* = 1 - (2/a)(\sqrt{1+a}-1) \leq 1$ , we see that the criterion for real real roots to equation 49 is  $b^* \leq b \leq 1/b^*$ . From equation 49 we also

see that in order for the roots to be real and positive we need  $b \leq 1$ . Hence to satisfy the instability criterion, equation 49, we must have

$$b \leq b^* \leq 1 \quad (51)$$

In the limit  $\Lambda_\pi \rightarrow \infty$ ,  $b^* \rightarrow 1$  and the criterion becomes the same as the one for loop 1, equation 33. Equation 51 can be rewritten as

$$a \geq \frac{4b}{(1-b)^2}, \quad \text{or} \quad \Lambda_\pi \geq \frac{-4\ell/v}{(1+\ell/v\kappa)^2} \quad (52)$$

The denominator of equation 52 is the same as equation 33 and when it is zero the critical value of  $\Lambda_\pi$  is forced to infinity. Between the roots of equation 33 there exist finite  $\Lambda_\pi$  values that satisfy equation 52. However we have not yet made use of the steady state equation which means that  $L$  is still a free parameter but we have found the values of  $\Lambda_\pi$  for which instabilities are possible. Let us elaborate on these results with a simple example.

Example. Lets us consider a second order reaction chain where  $\ell$  is given by equation 34. Combining equations 34 and 52 gives

$$\Lambda_\pi \geq \frac{8\xi v \kappa^2 (\kappa^2 + 2\xi \kappa + 1)}{\kappa^2 + (2\xi - \frac{v}{2\xi})\kappa + 1} \quad (53)$$

The roots of the denominator are given by equation 36 and they represent the looser bound of equation 51. At these roots  $\Lambda_\pi$  goes to infinity but between  $\kappa_-$  and  $\kappa_+$  the locus can be traced out, figure 8-7. As  $\Lambda_\pi$  drops from infinity the size of the region of possible instability shrinks and ultimately vanishes and the loop is stable

for all values of  $L$ . Hence for finite values of  $\Lambda_{\pi}$  the symmetry model is less likely to cause dynamic instabilities than the lumped controller. Similar results are obtained for higher values of  $n$ . We still have a free parameter  $L$  and one has to search over  $L$  in the regions shown in figure 8-7 for the locus of Hopf bifurcation points. Figure 8-8 shows the results of such search for  $n=3$  and  $v=5$ .

### 8.3.2. Constant removal rate.

Proceeding as for the lumped controller gives us the stability criterion

$$L^{1/v} \Lambda_{\pi} \geq \left( \frac{-\lambda_0}{v\Omega_m^2} \right) \left( \frac{1-\Omega_m}{\Omega_m} \right)^{1/v-1} \quad (54)$$

This is the identical result to equation 40 with  $L^{1/v} \Lambda_{\pi}$  for the symmetry model equivalent to  $\Lambda_{\pi}$  for the lumped controller. Hence all the results in section 8.2.2 apply here by simply changing  $\Lambda_{\pi}$  to  $L^{1/v} \Lambda_{\pi}$ .

### 8.3.3. Michaelis-Menten removal rate.

Using the Michaelis-Menten form for  $\Omega(\pi)$  transforms the criterion for instability into

$$\bar{\pi} \left( \bar{\pi}^2 + \frac{\Omega_m}{\kappa} \left( 2 + \left( \frac{v\kappa}{\lambda} \right) \left( 1 - \Omega_m \right) \right) \bar{\pi} + \left( \frac{\Omega_m}{\kappa} \right)^2 \left( 1 + \frac{v\kappa}{\lambda} \right) \right) + \frac{1}{\Lambda_{\pi}} \left( \bar{\pi} + \frac{\Omega_m}{\kappa} \right)^2 \leq 0 \quad (55)$$

Again if we let  $\Lambda_{\pi} \rightarrow \infty$  we recover the results from loop 1, in this case equation 42. When  $\Lambda_{\pi}$  is finite a second positive term is added

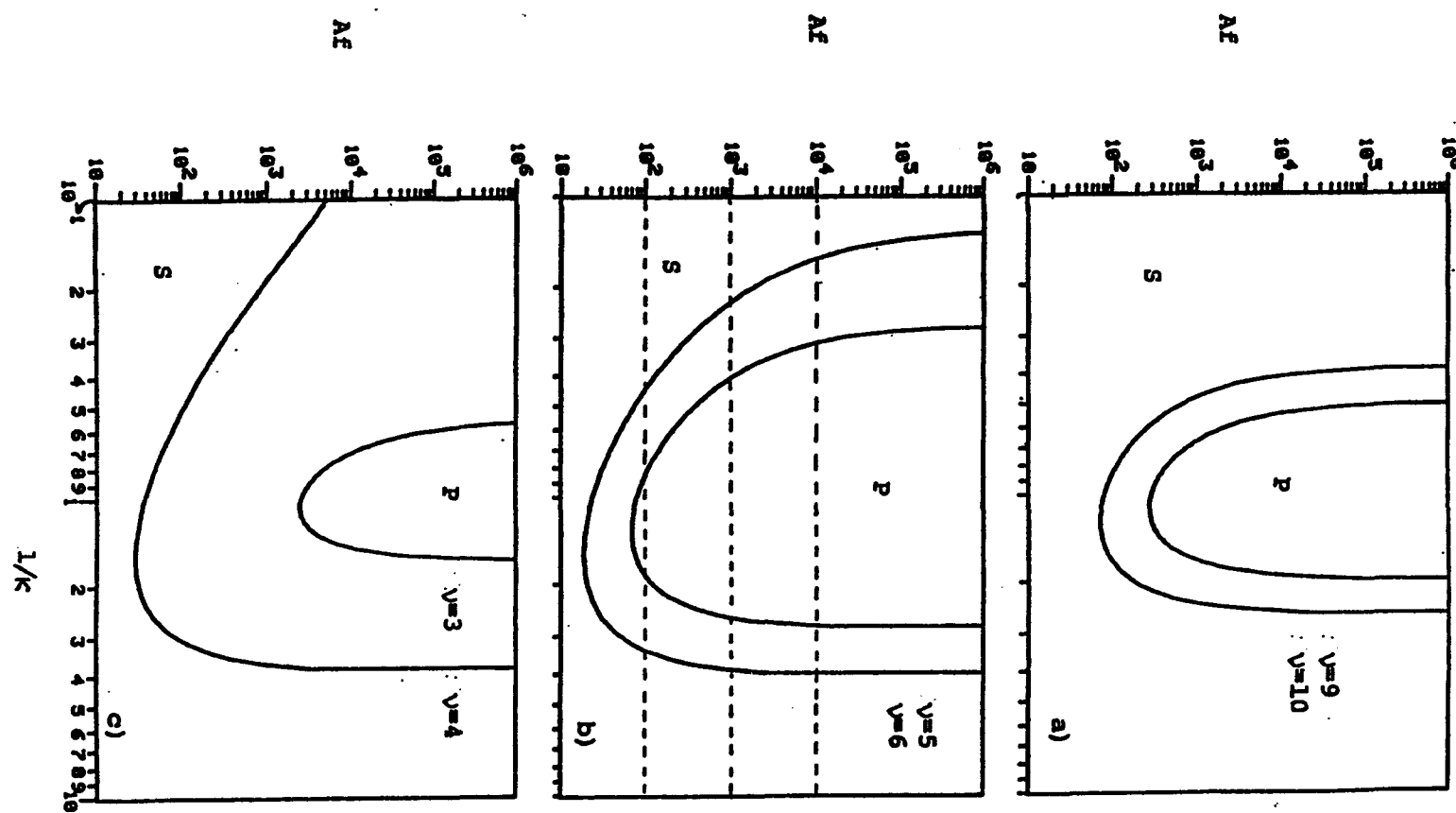


Figure 8-7. Regions of possible dynamic instabilities for loop 2 traced out in the  $\Delta F, (1/\kappa)$ -plane ( $P$  = region of possible instabilities,  $S$  = stable region). a)  $n=2$ ,  $v=9, 10$ , b)  $n=3$ ,  $v=5, 6$ , and c)  $n=4$ ,  $v=3, 4$ .

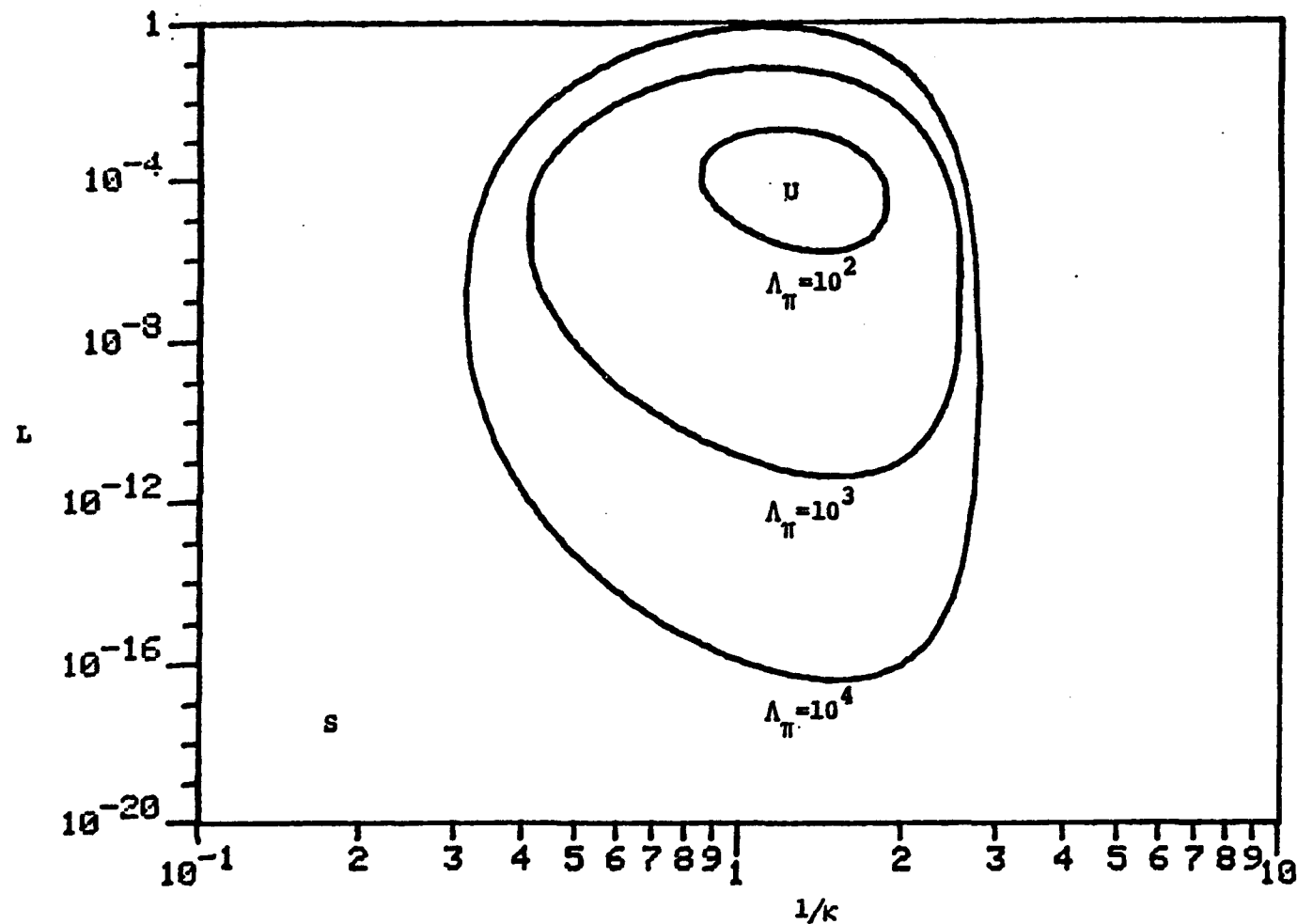


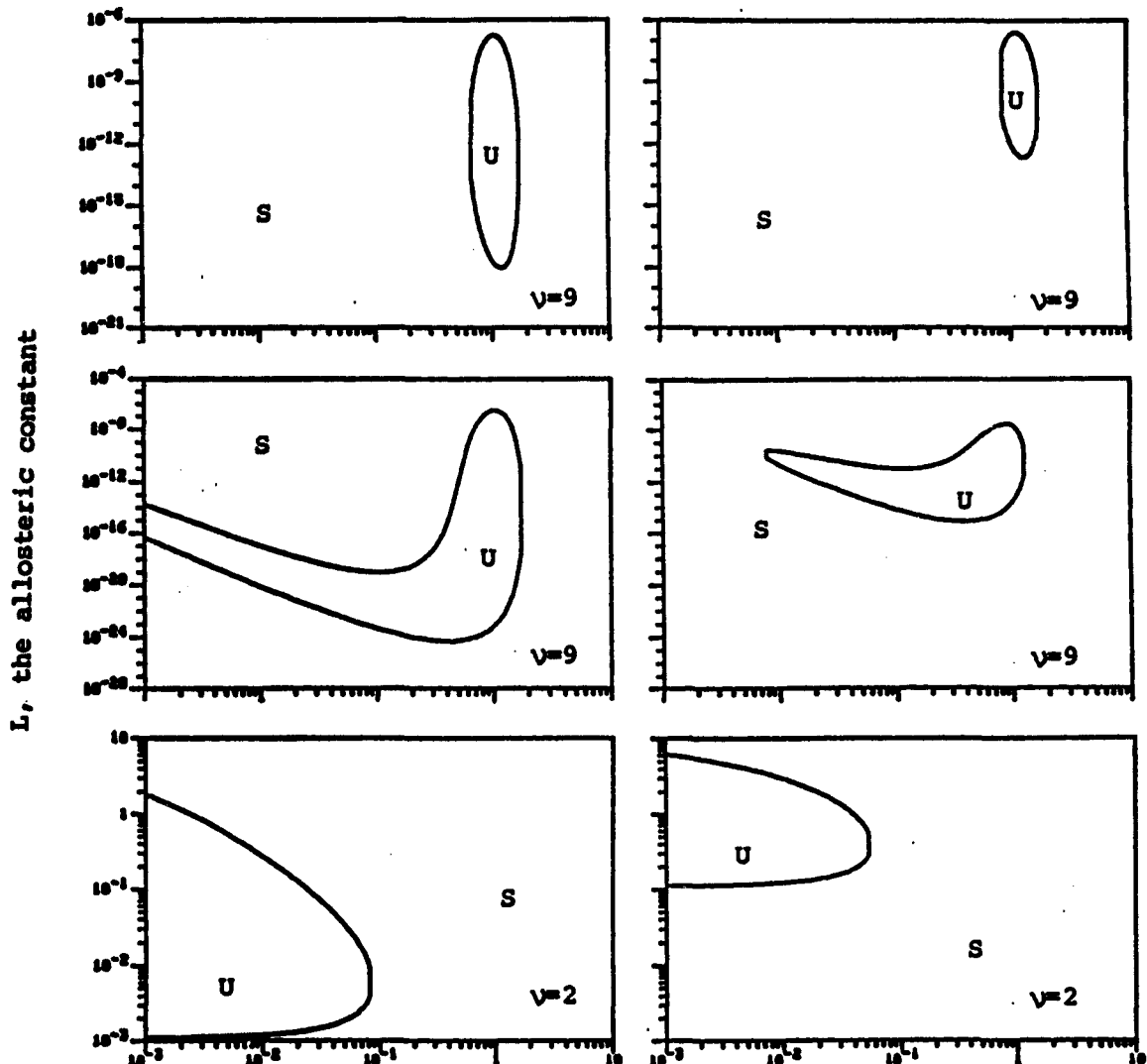
Figure 8-8. Instability regions for Loop 2 in the  $L, (1/\kappa)$ -plane. The curves shown correspond to the values of  $\Lambda_\pi$  indicated in figure 8-7b, curve 1,  $\Lambda_\pi = 100$ , curve 2,  $\Lambda_\pi = 1000$ , and curve 3,  $\Lambda_\pi = 10000$ .

to the first one making it less likely to find roots to this equation. Hence again we have the result that the symmetry mechanism gives a more stable control circuit. As an example we show how the results corresponding to first column of figure 8-4 for loop 1 changes with  $\Lambda_{\pi}$  in figure 8-9.

#### 8.4. Discussion.

Feedback regulation at the metabolic/genetic level has been subject to intensive study (e. g. Tyson and Othmer, 1978, and chapter 9). The results presented in this chapter provide answers to questions which have much discussed in the literature since the formulation of the well known Goodwin equations some twenty years ago. The extensive stability analysis, summarized in chapter 9, are incomplete but the analytical and numerical results of this chapter finally resolve the local stability issue. Furthermore we have been able to ascertain numerically the predictions of Mees and Rapp (1978) and Allwright (1981) that the bifurcated orbits at the Hopf bifurcation points are always stable for the Goodwin equations.

Our extension of the Goodwin equations, by introducing Michaelis-Menten kinetics for the removal rate, dramatically changes the conclusions derived from previous studies. One of the key results from the studies of the Goodwin equations, the linear limit for the removal rate, is that the degree of cooperativity,  $v$ , needed to cause instabilities is much higher than physiologically meaningful



1/k, the reciprocal of the pseudo-first order removal rate constant

**Figure 8-9.** Regions of unstable steady states for a loop with the symmetry model and Michaelis-Menten removal rate. The parameters are:  $\Omega_m = 10$  in the first row,  $= 1$  in the second row and  $= .1$  in the bottom row;  $\Lambda$  is 1000 in the first column and 100 in the second column,  $n=2$  for all the graphs. U denotes a region of unstable steady states and S a region of stable steady states.

values. However by allowing saturation features in the removal rate these results change and instability occurs for realistic values of  $v$ . In order to observe these instabilities the saturation velocity of the removal rate has to be lower than that of the regulatory enzyme,  $\Omega_m < 1$ . It is interesting to note here that the saturation velocities for key regulatory enzymes, such as phosphofructokinase in glycolysis, are typically much lower than for other enzymes in the same sequence. Hence according to our results, for the single control loop, that would virtually guarantee dynamic stability.

Furthermore the introduction of saturation velocity in the removal rate results in unstable Hopf bifurcations. These are the first reported unstable dynamic bifurcations in single biochemical control loops. Close to these conditions the equations can have two stable solutions, both a stable steady state and a stable limit cycle. This allows for creative functions where by varying the enzyme concentrations the cell could induce or eliminate oscillations; thus allowing for the generation of temporal signals, which are common in metabolic networks.

Finally the symmetry model is found to give more stable behavior than the lumped Hill-type controller. Depending on the dimensionless constant of inhibitor to the regulatory enzyme the symmetry model can yield stable operation where the lumped controller could not.

### 8.5. Summary.

The control loop considered herein is a linear reaction chain in which the end product of the reaction sequence feedback inhibits the first reaction in the sequence to produce feedback control. In our previous study in chapter 6 we found that the in general criteria for the existence of oscillatory solutions in such loops depend on: a) the kinetics of the regulatory enzyme controlling the first reaction, b) the kinetics of end product removal in, and c) the transport and kinetic properties of the reaction chain. Here we expand the results of chapter 6 by specifying all kinetics and we search the parameter space of biologically realistic rate laws for sustained oscillatory behavior. The effects of regulatory kinetics are examined here using two representative models for the regulatory enzyme: the lumped controller, based on Hill-type kinetics, and the symmetry model. The removal rate is assumed to be of the Michaelis-Menten type, and the reaction chain is assumed to be described by a dynamic linear operator.

Loops with Hill type inhibition and linear removal are identical to the well studied Goodwin equations. Here we present a complete survey of how the stability of these equations depends on model parameters much more extensive than published to date. The study is extended by incorporating saturation effects in the removal rate and such feature is shown to dramatically enlarge the instability regions and furthermore we find regions where the bifurcated solutions are unstable. This implies that there are parameter combinations where

the phase plane both has a stable equilibrium point and a stable limit cycle and under such conditions the loop is exitable, i. e. it can be forced from an asymptotically stable steady state to a sustained oscillatory behavior by a sufficient disturbance.

Using the symmetry model to describe the regulatory enzyme results in qualitatively similar, but more complex, results. It, however, is found to be less prone to cause dynamic instabilities.

## CHAPTER 9

## MATHEMATICAL MODELLING OF FEEDBACK INHIBITION;

## A REVIEW

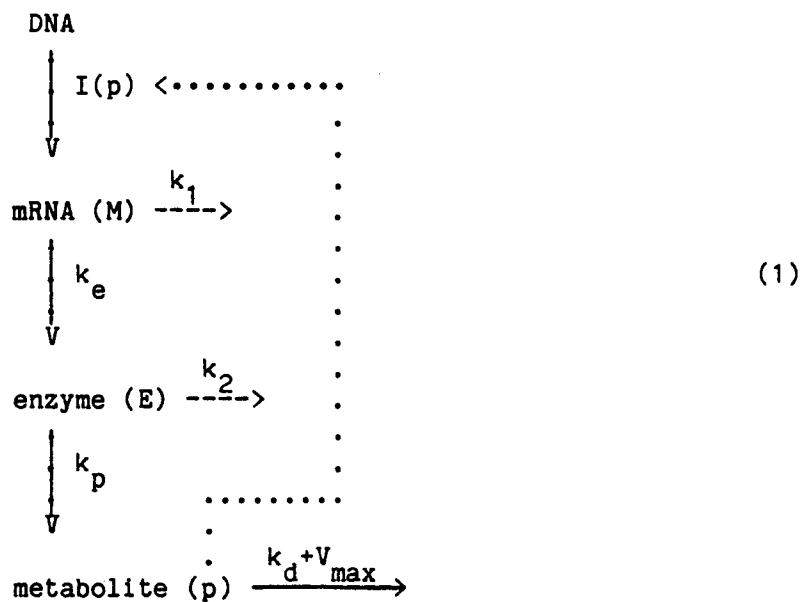
The observation of feedback regulation in metabolic networks in the 1950s (Umbarger, 1956, Yates and Pardee, 1956) motivated mathematical modelling. The first efforts to develop a plausible physiochemical model of feedback regulation of gene transcription were presented in the 1960s (Goodwin, 1963, 1965, 1966) and extended to metabolic regulation by Morales and McKay (1967). The model that these investigators developed has since been extensively studied. It is called, after the pioneer, the Goodwin equations or the Goodwin oscillator. Extensive mathematical literature on this model has accumulated, mostly in the 1970s and is briefly reviewed in this chapter. An extensive mathematical survey is found in Tyson and Othmer (1978).

The Goodwin equations are presented in subsection 9.1. Then we discuss the myriad of stability analyses developed for this simple model in subsection 9.2. Several extensions of the basic model have been considered and these are discussed in subsection 9.3. The survey concludes with a discussion on an alternative modelling

approach, which is not based on physical principles, subsection 9.4.

### 9.1. The Goodwin Equations.

The earliest effort to develop a physiochemical model of feedback regulation, was by Goodwin (1963, 1965, 1966). It was formulated to describe the dynamic behavior of a genetic operon regulated by feedback repression. He considered the scheme



where the concentrations of the chemical species are indicated in parentheses and the  $k_i$ 's are rate constants. The dynamic model consists of three differential equations:

a mass balance on mRNA,

$$\frac{dM}{dt} = Dk_m I(p) - k_1 M \quad (2)$$

a mass balance on the enzyme

$$\frac{dE}{dt} = k_e M - k_2 E \quad (3)$$

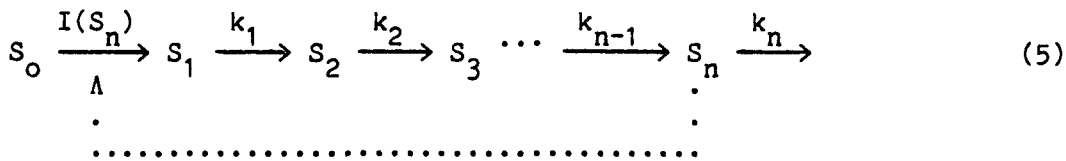
a mass balance on the end product

$$\frac{dp}{dt} = k_p E - k_d p - V_{max} \quad (4)$$

where  $t$  is time and  $D$  is the concentration of the operon (gene dosage),  $k_d$  is the growth rate constant ( $k_d = \ln(2)/t_d$ ,  $t_d$  is the mass doubling time) and  $V_{max}$  is the constant rate of utilization of end product. The function  $I(p)$  ( $= I_m / (1 + (L_p)^v)$ ) is identical to the lumped controller.

Analog simulations of these equations were presented by Goodwin (1965), using somewhat arbitrary numerical values for the different parameters. In particular he chose  $V_{max} = 0$  and  $v = 1$ . The analog simulations showed limit cycle behavior. These results were later shown to be in error by Griffith (1968a,b) who showed, using the Poincare-Bendixon criterion, than limit cycle behavior is impossible for the parameters used by Goodwin (1965), in particular he showed that  $v \geq 8$  is needed for limit cycles to appear.

Morales and McKay (1967) then extended this model to account for feedback inhibition at the metabolic level of the Yates-Pardee-Umbarger type as



where  $S_i$ 's represent metabolites and  $I(S_n)$  is the lumped controller.

The dynamic model of this system consists of  $n$  first order differential equations

$$\frac{dS_i}{dt} = I(S_n) - k_i S_i, \quad \frac{dS_i}{dt} = -k_i S_i + k_{i-1} S_{i-1}, \quad i = 2, 3, \dots, n \quad (6)$$

Again initial analog simulations by Morales and McKay (1967) showed oscillations which later were proven to be computer artifacts, Walter (1969b). These equations are also called the Goodwin equations since they are identical to equation (2)-(4) when  $V_{max}$  is zero, but are generalized in the sense that the linear part of the model can be of arbitrary dimension. Equations (6) are more prone to go unstable than equations (2)-(4) particularly if  $n$  is high (Walter, 1969, Hunding, 1974, Tyson and Othmer, 1978) or if a time delay is incorporated into the model (MacDonald, 1977b, Rapp, 1976a, Alwright, 1977a, 1981).

Although the initial papers showing oscillatory behavior were later shown in error these findings fueled interests in assessing the dynamic stability of the stationary point. The stability properties of this model have been extensively investigated, and below we will briefly review the different stability analyses, and the criteria for periodic solutions.

## 9.2. Stability Analysis of the Goodwin Equations.

The Goodwin equations are a set of  $n$  coupled non-linear differential equations. In general analytical solutions of such system of equations are difficult or impossible to obtain, even for such simple example as the Goodwin equations. Much can though be learned about the nature of the solutions from stability analysis.

Before proceeding to describe applications of the various stability analyses, some general results should be discussed.

Allwright (1977a) has shown that for  $v$  of unity the stationary point is a global attractor for all values of  $n$ . For other values of  $v$  ( $>1$ ) oscillatory behavior is possible. Tyson (1974), for  $n = 3$ , and Hastings and Tyson (1975) and Hastings et al., (1977), for all  $n$ , have shown that an unstable stationary point is a sufficient criterion for the existence of periodic solutions. Whether that periodic solution is a global unique attractor for all unstable stationary points remains to be shown. We start our discussion by looking at the characteristic equation for the Goodwin equations.

### 9.2.1. The characteristic equation.

For local stability analysis the mathematical description is linearized around the stationary point; here denoted with an overbar. The roots of the characteristic equation are then examined to assess the dynamic stability of the stationary point (see chapter 8). The material that follows is mostly taken from Hunding (1974).

The stationary point is found by equating the left side of equations (6) to zero. The so obtained steady state equations are

$$k_1 S_i = k_{i-1} S_{i-1}, \quad i = 2, 3, \dots, n \quad (7)$$

$$\bar{S}_1^{v+1} + \frac{1}{L_p} \left( \frac{k_n}{k_1} \right)^v \left( \bar{S}_1 - \frac{I_m}{k_1} \right) = 0 \quad (8)$$

Equation 8 is non-linear and is hard to solve analytically. The roots for  $v = 0, 1, 2, 3$ , and for  $v > 3$  for special parameter combinations are given by Walter (1969a).

Hunding (1974) proposes a variable transformation

$$N = \frac{I_m}{k_1 \bar{S}_1} \quad (9)$$

to simplify the steady state equations. Equation (8) transforms into

$$N(N-1)^{1/v} = \frac{I_m}{k_n L_p} L^{1/v} \quad (10)$$

The characteristic equation is found by linearizing equations 6 around the stationary point. Doing so one obtains

$$\frac{d\bar{S}'}{dt} = JS' \quad (11)$$

where

$$J = \begin{bmatrix} -k_1 & & & & I_p \\ k_1 & -k_2 & & & \\ & k_2 & -k_3 & & \\ & & k_3 & -k_4 & \\ & & & \ddots & \\ & & & & k_{n-1} & -k_n \end{bmatrix} \quad (12)$$

where  $I_p$  is the partial derivative of  $I(p)$  with respect to  $P$  and where  $\underline{S}'$  is a vector of deviation variables,  $\underline{S}' = \underline{S} - \bar{\underline{S}}$ .

Since  $J$  is a simple matrix, nearly a band matrix, the characteristic equation is easily derived

$$\prod_{i=1}^n (k_i + \lambda) - \frac{I_p}{k_n} \prod_{i=1}^n k_i = 0 \quad (13)$$

In general it is hard to solve for the roots of this equation. In the special case where all the reactions are identical, when  $k_1 = k_2 = \dots = k_n$ , is of special interest. This special case has been extensively discussed, and is the situation where for a given number of reactions the system is most easily destabilized (Othmer, 1976, Tyson and Othmer, 1978). This situation therefore represents a limiting case, which gives bounds on the stability region for any reaction chain of any dimension where the kinetic parameters are not identical.

Now equation 13 may be written as

$$(k + \lambda)^n = I_p k_{n-1} = -k \left(\frac{N-1}{N}\right)^v \quad (14)$$

and the eigenvalues are found to be

$$\lambda_m = k \left( -1 + \sqrt[n]{\frac{N-1}{N}} \exp\left(\frac{(1+2m)\pi i}{n}\right) \right) \quad (15)$$

The real part of the smallest eigenvalue is

$$\operatorname{Re}(\lambda) = k \left( -1 + \sqrt[n]{\frac{N-1}{N}} \cos\left(\frac{\pi}{n}\right) \right) \quad (16)$$

and it becomes positive at

$$v_{\min} = \frac{N}{N-1} \frac{1}{\cos^n(\frac{n}{\pi})} \quad (17)$$

Then for  $v > v_{\min}$  the real part is positive. This is a necessary condition for the existence of a limit cycle. Hence for a fixed  $n$ , there is a minimum number of inhibitor molecules that must bind to the regulatory enzyme in order to make the stationary point dynamically unstable. The exact bounds on the region of unstable steady states are presented in Othmer (1976) and much more extensive results are found in chapter 8.

A similar but weaker criterion has been derived by several authors, Viniegra-Gonzalez and Martinez (1968), Higgins et al., (1973), Othmer (1976) which are identical to equation 17 except the factor  $N/(N-1)$  is missing.

### 9.2.2. Hopf bifurcations.

A comprehensive description of Hopf bifurcations (Hopf, 1942) is found in Marsden and McCracken (1976), and a brief statement of the bare fundamentals is found in Tyson and Othmer (1978), Mees and Rapp (1978).

Recently Hopf bifurcation theory has attracted much attention because it is one of the few methods that can reliably establish the existence of limit cycles in systems of high order. It is, however, a local theory that only applies in the small and it makes predictions in small regions around the bifurcation point, in both

parameter and behavior space. Fortunately Hastings et al., (1977), have shown that for the Goodwin equations an unstable stationary point is a sufficient condition for the existence of a periodic solution. Furthermore the fact that the bifurcation results in a stable limit cycle has been established under certain conditions Mees and Rapp (1978), Allwright (1981), which seems to be always the case judging from the numerical results in chapter 8. Hence the bifurcation parameter needs not to be infinitesimally close to its critical value to obtain limit cycles. In general the theory does not give a range on the bifurcation parameter that guarantees periodic behavior.

A brief consideration of the theorem is pertinent here. Loosely speaking it states that if a set of ordinary differential equations,  $dx/dt = f(x, \xi)$ , depends on a real parameter  $\xi$  (the bifurcation parameter), and if on linearizing the equations around the stationary point, the Jacobian is found to have a pair of complex conjugate eigenvalues that cross the imaginary axis as  $\xi$  varies through some critical value  $\xi_0$ . Then for near critical values of  $\xi$  there exist limit cycles close to the stationary point. Furthermore one has to check for the sign on the real part of a complex number, the magic number given by Poore (1975, 1976), to assess the stability of the limit cycle, and also to assess whether the limit cycle exists for subcritical ( $\xi < \xi_0$ ) or supercritical ( $\xi > \xi_0$ ) values of the bifurcation parameter. The magic number has in general a complicated analytical form, equation 20 in chapter 8, but Allwright (1977b,

1981) has provided some simplification for equations like the Goodwin equations by using a transfer function representation for the linear part of the problem.

The first application of the Hopf bifurcation theory to the Goodwin equations came from Hunding (1974). As discussed above he considered the case where all the intermediary reactions are identical. By examining the real part of the eigenvalues he arrived at the criterion of equation 17 as a necessary condition for oscillatory behavior. The theory also gives an estimate of the period of oscillation simply as  $T = 2\pi/\text{Im}(\lambda_c)$  where  $\text{Im}(\lambda_c)$  the imaginary part of the eigenvalues crossing the imaginary axis, figure 9-1. The estimated period then is

$$T = \frac{2\pi}{k^n \sqrt{v \frac{N-1}{N}} \sin\left(\frac{\pi}{n}\right)} \quad (18)$$

MacDonald (1977a) was first to evaluate the magic number for the Goodwin equations. The expression for  $M_n$  is rather complicated, as is true for the  $M_n$  in general, but it simplifies in certain situations. For example if  $n \rightarrow \infty$ , it becomes apparent that  $v > 1$  is necessary for oscillatory behavior.

Mees and Rapp (1978), in a more comprehensive treatment, consider higher-order bifurcations. This mathematical development is probably of more mathematical interest than biological. Their results are summarized in table 9-1. The subscript on  $n_i$ , in the table, indicates how many reactions in the sequence are necessary to

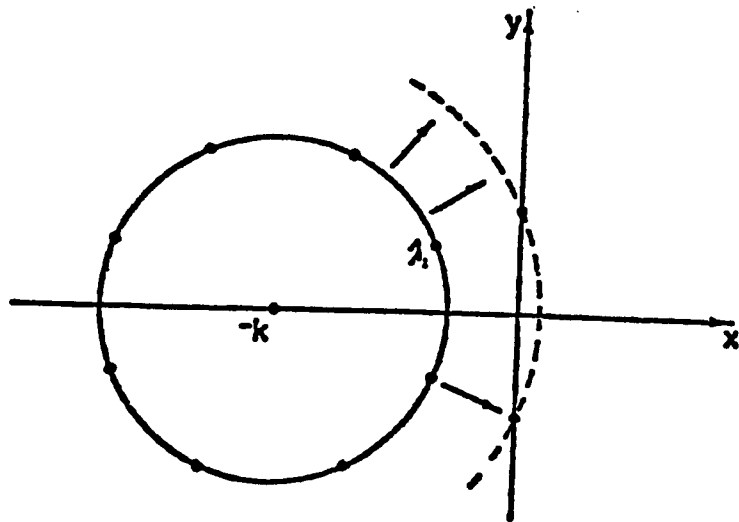


Figure 9-1. Figure illustrating the location of the eigenvalues for the Goodwin equations in the complex plane for the case where all the reactions are identical, taken from Hunding (1974).

degree of cooperativity v.

	$n_1$	$n_2$	$n_3$	$n_4$
<b>1</b>	<b>equilibrium attracting</b>			
2	8	65	179	350
5	4	29	78	151
10	3	21	55	106
15	3	18	47	91
20	3	16	43	82

Table 9-1. A table that contains the number of identical reactions,  $n_i$ , to give bifurcations of order  $i$  for a given degree of cooperativity  $v$  (from Mees and Rapp, 1978).

reach the  $i$ -th bifurcation. For example for  $v = 5$ , the necessary number of reactions to observe a second bifurcation is 29. It may be seen from this table that for parameters of biological interest,  $v < 4$ ,  $n = 10-15$ , there is virtually no way to observe a second bifurcation.

Mees and Rapp (1978) also examine the magic number. They conclude that "for  $2 < v < 5191$  and any fixed  $j$ , the Goodwin oscillator possesses an attracting limit cycle immediately after the first bifurcation, and a hyperbolic limit cycle immediately after each of the next  $j$  bifurcations, provided that  $n$  is sufficiently large."

Allwright (1981) applies his extension of bifurcation theory, Allwright (1977b), to the Goodwin equations. This extension basically shows that the Magic number can be written in such a way that the linear elements in the system occur only through their transfer function. This is useful and allows one to use characteristics of transfer functions to see through the heavy algebra involved in the evaluation of the magic number. Using this technique Allwright (1981) concludes that any bifurcation in the Goodwin equations when  $v > 2$  and the ratio  $g(iw)/g(0)$  ( $g$  is the transfer function for the linear part of the problem, and  $w$  is the imaginary part of the eigenvalue crossing into the right half plane) at the bifurcation point is at least  $1/2$  produces an attracting orbit existing when the stationary point is unstable. This is the most general analytical result derived from bifurcation theory to date for

the Goodwin equations.

### 9.2.3. Popov's theorem.

Othmer (1976) and Tyson and Othmer (1978) have applied this theorem (Popov, 1962) to the Goodwin equations, and obtained global stability bounds for the Goodwin equations. The basic idea behind the theorem is illustrated in figure 9-2. There the locus of the linear part of the problem is traced out in modified Nyquist coordinates,  $\text{Re}(g(i\omega))$ ,  $\omega \text{Im}(g(i\omega))$ . Then if a line through the point  $(0, -1/k)$ , where  $k$  is the maximum slope of the non-linear element, can be constructed such that the locus of the transfer function is strictly to the right of the line, then the system is globally stable. A detailed description of this theorem is found in Aizerman and Gantmacher (1964).

These two studies establish rigorously the fact that the case of all identical intermediary reactions is the most easily destabilized one, for fixed chain length  $n$  and degree of cooperativity  $v$ . Guaranteeing stability for this limiting case will also guarantee stability for all other rate constant for the same chain lenght and cooperativity.

Tyson and Othmer (1978) provide and excellent review of the Goodwin equations, and discuss both global and local stability results. The application of Popov's theorem, which provides global stability, leads to a definition of an important parameter, defined as

In order that the system (!) be absolutely stable in the sector  $[0, k]$  for the principal case, or in the sector  $[\epsilon, k]$  for the particular cases, it is sufficient that there exist in the  $W^*(\omega)$  plane a straight line, passing through the point on the real axis with abscissa  $-1/k$ , such that the modified frequency response  $W^*$  lies strictly to the right of it, and additionally, that for the particular cases the conditions for stability-in-the-limit be satisfied.

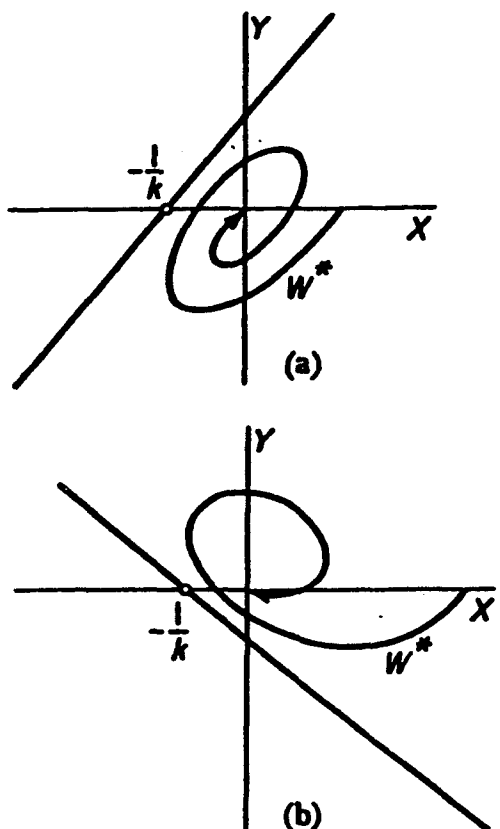


Figure 9-2. Graphical illustration of Popov's theorem, taken from Aizerman and Gantmacher (1964).

$$\phi = \prod_{i=1}^n k_i \quad (19)$$

Important values of  $\phi$  are bounded by  $\phi_0$  and  $\phi_{\max}$  which have the following meaning,

- if  $\phi < \phi_0$  the system is unstable
- if  $\phi_0 < \phi < \phi_{\max}$  local stability is guaranteed, but no information on global stability.
- if  $\phi_{\max} < \phi$  the system is globally stable.

Table 9-2 contains the bounds  $\phi_0$  and  $\phi_{\max}$  for a given chain length  $n$  and cooperativity  $v$ . Note that when  $\phi_0$  is zero stability of the stationary point is guaranteed. This is true for  $v$  equal to unity and any  $n$ . It also holds true for all  $v < 5$  and  $n < 5$ , which is the region of biological interest.

Othmer (1976) finds for the case where  $k_1 = k_2 = \dots = k_{n-1}$  bounds on the existence of oscillatory solutions in the  $L_p, k_n$ -plane. Two limiting cases of interest are: 1) when  $k_n$  is sufficiently small or large and for any  $L_p$ , and 2) when  $L_p$  is sufficiently small for any  $k_n > 0$ , then the steady state is asymptotically stable. Quantitative bounds are developed on the stability region, and a numerical example is given for  $v = 4$ ,  $n = 5$ ,  $k_1 = k_2 = k_3 = k_4 = 1$ . The stability region for this case is shown in figure 9-3. Computations of the amplitude and period of the oscillations for constant  $k_n$  or constant  $L_p$ , are given, as the other parameter ranges through the region of oscillations. Figure 9-4 shows these computations when  $L_p$  is

**GLOBAL STABILITY RESULTS FOR REPRESSIBLE  
SYSTEMS\***

$n =$	3	4	5	8	16	$\infty$
$p = 1$	0.00	0.00	0.00	0.00	0.00	0.00
	0.02	0.05	0.09	0.19	0.31	0.50
	0.00	0.00	0.00	0.01	0.21	0.50
	0.04	0.11	0.17	0.29	0.44	0.62
	0.00	0.00	0.01	0.31	0.58	0.84
	0.07	0.18	0.27	0.42	0.62	0.84
$p = 2$	0.00	0.00	0.22	0.54	0.78	0.99
	0.11	0.25	0.35	0.57	0.79	1.04
	0.00	0.15	0.40	0.69-	0.88	1.05
	0.14	0.36	0.46	0.69+	0.92	1.20
	1.00	1.00	1.00	1.00	1.00	1.00
$\infty$	1.13	1.25	1.35	1.53	1.74	2.00

\* For given  $n$  and  $p$  we tabulate  $\phi_v$  and  $\phi_{\min}$  as defined by Eqs. (43) and (51). Notice that  $\phi_v < \phi_{\min}$ , except for  $p = 3, n = \infty$ , when  $\phi_v = \phi_{\min}$ . For  $\phi < \phi_v$  the steady state is unstable if  $\kappa_1 = \dots = \kappa_n$ , or nearly so. For  $\phi > \phi_{\min}$  Popov's theorem assures global stability of the steady state. For  $\phi_v < \phi < \phi_{\min}$  the steady state is locally stable, but we make no claim about global stability.

Table 9-2. Global stability results for the Goodwin equations using Popov theorem, taken from Tyson and Othmer (1978).

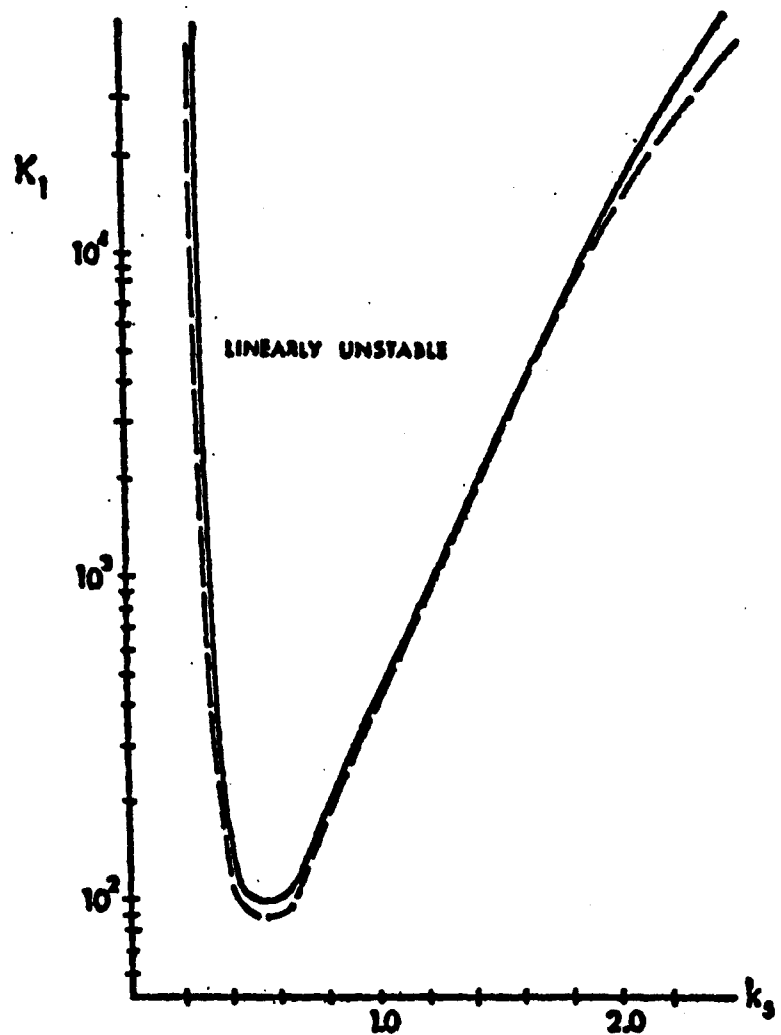


Figure 9-3. Regions of linear and global asymptotic stability for the Goodwin equations in the  $k_1, k_3$ -plane ( $n=5$ ,  $k_i = 1$  for  $i = 1, 2, 3, 4$ ,  $v = 4$ ). Solid curve = linear stability boundary, dashed curve = global stability boundary. Taken from Othmer (1976).

assigned a value of 2883, and  $k_n$  is allowed to range through the region of instability. Similarly figure 9-5 shows the analogous results when  $k_n$  is assigned a value of unity and  $L_p$  is allowed to range into the unstable region. The second case exhibits some interesting features. The amplitude is effectively constant over a large range of parameters. This would allow periodic operation of the reaction chain where the oscillations are not sensitive to variations in parameters. This type of insensitivity occurs often in living systems and its advantages are clear, in this case insensitivity to f. ex. mutations.

We note here that the global and local stability bounds are quite close, figure 9-3. Since dynamic instability is hard to obtain for physically realistic parameters, one is tempted to conclude the linear stability analysis gives all the information that one desires.

#### 9.2.4. The second method of Lyapunov.

This well know method for stability analysis gives global stability results, like Popov's theorem. It is, however, hard, in general, to apply to systems of high dimensionality.

The basic idea behind this method is illustrated in figure 9-6. This method involves the construction of a function  $V$ , called the Lyapunov function, that forms a closed trajectory around the

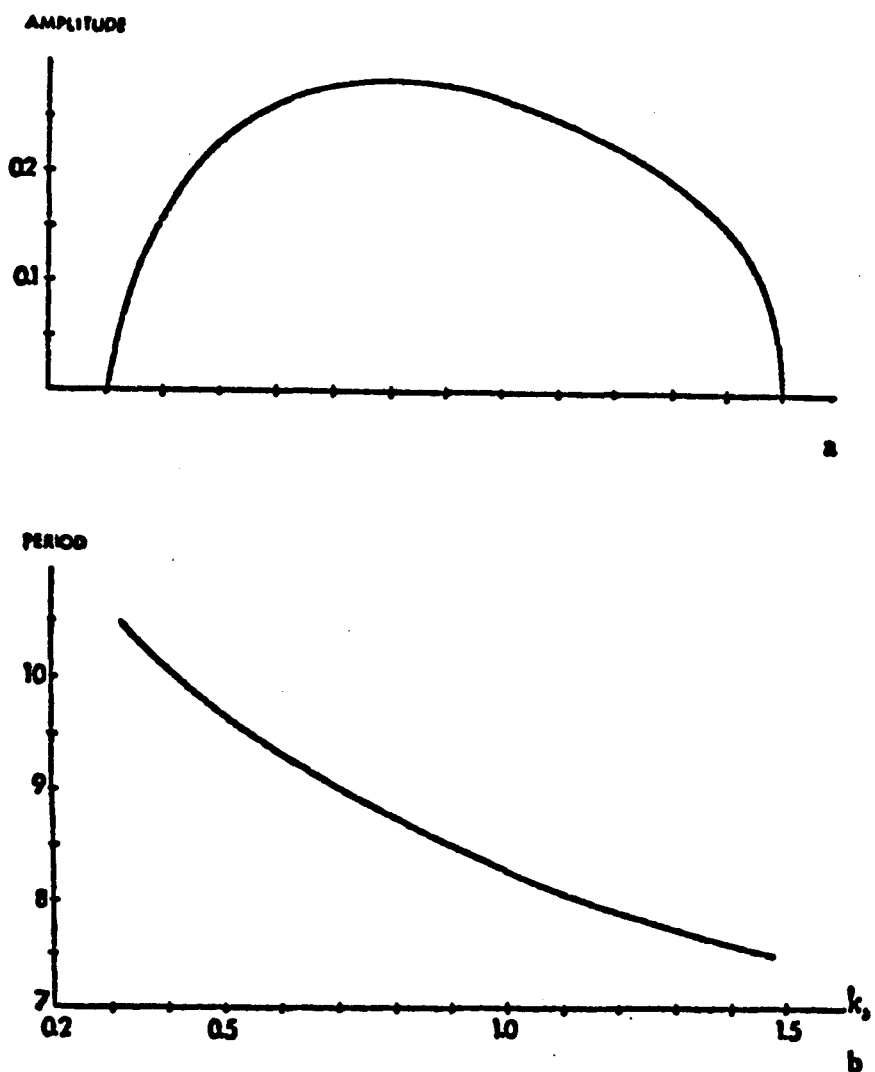


Figure 9-4. Amplitude and period versus  $k_5$  for oscillatory solutions in the Goodwin equations for the same parameter values as is figure 9-3 with  $L_p = 2883$ .

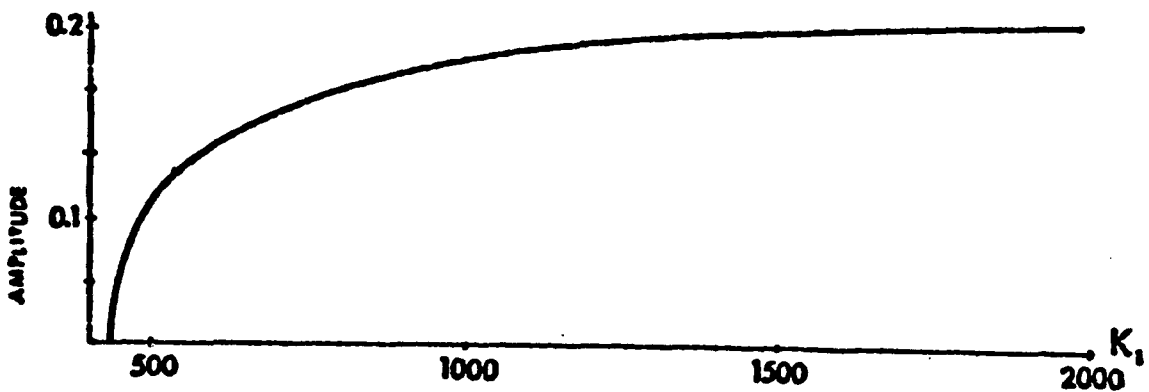


Figure 9-5. Amplitude versus  $L_p$  for oscillatory solutions in the Goodwin equations for the same parameter values as is figure 9-3 with  $k_5 = 1$ .

stationary point, which is normally transformed into the origin.

Then by forming the dot product of the gradient of  $V$  and  $dx/dt=f(x)$ ,

$$\frac{dV}{dt} = \nabla V \cdot f(x) \quad (20)$$

one can ensure stability if the function  $V$  can be constructed such that the derivative  $dV/dt$  is sign definite and opposite in sign to  $V$ , which is also sign definite. This will ensure that all trajectories in the phase plane will intersect the orbits of  $V$  in such away that they are moving towards the origin, figure 9-6. If such a function  $V$  can be constructed the stationary point is stable.

The main difficulty involved in the application of this method is the construction of the Lyapunov function  $V$ . The extent and utility of this technique is limited by this difficulty. At present the state of the art is that a general systematic procedure for the construction of  $V$  is only available for linear systems. A fuller discussion on the method and applications to biochemical systems is found in Walter (1972) and Stucki (1978).

Application of the Lyapunov method to the Goodwin equations came first from Walter (1969a,b). He used Lure's transformation (Lure, 1951) to obtain a canonical form of the Goodwin equations. For  $n = 1$  Walter finds that the stationary point is a global attractor. For  $n \geq 2$  limit cycle behavior cannot be excluded. A direct application of the technique, i. e. without the canonical transformation, combined with the Routh-Horowitch criterion yields similar results, Walter (1969a).

U an der Heiden (1976) obtains more extensive results for the

**Figure 9-6.** Graphical Illustration of Lyapunov functions.

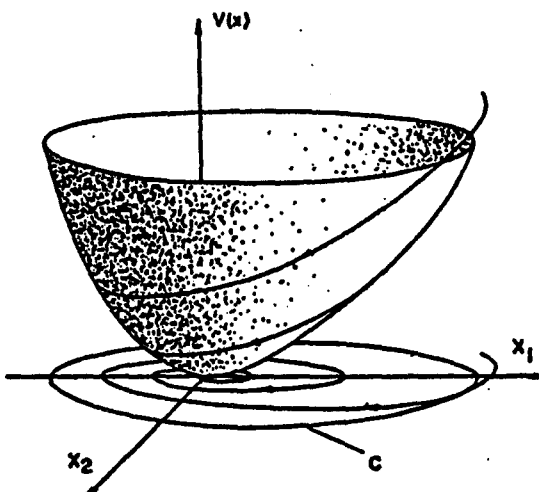


**FIG. 9-6.** Liapunov function. A trajectory on the Liapunov function in the  $V(x)$ - $x$  space and its projection onto the state plane is depicted for a two-dimensional case. The contour  $C$  is the projection of some value  $V(x) = \text{const}$ . of the Liapunov function on the state plane. For further details see text.

From Stuki (1978)

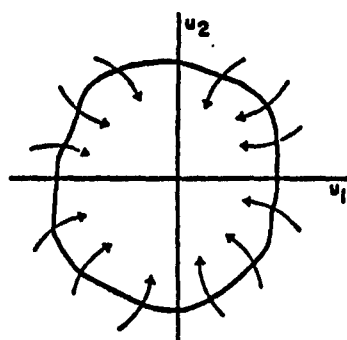


**Fig. 10.** Two-dimensional representation of trajectories intersecting a Lyapunov function toward the origin.

From Walter (1972)

Goodwin equations. He finds conditions that guarantee global stability. His general result is applicable for any dimension  $n$ , and the utility of this development has not been fully explored at present.

Lyapunov functions have also been applied to more complex feedback inhibition patterns in biochemical systems by Mees and Rapp (1978).

#### 9.2.5. Harmonic balancing.

The method of harmonic balancing is a commonly used technique for studying limit cycle behavior in non-linear control systems. Extensive reviews of this technique are available in the literature, f. ex. Hsu and Meyer (1968), and Mees (1972). This method has been applied to the Goodwin equations by Rapp (1975a,b,c, 1976a,b), using a first-order describing function. A nice summary is found in Rapp (1976b).

The method can be briefly described as follows. Equations 6 are rewritten as

$$\left( \prod_{i=1}^n (D+k_i) \right)[p] = I(p) \quad (21)$$

where  $D$  denotes the differentiation operator. The non-linear function is  $I(p)$ , and the reaction chain is the linear filter,

$$g(s) = \frac{1}{\prod_{j=1}^n (s+k_j)} \quad (22)$$

The output  $p$  and the non-linear function  $I(p)$  are now approximated

with a Fourier series as

$$p(t) = \operatorname{Re} \left( \sum_{k=0}^r z_k e^{ik\omega t} \right) \quad (23)$$

$$I(p(t)) = \operatorname{Re} \left( \sum_{k=0}^r a_k e^{ik\omega t} \right) \quad (24)$$

Letting the linear filter operate on  $I(p)$  a series of harmonic balancing equations is obtained,

$$g(0)a_0/z_0 = 1, g(i\omega)a_1/z_1 = 1, \dots, g(ir\omega)a_r/z_r = 1 \quad (25)$$

If these harmonic balancing equations can be satisfied, then a periodic solution exists, if not, then a periodic solution is not possible.

Solving the set of harmonic balancing equations is rather difficult. Two properties of the Goodwin equations make an approximate treatment possible. First, the Fourier series on  $I(p)$  converges very rapidly, and second is the low pass filter properties of  $g(s)$ . The harmonic contents of the pulses decreases rapidly as  $n$  increases. A nice discussion on the harmonic content of different pulses is found in Clements and Schelle (1963). These two simplifications make it possible to approximate the treatment and consider only the fundamental harmonic and the bias term, i. e. the two first harmonic equations of 25.

Rapp uses the method to develop a parameter  $T$ , which indicates the existence of periodic solutions. For  $T > 1$  periodic solutions may exist, but for  $T < 1$  limit cycles are excluded. The parameter  $T$  takes a maximum value when all the rate constants are identical

$$T_{\max} = v \cos^n \left( \frac{\pi}{n} \right) \quad (26)$$

This criterion resembles equation 17 but is a weaker condition. Extensive numerical results indicate that  $T$  is a good criterion for the existence of limit cycles. However the treatment is only approximate and some caution must be exercised at high values of  $n$ , Rapp and Mees (1977).

#### 9.2.6. Computational search.

An extensive numerical search for limit cycles was undertaken by Walter (1970), by simulating over 2500 cases. The results he obtained are in agreement with the theoretical developments discussed above. The simulations reveal an interesting characteristic of the limit cycles. Walter finds that in some cases that the fraction of the cycle time spent below the unstable stationary point is much higher than spent above. He suggests that this may explain the frequently observed precisely timed "spikes" in biological systems. He also finds that the amplitude of the oscillations are not highly sensitive to variations in some parameters, as Othmer (1976) did.

Mees and Rapp (1978) have presented a method to locate periodic solutions numerically without integrating the differential equations which is useful especially when one wants to locate unstable limit cycles.

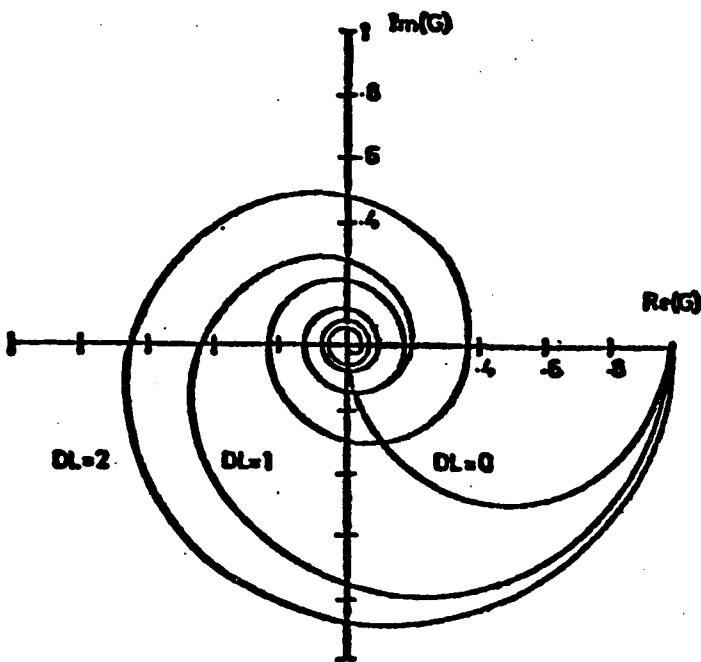
### 9.3. Modifications of the Goodwin Equations.

Several extensions and modifications of the basic Goodwin equations have been made. These make them more realistic and reveal more of the character of biochemical feedback loops. We start the discussion by looking at time delays, which may be interpreted as diffusional limitations (chapter 6). Then we discuss the inclusion of more realistic biochemical rate laws for the intermediary reactions.

#### 9.3.1. Time delays.

It is well known that time delays reduce the stability of control systems. Sometimes their effects are quite profound, and even small time delays may cause serious stability problems.

For the Goodwin equations some authors have examined the effects of time delays. Allwright (1977a) and MacDonald (1977b) have shown that for  $v$  of unity no oscillations are possible with a time delay in the loop. Rapp (1976b) derives similar results. He provides numerical examples illustrating the effects of time delays, figure 9-7. Using the harmonic balancing technique it is necessary for the locus of the roots of  $g(i\omega)$  in the complex plane to intersect the negative real axis, in order to satisfy the harmonic balancing equations and for limit cycles to occur. As this figure indicates the more the time delay the easier it is to obtain oscillatory behavior.



**Effect of increasing total delay,  $DL$ , on  $G(j\omega)$  for  $n = 1$ .**  
 $b_1 = 1$

Figure 9-7. Nyquist plot for the Goodwin equations illustrating the influence of increasing time delays. Taken from Rapp (1976b).

It is easy to visualize that if diffusional limitations occur, a time lag is introduced between the formation of the final product and the time at which it exerts inhibition. This will gravely effect the stability properties of the loop, as outlined above. One can thus partially rationalize, using controlability arguments, the general absence of diffusional limitations in living systems.

### 9.3.2. Different intermediate rate laws.

The first-order irreversible reactions in the Goodwin equations represent a highly idealized situation. Enzymes, in general, display more complex kinetic behavior. The simplest enzymatic reaction mechanism is the Michaelis-Menten mechanism, which is described by the quasi-steady state rate law (chapter 2),

$$\frac{dm_i}{dt} = - \frac{V_{m_i} m_i}{K_{m_i} + m_i} \quad (27)$$

It is believed that in general in vivo the concentration of the substrate is approximately equal to the Michaelis-Menten constant (Segel, 1975, Atkinson, 1977). This means that the reaction is operating close to, but away from the linear region.

Viniegra-Gonzalez (1973) extended the basic Goodwin equations to include Michaelis-Menten kinetics for the intermediate reactions. For the reaction chain with Michaelis-Menten intermediate reactions the Jacobian is

$$J = \begin{bmatrix} -a_1 & & & I_p \\ a_1 & -a_2 & & \\ & a_2 & -a_3 & \\ & & a_3 & -a_4 \\ & & & \ddots \\ & & & a_{n-1} & -a_n \end{bmatrix} \quad (28)$$

where

$$a_i = \frac{V_m K_m}{(K_m + m_i)^2} \quad (29)$$

and the characteristic equation becomes

$$\prod_{i=1}^n (a_i + \lambda) - \frac{I_p}{a_n} \prod_{i=1}^n a_i = 0 \quad (30)$$

Viniegra-Gonzalez conjectures, by analogy with equation 17, that

$$\frac{I_p}{a_n} = \frac{1}{\cos^n(\frac{\pi}{n})} \quad (31)$$

would imply  $\operatorname{Re}(\lambda) < 0$ . If  $m_i/K_m \ll 1$  then equation 31 reduces to the weaker form of equation 17. As before if the kinetic properties are distributed instability is less likely.

Another interesting result, obtained by Viniegra-Gonzalez, is a root locus diagram for the closed loop, using the linearized feedback parameter  $I_p$  as a variable, figure 9-8. The dotted lines represent the limiting case when all the  $a_i$ 's are equal. This case forms the asymptotes to the situations where the rate constants are not

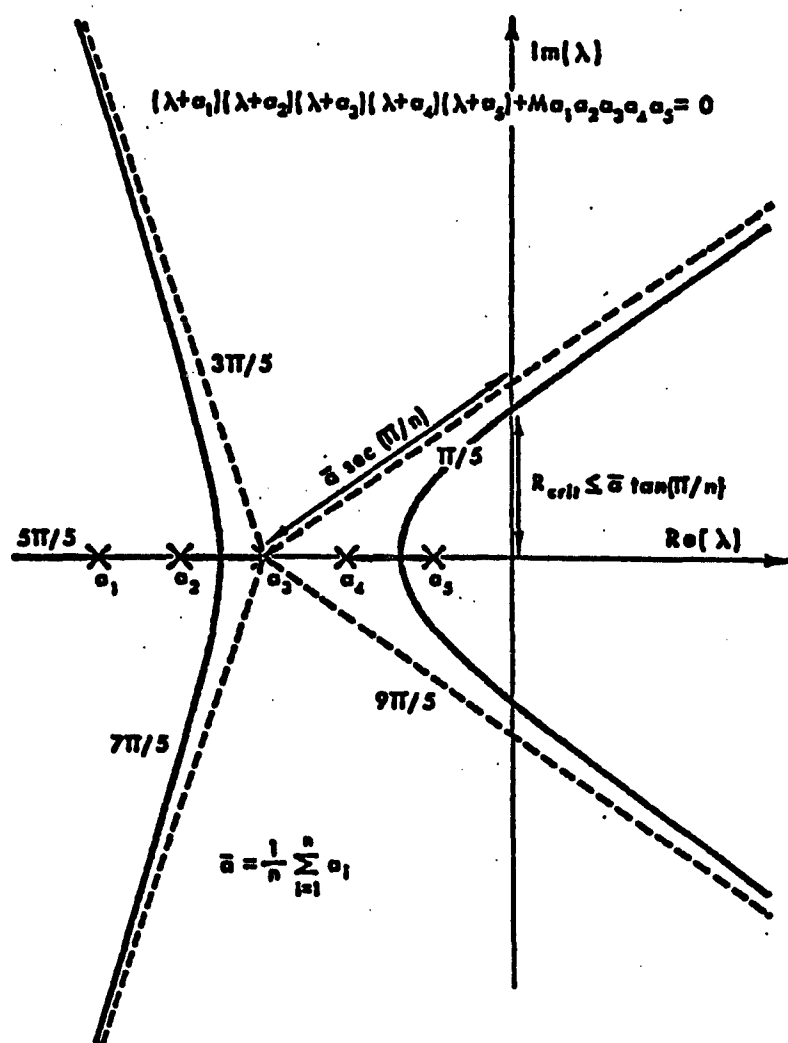
ROOT LOCUS OF A CHARACTERISTIC EQUATION ( $n = 5$ )

Figure 9-8. Root locus plot for the Goodwin equations. Taken from Viniegra-Gonzales (1973).

identical. For the case where all the reactions are identical only complex roots are possible, implying that the response is always damped oscillatory. However for small values of the feedback parameter and unequal a's, there are parameter combinations where the roots are purely real and negative. Presumably this is what we would expect to find in metabolic networks.

Walter (1970, 1971, 1974) has examined the effects of different intermediate rate laws on the stability of the loop. Aside from showing, using the Bendixon criterion for n=2, that the system is always stable for any rate laws of biological interest, most of his investigation is computational. His extensive simulations result in some heuristics: 1) the stability of the reaction chain with respect to the rate laws of the intermediate reactions is

sigmoidal < linear < hyperbolic

where the sigmoidal rate laws give the most stable system, 2) the characteristics of the oscillations is relatively insensitive to the model's parameters.

#### 9.4. Power Law Kinetics.

Savageau (1969, 1977) has proposed an alternative approach to the modelling of biochemical reaction networks. Instead of using physically derived rate laws, such as the Michaelis-Menten quasi-steady state rate law, he proposes that all biochemical kinetics can be approximated by a simple power law. This formalism

avoids the mathematically unattractive biochemical rate laws, described by ratios of polynomials.

In the power laws formalism the describing equations are

$$\frac{dm_i}{dt} = F_i^+ - F_i^- \quad (32)$$

where

$$F_i^+ = k_i^+ \prod_{j=1}^n m_j^{v_{ij}^+} \quad (33)$$

$$F_i^- = k_i^- \prod_{j=1}^n m_j^{v_{ij}^-} \quad (34)$$

and the  $k_i$ 's are the apparent rate constants and  $v_{ij}^+$  is the apparent kinetic order of the reaction with respect to  $m_j$ , for the net formation of  $m_i$  and  $k_i^-$ ,  $v_{ij}^-$  have equivalent meaning for the net disappearance of  $m_i$ . Equations 33 and 34 can be transformed into a linear set of equations by making a logarithmic transformation. This greatly simplifies the mathematics, now being linear. Savageau (1969, 1971) has argued that the range where the power law approximation is applicable is much wider than direct linearization, and is wide enough to cover the physiological situations of interest.

Savageau (1974, 1975) has applied his power law approach to the Goodwin reaction scheme. He derives a criterion for the stability of the stationary point as which is strikingly similar to that of equation 17. He obtains these results with considerably more ease than is needed for the derivation of equation 17. Savageau also arrives at the conclusion that the case with all equal reactions is the least stable situation.

The physiological function of biosynthetic pathways in general seems to be to keep the supply of the monomer it produces a constant. Its operation is not expected to be periodic. It is also expected to be perturbed by two kinds of disturbances, changes that effect the supply and the demand of initial substrate and final product respectively. With this in mind Savageau (1974) examines the ability of the reaction chain to cope with these disturbances. He finds the feedback inhibition scheme to be optimal. The loop accomplishes its task while minimizing the concentration of the intermediate metabolites.

The mathematical simplicity of Savageau's formalism is attractive. He obtains much the same conclusions as the more rigorous methods, but much more easily. His technique is summarized in Savageau (1977).

## CHAPTER 10

## CONCLUSIONS AND RECOMMENDATIONS

I hope that this thesis will be the starting point of comprehensive engineering modelling studies of biochemical reaction networks. Such studies seem timely in view of the rapidly growing knowledge about the detailed molecular structure and function of living matter and the currently developing capability to alter organism at this level through genetic engineering. The metabolic reaction network provides an excellent starting point for such modelling efforts both since it is chemically well known, and the fundamental physical laws can be applied, and since it is of much practical importance in such diverse areas as fermentations, chemotherapy and toxicology.

The chemical engineering training is particularly well suited background, because of the proper combination of disciplines, to carry out metabolic/genetic modelling studies. It is perhaps the most important contribution of this thesis to initiate such a study. On a more technical level the thesis contains fundamental work on two basic topics involved, biochemical dynamics and simple biochemical control loops, and it sets the tone for the mathematical methodology

needed and provides a basis for further work. I believe it makes significant contributions to both these topics, an issue that I wish to discuss in some more detail.

### 10.1. Conclusions.

#### 10.1.1. Biochemical reaction dynamics.

The basic problem with mass action kinetic models of biochemical reaction mechanisms is mathematical intractability; explicit analytical solutions for the concentration profiles cannot be obtained even for the most simple situations. This leaves us with the problem of exploring the qualitative features of the solutions and their parametric sensitivity through some approximate means. The procedure that we have used is as follows:

- 1) The model. First we write down the reaction mechanism under investigation and formulate a model based on the law of mass action.
- 2) Scaling. Such models contain a large number of parameters, both kinetic and concentration related, and we concentrate these into the minimum number of dimensionless property ratios through judicious scaling. The distinction between kinetic and concentration dependent effects is important: the kinetic constants are specified by the genes and can be taken, as a first

approximation, to be constant but the concentrations of enzymes and metabolites can change from one physiological state to another. Hence we have tried to separate the two during the scaling procedure and isolate dimensionless parameters containing only kinetic properties from those containing species concentrations.

It is pertinent to note that the kinetic constants are, strictly speaking, not invariant; they depend primarily on temperature and pH. Biological systems are normally isothermal so temperature can be regarded as essentially constant but the pH may vary especially if abnormal or pathological situations develop. Inspite of these considerations it is conceptually useful to separate the kinetic parameters and treating them as constants especially when one studies the normal physiological state.

3) Full linear analysis. The next problem is to solve the scaled mass action kinetic model which, as discussed above, is normally impossible. As a first approximation we have linearized these models and examined the properties of the full -- including a study of the normal modes -- linear solution.

This procedure is useful for several purposes and yields several important results.

1) Exploratory purposes. The two factors that characterize the linear solution are the eigenvalues, or the relaxation times, and the modes that give measures of dynamic interactions. One can simply compute these as a functions of the dimensionless property

ratios and thereby examine how a particular kinetic or concentration related property change these two key characteristics.

2) Understanding and justification of approximations. The combination of the time constants and the modes gives an extremely useful result: the justification and understanding of frequently used approximations to simplify kinetic behavior.

The widely used quasi-steady state assumption is interpreted as a reduction in dynamic interactions under conditions where the relaxation times are well separated. If a variable becomes fast and dynamic interactions are reduced then the transients of this particular variable becomes unimportant and hence its temporal derivative can be equated to zero. Study of one-way interactions sheds light on the meaning and applicability of singular perturbations (section 2.4). The important criterion,  $\epsilon_t \ll K_m \ll s_t$ , for the applicability of the quasi-steady state assumption is obtained.

Similarly the quasi-equilibrium assumption is interpreted within this framework. Under certain conditions a fast mode appears whose steady state equation is simply the equilibrium relationship for a particular step in the reaction mechanism. Then if one relaxes this mode it is equivalent to making the quasi-equilibrium assumption but here we have a basis for doing so: the fast mode is dynamically independent and it describes the motion towards the equilibrium state. Hence ignoring the dynamics

of this mode is equivalent to saying; lets ignore the fast transients since they are all associated with the equilibration of this particular step.

3) Approximation to transient behavior. Physiological conditions are apparently such that the reactions operate in what is known as the "linear region" or the substrate concentrations are at or below their binding constants. Under those conditions the kinetic description is weakly non-linear and the linear solution is a good approximation to transient behavior. The most serious non-linear effects are saturation kinetics and if we approach the saturation region the linear approximation becomes inadequate.

4) Estimation of relative diffusional and reaction response times. Another advantage of the linear solution is that an explicit expression for the fastest time constant can be obtained and compared to expected diffusional response times. Such comparison indicates, as has been discussed previously by several authors, that diffusional limitations seem unimportant under intracellular conditions, see appendix A.

5) Relating "macro-and-microscopic" kinetic properties. The linear description gives us the opportunity to express the overall kinetic characteristics of enzymatic reaction chains in terms of temporal moments which have well characterized physical significance. The moments for simple reaction chains (chapter 5) can be obtained in terms of all the kinetic parameters, or the properties of the

individual reactions. Hence the moments gives us the important link between detailed ("microscopic") and overall ("macroscopic") kinetic properties and enable us to predict overall dynamic behavior and assessing which individual kinetic parameters contribute most significantly to the overall kinetics. The limitations on this development are, however, not yet clear.

Hence through the process of judicious scaling and full linear analysis we have been able to examine many important issues of biochemical kinetics.

#### 10.1.2. Biochemical Regulation.

Metabolism is characterized by a tangle of control loops. The simplest of these is a single loop with feedback regulation, which we call simply the single biochemical control loop. The second part of the thesis deals with these single biochemical control loops and the procedure that the analysis follows is now outlined.

1) Structural model. The single feedback loop has been used to model regulation on several levels on biology, such as metabolic, genetic, cell density, nervous system and ecological regulation. These models are all structurally similar although the details may differ from model to model. The study of metabolic/genetic regulation has perhaps advanced the furthest, through study of the Goodwin equations and variants thereof (chapters 8 and 9).

We therefore begun the analysis by examining the the properties

of the structure of these models to see what characteristics are independent of model details but which depend only on the structure of the model. As before we scale the equations to separate kinetic from concentration dependent effects.

2) Local stability analysis. The basic results from local stability analysis, chapter 6, are that positive and negative feedback is capable of exhibiting multiple steady states and sustained oscillations respectively, the two simplest kinds of dissipative structures. General criteria for each type of bifurcation is presented. The criteria for multiple steady states depends only on the partial derivatives with respect to the end product concentration of the non-linear elements in the model evaluated at the steady states. The criteria contains in addition to these partial derivatives properties of the dynamic operator describing the reaction chain. The size of the instability regions is most heavily influenced by the order of the dynamic description and the appearance of a transporation lag. Both of these factors are found to be unimportant under physiological conditions suggesting that evolution has a selection bias towards robust control structures.

3) Mapping general results into specific parameter spaces. The general results from the local stability analysis really breaks the study down into two parts.

In chapter 7 we study feedback activation and specify kinetic

models for the reaction rates that were left unspecified in the general bifurcation criteria. We use rate laws that are commonly used to describe kinetics of regulatory enzymes; the lumped model based on Hill-type kinetics, and the well known symmetry model. The basic results are that the region of multiple steady states can be mapped out in a parameter space consisting of purely dimensionless kinetic parameters. Bounds on these kinetic parameters are obtained. The reaction has to be accelerated over a certain minimum threshold value and the end product's affinity for the regulatory enzyme relative to the removal enzyme must exceed a critical value in order for multiplicities to appear. However the regions of multiple steady states in this kinetic parameter space can be moved around by modifying the amounts of metabolites and/or enzymes present. This gives the cell certain decision making capabilities: the flux through the loop can be switched to a higher rate of utilization when a critical amount of initial substrate is exceeded and similarly it can be switched down when the initial substrate drops below a certain critical level. Hence positive feedback allows for creative functions at the metabolic level.

Analogously in chapter 8 we map the criteria for dynamic bifurcations out into the parameter spaces formed by parameters of the lumped controller and the symmetry model. Here we are able to resolve questions concerning the dynamic stability of the well known Goodwin equations, which form a special limit of our general case.

These equations have been extensively discussed in the literature for about twenty years (chapter 9). Our study of the basic Goodwin equations including saturation effects in the removal rate dramatically alter the main conclusion derived from extensive analysis of these equations; that instability is not observed for realistic values of the parameters. We also make another important finding; unstable Hopf bifurcations. Similarly to the creative functions introduced by the multiple steady state solutions this feature allows for switching between a stable steady state and a stable limit cycle for the same set of parameters ! Here we get a trigger mechanism; critical values of certain concentration can either induce or quench oscillations. Another creative function that allows the cell to generate temporal signals. This study is incomplete at present.

Two other general comments should be made. First the static bifurcations are much easier to deal with, both analytically and numerically, than the dynamic bifurcations. The reason is that they do not depend on the dynamic character of the model but only the steady state condition. Second the symmetry model is less likely to show both types of bifurcations, static and dynamic, than the lumped controller.

These two chapters, 7 and 8, contain a comprehensive survey of the occurrence of simple bifurcations and their parameter sensitivity in the simplest of biological regulatory structures.

## 10.2. Recommendations.

The work presented here is only the beginning of a major research topic; the quantification of the dynamic structure and function of metabolic networks. Several extensions of the present work should be considered.

### 10.2.1. Branched Pathways.

Once we have a comprehensive understanding of how a single control loop functions and how the various parameters influence its behavior the next logical question is; how do metabolic control loops interact? Here we are referring to basically two situations; multiple control loops over branched pathways such as found in the biosynthetic sequences leading to amino and nucleic acids, and multiple control loops on a single reaction chain, such as glycolysis.

In the former case the question basically is how are the production rates of each end product controlled; are the loops designed such that the cell can produce each endproduct without changing the production rates of the other end products; in other words are these production rates dynamically decoupled?

In the latter situation it seems more a question of how to simultaneously regulate the multiple objectives of glycolysis: production of cofactors, such as ATP (chemical energy) and NADH (redox potential), and carbon skeletons for biosynthesis. Some

progress towards this end has been made in the analysis of glycolysis in the red blood cell (Palsson, Liao and Lightfoot, 1984). These preliminary results indicate that there is an inherent dynamic structure that allows for the three different objectives to be meet, apparently dynamically independently of each other! These three objectives are production of ATP, of NADH, and of 2,3-DPG (a bi-phosphorylated three-carbon sugar used to regulate the saturation curve of oxygen to Hemoglobin). Hence there is a dynamic structure in place that has a well defined function: teleology extended to metabolic dynamics!

#### 10.2.2. Hierarchical loops.

Once the regulation at the metabolic level has been reasonably well studied it is timely to ask the question: how do genetic/metabolic controls interact? It has been known for some time that metabolites regulate both metabolic fluxes by regulating enzyme activities but they also regulate gene expression (chapter 1, figure 1-5). A model of such hierarchical control can be easily formulated by a simple extension of the Goodwin equations by allowing dynamics in the metabolic part of the model. Such model is really in the form of a cascade control loop where the inner loop is the metabolic control loop operating on a time scale of roughly minutes. The outer, slower, loop, operating roughly on the time scale of about an hour, then resets the setpoint for the inner loop by modifying the amount of regulatory enzyme present.

Finally regulation of gene expression is becoming increasingly important in this age of genetic engineering. To produce protein in genetically engineered bacteria one wants to be able to control the operons on the plasmids in such a way that they are "off" during the growth phase of the bacteria and once the stationary phase is reached one would like to turn the operon "on" so that the production of the desired protein is initiated.

## REFERENCES

- Adair, C. S. (1925), "The Hemoglobin System. VI The Oxygen Dissociation Curve of Hemoglobin," *J. Biol. Chem.*, 63, 529-545
- Aizerman, D. G. and F. R. Gantmacher (1964), "Absolute Stability of Regulator Systems," Holden-Day, San Francisco, California
- Albery, W. J. and J. R. Knowles (1976), "Evolution of Enzyme Function and the Development of Catalytic Efficiency," *Biochem.*, 15, 5631-5640
- Albery, W. J. and J. R. Knowles (1977), "Efficiency and Evolution of Enzyme Catalysis," *Angew. Chem. Int. Ed. Engl.*, 16, 285-293
- Alberty, R. A. (1959), "The Rate Equation for an Enzymatic Reaction," in P. D. Boyer, H. Lardy and K. Myrback editors, "The Enzymes", 2nd Edition chapter 3, 1, pages 143-155, Academic Press, New York
- Allwright, D. J. (1977a), "A Global Stability Criterion for Simple Control Loops," *J. Math. Biol.*, 4, 363-373
- Allwright, D. J. (1977b), "Harmonic Balance and the Hopf Bifurcation," *Math. Proc. Cambridge Philos. Soc.*, 82, 453-467
- Allwright, D. J. (1981), "The Hopf Bifurcation in Some Biochemical Control Loops," *J. Math. Biol.*, 11, 85-93
- Aris, R. (1975), "The Mathematical Theory of Diffusion in Permeable Catalysts," Vol I and II, Clarendon Press, Oxford, London
- Atkins, G. L. and I. A. Nimmo (1980), "Current Trends in the Estimation of Michaelis-Menten Parameters," *Ana. Biochem.*, 104, 1-9
- Atkinson, D. E. (1970), "Enzymes as Control Elements in Metabolic Regulation," in P. D. Boyer editor, "The Enzymes," 3rd edition chapter 9, 1, 461-489, Academic Press, New York
- Atkinson, D. E. (1971), "Adenine Nucleotides as Universal Stoichiometric Metabolic Coupling Agents," *Adv. Enzyme Regul.*, 9, 207-219

- Atkinson, D. E. (1977), "Cellular Energy Metabolism and its Regulation," Academic Press, New York
- Block, K. and D. Vance (1977), "Control Mechanisms in the Synthesis of Saturated Fatty acids," Annu. Rev. Biochem., 46, 263-298
- Bodenstein, M. and H. Lutkemeyer (1925), "Die Photochemische Bildung von Bromwasserstoff und die Bildungsgeschwindigkeit der Brommolekel aus den Atomen," Z. Phys. Chem., 114, 208-236
- Boiteux, A., B. Hess and E. E. Sel'kov (1980), "Creative Functions of Instability and Oscillations in Metabolic Systems," Curr. Top. Cell. Reg., 17, 171-203
- Borkenhagen, L. F. and E. P. Kennedy (1958), "Enzymatic Equilibration of L-Serine with O-Phospho-L-Serine," Biochim. Biophys. Acta, 28, 222-223
- Bourget, P. A. and G. C. Tremblay (1972), "Control of Pyrimidine Biosynthesis in Rat Liver by Feedback Inhibition of Aspartate Carbamyltransferase," Biochem. Biophys. Res. Commun., 46, 752-756
- Bowen, J. R., A. Acrivos and A. K. Oppenheim (1963), "Singular Perturbation Refinement to Quasi-Steady State Approximation in Chemical Kinetics," Chem. Eng. Sci., 18, 177-188
- Bresnick, E. and K. Blatchford (1964), "Inhibition of Dihydroorotase by Purines and Pyrimidines," Biochim. Biophys. Acta, 81, 150-157
- Briggs, G. E. and J. B. S. Haldane (1925), "A Note on the Kinetics of Enzyme Action," Biochem. J., 19, 338-339
- Careri, G., P. Fasella and E. Gratton (1975), "Statistical Time Events in Enzymes: A Physical Assessment," CRC Crit. Rev. Biochem., 3, 141-164.
- Carslaw, H. S. and J. C. Jaeger (1959), "Conduction of Heat in Solids," 2nd Edition, Oxford University Press
- Carson, E. R., C. Cobelli and L. Finkelstein (1983), "The Mathematical Modelling of Metabolic and Endocrine Systems," John Wiley and Sons, New York
- Chance, B. (1943), "The Kinetics of the Enzyme-Substrate Compound of Peroxidase," J. Biol. Chem., 151, 553-577
- Chance, B., J. J. Higgins and D. Garfinkel (1962), "Analogue and Digital Computer Representations of Biochemical Processes," Federation Proceedings, 21, 75-86

- Chance, B., E. K. Pye, A. K. Ghosh and B. Hess (1973) editors, "Biological and Biochemical Oscillators," Academic Press, New York
- Cleland, W. W. (1975), "What Limits the Rate of an Enzyme-Catalyzed Reaction?", *Acc. Chem. Res.*, 8, 145-151
- Clements, W. C. and K. B. Schnelle (1963), "Pulse Testing for Dynamic Analysis," *Ind. Eng. Chem. Proc. Devel.*, 2, 94-102
- Citri, N. (1973), "Conformational Adaptability in Enzymes," *Adv. Enzymol.*, 37, 397-647
- Cohn, M. and K. Horibata (1959), "Inhibition by Glucose of the Induced Synthesis of the  $\beta$ -Galactoside-Enzyme System of Escherichia Coli. Analysis of Maintenance," *J. Bacteriol.*, 78, 601-612
- Cornish-Bowden, A. (1979), "Fundamentals of Enzyme Kinetics," Butterworths, London
- Coughanover, D. R. and L. B. Koppel (1965), "Process Systems Analysis and Control," McGraw-Hill, New York
- Crandall, M. G. and P. H. Rabinowitch (1981), "Mathematical Theory of Bifurcation," in C. Bardos and D. Bessis editors, "Bifurcation Phenomena in Physics and Related Topics," pages 3-46, D. Reidel Publishing Company, Boston
- Crooke, P. S., R. D. Tanner and R. Aris (1979), "The Role of Dimensionless Parameters in the Briggs-Haldane and Michaelis-Menten Approximations," *Chem. Eng. Sci.*, 34, 1354-1357
- Darvey, I. G. and R. F. Maltak (1967), "An Investigation of a Basic Assumption in Enzyme Kinetics Using Results of the Geometric Theory of Differential Equations," *Bull. Math. Biophys.*, 29, 335-341
- Darvey, I. G., A. H. Klotz and M. Ritter (1978), "On the Kinetics of Enzyme Action," *Bull. Math. Biol.*, 40, 727-734
- Doedel E. J. (1984), "Continuation Techniques in the Study of Chemical Reaction Schemes," in K. I. Gross editor, Proc. Special Year in Energy Math., University of Wyoming, SIAM Publ.
- Doedel E. J. and R. F. Heinemann (1983), "Numerical Computation of Periodic Solution Branches and Oscillatory Dynamics of the Stirred Tank Reactor with A  $\rightarrow$  B  $\rightarrow$  C Reactions," *Chem. Eng. Sci.*, 38, 1493-1499
- Doedel E. J., A. D. Jepson, and H. B. Keller (1984) "Numerical

Methods for Hopf Bifurcations and Continuation of Periodic Solution Paths," in R. Glowinski and J. L. Lions, "Computing Methods in Applied Sciences and Engineering VI, North-Holland, Amsterdam

Eigen, M. (1971), "Self-Organization of Matter and the Evolution of Biological Macromolecules," *Naturwissenschaften*, 58, 465

Eigen, M. and P. Schuster (1979), "The Hypercycle - A Principle of Natural Self-organization," Springer-Verlag, Heidelberg

Ferdinand, W. (1977), "The Enzyme Molecule," John Wiley and Sons, London

Filon, L. N. G. (1928), "On a Quadrature Formula for Trigonometric Integrals," *Proc. Roy. Soc. Edinburgh*, 49, 38-47

Garfinkel, D., L. Garfinkel, M. Pring, S. B. Green and B. Chance (1970), "Computer Applications to Biochemical Kinetics," *Ann. Rev. Biochem.*, 39, 473-498

Garfinkel, D. and M. C. Kohn (1980), "Computer Modeling of Cardiac Energy Metabolism," in W. E. Jacobus and J. S. Ingwall editors, "Heart Creatine Kinase," chapter 5, 48-62, Williams and Wilkins, Baltimore

Gibilaro, L. G. and F. P. Lees (1969), "The Reduction of Complex Transfer Function Models to Simple Models Using the Method of Moments," *Chem. Eng. Sci.*, 24, 85-93

Glandsdorff, P. and I. Prigogine (1971), "Thermodynamic Theory of Structure, Stability, and Fluctuations," John Wiley and Sons, London

Goldbeter, A. and S. R. Caplan (1976), "Oscillatory Enzymes," *Annu. Rev. Biophys. Bioeng.*, 5, 449-476

Goldbeter, A. and P. Nicolis (1976), "An Allosteric Enzyme Model with Positive Feedback Applied to Glycolytic Oscillations," *Prog. Theor. Biol.*, 4, 65-160

Goodridge, A. B. (1973), "Regulation of the Activity of Acetyl CoA Carboxylase by Palmitoyl CoA and Citrate," *J. Biol. Chem.*, 247, 6946-6952

Goodwin, B. C. (1963), "Oscillatory Organization in Cells, A Dynamic Theory of Cellular Control Processes," Academic Press, New York

Goodwin, B. C. (1965), "Oscillatory Behaviour in Enzymatic Control Processes," *Adv. Enzyme Reg.*, 3, 425-438

- Goodwin, B. C. (1966), "An Entrainment Model for Timed Enzyme Synthesis in Bacteria," *Nature*, 209, 479-481
- Griffith, J. S. (1968a), "Mathematics of Cellular Control Processes, I. Negative Feedback to One Gene," *J. theor. Biol.*, 20, 202-208
- Griffith, J. S. (1968b), "Mathematics of Cellular Control Processes, II. Positive Feedback to One Gene," *J. theor. Biol.*, 20, 209-216
- Guertin, E. W., J. P. Sørensen and W. E. Stewart (1977), "Exponential Collocation of Stiff Reactor Models," *Computers and Chem. Engng.*, 1, 197-203
- Gutfreund, H. (1955), "Steps in the Formation and Decomposition of Some Enzyme-Substrate Complexes," *Discussions of the Faraday Society*, 20, 167-173
- Haldane, J. B. S. (1930), in R. H. A. Plimer and F. G. Hopkins editors, "The Enzymes," page 81, Longmans Green, London
- Hamer, J. W., T. A. Akramov and W. H. Ray (1981), "The Dynamic Behavior of Continuous Polymerization Reactors - II," *Chem. Eng. Sci.*, 36, 1897-1914
- Hammes, G. G. and P. R. Schimmel (1970), "Rapid Reactions and Transient States," in P. D. Boyer editor, "The Enzymes," Chapter 2, 2, 67-114, Academic Press, New York
- Hammes, G. G and C-W Wu (1974), "Kinetics of Allosteric Enzymes," *Ann. Rev. Biophys. Bioeng.*, 3, 1-33
- Hastings, S. and J. Tyson (1975), "Oscillations in Negative Feedback Cellular Control Processes," *Biophys. Soc.*, 179a
- Hastings, S., J. Tyson and D. Webster (1977), "Existence of Periodic Solutions for Negative Feedback Cellular Control Systems," *J. Diff. Eq.*, 25, 39-64
- Hearon, J. Z. (1953), "The Kinetics of Linear Systems with Special Reference to Periodic solutions," *Bull. Math. Biophys.*, 15, 121-141
- Heineken, F. G., H. M. Tsuchyia and R. Aris (1967), "On the Mathematical Status of the Pseudo-Steady State Hypothesis in Biochemical Kinetics," *Math. Biosci.*, 1, 95-113
- Heinrich, R. and T. A. Rapoport (1974), "A Linear Steady-State Treatment of Enzymatic Chains: General Properties, Control and Effector Strength," *Eur. J. Biochem.*, 42, 89-95
- Heinrich, R. and T. A. Rapoport (1975), "Mathematical Analysis of

- Multienzyme Systems, II Steady State and Transient Control,"  
BioSystems 7, 130-136
- Heinrich, R., S. M. Rapoport and T. A. Rapoport (1977), "Metabolic Regulation and Mathematical Models," Prog. Biophys. Molec. Biol., 32, 1-82
- Henri, V. (1903), "Lois generalis de l'action des diastases," Hermann, Paris
- Herman, R. H., R. M. Cohn and P. D. McNamara editors (1979), "Principles of Metabolic Control in Mammalian Systems," Plenum Press, New York
- Hess, B. and A. Boiteux (1971), "Oscillatory Phenomena in Biochemistry," Annu. Rev. Biochem., 40, 237-258
- Hess, B., A. Boiteux and H. G. Busse (1975), "Spatiotemporal Organization in Chemical And Cellular Systems," Adv. Chem. Phys., 29, 137-168
- Higgins, J. (1964), "A Chemical Mechanism for Oscillation of Glycolysis Intermediates in Yeast Cells," Proc. Natl. Acad. Sci., 51, 989-994
- Higgins, J. (1967), "The Theory of Oscillatory Reactions," Ind. Eng. Chem., 59, 18-62
- Higgins, J., R. Frenkel, E. Hulme, A. Lucas and G. Rangazas (1973), "The Control Theoretic Approach to the Analysis of Glycolytic Oscillations," in B. Chance, E. K. Pye, A. K. Ghosh and B. Hess (1973) editors, "Biochemical and Biological Oscillations," pages 127-175, Academic Press, New York
- Hill, A. V. (1910), "The Possible Effects of the Aggregation of the Molecules of Haemoglobin on its Dissociation Curves," J. Physiol. (Proceedings), 40, iv-vii
- Hirschfelder, J. O. (1957), "Pseudostationary State Approximation in Chemical Kinetics," J. Chem. Phys., 26, 271-273
- Hommes, F. A. (1962a), "The Integrated Michaelis-Menten Equation," Arch. Biochem. Biophys., 96, 28-31
- Hommes, F. A. (1962b), "Analog Computer Studies of a Simple Enzyme-Catalyzed Reaction," Arch. Biochem. Biophys., 96, 32-36
- Hopf, E. (1942), "Abzweigung Einer Periodischen Losung von Einer Stationaren Eines Differential-Systems," Ber. Verh. Sachs. Acad. Wiss. Leibzig. Math. Nat. Kl., 95, 3-22

- Hsu, J. C. and A. U. Meyer (1968), "Modern Control Principles and Application," McGraw-Hill, New York
- Hunding, A. (1974), "Limit Cycles in Enzyme Systems with Non-Linear Feedback," *Biophys. Struct. Mech.*, 1, 47-54
- Ignatik, R., M. A. B. Deakin and C. Fandry (1981), "Phase-Plane Analysis of the Michaelis-Menten Reaction Equations," *Bull. Math. Biol.*, 43, 361-370
- Ignatik, R. and M. A. B. Deakin (1981), "Asymptotic Analysis of the Michaelis-Menten Reaction Equations," *Bull. Math. Biol.*, 43, 375-388
- Jacob, F. and J. Monod (1961), "Genetic Regulatory Mechanisms in the Synthesis of Proteins," *J. Mol. Biol.*, 3, 318-356
- Kacser, H. (1983), "The Control of Enzymes in Vivo: Elasticity Analysis of the Steady State," *Biochem. Soc. Trans.*, 601st meeting Aberdeen, 11, 35-40
- Kacser, H. and J. A. Burns (1973), "The Control of Flux," *Symp. Soc. Exp. Biol.*, 27, 65-104
- Kacser, H. and J. A. Burns (1979), "Molecular Democracy: Who Shares the Controls ?," *Biochem. Soc. Trans.*, *Biochem. Rev.*, 7, 1149-1160
- Katiyar, S. S. and J. W. Porter (1977), "Minireview: Mechanism of Fatty Acid Synthesis," *Life Sci.*, 20, 737
- Katunuma, N., Y. Matsuda and Y. Kuroda (1970), "Phylogenetic Aspects of Different Regulatory Mechanism of Glutamine Metabolism," *Adv. Enzyme Regulation*, 8, 73-82
- Kerson, L. A. and S. H. Appel (1968), "Kinetic Studies on Rat Liver Carbamylphosphate Synthetase," *J. Biol. Chem.*, 243, 4279-4285
- Kohn, M. C., L. M. Whitley and D. Garfinkel (1979), "Instantaneous Flux Control Analysis for Biochemical Systems," *J. ther. Biol.*, 76, 437-452
- Koshland, D. E., G. Nemethy and D. Filmer (1966), "Comparison of Experimental Binding Data and Theoretical Models in Proteins Containing Subunits," *Biochemistry*, 5(1), 365-385
- Krebs, H. A. (1972), "The Pasteur Effect and the Relations Between Respiration and Fermentation," *Essays Biochem.*, 8, 1-34
- Kurganov, B. I. (1983), "Allosteric Enzymes: Kinetic Behavior," Wiley, New York

- Lane, A. N. (1982), "The Dependence of Flux, Sensitivity and Response of the Flux on the Concentrations of Substrate and Modifiers of Cooperative Enzymes," *J. theor. Biol.*, 99, 491-508
- Laidler, K. J. (1955), "Theory of the Transient Phase in Kinetics with Special Reference to Enzyme Systems," *Can. J. Chem.*, 33, 1614-1624
- Levine, R. L., N. J. Hoogenraadand and N. Kretchmer (1974), "A Review: Biological and Clinical Aspects of Pyrimidine Metabolism," *Pediat. Res.*, 8, 724-734
- Lim, H. C. (1973), "On Kinetic Behavior at High Enzyme Concentrations," *AIChE J.*, 19, 659-661
- Lin, C. C. and L. A. Segel (1974), "Mathematics Applied to Deterministic Problems in the Natural Sciences," MacMillan Publishing Company Inc., New York
- Lur'e, A. I. (1951), "Certain Non-linear Problems in the Theory of Automatic Control," Gostekhizat, Moscow
- MacDonald, N. (1977a), "Bifurcation Theory Applied to a Simple Model of a Biochemical Oscillator," *J. theor. Biol.*, 65, 727-734
- MacDonald, N. (1977b), "Time Lag in a Model of a Biochemical Reaction Sequence with End Product Inhibition," *J. theor. Biol.*, 67, 549-556
- MacKay, M. C. and L. Glass (1977), "Oscillation and Chaos in Physiological Control Systems" *Science*, 197, 287-289
- Mahler, H. R. and E. M. Cordes (1971), "Biological Chemistry," 2nd edition, Harper and Row Publishers Incorporated, New York
- Marsden, J. E. and M. McCracken (1976), "The Hopf Bifurcation Theory and its Applications," Springer-Verlag, New York
- Masters, C. J. (1977), "Metabolic Control and the Microenvironment," *Curr. Top. Cell. Reg.*, 12, 75-105
- May, R. M. (1974), "Biological Populations with Nonoverlapping Generations: Stable Points Stable Cycles and Chaos," *Science*, 186, 645-647
- May, R. M. (1976), "Simple Mathemtical Models with Very Complicated Dynamics," *Nature*, 261, 459-467
- Mees, A. (1972), "The Describing Function Matrix," *J. Inst. Maths. Applies.*, 10, 49-67

- Mees, A. I. and P. E. Rapp (1978), "Periodic Metabolic Systems: Oscillations in Multiple-Loop Negative Feedback Biochemical Control Networks," *J. Math. Biol.*, 5, 99-114
- Meiske, W. (1978), "An Approximate Solution of the Michaelis-Menten Mechanism for Quasi-Steady State and Quasi-Equilibrium," *Math. Biosci.*, 42, 63-71
- Michaelis, L. and M. Menten (1913), "Die Kinetik der Invertinwirkung," *Biochim. Z.*, 49, 333-369
- Miller, W. G. and R. A. Alberti (1958), "Kinetics of the Reversible Michaelis-Menten Mechanism and the Applicability of the Steady-State Approximation," *J. Am. Chem. Soc.*, 80, 5146-5151
- Monod, J., J-P. Changeux and F. Jacob (1963), "Allosteric Proteins and Cellular Control Systems," *J. Mol. Biol.*, 6, 306-329
- Monod, J., J. Wyman and J-P Changeux (1965), "On the Nature of Allosteric Transitions, A Plausible Model," *J. Mol. Biol.*, 12, 88-118
- Monod, J. (1971), "Chance and Necessity," Vintage Books, New York
- Morales, M. F. and D. E. Goldman (1955), "A Note on the Differential Equation of Simple Enzyme Kinetics," *J. Am. Chem. Soc.*, 77, 6069-6070
- Morales, M. and D. McKay (1967), "Biochemical Oscillations in Controlled Systems," *Biophys. J.*, 7, 621-625
- Nazarenko, V. G. and E. E. Sel'kov (1978), "Self-Oscillations as the Most Probable Mode of Existence of Density-Controlled Cell Populations," *Int. J. Chronobiol.*, 5, 345-367
- Neuhaus, F. C. and W. L. Byme (1958), "O-Phosphoserine Phosphatase," *Biochim. Biophys. Acta*, 28, 223-224
- Newsholme, E. A. and C. Start (1973), "Regulation in Metabolism," John Wiley and Sons, New York
- Norvick, A. and M. Weiner (1957), "Enzyme Induction as an All-or-None Phenomenon," *Proc. Nat. Acad. Sci. (USA)*, 43, 553-566
- Norvick, A. and M. Weiner (1959), in *Proc. Symp. Molec. Biology*, page 78, University of Chicago Press, Chicago
- Nicolis, G. and Prigogine (1977), "Self-Organization in Nonequilibrium Systems: From Dissipative Structures to Order Through Fluctuation," John Wiley and Sons, New York

- O'Mathua, D. (1971), "The Differential Equations of Enzyme Reaction Kinetics - the Regularisation of a Singular Perturbation," Proc. R. Ir. Acad. Sci., 71A, 27-51
- Orsi, B. A. and W. W. Cleland (1972), "Inhibition and Kinetic Mechanisms of Rabbit Muscle Glyceraldehyde-3-Phosphate Dehydrogenase," Biochem., 11, 102-109
- Othmer, H. G. (1976), "The Qualitative Dynamics of a Class of Biochemical Control Circuits," J. Math. Biol., 3, 53-78
- Otten, H. A. and L. N. M. Duysens (1973), "An Extension of the Steady-State Approximation of the Kinetics of Enzyme-Containing Systems," J. theor. Biol., 39, 387-396
- Otten, H. A. (1974), "Some Remarks on the Michaelis-Menten Kinetic Equations," Math. Biosci., 19, 155-161
- Park, D. J. M. (1974), "The Hierarchical Structure of Metabolic Networks and the Construction of Efficient Metabolic Simulators," J. theor. Biol., 46, 31-74
- Passonneau, J. V. and O. H. Lowry (1963), "P-Fructokinase and the Control of the Citric Acid Cycle," Biochem. Biophys. Res. Commun., 13, 372-379
- Poore, A. B. (1975), "Bifurcation of Periodic Orbits in a Chemical Reactor Problem," Math. Biosci., 26, 99-107
- Poore, A. B. (1976), "On the Theory and Application of the Hopf-Fredrichs Bifurcation Theory," Arch. Ration. Mech. Anal., 60, 371-393
- Popov, V. M. (1962), "Absolute Stability of Non-Linear Control Systems of Automatic Control," Autom. Remote Control, 22, 857-875
- Prigogine, I. and I. Stengers (1983), "Order out of Chaos," Bantam Books, New York
- Puric, D. L. and H. J. Fromm (1973), "Additional Factors Influencing Enzyme Responses to the Adenyl Energy Charge," J. Biol. Chem., 248, 461-466
- Rapoport, T. A., R. Heinrich and S. M. Rapoport (1976), "The Regulatory Principles of Glycolysis in Erythrocytes In Vivo and In Vitro," Biochem. J., 154, 449-469
- Rapp, P. E. (1975a), "Biochemical Oscillators - A Search Procedure," Math. Biosci., 23, 289-303

- Rapp, P. E. (1975b), "A Theoretical Investigation of a Large Class of Biochemical Oscillators," *Math. Biosci.*, 25, 165-188
- Rapp, P. E. (1975c), "Analytical Procedures for Large Dimensional Non-Linear Biochemical Oscillators," *BioSyst.*, 7, 92-100
- Rapp, P. E. (1976a), "Analysis of Biochemical Phase Shift Oscillators by a Harmonic Balancing Technique," *J. Math. Biol.*, 3, 203-224
- Rapp, P. E. (1976b), "Mathematical Techniques for the Study of Oscillations in Biochemical Control Loops," *Ins. Math. Appl.*, 12, 11-21
- Rapp, P. E. (1983), "Biological Applications of Control Theory," in L. A. Segel editor, "Mathematical Models in Molecular and Cellular Biology," chapter 3, 146-247, Cambridge University Press, Cambridge
- Rapp, P. E. and A. I. Mees (1977), "Spurious Predictions of Limit Cycles in a Non-Linear Feedback System by the Describing Function Method," *Int. J. Control.*, 26, 821-829
- Reich, J. G. (1984), "Dynamic and Regulatory Characteristics of Cellular Metabolism," presented at the annual meeting of the American Institute of Chemical Engineers, session 43, San Francisco
- Reich, J. G. and E. E. Sel'kov (1974), "Mathematical Analysis of Metabolic Networks," *FEBS Lett.*, 40, S119-S127
- Reich, J. G. and E. E. Sel'kov (1981), "Energy Metabolism of the Cell," Academic Press, New York
- Roberts, R. B., P. H. Abelson, D. V. Crowie, E. T. Bolton, and R. J. Britten (1955), "Studies on Biosynthesis in Echerichia Coli," Carnegie Institute, Washington D. C., Publ. No 607
- Rosen, R. (1970), "Dynamical Systems Theory in Biology," vol 1, Wiley, New York
- Roughton, F. J. W., E. C. DeLand, J. C. Kernohan and J. W. Severinghaus (1972), in M. Rorth and P. Astrup editors, "Oxygen Affinity of Hemoglobin and Red Cell Acid Base States," pages 73-83, Academic Press, New York
- Rubinow, S. I. (1975), "Introduction to Mathematical Biology," chapter 2, John Wiley and Sons, New York
- Rubinow, S. I. and L. A. Segel (1981), "Positive and Negative Cooperativity," in L. A. Segel editor, "Mathematical Models in

- Molecular and Cellular Biology," section 1.4, pages 39-54,  
Cambridge University Press, Cambridge
- Savageau, M. A. (1969), "Biocemical System Analysis. II. The Steady State Solution for an n-pool System Using a Power Law Approximation," *J. theor. Biol.*, 25, 370-379
- Savageau, M. A. (1971), "Concepts Relating the Behavior of Biochemical Systems to their Underlying Molecular Properties," *Arch. Biochem. Biophys.*, 145, 612-621
- Savageau, M. A. (1974), "Optimal Design of Feedback Control by Inhibition: Steady State Considerations," *J. Mol. Evol.*, 4, 139-156
- Savageau, M. A. (1975), "Optimal Design of Feedback Control by Inhibition: Dynamic Considerations," *J. Mol. Evol.*, 5, 199-222
- Savageau, M. A. (1977), "Biochemical Systems Analysis: A Study of Function and Design in Molecular Biology," Addison-Wesley, Reading, Mass
- Schauer, M. and R. Heinrich (1979), "Analysis of the Quasi-Steady State Approximation for an Enzymatic One-Substrate Reaction," *J. theor. Biol.*, 79, 425-442
- Segal, H. L. (1959), "The Development of Enzyme Kinetics," in P. D. Boyer, H. Lardy and K. Myrback editors, "The Enzymes" 2nd edition, chapter 1, 1, 1-48, Academic Press, New York
- Segel, L. A. (1975), "Enzyme Kinetics," Wiley, New York
- Siperstein, M. D. and V. M. Fagan (1964), "Studies on the Feedback Regulation of Cholesterol Synthesis," *Adv. Enzyme Regul.*, 2, 249-264
- Sols, A. (1981), "Multimodulation of Enzyme Activity," *Curr. Top. Cell. Reg.*, 19, 77-101
- Spiegel, M. R. (1978), "Mathematical Handbook of Formulas and Tables," Schaum's outline series, McGraw-Hill, New York
- Srere, P. A. (1967), "Enzyme Concentrations in Tissues," *Science*, 158, 936-937
- Srere, P. A. (1970), "Enzyme Concentrations in Tissues II. An Additional List," *Biochem. Medicine*, 4, 43-46
- Stadtman, E. R. (1966), "Allosteric Regulation of Enzyme Activity," *Adv. Enzymol.*, 28, 41-154

- Stadtman, E. R. (1970), "Mechanisms of Enzyme Regulation in Metabolism;" in P. D. Boyer editor, "The Enzymes," 3rd edition, chapter 8, 1, 297-359, Academic Press, New York
- Stayton, M. M. and H. J. Fromm (1979), "A Computer Analysis of the Validity of the Integrated Michaelis-Menten Equation," *J. theor. Biol.*, 78, 309-323
- Stucki, J. W. (1978), "Stability Analysis of Biochemical Systems - A Practical Guide," *Prog. Biophys. Molec. Biol.*, 33, 99-187
- Swoboda, P. A. T. (1955), *Disc. Faraday. Soc.*, 20, 275-277
- Swoboda, P. A. T. (1957a), "The Kinetics of Enzyme Action," *Biochim. Biophys. Acta*, 23, 70-80
- Swoboda, P. A. T. (1957b), "The Kinetics of Enzyme Action. II. The Terminal Phase of the Reaction," *Biochim. Biophys. Acta*, 25, 132-135
- Tatibana, M. and K. Ito (1967), "Carbamylphosphate Synthetase of the Hematopoietic Mouse Spleen and the Control of Pyrimidine Biosynthesis," *Biochem. Biophys. Res. Commun.*, 26, 221-227
- Tikhonov, A. N. (1948), "On the Dependence of the Solutions of Differential Equations on a Small Parameter," *Mat. Sb.*, 22, 193-204
- Tikhonov, A. N. (1952), "Systems of Differential Equations with Small Parameters at the Derivatives," *Mat. Sb.*, 31, 575-586
- Tornheim, K. (1980), "Co-Ordinate Control of Phosphofructokinase and Pyruvate Kinase by Fructose Diphosphate, A Mechanism for Amplification and Step Changes in Regulation of Glycolysis in Liver," *J. theor. Biol.*, 85, 199-222
- Tsutsumi, E. and F. Takenaka (1969), "Inhibition of Pyruvate Kinase by Free Fatty Acids in the Rat Heart Muscle," *Biochim. Biophys. Acta*, 171, 355-357
- Tubbs, P. K. (1963), "Inhibition of Citrate Formation of Long Chain Thioesters of Coenzyme A as a Possible Control Mechanism in Fatty Acid Biosynthesis," *Biochim. Biophys. Acta*, 70, 608-609
- Tyson, J. J. (1974), "On the Existence of Periodic Solutions in Negative Feedback Cellular Processes," *J. Math. Biol.*, 1, 311-315
- Tyson, J. J. (1983), "Periodic Enzyme Synthesis and Oscillatory Repression: Why is the Period of Oscillation Close to the Cell Cycle Time?" *J. theor. Biol.*, 103, 313-328

- Tyson, J. J. and H. G. Othmer (1978), "The Dynamics of Feedback Control Circuits in Biochemical Pathways," *Prog. Theor. Biol.*, 5, 1-62
- Umbarger, H. E. (1956), "Evidence for a Negative-Feedback Mechanism in the Biosynthesis of Isoleucine," *Science*, 123, 848
- U. van der Heiden (1976), "Stability Properties of Neural and Cellular Control Systems," *Math. Biosci.*, 31, 275-283
- Vergonnet, G. and H. J. C. Berendsen (1970), "Evaluation of the Steady-State Approximation in a System of Coupled Rate Equations," *J. theor. Biol.*, 28, 155-173
- Viniegra-Gonzalez, G. and H. Martiniez (1968), "Stability of Biochemical Feedback Systems," *Proc. Biophys. Soc. Abstracts*, 13, A210
- Viniegra-Gonzales, G. (1973), "Stability Properties of Metabolic Pathways with Feedback Interactions," in B. Chance, E. K. Pye, A. K. Ghosh and B. Hess (1973) editors, "Biological and Biochemical Oscillators," pages 41-59, Academic Press, New York
- Volkenshtein, M. V. (1969), "Enzyme Physics," Plenum, New York
- Volkenstein, M. V. and N. B. Goldsein (1966), "Allosteric Enzyme Models and their Analysis by the Theory of Graphs," *Biochim. Biophys. Acta*, 115, 478-485
- Volpe, J. J., and P. R. Vagelos (1976), "Mechanisms and Regulation of Biosynthesis of Saturated Fatty Acids," *Physiol. Rev.*, 56, 339-417
- Walter, C. F. (1969a), "Stability of Controlled Biological Systems," *J. theor. Biol.*, 23, 23-38
- Walter, C. F. (1969b), "The Absolute Stability of Certain Types of Controlled Biological Systems," *J. theor. Biol.*, 23, 39-52
- Walter, C. F. (1969c), "Oscillations in Controlled Biochemical Systems," *Biophys. J.*, 9, 863-872
- Walter, C. F. (1970), "The Occurrence and the Significance of Limit Cycle Behavior in Controlled Biochemical Systems," *J. theor. Biol.*, 27, 259-272
- Walter, C. F. (1971), "The Stability of Multi-Enzyme Systems with Feedback," *Proc. First Europ. Biophys. Congress Y111/7*, Broda et al. editors., pages 459-464
- Walter, C. F. (1972), "Kinetic and Thermodynamic Aspects of

Biological and Biochemical Control Mechanisms," in "Biochemical Regulatory Mechanisms in Eukaryotic Cells," E. Kun and S. Grisolia editors, pages 355-489, John Wiley and Sons

Walter, C. F. (1974a), "Some Dynamic Properties of Linear, Hyperbolic and Sigmoidal Multi-Enzyme Systems with Feedback Control," *J. theor. Biol.*, 44, 219-240

Walter, C. F. (1974), "The Validity of Using a Quasi-Steady State Approximation for the Reversible Michaelis-Menten Mechanism of Enzyme Action," *J. theor Biol.*, 44, 1-5

Walter, C. F. and M. F. Morales (1964), "An Analogue Computer Investigation of Certain Issues in Enzyme Kinetics," *J. Biol. Chem.*, 239, 1277-1283

Watson, J. D. (1976), "Molecular Biology of the Gene," W. A. Benjamin, Inc, Menlo Park, California

Weber, G., M. A. Lea and N. B. Stamm (1968), "Sequential Feedback Inhibition and Regulation of Liver Carbohydrate Metabolism Through Control of Enzyme Activity," *Adv. Enzyme Regul.*, 6, 101-123

Wei, J. and C. D. Prater (1962), "The Structure and Analysis of Complex Reaction Systems," *Adv. in Catalysis*, 13, 203-392

Weisz, P. B. (1973), "Diffusion and Chemical Transformation," *Science*, 179, 433-440

Whitehead, E. (1970), "The Regulation of Enzyme Activity and Allosteric Transition," *Prog. Biophys. Mol. Biol.*, 21, 321-397

Wieland, O. and L. Weiss (1963), "Inhibition of Citrate-Synthetase by Palmitoyl Coenzyme A," *Biochem. Biophys. Res. Commun.*, 13, 26-31

Wong, J. T-F. (1965), "On the Steady State Method of Enzyme Kinetics," *J. Am. Chem. Soc.*, 87, 1788-1793

Wright, B. E. and P. J. Kelly (1981), "Kinetic Models of Metabolism in Intact Cells, Tissues, and Organisms," *Curr. top. Cell. Reg.*, 19, 103-158

Wyngaarden, J. B. and D. M. Ashton (1959), "The Regulation of Activity of Phosphoribosylpyrophosphate Amidotransferase by Purine Ribonucleotides: A Potential Feedback Control of Purine Biosynthesis," *J. Biol. Chem.*, 234, 1492-1496

Yagil, G. and E. Yagil (1971), "On the Relation Between Effector Concentration and the Rate of Induced Enzyme Synthesis,"

Biophys. J., 11, 11-27

Yang, C-C. (1953), "Solution of Enzyme Kinetics by the Reversion Method," Arch. Biochem. Biophys., 51, 419-427

Yates, R. A. and A. B. Pardee (1956), "Control of Pyrimidine Biosynthesis in Escherichia Coli by a Feedback Mechanism," J. Biol. Chem., 21, 321-397

## APPENDIX A

## DIFFUSIONAL EFFECTS

Here we seek conditions under which diffusional response to changes in boundary conditions is fast compared to all other time scales of interest and where the position dependence of species concentration is negligible, thus seeking to justify the assumption that diffusional effects are insignificant. We begin by noting that a large amount of accumulated experience suggests that diffusional transients will die out with a time constant,  $\tau_{\text{diff}} = l^2/D$ . Here  $D$  is the effective binary diffusion coefficient, which for most solutes falls in the range  $10^{-6} - 10^{-5} \text{ cm}^2/\text{sec}$ , and  $l$  is the diffusion distance to the least accessible point in the system. This is readily demonstrated for zero and first order kinetics from exact solutions for a variety of simple shapes (Carslaw and Jaeger, 1959). Its use under more general circumstances cannot be justified rigorously, but as discussed in Aris (1975) it appears reasonable. We next note that the importance of spatial concentration gradients can often be assessed in terms of a single parameter  $\phi$  (Weisz, 1973, Aris, 1975) which is a ratio of two time constants,  $\phi = \tau_{\text{diff}}/\tau_{\text{rxn}}$ .

Briefly it has been found that diffusional resistance is unimportant if  $\phi$  is less than about unity.

For the reaction time constant,  $\tau_{rxn}$ , we can use the time constant for the faster time scale,  $\tau_2$ . If we assume  $\tau_2$  to be given as  $\tau_2 = Q\bar{e}\epsilon^2$  (equations 37 and 39 of chapter 2, provided that  $Q\bar{e}\epsilon^2$  is small compared with unity) we estimate the reaction time constant to be

$$\tau_2 = \frac{\tau_2}{k_1 e_t} = \frac{(e_t/K_m)(\bar{e}/e_t)}{k_1 e_t} = \left(\frac{1}{k_2 + k_{-1}}\right)\left(\frac{\bar{e}}{e_t}\right) < \frac{1}{k_2 + k_{-1}} \quad (A1)$$

in dimensioned form. Typically  $k_2 \ll k_{-1}$  (or St small) and reasonable values of  $k_{-1}$  for cytosolic enzymes are  $\leq 10^3 \text{ sec}^{-1}$  (Hammes and Schimmel, 1970, and Mahler and Cordes, 1971). Now we can estimate the diffusional paths required to make  $\phi$  greater than unity as

$$l > \sqrt{D/(k_2 + k_{-1})} \approx 1 \mu\text{m} \quad (A2)$$

by using the above assumptions. For mitochondrial enzymes  $k_{-1}$  can be as high as  $10^{-5} \text{ sec}^{-1}$  and then  $l$  must be less than about .1  $\mu\text{m}$ . These conservative estimates of diffusional paths correspond very well to expected intra-cellular dimensions and diffusional resistance is not expected to have major effects on metabolic dynamics.

## APPENDIX B

## ON THE DYNAMICS OF TWO DIMENSIONAL LINEAR SYSTEMS

Approximate eigenvalues. The eigenvalues of a two dimensional linear system,  $dx/dt = Ax = MAM^{-1}x$  are given by

$$\lambda_1, \lambda_2 = \frac{1}{2}(\text{tr}(A) \pm \sqrt{\text{tr}(A)^2 - 4\det(A)}) \quad (\text{B1})$$

$$= \frac{1}{2}\text{tr}(A)(1 \pm \sqrt{1-\delta}) \quad (\text{B2})$$

where  $\delta = 4\det(A)/\text{tr}(A)^2$ . When the parameter  $\delta$  becomes small approximate expressions for the eigenvalues may be obtained using the series

$$\sqrt{1+y} = 1 + \frac{1}{2}y - \frac{1}{2 \cdot 4}y^2 + \dots \quad -1 < y < 1 \quad (\text{B3})$$

Substituting  $-\delta$  for  $y$  we obtain

$$\lambda_1, \lambda_2 = \frac{1}{2}\text{tr}(A)(1 \pm (1-\delta/2-\delta^2/8 - \dots)) \quad (\text{B4})$$

or

$$\lambda_1 = \text{tr}(A), \quad \lambda_2 = \det(A)/\text{tr}(A) \quad (\text{B5})$$

and the time constants become

$$\tau_1 = -1/\lambda_1 = -1/\text{tr}(A), \quad \tau_2 = -1/\lambda_2 = -\text{tr}(A)/\det(A) \quad (\text{B6})$$

Modal analysis. To obtain the modes of the  $2 \times 2$  system we must find the matrix  $M$  which relates the modes  $\underline{m}$  to the variables  $\underline{x}$  by  $\underline{m} = M^{-1}\underline{x}$  where the matrix  $M$  is defined by

$$M^{-1} = \begin{pmatrix} \underline{u}_1 \\ \underline{u}_2 \end{pmatrix} = \begin{pmatrix} u_{11} & u_{12} \\ u_{21} & u_{22} \end{pmatrix} \quad (B7)$$

where  $\underline{u}_1$  and  $\underline{u}_2$  are the eigenrows of the system. The eigenrows are found by solving  $\underline{u}_i(A - \lambda_i I) = \underline{0}$  as

$$\begin{aligned} (a_{11} - \lambda_1)u_{11} + a_{21}u_{12} &= 0 \\ (a_{11} - \lambda_2)u_{21} + a_{21}u_{22} &= 0 \end{aligned} \quad (B8)$$

or

$$\begin{aligned} \frac{u_{12}}{u_{11}} &= \frac{\lambda_1 - a_{11}}{a_{12}} = c_1 \\ \frac{u_{21}}{u_{22}} &= \frac{a_{12}}{\lambda_2 - a_{11}} = c_2 \end{aligned} \quad (B9)$$

Since the eigenvectors are only specified up to a constant we can choose

$$\begin{aligned} \underline{u}_1 &= (1, c_1) \text{ for } c_1 < 1 \\ &= (c_1^{-1}, 1) \text{ for } c_1 > 1 \\ \underline{u}_2 &= (c_2, 1) \text{ for } c_2 < 1 \\ &= (1, c_2^{-1}) \text{ for } c_2 > 1 \end{aligned} \quad (B10)$$

So that the variables contributing more to a mode has a weighting of unity. If either  $c_1$  or  $c_2$  vanish we have a one-way decoupled system, that is  $m_1 \rightarrow x_1$  or  $m_2 \rightarrow x_2$  for  $c_1 \rightarrow 0$  and  $c_2 \rightarrow 0$ , respectively.

However if both  $c_1, c_2 \rightarrow 0$  then  $M^{-1} \rightarrow I$  then we have a completely decoupled system, since  $\underline{m} \rightarrow \underline{x}$ . Hence the  $c_i$ 's can be interpreted as measures of interactions.

## APPENDIX C

## NUMERICAL EVALUATION OF THE FREQUENCY RESPONSE

The input pulse. When selecting the input pulse one has to make sure that the chosen pulse will have sufficient frequency content over the frequency range of interest. We have chose for this purpose two different types of input pulses.

- 1) The  $n^{\text{th}}$  order ramp pulse. This pulse has the mathematical form

$$\begin{aligned}\psi(t) &= h(t/t_1)^n, \quad 0 \leq t \leq t_1 \\ &= 0 \quad \text{otherwise}\end{aligned}\tag{C1}$$

and it derives its name from the shape of the pulse when  $n = 1$ . Here  $h$  is the height of the pulse,  $t_1$  is the duration of the pulse and  $n$  is the order of the pulse.

The Fourier integral transform of the input is generated by computing the integral

$$\int_0^{t_1} \psi(t) e^{-i\omega t} dt = t_1 h \left( \int_0^1 \tau^n \cos(a\tau) d\tau - i \int_0^1 \tau^n \sin(a\tau) d\tau \right) \tag{C2}$$

with  $\tau = t/t_1$  and  $a = t_1\omega$ , over all the frequencies of interest. The integrals may be rewritten as

$$\int_0^{t_1} \psi(t) e^{-i\omega t} dt = t_1 h(c_1^n|_0^1 - s_0^n|_0^1) \\ = t_1 h((c_1^n - c_0^n) - i(s_1^n - s_0^n)) \quad (C3)$$

where  $c_\tau^n$  and  $s_\tau^n$  are the sequences

$$c_\tau^n = \left(\frac{\tau}{a}\right) \sin(a\tau) + \left(\frac{n\tau}{a^2}\right) \cos(a\tau) - \frac{n(n-1)}{a^2} c_\tau^{n-2} \quad (C4)$$

$$s_\tau^n = \left(\frac{-\tau}{a}\right) \cos(a\tau) + \left(\frac{n\tau}{a^2}\right) \sin(a\tau) - \frac{n(n-1)}{a^2} s_\tau^{n-2}$$

To compute these sequences one needs the startup values

$$c_\tau^0 = \sin(a\tau)/a, \quad s_\tau^0 = -\cos(a\tau)/a \quad (C5)$$

for even values of n

$$c_\tau^1 = \cos(a\tau)/a^2 - \tau \sin(a\tau) \\ s_\tau^1 = \sin(a\tau)/a^2 - \tau \cos(a\tau) \quad (C6)$$

for odd values of n. The frequency content of this pulse is shown in figure C-1, where the amplitude has been normalized to its value at zero frequency

$$\int_0^{t_1} \psi(t) dt = \frac{ht_1}{n+1} \quad (C7)$$

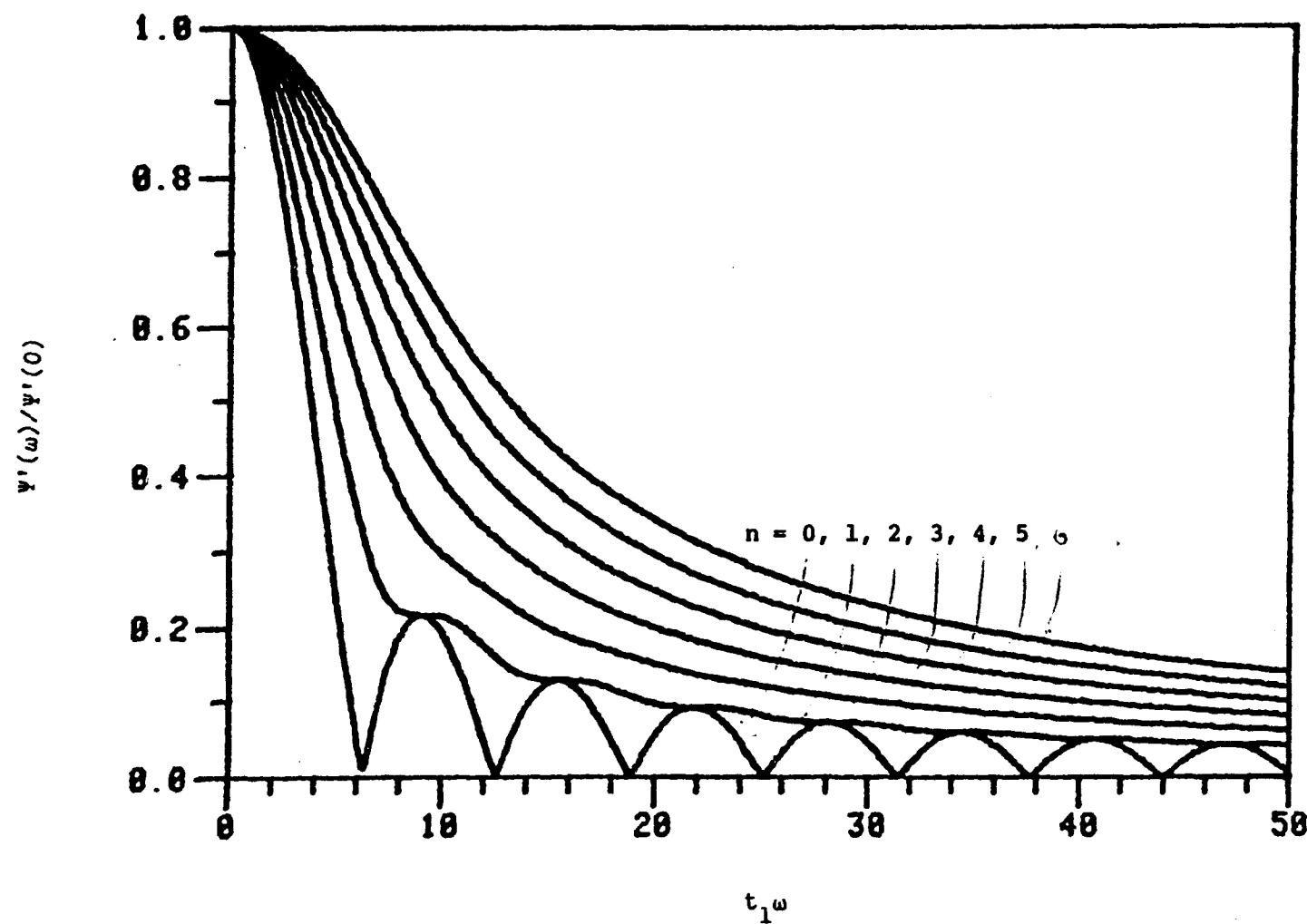
2) The n-th order triangular pulse. This pulse is described by

$$\psi(t) = h(t/t_1)^n, \quad 0 \leq t \leq t_1 \\ = h(2-t/t_1)^n, \quad t_1 \leq t \leq 2t_1 \\ = 0, \quad \text{otherwise} \quad (C8)$$

The Fourier integral transforms of this pulse is

$$\int_0^{2t_1} \psi(t) e^{-i\omega t} dt = t_1 h(\int_0^1 \tau^n e^{-iat} d\tau + \int_1^2 (2-\tau)^n e^{-iat} d\tau) \quad (C9)$$

Figure C-1. Frequency content of the n-th order ramp pulse.



where the first integral is identical to the one for the ramp pulse.

After some algebraic manipulation equation C9 can be rewritten as

$$\int_0^{t_1} \psi(t) e^{-i\omega t} dt = t_1 h((\cos(2a)-1)(C_1^n - C_0^n) + \sin(2a)(S_1^n - S_0^n) + i((\cos(2a)-1)(S_1^n - S_0^n) - \sin(2a)(C_1^n - C_0^n))) \quad (C10)$$

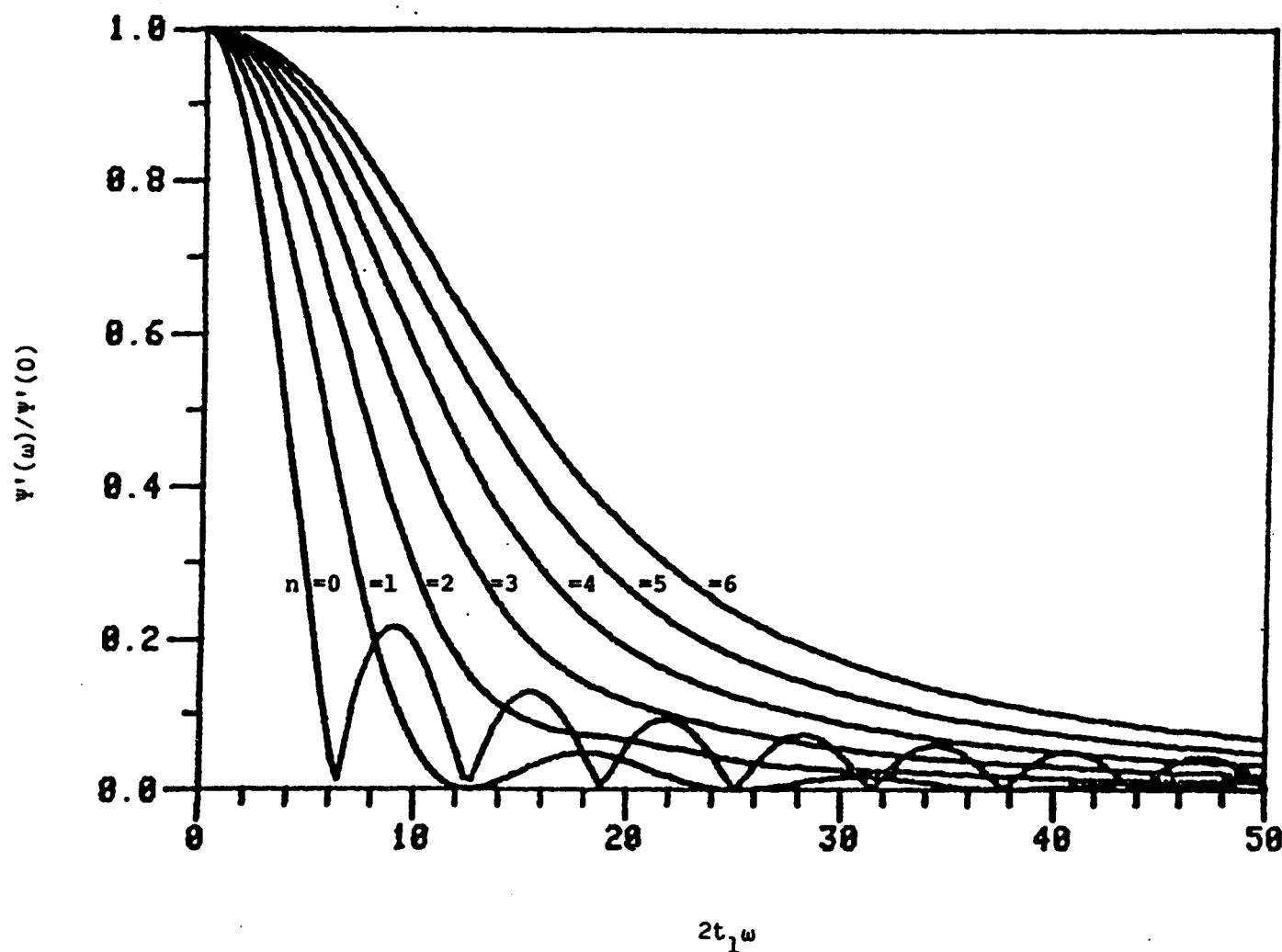
with  $C_\tau^n$  and  $S_\tau^n$  defined by equations C8 and C6. The frequency content is shown in figure C-2 and again it has been normalized to the amplitude at zero frequency as

$$\int_0^{t_1} \psi(t) dt = \frac{ht_1}{n+1} \quad (C11)$$

For  $n = 0$  the pulses are equivalent both being square. Once the desired frequency range has been determined one selects the pulse duration and order from figures C-1 and C-2 to ensure that all frequencies in that range will be excited.

The output. The Fourier integral transform for the output must be evaluated numerically. These computations are readily carried out using available computer software. The concentration profile may be generated by a differential equation integrating package for stiff equations and for integration of the numerator of equation 48 in chapter 5 we have successfully used Filon's extension (Filon, 1928, see also Clements and Schelle, 1963) of the Simpson's quadrature to trigonometric functions.

Figure C-2. Frequency content of the n-th order triangular pulse.



## APPENDIX D

## EVALUATION OF PARAMETERS FOR LOW ORDER TRANSFER FUNCTIONS

In this appendix we shall show how the parameters of low order transfer functions relate to their moments. Then if one desired to use these low order transfer functions for dynamic representation of more complex transfer functions then all one has to do is to substitute the moments of the high order transfer functions into the expressions developed below, and summarized in table 5-2, to obtain the parameters of the reduced description.

First order system. The first order transfer function is given by

$$g(s) = \frac{1}{\tau s + 1}, \quad \text{and } p(s) = \tau s + 1 \quad (\text{D1})$$

with  $p_0 = 1$  and  $p'_0 = \tau$ . Hence from the moment equations (only equation 42 in chapter 5 in this case) we get that  $\tau = M_1$ .

Second order system. The general form for a second order transfer function is

$$g(s) = \frac{1}{\tau^2 s^2 + 2\zeta\tau s + 1} = \frac{1}{(\tau_1 s + 1)(\tau_2 s + 2)} \quad (\text{D2})$$

and to evaluate the two moments of this transfer function we need the

derivatives of the pole polynomial,  $p(s) = \tau^2 s^2 + 2\zeta\tau s + 1$ , evaluated at  $s = 0$  which are

$$p_0 = 1, \quad p'_0 = 2\zeta\tau, \quad p''_0 = 2\tau^2 \quad (D3)$$

The moment equations, equations 42 and 43 in chapter 5, take the form

$$M_1 = 2\tau\zeta, \quad T_2 = (M_1)^2 - 2\tau^2 \quad (D4)$$

and they can be solved explicitly for the parameters of the second order system as

$$\tau^2 = (M_1^2 - T_2)/2, \quad \zeta = M_1/2\tau, \quad \tau_1, \tau_2 = \tau(\zeta \pm \sqrt{\zeta^2 - 1}) \quad (D5)$$

Third order system. A third order system will always have a real root and we write the transfer function in a general form as

$$g(s) = \frac{1}{(\tau_a s + 1)((\tau_b s)^2 + 2\zeta\tau_b s + 1)} = \frac{1}{(\tau_1 s + 1)(\tau_2 s + 1)(\tau_3 s + 1)} \quad (D6)$$

To evaluate three moments we need three derivatives evaluated at  $s = 0$

$$p'_0 = \tau_a + 2\zeta\tau_b \quad (D7)$$

$$p''_0 = 4\zeta\tau_a\tau_b + 2(\tau_b)^2 \quad (D8)$$

$$p'''_0 = 6\tau_a(\tau_b)^2 \quad (D9)$$

Substituting into the moment equations, equations 42-44 of chapter 5 we obtain equations that cannot be solved explicitly for the parameters. The first time constant  $\tau_a$  is computed as the root of the cubic equation

$$\tau_a^3 - M_1\tau_a^2 + (M_1 - T_2)\tau_a/2 - (T_3 - M_3 - 3T_2M_1)/6 = 0 \quad (D10)$$

and then the other two parameters may be evaluated from the relations

$$\tau_b^2 = (T_3 + M_1^3 - 3T_2 M_1) / 6\tau_a \quad (D11)$$

$$\xi = (M_1 - \tau_a) / 2\tau_b \quad (D12)$$

or

$$\tau_1 = \tau_a, \quad \tau_2, \tau_3 = \tau_b (\xi \pm \sqrt{\xi^2 - 1}) \quad (D13)$$

## APPENDIX E

## PROGRAM LISTINGS

This appendix contains a listing of programs used to compute figures in chapters 2, 5 and 8. The routines are well documented and need no further explanation.

The first program computes the transient response of the Michealis-Menten reaction mechanism and it is fairly typical for the programs used to generate the transient response curves presented in this thesis.

Secondly I include two programs that are used to generate the frequency response curves in chapter 5, both for the high order linearized model and the low order approximate models.

Thirdly I list a set of programs that are used to generate the local stability results in chapter 8. I would like mention that these programs are not written for computational efficiency but rather with robustness in mind. For example I use the regula falsi method to locate roots even though it is less efficient than more sophisticated algorithms. This is done since convergence for regula falsi is guaranteed, if the root has been bracketed. It is the

author's opinion that one should not, in this day and age of cheap computational power, in general spend a lot of time completing sophisticated numerical schemes when the computations can be obtained quicker, in real time, with simpler but robust numerical procedures even though it costs use more CPU time.

Program to Simulate the Transient Response of  
Michaelis-Menten Reaction Mechanism.

```

C-----0-----0-----0-----0-----0-----0-----0-----
C A program that computes the dynamic response of the Michaelis-Menten
C reaction mechanism:
C
C     I           (k1)           (k2)           R
C     ----> S + E <=====> X <=====> E + P ----->
C                   (k-1)          (k-2)
C
C The differential equations are:
C
C for the substrate
C
C 
$$\frac{d(\sigma)}{d(\tau)} = -\sigma + \frac{\chi}{1+S} + \sigma\chi + \frac{\Psi}{1+S} \quad (1)$$

C
C and for the intermediate complex
C
C 
$$\frac{d(\chi)}{d(\tau)} = \frac{S\cdot Q_s}{K_{eq}\cdot M_r} + \left(1 - \frac{S}{K_{eq}}\right)\sigma - \left(1 + \frac{S\cdot Q_s}{K_{eq}\cdot M_r}\right)(\chi + 1) \quad (2)$$

C
C The scaled variables are:
C     the substrate            $\sigma = s/K_m$ 
C     the intermediate          $\chi = x/(et)$ 
C     the input flux            $\Psi = I/(k_2)(et)$ 
C
C The physical parameters are:
C     the total enzyme concentration    $(et)$ 
C     the total substrate           "       $(st)$ 
C     the Michaelis constant         $K_m = ((k-1)+(k2))/(k1)$ 
C     the input flux                 $I$ 
C     the removal flux               $R$ 
C
C The dimensionless parameters are:
C     the Quasi-steady state number  $Q_s = (et)/K_m$ 
C     the Mass ratio                $M_r = (et)/(st)$ 
C     the Sticyness number         $S_t = (k2)/(k-1)$ 
C     the Equilibrium constant     $K_{eq} = (k1)(k2)/(k-1)(k-2)$ 
C     the scaled time              $\tau = (k1)(et)t$ 

```

```

C-----0-----0-----0-----0-----0-----0-----0-----
C the following solutions are stored in the vector Y(I)
C
C      the exact solution
C          Y(1) - the substrate
C          Y(2) - the intermediate
C
C      the linear solution
C          Y(3) - the substrate
C          Y(4) - the intermediate
C
C      the quasi-steady state solution
C          Y(5) - the substrate
C
C      the quasi-equilibrium solution
C          Y(6) - the substrate
C
C      the zeroth order inner solution
C          Y(7) - the intermediate
C-----0-----0-----0-----0-----0-----0-----0-----

IMPLICIT DOUBLE PRECISION(A-H,O-Z)
COMMON/BLK1/ST,STR,KEQ,QS,PSI,MR,TON,TOFF,DELPSI
COMMON/BLK2/A1,A2,A3,A4,C1,C2
COMMON/BLK3/SIGMA,IOPEN
DOUBLE PRECISION KEQ,MR
DIMENSION Y(7)

98  WRITE(5,99)
99  FORMAT(' Open system ? [Y/N] ',$,)
READ(5,206) IOPEN
IF(IOPEN.EQ.'Y') GO TO 100
GO TO 11
C-----0-----0-----0-----0-----0-----0-----0-----

100  WRITE(5,101)
101  FORMAT(' Enter St, Keq, Qs, Sigma, Psi ',$,)
READ(5,*) ST,KEQ,QS,SIGMA,PSI
CHI=((1.D0+ST)*SIGMA-ST*PSI)/(1.D0+(1.D0+ST)*SIGMA)
PI=KEQ*(SIGMA-PSI*(1.D0+SIGMA))/(1.D0+ST*PSI)
MR=QS/(SIGMA+QS*CHI+PI)
WRITE(5,102) SIGMA,CHI,PI,MR
102  FORMAT(' The steady state concentrations are',//,
1  ' sigma=',1PE15.5,' chi  =',1PE15.5,' ,
2  ' pi   =',1PE15.5,' Mr    =',1PE15.5')
GO TO 200
11   WRITE(5,103)
103  FORMAT(' Enter sigma, chi, St, Keq, Qs, Mr ',$,)
READ(5,*) SIGMA,CHI,ST,KEQ,QS,MR
GO TO 21
C-----0-----0-----0-----0-----0-----0-----0-----

Compute Jacobian
200  EPS=1.D0-CHI
     A1=-EPS

```

```

A2=(1.D0+ST*PSI)/((1.D0+ST)*EPS)
A3=(1.D0-ST/KEQ)*EPS/QS
A4=-(1.D0+ST*QS*EPS**2/KEQ)/(QS*EPS)
GO TO 22
21 A1=-1.D0+CHI
A2=1.D0/(1.D0+ST)+SIGMA
A3=(1.D0-ST/KEQ)*(1.D0-CHI)/QS
A4=2.D0*ST*QS*CHI/KEQ-(1.D0+ST*QS*(1.D0+1.D0/MR)/KEQ+
1 (1.D0-ST/KEQ)*SIGMA)
A4=A4/QS
Compute the time constants
22 TR=A1+A4
DET=A1*A4-A2*A3
T1=(TR+DSQRT(TR**2-4.D0*DET))/2.D0
T2=(TR-DSQRT(TR**2-4.D0*DET))/2.D0
T1=-1.D0/T1
T2=-1.D0/T2
TRATIO=T1/T2
Compute constants of linearization
C1=-SIGMA+CHI/(1.D0+ST)+SIGMA*CHI+ST*PSI/(1.D0+ST)
C1=C1-A1*SIGMA-A2*CHI
DET=1.D0/MR+(KEQ/ST-1)*SIGMA/QS
TR=(1.D0+KEQ/(ST*QS)+DET)
C2=(ST/KEQ)*(CHI**2-TR*CHI+DET)-A3*SIGMA-A4*CHI
Compute modal matrix
ALPHA=(-1.D0/T1-A1)/A3
BETA=A3/(-1.D0/T2-A1)
V1=1.D0
V2=ALPHA
DIV=DMAX1(V1,V2)
V1=V1/DIV
V2=V2/DIV
V3=BETA
V4=1.D0
DIV=DMAX1(V3,V4)
V3=V3/DIV
V4=V4/DIV
WRITE(5,201) A1,A2,A3,A4
201 FORMAT(' The Jacobian is',/,2(1PE15.5),/,2(1PE15.5)/)
WRITE(5,202) T1,T2
202 FORMAT(' The time constants are',/,2(1PE15.5),/)
WRITE(5,203) TRATIO
203 FORMAT(' The ratio between the time constants is ',/,1PE15.5/)
WRITE(5,204) V1,V2,V3,V4
204 FORMAT(' The modal matrix is',/,2(1PE15.5),/,2(1PE15.5)/)
WRITE(5,205)
205 FORMAT(' Another set of parameters ? [Y/N]      ',,$)
READ(5,206) ISET
FORMAT(A1)
IF(ISET.EQ.'Y') GO TO 98
206

```

```

C-----0-----0-----0-----0-----0-----0-----0-----
C specify time scaling factor
      TSCALE = 1.0D0
      WRITE (5,301)
301   FORMAT(' Do you want to scale time ? [Y/N]           ', '$')
      READ (5,206) ISCALE
      IF (ISCALE.NE.'Y') GO TO 31
      WRITE (5,302)
302   FORMAT(' Scale to Tau1 = 1, Tau2 = 2, other = 3           ', '$')
      READ(5,*) ISCALE
      IF(ISCALE.EQ.1) TSCALE=T1
      IF(ISCALE.EQ.2) TSCALE=T2
      IF(ISCALE.NE.3) GO TO 31
      WRITE (5,303)
303   FORMAT (' Enter scaling factor           ', '$')
      READ (5,*) TSCALE
31    WRITE(5,304)
304   FORMAT(' Enter final time and    of points           ', '$')
      READ(5,*) TFIN,IPTS
      DEL=TFIN/DFLOAT(IPTS-1)
C-----0-----0-----0-----0-----0-----0-----0-----
C set parameters for EPISODE
      WRITE(5,305)
305   FORMAT(' Standard settings for EPISODE ? [Y/N]           ', '$')
      READ(5,206) ISET
      H=T2/(1000.0D0*TSCALE)
      EP=1.D-5
      IMETH=22
      IF(ISET.EQ.'Y') GO TO 32
      WRITE(5,306)
306   FORMAT(' Enter the method to be used by EPISODE           ', '$')
      READ (5,*) IMETH
      WRITE(5,307)
307   FORMAT(' Enter the error tolerance           ', '$')
      READ(5,*) EP
32    IF(IOPEN.NE.'Y') GO TO 42
C-----0-----0-----0-----0-----0-----0-----0-----
C specify the initial conditions
400   WRITE(5,401)
401   FORMAT(' Are the stst conditions your IC ? [Y/N]           ', '$')
      READ(5,206) IC
      IF(IC.NE.'Y') GO TO 41
      WRITE(5,403)
403   FORMAT(' Enter Ton, Toff, Delta-Psi           ', '$')
      READ(5,*) TON,TOFF,DELPSI
      TON=TON*TSCALE
      TOFF=TOFF*TSCALE
      DELPSI=ST*DELPSI/(1.0D0+ST)
      GO TO 42
41    WRITE(5,402)
402   FORMAT(' Enter the IC for sigma and chi           ', '$')

```

```

        READ(5,*) SIGMA,CHI
42      WRITE(5,404)
404      FORMAT(' Do you want to record data as deviation    ',/
1           ' from the initial conditions ? [Y/N]          ',,$)
           READ(5,206) IDEV
           IF(IDEV.NE.'Y') GO TO 43
           WRITE(5,405)
405      FORMAT(' record sigma as % deviation from ICs ? [Y/N]    ',,$)
           READ(5,206) IPER

C initial conditions
43      Y(1)=SIGMA
           Y(2)=CHI
           Y(3)=SIGMA
           Y(4)=CHI
           Y(5)=SIGMA
           Y(6)=SIGMA
           Y(7)=CHI
           DET=1.D0/MR+(KEQ/ST-1.D0)*SIGMA/QS
           TR=(1.D0+KEQ/(ST*QS)+DET)
           XQSI=(TR-DSQRT(TR**2-4.D0*DET))/2.D0
           STR=1.D0/(1.D0+ST)
           XQEI=SIGMA/(STR+SIGMA)
           IF(IDEV.EQ.'Y') GO TO 44
           S1=Y(1)
           X1=Y(2)
           S2=Y(3)
           X2=Y(4)
           S3=Y(5)
           X3=XQSI
           S4=Y(6)
           X4=XQEI
           X5=Y(7)
           GO TO 45

C if deviation from the IC's is desired
44      S1=0.D0
           X1=0.D0
           S2=0.D0
           X2=0.D0
           S3=0.D0
           X3=XQSI-CHI
           S4=0.D0
           X4=XQEI-CHI
           X5=0.D0
45      INDEX=1
           DEL=DEL*TSCALE
           TOUT=DEL
           T=0.D0
           NUMODE=6
           IF(IOPEN.NE.'Y') NUMODE=7
           CALL ASSIGN(1,'MMDYN.DAT')
           WRITE(1) SNGL(T),SNGL(S1),SNGL(X1),SNGL(S2),SNGL(X2),

```

```

1 SNGL(S3),SNGL(X3),SNGL(S4),SNGL(X4),SNGL(X5)
C-----0-----0-----0-----0-----0-----0-----0-----
500 DO 1 I1=1,IPTS-1
      CALL DDRIVE(NUMODE,T,H,Y,TOUT,EP,3,IMETH,INDEX)
      TIME = TOUT/TSCALE
      DET=1.D0/MR+(KEQ/ST-1.D0)*Y(5)/QS
      TR=(1.D0+KEQ/(ST*QS)+DET)
      XQS=(TR-DSQRT(TR**2-4.D0*DET))/2.D0
      XQE=Y(6)/(STR+Y(6))
      IF(IDEV.EQ.'Y') GO TO 51
      S1=Y(1)
      X1=Y(2)
      S2=Y(3)
      X2=Y(4)
      S3=Y(5)
      X3=XQS
      S4=Y(6)
      X4=XQE
      X5=Y(7)
      GO TO 52
51   S1=Y(1)-SIGMA
      X1=Y(2)-CHI
      S2=Y(3)-SIGMA
      X2=Y(4)-CHI
      S3=Y(5)-SIGMA
      X3=XQS-CHI
      S4=Y(6)-SIGMA
      X4=XQE-CHI
      X5=Y(6)-CHI
      IF(IPER.NE.'Y') GO TO 52
      S1=S1*100.D0/SIGMA
      S2=S2*100.D0/SIGMA
      S3=S3*100.D0/SIGMA
      S4=S4*100.D0/SIGMA
52   WRITE(1) SNGL(TIME),SNGL(S1),SNGL(X1),SNGL(S2),SNGL(X2),
      1 SNGL(S3),SNGL(X3),SNGL(S4),SNGL(X4),SNGL(X5)
1     TOUT=TOUT+DEL
      STOP
      END

```

```

SUBROUTINE DDIFUN(N,T,Y,YD)
C-----0-----0-----0-----0-----0-----0-----0-----
C subroutine that evaluates the RHS of the differential equations
      IMPLICIT DOUBLE PRECISION(A-H,O-Z)
      COMMON/BLK1/ST,STR,KEQ,QS,PSI,MR,TON,TOFF,DELPsi
      COMMON/BLK2/A1,A2,A3,A4,C1,C2
      COMMON/BLK3/SIGMA,IOPEN
      DOUBLE PRECISION KEQ,MR

```

```

DIMENSION Y(7),YD(7)
C-----0-----0-----0-----0-----0-----0-----0-----0
C exact solution
YD(1)=-Y(1)+Y(2)/(1.D0+ST)+Y(1)*Y(2)+ST*PSI/(1.D0+ST)
DET=1.D0/MR+(KEQ/ST-1.D0)*Y(1)/QS
TR=(1.D0+KEQ/(ST*QS)+DET)
YD(2)=Y(2)**2-TR*Y(2)+DET
YD(2)=YD(2)*ST/KEQ
C-----0-----0-----0-----0-----0-----0-----0-----0
C linear solution
YD(3)=C1+A1*Y(3)+A2*Y(4)
YD(4)=C2+A3*Y(3)+A4*Y(4)
C-----0-----0-----0-----0-----0-----0-----0-----0
C quasi-steady state solution
DET=1.D0/MR+(KEQ/ST-1)*Y(5)/QS
TR=(1.D0+KEQ/(ST*QS)+DET)
XQS=(TR-DSQRT(TR**2-4.D0*DET))/2.D0
YD(5)=-Y(5)+XQS/(1.D0+ST)+XQS*Y(5)+ST*PSI/(1.D0+ST)
C-----0-----0-----0-----0-----0-----0-----0-----0
C quasi-equilibrium solution
XQE=Y(6)/(STR+Y(6))
DPIDT=ST*(XQE-PSI)*STR
FACTOR=QS*STR/(STR+Y(6))**2+1.D0
FACTOR=1.D0/FACTOR
YD(6)=-FACTOR*DPIDT
IF(IOPEN.EQ.'Y') GO TO 10
C-----0-----0-----0-----0-----0-----0-----0-----0
C zeroth order inner solution
DET=1.D0/MR+(KEQ/ST-1.D0)*SIGMA/QS
TR=(1.D0+KEQ/(ST*QS)+DET)
YD(7)=Y(7)**2-TR*Y(7)+DET
YD(7)=YD(7)*ST/KEQ
10 IF(T.LE.TON.OR.T.GE.TOFF) RETURN
C-----0-----0-----0-----0-----0-----0-----0-----0
C disturbance
YD(1)=YD(1)+DELPSI
YD(3)=YD(3)+DELPSI
YD(5)=YD(5)+DELPSI
YD(6)=YD(6)+DELPSI*FACTOR
RETURN
END

```

```

SUBROUTINE DPDERV(N,T,Y,PD,M)
C-----0-----0-----0-----0-----0-----0-----0-----0
C subroutine that evaluates the partial derivatives of the RHS of the
C differential equations (i. e. the Jacobian)
IMPLICIT DOUBLE PRECISION(A-H,O-Z)
COMMON/BLK1/STR,KEQ,QS,PSI,MR,TON,TOFF,DELPSI

```

```

COMMON/BLK3/SIGMA,IOPEN
COMMON/BLK2/A1,A2,A3,A4,C1,C2
DOUBLE PRECISION KEQ,MR
DIMENSION Y(7),PD(7,7)
C-----0-----0-----0-----0-----0-----0-----0-----0-
C initialize PD
    DO 1 I1=1,7
    DO 1 I2=1,7
1     PD(I1,I2)=0.D0
C-----0-----0-----0-----0-----0-----0-----0-----0-
C for exact solution
    PD(1,1)=-1.D0+Y(2)
    PD(1,2)=1.D0/(1.D0+ST)+Y(1)
    PD(2,1)=(1.D0-ST/KEQ)*(1.D0-Y(2))/QS
    PD(2,2)=2.D0*ST*QS*Y(2)/KEQ-(1.D0+ST*QS*(1.D0+1.D0/MR)/KEQ+
1     (1.D0-ST/KEQ)*Y(1))
    PD(2,2)=PD(2,2)/QS
C-----0-----0-----0-----0-----0-----0-----0-----0-
C for linear part
    PD(3,3)=A1
    PD(3,4)=A2
    PD(4,3)=A3
    PD(4,4)=A4
C-----0-----0-----0-----0-----0-----0-----0-----0-
C for qss solution
    DETDS=(KEQ/ST-1.D0)/QS
    DET=1.D0/MR+DETDS*Y(5)
    TR=(1.D0+KEQ/(ST*QS)+DET)
    SQ=DSQRT(TR**2-4.D0*DET)
    XQS=(TR-SQ)/2.D0
    XQSDS=.5D0*(1.D0-(TR-2.D0)/SQ)*DETDS
    PD(5,5)=-1.D0+XQS+(STR-Y(5))*XQSDS
C-----0-----0-----0-----0-----0-----0-----0-----0-
C for qea solution
    BE=QS*STR/(STR+Y(6)**2+1.D0)
    BE=1.D0/BE
    BEDS=2.D0*QS*STR*BE**2/(Y(6)+STR)**3
    GA=Y(6)/(STR+Y(6))
    GADS=STR/(STR+Y(6))**2
    PD(6,6)=-ST*STR*(BE*GADS+BEDS*GA)
    IF(IOPEN.EQ.'Y') RETURN
C-----0-----0-----0-----0-----0-----0-----0-----0-
C for the zeroth order inner solution
    DET=1.D0/MR+(KEQ/ST-1.D0)*SIGMA/QS
    TR=(1.D0+KEQ/(ST*QS)+DET)
    PD(7,7)=2.D0*Y(7)-TR
    PD(7,7)=PD(7,7)*ST/KEQ
    RETURN
    END

```

Programs to Compute the Frequency Response of  
Linearized Chains of Irreversible Michaelis-Menten  
Reactions and Low Order Transfer Functions.

```

C-----0-----0-----0-----0-----0-----0-----0-----
C Generate Fourier integral transform (FIT) for
C a transfer function:
C
C           t=infinity
C                   x(t)exp(-i*omega) dt
C           t=0
C   G(i*omega)= -----
C                   t=Tp
C                   i(t)exp(-i*omega) dt
C           t=0
C
C For the output x(t) the program uses data stored on file DPR0.DAT
C in the form (Time,output) and this data is integrated
C using the following quadratures:
C 1) trapezoidal rule, see Luyben (1973) pg 285-291
C 2) Filon's method, see Clements and Scnelle (1963) IEC
C Proc. Des. Devel. vol 2, 94-102.
C
C For the input i(t) we use two kinds of pulses:
C 1) n-th order ramp (ITYPE=1, with Tp=T1) or
C 2) n-th order triangle (ITYPE=2 with Tp=2*T1).
C The FIT of both types of inputs can be obtained analytically.
C-----0-----0-----0-----0-----0-----0-----0-----

      IMPLICIT DOUBLE PRECISION(A-H,O-Z)
      DOUBLE PRECISION IM,IM1,IM2
      DATA IYES/'Y'
      PI=3.1415926535D0
C-----0-----0-----0-----0-----0-----0-----0-----
Choose parameters for simulation
      WRITE(5,101)
101   FORMAT(
      1 ' Enter W-min, W-max, and    of pts          ',,$)
      READ(5,*) WMIN,WMAX,NPTS
      DELW=(DLOG(WMAX)-DLOG(WMIN))/DFLOAT(NPTS-1)
      WRITE(5,102)
102   FORMAT(
      1 ' Enter the    of 180 degree shifts (=1 for Phi>90) ',,$)
      READ(5,*) X180
      WRITE(5,103)
103   FORMAT(' Enter quadrature method for output',/,
      1 ' 1:trapizoidal, 2:Filon method [1/2]          ',,$)
      READ(5,*) METHOD
C-----0-----0-----0-----0-----0-----0-----0-----
C Read information about the input pulse
      CALL ASSIGN(1,'MOM.DAT')
      READ(1) SIZE,TL,DEL,IPTS,NPUL,ITYPE,GAIN
      CALL CLOSE(1)
      JPTS=(IPTS-1)/2

```

```

C-----0-----0-----0-----0-----0-----0-----0-----0-----0-----
C Set printing specifications
      WRITE(5,104)
104   FORMAT(
      1 ' Write AR and W in linear form=1, with logs taken=2      ',,$)
      READ(5,*) ILOG
      WRITE(5,105)
105   FORMAT(
      1 ' Do you want some printout ? [Y/N]                      ',,$)
      READ(5,106) IPR
106   FORMAT(A1)
      CALL ASSIGN(2,'DPRO.DAT')
      IF(IPR.NE.IYES) GO TO 100
      WRITE(5,107)
107   FORMAT(
      1 ' Term=5, LP=6  [5/6]                                     ',,$)
      READ(5,*) IW1
C-----0-----0-----0-----0-----0-----0-----0-----0-----0-----
Compute FIT for output at zero frequency
      READ(2) R1,X1
      IF(METHOD.EQ.2) GO TO 200
      XZERO=X1/2.D0
      DO 1 I1=2,IPTS
      READ(2) R1,X2
      XZERO=DEL*(X1+X2)/2.D0+XZERO
1      X1=X2
      GO TO 300
200   XZERO=0.D0
      READ(2) T1,X1
      DO 2 I2=1,JPTS
      READ(2) T1,X2
      READ(2,END=300) T1,X3
      XZERO=XZERO+DEL*(X1+4.D0*X2+X3)/3.D0
2      X1=X3
C-----0-----0-----0-----0-----0-----0-----0-----0-----0-----
300   WRITE(IWI,108) SIZE,TL,GAIN,NPUL,ITYPE,IPTS,XZERO
108   FORMAT(//' Parameters for the pulse://,
      1 ' size of pulse           ',IPE12.4./,
      2 ' length of pulse         ',IPE12.4./,
      3 ' gain                   ',IPE12.4./,
      4 ' order of pulse          ',I12./,
      5 ' type of pulse (1=ramp, 2=triangle) ',I12./,
      6 ' number of data points   ',I12./,
      7 ' integral over x a zero frequency ',IPE12.4//)
      WRITE(IWI,201)
201   FORMAT(2X,'Frequency',7X,'AR',9X,'Phi',11X,'Re',9X,'Im',9X,
      1 'ARinp//')

```

```

C-----0-----0-----0-----0-----0-----0-----0-----0
C Loop 3 computes the FIT for input and output
100    W=WMIN
        SAV=1.D0
        XM=0.D0
        CALL ASSIGN(3, 'CHBODE.DAT')
        DO 3 I3=1,NPTS
C-----0-----0-----0-----0-----0-----0-----0-----0
Compute the FIT for the input:
C      n
C      int(X cos(X)dX = CN = (alpha-n)*cos(X)+(beta-n)*sin(X)
C      n
C      int(X sin(x)dX = SN = (alpha-n)*cos(X)-(beta-n)*sin(X)
C
C-----0-----0-----0-----0-----0-----0-----0-----0
A=W*TL
COSA=DCOS(A)
SINA=DSIN(A)
C-----0-----0-----0-----0-----0-----0-----0-----0
C evaluate alpha-n and beta-n at 0 and 1 for the integrals
      IF(NPUL.EQ.0) ALNO=0.D0
      IF(NPUL.EQ.0) BEN0=1.D0
      IF(NPUL.EQ.0) ALN1=0.D0
      IF(NPUL.EQ.0) BEN1=1.D0
C N=1
      IF(NPUL.EQ.1) ALNO=1.D0
      IF(NPUL.EQ.1) BEN0=0.D0
      IF(NPUL.EQ.1) ALN1=1.D0
      IF(NPUL.EQ.1) BEN1=A
C N=2
      IF(NPUL.EQ.2) ALNO=0.D0
      IF(NPUL.EQ.2) BEN0=-2.D0
      IF(NPUL.EQ.2) ALN1=2.D0*A
      IF(NPUL.EQ.2) BEN1=A**2-2.D0
C N=3
      IF(NPUL.EQ.3) ALNO=-6.D0
      IF(NPUL.EQ.3) BEN0=0.D0
      IF(NPUL.EQ.3) ALN1=3.D0*A**2-6.D0
      IF(NPUL.EQ.3) BEN1=A*(A**2-6.D0)
C N=4
      IF(NPUL.EQ.4) ALNO=0.D0
      IF(NPUL.EQ.4) BEN0=24.D0
      IF(NPUL.EQ.4) ALN1=A*(4*A**2-24.D0)
      IF(NPUL.EQ.4) BEN1=A**4-12.D0*A**2+24.D0
C N=5
      IF(NPUL.EQ.5) ALNO=120.D0
      IF(NPUL.EQ.5) BEN0=0.D0
      IF(NPUL.EQ.5) ALN1=5*A**4-60.D0*A**2+120.D0
      IF(NPUL.EQ.5) BEN1=(A**4-20.D0*A**2+120.D0)*A
C N=6

```

```

IF(NPUL.EQ.6) ALNO=0.D0
IF(NPUL.EQ.6) BEN0=-720.D0
IF(NPUL.EQ.6) ALN1=A*(6.D0*A**4-120*A**2+720.D0)
IF(NPUL.EQ.6) BEN1=A**6-30.D0*A**4+360.D0*A**2-720.D0
C-----0-----0-----0-----0-----0-----0-----0-----
C normalize input integrals
  DIVIDE=A**(NPUL+1)
  ALNO=ALNO/DIVIDE
  BEN0=BEN0/DIVIDE
  ALN1=ALN1/DIVIDE
  BEN1=BEN1/DIVIDE
  CN1=ALN1*COSA+BEN1*SINA
  SN1=ALN1*SINA-BEN1*COSA
  CNO=ALNO
  SNO=-BENO
  CD=CN1-CNO
  SD=SN1-SNO
  COS2A=DCOS(2*A)
  SIN2A=DSIN(2*A)
C-----0-----0-----0-----0-----0-----0-----0-----
C if n-th order ramp
  IF(ITYPE.EQ.1) COS2A=0.D0
  IF(ITYPE.EQ.1) SIN2A=0.D0
C-----0-----0-----0-----0-----0-----0-----0-----
Compute the real ang immaginary part of the input
  DENOMR=((COS2A+1.D0)*CD+SIN2A*SD)*TL*SIZE
  DENOMI=((COS2A-1.D0)*SD-SIN2A*CD)*TL*SIZE
  ARINP=DSQRT(DENOMR**2+DENOMI**2)
C-----0-----0-----0-----0-----0-----0-----0-----
Calculate FIT for the output on file DPR0.DAT
  REWIND 2
  IF(METHOD.EQ.2) GO TO 400
C Trapizoidal quadrature
  DELTA=DEL*W**2
  COSW=DCOS(DEL*W)
  SINW=DSIN(DEL*W)
  RE1=(COSW-1.D0)/DELTA
  RE2=RE1+SINW/W
  IM=SINW/DELTA
  IM1=1.D0/W-IM
  IM2=COSW/W-IM
  T=DEL
  READ(2) R1,X1
  RE=X1*RE2
  IM=X1*IM2
  GNUMR=RE*COSW+IM*SINW
  GNUMI=IM*COSW-RE*SINW
  DO 4 I4=2,IPTS
    READ(2) R1,X2
    RE=X2*RE2-X1*RE1

```

```

IM=X2*IM2-X1*IM1
COST=DCOS(W*T)
SINT=DSIN(W*T)
GADDR=RE*COST+IM*SINT
GADDI=IM*COST-RE*SINT
GNUMR=GNUMR+GADDR
GNUMI=GNUMI+GADDI
REL1=DSQRT(GADDR**2+GADDI**2)
REL2=DSQRT(GNUMR**2+GNUMI**2)
IF(REL2.GT.0.) REL=REL1/REL2
IF(REL.LT.1.D-5) GO TO 500
X1=X2
4      T=T+DEL
      GO TO 500
C Filon's method
400    THETA=DEL*W
      SINTH=DSIN(THETA)
      COSTH=DCOS(THETA)
      SIN2TH=DSIN(2.D0*THETA)
      AL=(1.D0+SIN2TH/(2.D0*THETA)-2.D0*(SINH/THETA)**2)/THETA
      BE=(2.D0/THETA**2)*(COSTH**2+1.D0-SIN2TH/THETA)
      GA=(4.D0/THETA**2)*(SINH/THETA-COSTH)
      READ(2) T1,X1
      GNUMR=0.D0
      GNUMI=0.D0
      DO 5 I5=1,JPTS
      READ(2) T2,X2
      READ(2) T3,X3
      Y1=X1*DCOS(T1*W)
      Y2=X2*DCOS(T2*W)
      Y3=X3*DCOS(T3*W)
      Z1=X1*DSIN(T1*W)
      Z2=X2*DSIN(T2*W)
      Z3=X3*DSIN(T3*W)
      S2=(Y1+Y3)/2.D0
      GADDR=DEL*(AL*(Z3-Z1)+BE*S2+GA*Y2)
      S2=(Z1+Z3)/2.D0
      GADDI=DEL*(AL*(Y1-Y3)+BE*S2+GA*Z2)
      GNUMR=GNUMR+GADDR
      GNUMI=GNUMI-GADDI
      REL1=DSQRT(GADDR**2+GADDI**2)
      REL2=DSQRT(GNUMR**2+GNUMI**2)
      IF(REL2.GT.0.) REL=REL1/REL2
      IF(REL.LT.1.D-5) GO TO 500
      X1=X3
      T1=T3
5      RE=(GNUMR*DENOMR+GNUMI*DENOMI)/ARINP**2
      IM=(GNUMI*DENOMR-GNUMR*DENOMI)/ARINP**2
      AR=DSQRT(RE**2+IM**2)/GAIN
      SIGN=RE*SAV

```

```
IF(SIGN.LT.0) XM=XM+1.D0
IF(XM.GT.X180) XM=X180
SAV=RE
PH=DATAN(IM/RE)*180.D0/PI-180.D0*XM
WLOG=W
IF(ILOG.EQ.2) WLOG=DLOG10(W)
ARLOG=AR
IF(ILOG.EQ.2) ARLOG=DLOG10(AR)
WRITE(3) SNGL(WLOG),SNGL(ARLOG),SNGL(PH),SNGL(RE),SNGL(IM),
1 SNGL(ARINP)
IF(IPR.EQ.IYES) WRITE(IWI,202) WLOG,ARLOG,PH,RE,IM,ARINP
202 FORMAT(6(1PE12.4))
3 W=DEXP(DLOG(W)+DELW)
CALL CLOSE(2)
CALL CLOSE(3)
STOP
END
```

```

C-----0-----0-----0-----0-----0-----0-----0-----0
C A program that calculates the frequency response of an approximate
C transfer function given the moments of a higher order transfer
function.
C-----0-----0-----0-----0-----0-----0-----0-----0
      IMPLICIT DOUBLE PRECISION(A-H,O-Z)
      DIMENSION ROOT(3),VAL(3)
      DOUBLE PRECISION IM,M1,M2,M3
      DATA IYES/'Y'/
      PI=3.1415926535D0
C-----0-----0-----0-----0-----0-----0-----0-----0
C 1.0 Calculate the moments of the linearized model
      WRITE(5,101)
101   FORMAT(
     1 ' Enter the number of reactions (<11)           ',$,)
      READ(5,*) NUM
      WRITE(5,102)
102   FORMAT(
     1 ' Enter the steady state flux                 ',$,)
      READ(5,*) PSI
      WRITE(5,103)
103   FORMAT(
     1 ' Write out some results ? [Y/N]             ',$,)
      READ(5,104) IPR
104   FORMAT(A1)
      IF(IPR.EQ.IYES) WRITE(5,105)
105   FORMAT(
     1 ' Write results on the screen=5, the LP=6 [5/6] ',$,)
      IF(IPR.EQ.IYES) READ(5,*) IWI
      IF(IPR.EQ.IYES) WRITE(IWI,106)
106   FORMAT(' Rxn ',6X,'Tau1',8X,'Tau2',10X,'Bi',11X,'Sa',10X,'St',
     1 10X,'Qs',8X,'Sigma-bar',4X,'Chi-bar',/)
C-----0-----0-----0-----0-----0-----0-----0-----0
C get the dimensionless numbers from file KIN.DAT
      CALL ASSIGN(1,'KIN.DAT')
      GAIN=1.D0
      DO 1 I1=1,NUM
      READ(1,*) BI,SA,ST,QS
C solve for the steady state
      GAIN=GAIN*SA
      PS=PSI*GAIN
      SS=PS/(1.D0-PS)
      XS=PS
Compute the sub-Jacobian matrix
      A11=-(1.D0-XS)
      A12=1.D0/(1.D0+ST)+SS
      A21=(1.D0-XS)/QS
      A22=-1.D0/(QS*(1.D0-XS))
Compute the eigenvalues
      DET=(A11*A22-A21*A12)/BI**2

```

```

TR=(A11+A22)/BI
DIS=DSQRT(TR**2/4.D0-DET)
T1=TR/2.D0+DIS
T1=-1.D0/T1
T2=TR/2.D0-DIS
T2=-1.D0/T2
IF(IPR.EQ.IYES) WRITE(IWI,107) I1,T1,T2,BI,SA,ST,QS,SS,XS
107 FORMAT(1X,I3,4X,8(1PE11.3,1X))
M1=M1+T1+T2
M2=M2+T1**2+T2**2
1 M3=M3+2.D0*(T1**3+T2**3)
CALL CLOSE(1)
T2=M2
T3=M3
IF(IPR.EQ.IYES) WRITE(IWI,108) M1,T2,T3
108 FORMAT(// ' The moments are: ',/
1 ' First moment, M1=',1PE11.3,/
2 ' Second moment around the mean, T2=',1PE11.3,/
3 ' Third moment around the mean, T3=',1PE11.3)
C-----0-----0-----0-----0-----0-----0-----0-----
C 2.0 Approximate model
200 WRITE(5,201)
201 FORMAT(
1 ' Enter the approximate model order 1, 2, or 3 [1/2/3] ',,$)
READ(5,*) IORDER
CALL ASSIGN(2,'TIME.DAT')
WRITE(2) IORDER
IF(IORDER.EQ.3) GO TO 50
IF(IORDER.EQ.2) GO TO 40
C-----0-----0-----0-----0-----0-----0-----0-----
C 3.0 first order transfer function.
TAU=M1
IF(IPR.EQ.IYES) WRITE(IWI,301) TAU
301 FORMAT(
1 ' The time constant for the first order system is Tau = ',
2 1PE12.4)
WRITE(2) TAU
GO TO 60
C-----0-----0-----0-----0-----0-----0-----0-----
C 4.0 second order transfer function
40 DIFF=M1**2-T2
IF(DIFF.GT.0.D0) GO TO 41
WRITE(5,401)
401 FORMAT(/' M1**2 is less than T2'/)
DIFF=-DIFF
41 TAU=DSQRT(.5D0*DIFF)
EPS=.5D0*M1/TAU
IF(IPR.EQ.IYES) WRITE(IWI,402) TAU,EPS
402 FORMAT(//
1 ' Parameters for the second order system: ',/

```

```

2   ' Tau = ',1PE12.4,/, ' Eps = ',1PE12.4,/, ' or')
CALL SEC(TAU,EPS,TARE1,TAIM1,TARE2,TAIM2)
IF(IPR.EQ.IYES) WRITE(IWI,403) TARE1,TAIM1,TARE2,TAIM2
403 FORMAT(' Tau1 = ',1PE12.4,' +I*',1PE12.4,/
1 ' Tau2 = ',1PE12.4,' +I*',1PE12.4)
WRITE(2) TAU,EPS
GO TO 60
C-----0-----0-----0-----0-----0-----0-----
C 5.0 third order transfer function
50   A1=-M1
      A2=.5D0*(M1**2-T2)
      A3=-(T3+M1**3-3.D0*T2*M1)/6.D0
      Q=(3.D0*A2-A1**2)/9.D0
      R=(9.D0*A1*A2-27.D0*A3-2.D0*A1**3)/54.D0
      D=Q**3+R**2
      IF(D)>52,51,51
      S=(R+DSQRT(D))
      IF(S.LT.0.D0) S=-(-S)**.333333
      IF(S.GE.0.D0) S=S**.333333
      T=(R-DSQRT(D))
      IF(T.LT.0.D0) T=-(-T)**.333333
      IF(T.GE.0.D0) T=T**.333333
      TAUa=S+T-A1/3.D0
      IF(TAUa.GE.0.D0) GO TO 53
      WRITE(5,503)
503  FORMAT(1X,'*** TAUa IS NEGATIVE ***')
      TAUa=-TAUa
      GO TO 53
52   XX=2.D0*DSQRT(-Q)
      PH=DACOS(R/DSQRT(-Q**3))
      ROOT(1)=XX*DCOS(PH/3.D0)-A1/3.D0
      ROOT(2)=XX*DCOS((PH+2.D0*PI)/3.D0)-A1/3.D0
      ROOT(3)=XX*DCOS((PH+4.D0*PI)/3.D0)-A1/3.D0
      DO 5 I5=1,3
      5   VAL(I5)=ROOT(I5)**3+A1*ROOT(I5)**2+A2*ROOT(I5)+A3
      WRITE(5,505)(ROOT(I),I=1,3),(VAL(I),I=1,3)
505  FORMAT(' The roots are: ',/
1   3(1X,1PE12.4),/,'
2   ' and their functional values are:',/,'
3   3(1X,1PE12.4),/,'
4   ' Which one do you want 1,2 or 3
      READ(5,*) IR
      TAUa=ROOT(IR)
      CALL NEWTON(TAUa,A1,A2,A3,IYES)
      TAUB=DSQRT(-A3/TAUa)
      EPS=(M1-TAUa)/(2.D0*TAUB)
      TAU=TAUa
      IF(TAUB.GT.TAUa) TAU=TAUB
      IF(IPR.EQ.IYES) WRITE(IWI,506) TAUa,TAUB,EPS
506  FORMAT(/' Parameters for the third order system: ',/

```

```

1   ' TauA = ',1PE 12.4,/, ' TauB = ',1PE 12.4,/,,
2   ' Eps = ',1PE 12.4,//' or' /)
TAU3=TAUA
CALL SEC(TAUB,EPS,TARE1,TAIM1,TARE2,TAIM2)
IF(IPR.EQ.IYES) WRITE(IWI,403) TARE1,TAIM1,TARE2,TAIM2
IF(IPR.EQ.IYES) WRITE(IWI,507) TAU3
507  FORMAT(' Tau3 = ',1PE 12.4)
      WRITE(2) TAUB,TAUA,EPS
C-----0-----0-----0-----0-----0-----0-----0-----
C 6.0 Compute the frequency response
60   CALL CLOSE(2)
      WRITE(5,601)
601   FORMAT(/////
1   ' Enter Wmin,max and      of pts                      ',,$)
      READ(5,*) WMIN,WMAX,NPTS
      PHI=-90.0*DFLOAT(IORDER)
      CORNER=1.0/TAU
      TMAX=-DFLOAT(IORDER)*DLOG10(WMAX/CORNER)
      TMAX=DEXP(DLOG(10.0)*TMAX)
      S1=1
      CALL ASSIGN(3,'CORNER.DAT')
      WRITE(3) SNGL(WMIN),SNGL(PHI),SNGL(CORNER),S1
      WRITE(3) SNGL(WMAX),SNGL(PHI),SNGL(WMAX),SNGL(TMAX)
      CALL CLOSE(3)
      WRITE(5,602)
602   FORMAT(
1   ' Print out results for Bode diagram ? [Y/N]          ',,$)
      READ(5,104) IPR1
      IF(IPR1.EQ.IYES) WRITE(5,603)
603   FORMAT(
1   ' Term=5, LP=6  [5/6]                                     ',,$)
      IF(IPR1.EQ.IYES) READ(5,*) IWI
C-----0-----0-----0-----0-----0-----0-----0-----
      IF(IPR1.EQ.IYES) WRITE(IWI,604)
604   FORMAT(/,7X,'W',12X,'AR',12X,'PH',12X,'RE',12X,'IM',/)
      DWL=(DLOG(WMAX)-DLOG(WMIN))/DFLOAT(NPTS-1)
      W=WMIN
      CALL ASSIGN(4,'CHBODA.DAT')
C-----0-----0-----0-----0-----0-----0-----0-----
      DO 6 I6=1,NPTS
      IF(IORDER.EQ.3) GO TO 61
      IF(IORDER.EQ.2) GO TO 63
      BB=TAU*W
      AA=1.0
      GO TO 62
C-----0-----0-----0-----0-----0-----0-----0-----
63   AA=1.0-(TAU*W)**2
      BB=2.0*TAU*EPS*W
      GO TO 62

```

```

C-----0-----0-----0-----0-----0-----0-----0-----0
51      AA=1.D0-(TAUB+2.D0*EPS*TAUA)*TAUB*W**2
          BB=W*(TAUA*(1.D0-(TAUB*W)**2)+2.D0*EPS*TAUB)
C-----0-----0-----0-----0-----0-----0-----0-----0
62      AR=DSQRT(1.D0/(AA**2+BB**2))
          PH=DATAN(-BB/AA)*180.D0/PI
          IF(AA.LT.0.D0) PH=PH-180.D0
          DE=AA**2+BB**2
          RE=AA/DE
          IM=-BB/DE
          WRITE(4) SNGL(W),SNGL(AR),SNGL(PH),SNGL(RE),SNGL(IM)
          IF(IPR1.EQ.IYES) WRITE(IWI,605) W,AR,PH,RE,IM
605      FORMAT(5(1PE14.5))
          W=DLOG(W)+DWL
6       W=DEXP(W)
          CALL CLOSE(4)
C-----0-----0-----0-----0-----0-----0-----0-----0
          WRITE(5,606)
606      FORMAT(
1      ' Try another model ? [Y/N] ',$,)
          READ(5,104) IANS
          IF(IANS.EQ.IYES) GO TO 200
          STOP
          END

```

```

C-----0-----0-----0-----0-----0-----0-----0-----0
          SUBROUTINE SEC(T,E,TR1,TI1,TR2,TI2)
          IMPLICIT DOUBLE PRECISION(A-H,O-Z)
          EI=E**2-1.D0
          IF(EI.GE.0.D0) GO TO 1
          EI=DSQRT(-EI)
          TR1=T**E
          TI1=T**EI
          TR2=TR1
          TI2=-TI1
          RETURN
C-----0-----0-----0-----0-----0-----0-----0-----0
1      EI=DSQRT(EI)
          TR1=T*(E+EI)
          TR2=T*(E-EI)
          TI1=0.D0
          TI2=0.D0
          RETURN
          END

```

```
C-----0-----0-----0-----0-----0-----0-----0-----0--  
      SUBROUTINE NEWTON(X,A1,A2,A3,IYES)  
      DOUBLE PRECISION X,A1,A2,A3,SAV,DU,DN  
      WRITE(5,101)  
101   FORMAT(  
     1  ' do you want to see the iterations.... [Y/N]           ', $)  
          READ(5,102) IPR  
102   FORMAT(A1)  
          DU=A3+X*(A2+X*(A1+X))  
          DO 1 I1=1,50  
          DN=A2+X*(2.D0*A1+3.D0*X)  
          SAV=X  
          X=X-DU/DN  
          DU=A3+X*(A2+X*(A1+X))  
          IF(IPR.EQ.IYES) WRITE(5,103) I1,X,DU  
103   FORMAT(' AFTER ',I3,' ITERATIONS X= ',E26.16,' F(X)= ',E15.8)  
1       IF(DABS(SAV-X).LT.1.D-10) GO TO 2  
2       RETURN  
END
```

**Programs to Compute the Loci Defining the onset of  
Dynamic Instability for the Single Biochemical Control Loop.**

```

C-----0-----0-----0-----0-----0-----0-----0-----0-----0-----
C A program that computes the critical value of Binding constant for
C dynamic bifurcations for a single biochemical control loop with
C lumped negative controller and Michaelis-Menten type removal
C-----0-----0-----0-----0-----0-----0-----0-----0-----
C The subroutines are
C     BLOC   : computes the value of the criterion at
C                 pi-->0 or Binding constant-->infinity
C     CRVL   : Finds the critical value of Binding constant
C                 given all other parameters.
C     MAGNUM : calculates the magic number at the critical point
C     STSTCO : computes the steady state concentration of pi
C     LOCIN  : calculates the critical locus in the
C                 Omega-sub-pi,Psi-sub-pi plane.
C
C The physical variables are:
C   for the reaction chain
C     IORD   : order of reaction chain
C     XI     : the damping factor
C     PHI    : relative time constant of the first and second
C                 order subsystems in a third order transfer function
C   for the removal rate
C     KAPPA  : pseudo-first order rate constant
C     OMEGA  : saturation velocity
C   for the input rate
C     LAMBDA : binding constant for enzyme-substrate association
C     NU(RNU): Hill coefficient, degree of cooperativity
C
C The error tolerance parameters are
C     FTOL   : error tolerance on the function in question
C     RTOL   : error tolerance on the root
C     ITRTOL : maximum number of iterations per root evaluation
C
C The I/O parameters are
C     IWRITE : default write drive
C     IREAD  : default read drive
C     IDEV   : device that output is directed to
C     IWRIT1 : "      "  debug computations are directed to
C     IBUGP  : is Y if computations on steady state con's are debugged
C     IBUGL  : "      "      Bind.const. evaluations "
C     IBUGM  : "      "      magic   evaluations "
C-----0-----0-----0-----0-----0-----0-----0-----0-----
IMPLICIT DOUBLE PRECISION(A-H,O-Z)
COMMON/BL/IORD,XI,PHI,LAMBDA,RNU,IBUG,IBUGW,IWRITE,
1 RTOL,FTOL,ITRTOL
DOUBLE PRECISION LAMBDA,L,KAPPA,KAP,KAPP,DLOG,DEXP,DBLE,DABS
EXTERNAL BL
DIMENSION XI(5),PHI(5),TAUR(10),TAUI(10)

```

```

C-----0-----0-----0-----0-----0-----0-----0-----0-----0-----
C set I/O device numbers
    IREAD=5
    IWRITE=5
    L=1.D0
92    FORMAT(A1)
C-----0-----0-----0-----0-----0-----0-----0-----0-----0-----
C if instructions is to be read from a data file
90    CALL CLEAR
        WRITE(IWRITE,99)
99    FORMAT(' Program to compute the locus of dynamic bifurcations'/
1          '           in single biochemical control loops'/
2          '           with lumped controller and Michaelis-Menten removal'//
3          '           Version for PDP 11/55 - September 1983'//'
4          '           by Bernhard Palsson'//'
5          ' Input instructions from a data file ? [Y/N] ',\$)
        READ(IREAD,92) INSTR
        IF(INSTR.EQ.'Y') GO TO 400
        WRITE(IWRITE,98)
98    FORMAT(' Options currently available:'/
1          ' Ratio versus kappa = 1',/,'
2          ' Ratio versus Omega = 2','
3          ' 4X, Your choice ? ',\$)
        READ(IREAD,*) IPLOT
        WRITE(IWRITE,96)
96    FORMAT(' Input rate law',/,'
1          ' Lumped negative = 1',/,'
2          ' Symmetry model = 2',7X,' Your choice ? ',\$)
        READ(IREAD,*) LOOP
        IF(LOOP.EQ.1) WRITE(IWRITE,95)
95    FORMAT(' 1) ratio = Lambda, 2) ratio = Af ? [1/2] ',\$)
        IF(LOOP.EQ.1) READ(IREAD,*) IRATIO
        WRITE(IWRITE,97)
97    FORMAT('/// Any corrections ? [Y/N] ',\$)
        READ(IREAD,92) ICORR
        IF(ICORR.EQ.'Y') GO TO 90
C-----0-----0-----0-----0-----0-----0-----0-----0-----0-----
C set I/O parameters
100   CALL CLEAR
        WRITE(IWRITE,101)
101   FORMAT(' Enter control parameters for printing',///
1          '           Print out values of Binding constant ? [Y/N] ',\$)
        READ(IREAD,92) IPR
        IF(IPR.NE.'Y') GO TO 11
        WRITE(IWRITE,102)
102   FORMAT(' Device number ? ',\$)
        READ(IREAD,*) IDEV
11     WRITE(IWRITE,103)
103   FORMAT(' Write results on file for plotting ? [Y/N] ',\$)
        READ(IREAD,92) IDATA

```

```

      WRITE(IWRITE, 104)
104    FORMAT(' Debug computations ?           [Y/N] ',\$)
      READ(IREAD,92) IANS
      IF(IANS.NE.'Y') GO TO 12
      WRITE(IWRITE,105)
105    FORMAT(' Computations of Binding constant ?   [Y/N] ',\$)
      READ(IREAD,92) IBUGL
      WRITE(IWRITE,106)
106    FORMAT(' Computations of pi-stst ?          [Y/N] ',\$)
      READ(IREAD,92) IBUGP
      WRITE(IWRITE,107)
107    FORMAT(' Computation of the magic   ?         [Y/N] ',\$)
      READ(IREAD,92) IBUGM
      WRITE(IWRITE,108)
108    FORMAT(' Computation of the critical frequency [Y/N] ',\$)
      READ(IREAD,92) IBUGW
      WRITE(IWRITE,102)
      READ(IREAD,*) IWRIT1
12     WRITE(IWRITE,97)
      READ(IREAD,92) ICORR
      IF(ICORR.NE.'Y') GO TO 200
      WRITE(IWRITE,109)
109    FORMAT(' Correct this screen = 1, previous screen = 2 ',\$)
      READ(IREAD,*) ICORR
      IF(ICORR.EQ.1) GO TO 100
      GO TO 90
C-----0-----0-----0-----0-----0-----0-----0-----0-----
C set control parameters for computations
200    CALL CLEAR
      WRITE(IWRITE,201)
201    FORMAT(' Enter control parameters for computations://',
     1           ' of pts to be computed on the loci           ',\$)
      READ(IREAD,*) IPTS
      WRITE(IWRITE,202)
202    FORMAT(' Logarithmic spacing of points ?           [Y/N] ',\$)
      READ(IREAD,92) ILOG
      WRITE(IWRITE,203)
203    FORMAT(' Multiplication on Binding constant during search   ',\$)
      READ(IREAD,*) FACTOR
      WRITE(IWRITE,204)
204    FORMAT(' of Binding constant values to be located (1 or 2) ',\$)
      READ(IREAD,*) LAMNUM
      IF(IDATA.NE.'Y'.OR.LAMNUM.EQ.1) GO TO 21
      WRITE(IWRITE,205)
205    FORMAT(' Do you want to merge data files ?           [Y/N] ',\$)
      READ(5,92) MERGE
      IF(MERGE.NE.'Y') GO TO 21
      WRITE(IWRITE,206)
206    FORMAT('                               first point ?       [Y/N] ',\$)
      READ(IREAD,92) MERGE1

```

```

      WRITE(IWRITE,207)
207   FORMAT('                               last point ?          [Y/N] ',,$)
      READ(IREAD,92) MERGE2
21     WRITE(IWRITE,208)
208   FORMAT(' Other than standard error tolerances ?      [Y/N] ',,$)
      READ(IREAD,92) IANS
      RTOL=1.D-14
      FTOL=1.D-14
      ITRTOL=100
      IF(IANS.EQ.'Y') GO TO 22
      GO TO 23
22     WRITE(IWRITE,209) RTOL
209   FORMAT(/'      The error tolerance on the root is    ',1PD15.5,/
1           '      change this value ? [Y/N] ',,$)
      READ(IREAD,92) IANS
      IF(IANS.NE.'Y') GO TO 24
      WRITE(IWRITE,210)
210   FORMAT( '                           Enter new value ',,$)
      READ(IREAD,*) RTOL
24     WRITE(IWRITE,211) FTOL
211   FORMAT( ' The error tolerance on the function is   ',1PD15.5,/
1           '      change this value ? [Y/N] ',,$)
      READ(IREAD,92) IANS
      IF(IANS.NE.'Y') GO TO 25
      WRITE(IWRITE,210)
      READ(IREAD,*) FTOL
25     WRITE(IWRITE,212) ITRTOL
212   FORMAT( ' The maximum number of iterations is   ',I7,/
1           '      change this value ? [Y/N] ',,$)
      READ(IREAD,92) IANS
      IF(IANS.NE.'Y') GO TO 23
      WRITE(IWRITE,210)
      READ(IREAD,*) ITRTOL
23     WRITE(IWRITE,97)
      READ(IREAD,92) ICORR
      IF(ICORR.NE.'Y') GO TO 300
      WRITE(IWRITE,109)
      READ(IREAD,*) ICORR
      IF(ICORR.EQ.1) GO TO 200
      GO TO 100
C-----0-----0-----0-----0-----0-----0-----0-----0-----
C Enter parameters physical constants
300   CALL CLEAR
      WRITE(IWRITE,301)
301   FORMAT(' Enter:',//,
1           ' transfer function order, nu ',,$)
      READ(IREAD,*) IORD,NU
      RNU=DFLOAT(NU)
      IODD=MOD(IORD,2)
      N3=IORD/2

```

```

IF(IORD.EQ.1) GO TO 31
DO 3 I3=1,N3
WRITE(IWRITE,302) I3
302 FORMAT(' Enter for subsystem ',I2,' xi and phi ',,$)
READ(IREAD,*) XI(I3),PHI(I3)
IF(XI(I3).GE.1.D0) GO TO 35
TAUI(2*I3-1)=DSQRT(1.D0-XI(I3)**2)/PHI(I3)
TAUR(2*I3-1)=-XI(I3)/PHI(I3)
TAUI(2*I3) =-TAUI(2*I3-1)
TAUR(2*I3) =TAUR(2*I3-1)
DIV=TAUR(2*I3-1)**2+TAUI(2*I3-1)**2
TAUR(2*I3-1)=-TAUR(2*I3-1)/DIV
TAUR(2*I3)=-TAUR(2*I3)/DIV
TAUI(2*I3-1)=TAUI(2*I3-1)/DIV
TAUI(2*I3)=TAUI(2*I3)/DIV
GO TO 3
35 DIS=DSQRT(XI(I3)**2-1.D0)
TAUR(2*I3-1)=(-XI(I3)-DIS)/PHI(I3)
TAUR(2*I3-1)=-1.D0/TAUR(2*I3-1)
TAUR(2*I3) =(-XI(I3)+DIS)/PHI(I3)
TAUR(2*I3) =-1.D0/TAUR(2*I3)
TAUI(2*I3-1)=0.D0
TAUI(2*I3) =0.D0
3 WRITE(IWRITE,303) (TAUR(J),TAUI(J),J=2*I3-1,2*I3)
303 FORMAT(' The time constants are tau =',1PD15.5,' + i*',1PD15.5/
      , ' tau =',1PD15.5,' + i*',1PD15.5)
      1 IF(IODD.EQ.0) GO TO 32
31 WRITE(IWRITE,304)
304 FORMAT(' Enter phi ',,$)
READ(IREAD,*) PHI(N3+1)
TAUR(IORD)=PHI(N3+1)
TAUI(IORD)=0.D0
WRITE(IWRITE,305) TAUR(IORD),TAUI(IORD)
305 FORMAT(' The time constants is tau =',1PD15.5,' + i*',1PD15.5)
32 IF(LOOP.EQ.1.OR.IPLOT.EQ.1) GO TO 33
WRITE(IWRITE,306)
306 FORMAT(' Enter LAMBDA ',,$)
READ(IREAD,*) LAMBDA
33 IF(IPLOT.EQ.2) GO TO 700
C-----0-----0-----0-----0-----0-----0-----0-----0-----
C for instruction file
400 CONTINUE
C-----0-----0-----0-----0-----0-----0-----0-----0-----
C Compute the binding constant as a function of Kappa
500 WRITE(IWRITE,501)
501 FORMAT(' Enter 1/Omega ',,$)
READ(IREAD,*) OMEGA
OMEGA=1.D0/OMEGA
WRITE(IWRITE,502)
502 FORMAT(' Locate roots on b+1=0 ? [Y/N] ',,$)

```

```

READ(IREAD,92) IANS
IF(IANS.NE.'Y'.AND LOOP.EQ.1) GO TO 54
IF(IANS.NE.'Y'.AND LOOP.EQ.2) GO TO 51
WRITE(IWRITE,503)
503 FORMAT(' Enter initial guess for the smaller root ',,$)
READ(IREAD,*) ROOT
WRITE(IWRITE,504)
504 FORMAT(' Debug computations ? [Y/N] ',,$)
READ(IREAD,92) IBUGB
CALL BLOC(ROOT,LAMBDA,RNU,1,IORD,XI,PHI,RTOL,FTOL,
1 ITRTOL,IWRITE,IBUGB,IBUGW)
FMAX=1.D0/ROOT
ROOT=ROOT*1.001D0
CALL BLOC(ROOT,LAMBDA,RNU,1,IORD,XI,PHI,RTOL,FTOL,
1 ITRTOL,IWRITE,IBUGB,IBUGW)
FMIN=1.D0/ROOT
WRITE(IWRITE,505) FMIN,FMAX
505 FORMAT(/' Reciprocals of the roots for loop of type 1 are :',/,
1 ' 1/Kappa1 ',1PD15.5,/,
2 ' 1/Kappa2 ',1PD15.5)
IF(LOOP.EQ.1) GO TO 53
FMA=0.99D0/FMIN
FMI=1.01D0/FMAX
FMIN=DFMIN(FMI,FMA,BL,1.D-8)
LAMBDA=BL(FMIN)
FMIN=1.D0/FMIN
WRITE(IWRITE,506) LAMBDA,FMIN
506 FORMAT(
1 ' Minimum value of LAMBDA for instability is ',1PD15.5,/,
2 ' and occurs at 1/kappa = ',1PD15.5,/,
3 ' Enter your choise for LAMBDA ',,$)
READ(IREAD,*) LAMBDA
ROOT=1.00001D0/FMAX
CALL BLOC(ROOT,LAMBDA,RNU,LOOP,IORD,XI,PHI,RTOL,FTOL,
1 ITRTOL,IWRITE,IBUGB,IBUGW)
FMAX=1.D0/ROOT
ROOT=1.D0/FMIN
CALL BLOC(ROOT,LAMBDA,RNU,LOOP,IORD,XI,PHI,RTOL,FTOL,
1 ITRTOL,IWRITE,IBUGB,IBUGW)
FMIN=1.D0/ROOT
WRITE(IWRITE,507) FMIN,FMAX
507 FORMAT(
1 ' Reciprocals of the roots for loop of type 2 are :',/,
2 ' 1/Kappa1 ',1PD15.5,/,
3 ' 1/Kappa2 ',1PD15.5)
53 WRITE(IWRITE,508)
508 FORMAT(' Use roots as limits on locus ? [Y/N] ',,$)
READ(IREAD,92) IANS
IF(IANS.NE.'Y') GO TO 54
WRITE(IWRITE,5081)

```

```

5081 FORMAT(' Enter fraction of intervall to be searched ? ',\$)
      READ(IREAD,*) FRAC
      FRAC=FRAC+(1.DO-FRAC)/2.DO
      RANGE=FMAX-FMIN
      FMIN=FMIN+(1.DO-FRAC)*RANGE
      FMAX=FMAX-(1.DO-FRAC)*RANGE
      GO TO 52
51      WRITE(IWRITE,5082)
5082 FORMAT(' Enter LAMBDA ',\$)
      READ(IREAD,*) LAMBDA
54      WRITE(IWRITE,509)
509   FORMAT(' Enter 1/Kappa-min,max ',\$)
      READ(IREAD,*) FMIN,FMAX
52      WRITE(IWRITE,510)
510   FORMAT(' Enter range of values to search over:/',
1           ' Binding constant-min, Binding constant-max ',\$)
      READ(IREAD,*) PMIN,PMAX
      WRITE(IWRITE,97)
      READ(IREAD,92) ICORR
      IF(ICORR.NE.'Y') GO TO 550
      WRITE(IWRITE,109)
      READ(IREAD,*) ICORR
      IF(ICORR.EQ.1) GO TO 300
      GO TO 200
550   CALL CLEAR
      IF(IDATA.EQ.'Y') CALL ASSIGN(2,'L1.DAT')
      IF(LAMNUM.EQ.2.AND.IDATA.EQ.'Y') CALL ASSIGN(3,'L2.DAT')
      DEL=(FMAX-FMIN)/DFLOAT(IPTS-1)
      IF(ILOG.EQ.'Y') DEL=(DLOG(FMAX)-DLOG(FMIN))/DFLOAT(IPTS-1)
      KAP=FMIN
      IF(IPR.EQ.'Y') WRITE(IDEV,511) IORD,OMEGA,FMIN,FMAX
511   FORMAT(13X,' PARAMETER SUMMARY ',//,' For the reaction chain',//,
1           2X,' order of the reaction chain:',I5,//,
4           ' For the removal rate',//,
5           2X,' saturation velocity      :',1PD15.5,/,
6           2X,' range on 1/Kappa       :',2(1PD15.5),/)
      IF(IPR.EQ.'Y') WRITE(IDEV,512) NU,PMIN,PMAX
512   FORMAT(
1           ' For the input rate',//,
2           2X,' Degree of cooperativity    :',I5,/,
3           2X,' Range on Lambda          :',2(1PD15.5),///)
      IF(IPR.EQ.'Y'.AND.LAMNUM.EQ.1) WRITE(IDEV,513)
513   FORMAT(
1           ' _____ /',
2           ' first order      Binding      Poores      product',//,
3           ' rate constant     constant     Magic number  concentration',//,
4           ' 1/Kappa           pi',/)
      IF(IPR.EQ.'Y'.AND.LAMNUM.EQ.2) WRITE(IDEV,514)
514   FORMAT(
1           ' _____ /'

```

```

2 ,-----')
IF(IPR.EQ.'Y'.AND.LAMNUM.EQ.2) WRITE(IDEV,515)
515 FORMAT(
1 '      first order      Binding      Poores      Binding      '
2 '      Poores',/
3 '      rate constant     constant     Magic number     constant      '
4 '      Magic number',/
5 '      1/Kappa           1           1           2           '
6 '      2')'
C-----0-----0-----0-----0-----0-----0-----0-----0-----
C a DO-loop that computes the critical value of Binding constant and the
C magic number as a function of 1/kappa.
600 DO 6 I6=1,IPTS
      KAPPA=1.D0/KAP
      CALL CRVL(PI,LAMBDA,L,RNU,LOOP,KAPPA,OMEGA,IORD,XI,PHI,RTOL,
1 FTOL,ITRTOL,IBUGL,IBUGP,IBUGW,IWRIT1,PMIN,PMAX,FACTOR,1)
      IF(LOOP.EQ.1) BIND1=LAMBDA
      IF(LOOP.EQ.2) BIND1=L
      IF(BIND1.GE.PMAX) GO TO 61
      SAV1=X1
      CALL MAGNUM(X1,ISIGN,IORD,TAUR,TAUI,XI,PHI,LAMBDA,L,
1 NU,RNU,LOOP,KAPPA,OMEGA,PI,IBUGM,IBUGW,IWRIT1,RTOL,FTOL,ITRTOL)
      IF(IDATA.NE.'Y') GO TO 62
      IF(SAV1*X1.GE.0.D0.OR.I6.EQ.1) GO TO 62
      IF(IRATIO.EQ.2) BIND1=BIND1*OMEGA/KAPPA
      WRITE(2) SNGL(KAP),SNGL(BIND1),SNGL(X1),SNGL(PI)
      CALL CLOSE(2)
      CALL ASSIGN(2,'L3.DAT')
62   IF(IRATIO.EQ.2.AND.SAV1*X1.GE.0.D0) BIND1=BIND1*OMEGA/KAPPA
      IF(IDATA.EQ.'Y') WRITE(2) SNGL(KAP),SNGL(BIND1),SNGL(X1),
1 SNGL(PI)
      Check if there are more than one BIND values to be calculated
      IF(LAMNUM.EQ.1) GO TO 63
      IF(MERGE1.EQ.'Y'.AND.IDATA.EQ.'Y')
1 WRITE(3) SNGL(KAP),SNGL(BIND1),SNGL(X1),SNGL(PI)
      MERGE1='N'
      C new minimum value on the range to search over
      IF(LOOP.EQ.1) BIND2=LAMBDA
      IF(LOOP.EQ.2) BIND2=L
      PMI=BIND2*1.001D0
      CALL CRVL(PI,LAMBDA,L,RNU,LOOP,KAPPA,OMEGA,IORD,XI,PHI,RTOL,
1 FTOL,ITRTOL,IBUGL,IBUGP,IBUGW,IWRIT1,PMI,PMAX,FACTOR,1)
      IF(LOOP.EQ.1) BIND2=LAMBDA
      IF(LOOP.EQ.2) BIND2=L
      IF(BIND2.GE.PMAX) GO TO 64
      SAV2=X2
      CALL MAGNUM(X2,ISIGN,IORD,TAUR,TAUI,XI,PHI,LAMBDA,L,
1 NU,RNU,LOOP,KAPPA,OMEGA,PI,IBUGM,IBUGW,IWRIT1,RTOL,FTOL,ITRTOL)
      Check for sign change on the magic number
      IF(IDATA.NE.'Y') GO TO 65

```

```

IF(SAV2*X2.GE.0.D0.OR.I6.EQ.1) GO TO 65
IF(IRATIO.EQ.2) BIND2=BIND2*OMEGA/KAPPA
WRITE(3) SNGL(KAP),SNGL(BIND2),SNGL(X2),SNGL(PI)
CALL CLOSE(3)
CALL ASSIGN(3,'L4.DAT')
C if both roots of BIND are found
65   IF(IRATIO.EQ.2.AND.SAV2*X2.GE.0.D0) BIND2=BIND2*OMEGA/KAPPA
      IF(IDATA.EQ.'Y') WRITE(3) SNGL(KAP),SNGL(BIND2),SNGL(X2),
      1 SNGL(PI)
      IF(IPR.EQ.'Y') WRITE(IDEV,601) KAP,BIND1,X1,BIND2,X2
601   FORMAT(1X,5(1PD15.5))
      IF(MERGE2.NE.'Y') GO TO 66
      BIND=BIND1
      KAPP=KAP
      GO TO 66
C if one value of BIND exists
64   IF(IPR.EQ.'Y') WRITE(IDEV,602) KAP,BIND1,X1
602   FORMAT(1X,3(1PD15.5),6X,'no second root')
      IF(MERGE2.NE.'Y') GO TO 66
      BIND=BIND1
      KAPP=KAP
      GO TO 66
C if neither root is found
61   IF(IPR.EQ.'Y') WRITE(IDEV,604) KAP
604   FORMAT(1X,1PD15.5,8X,'no root')
      GO TO 66
C if one value of BIND is to be computed
63   IF(IPR.EQ.'Y') WRITE(IDEV,603) KAP,BIND1,X1,PI
603   FORMAT(1X,4(1PD15.5))
      IF(MERGE2.NE.'Y') GO TO 66
      BIND=BIND1
      KAPP=KAP
66   IF(ILOG.EQ.'Y') KAP=DEXP(DLOG(KAP)+DEL)
6   IF(ILOG.NE.'Y') KAP=KAP+DEL
      IF(IDATA.EQ.'Y'.AND.MERGE2.EQ.'Y'.AND.LAMNUM.EQ.2)
      1 WRITE(3) SNGL(KAPP),SNGL(BIND),SNGL(X1),SNGL(PI)
      GO TO 1000
C-----0-----0-----0-----0-----0-----0-----0-----
C Calculate the locus of Binding constant versus 1/Omega-max
700   WRITE(IWRITE,701)
701   FORMAT(' Enter 1/Kappa ',\$)
      READ(IREAD,*) KAPPA
      KAPPA=1.D0/KAPPA
      WRITE(IWRITE,702)
702   FORMAT(' Enter 1/Omega-min, 1/Omega-max ',\$)
      READ(IREAD,*) OMI,OMA
      DEL=(OMA-OMI)/DFLOAT(IPTS-1)
      IF(ILOG.EQ.'Y') DEL=(DLOG(OMA)-DLOG(OMI))/DFLOAT(IPTS-1)
      WRITE(IWRITE,510)
      READ(IREAD,*) PMIN,PMAX

```

```

      WRITE(IWRITE,97)
      READ(IREAD,92) ICORR
      IF(ICORR.NE.'Y') GO TO 750
      WRITE(IWRITE,109)
      READ(IREAD,*) ICORR
      IF(ICORR.EQ.1) GO TO 300
      GO TO 200
 750   CALL CLEAR
      IF(IDATA.EQ.'Y') CALL ASSIGN(2,'L1.DAT')
      IF(LAMNUM.EQ.2.AND.IDATA.EQ.'Y') CALL ASSIGN(3,'L2.DAT')
      OM=OMI
      IF(IPR.EQ.'Y') WRITE(IDEV,706) IORD,KAPPA,OMI,OMA
 706   FORMAT(13X,' PARAMETER SUMMARY ',//,' For the reaction chain',//,
     1 2X,' order of the reaction chain:',I5,//,
     4 2X,' for the removal rate',//,
     5 2X,' first order rate constant ',1PD15.5,//,
     6 2X,' range on 1/Omega: ',2(1PD15.5),//)
      IF(IPR.EQ.'Y') WRITE(IDEV,512) NU,PMIN,PMAX
      IF(IPR.EQ.'Y'.AND.LAMNUM.EQ.1) WRITE(IDEV,704)
 704   FORMAT(
     1  ' _____'//,
     2  ' Saturation Binding Poores product',//,
     3  ' velocity constant Magic number concentration',//,
     4  ' 1/Omega pi',//)
      IF(IPR.EQ.'Y'.AND.LAMNUM.EQ.2) WRITE(IDEV,514)
      IF(IPR.EQ.'Y'.AND.LAMNUM.EQ.2) WRITE(IDEV,705)
 705   FORMAT(
     1  ' Saturation Binding Poores Binding ',
     2  ' Poores',//,
     3  ' velocity constant Magic number constant ',
     4  ' Magic number',//,
     5  ' 1/Omega 1 1 2 ',
     6  ' 2 ')
C-----0-----0-----0-----0-----0-----0-----0-----0-----
C a DO-loop that computes the critical value of Binding constnats and
the
C magic number as a function of 1/Omega.
 800   DO 8 I8=1,IPTS
      OMEGA=1.DO/OM
      CALL CRVL(PI,LAMBDA,L,RNU,LOOP,KAPPA,OMEGA,IORD,XI,PHI,RTOL,
     1 FTOL,ITRTOL,IBUGL,IBUGP,IBUGW,IWRIT1,PMIN,PMAX,FACTOR,1)
      IF(LOOP.EQ.1) BIND1=LAMBDA
      IF(LOOP.EQ.2) BIND1=L
      IF(BIND1.GE.PMAX) GO TO 81
      SAV1=X1
      CALL MAGNUM(X1,ISIGN,IORD,TAUR,TAUI,XI,PHI,LAMBDA,L,
     1 NU,RNU,LOOP,KAPPA,OMEGA,PI,IBUGM,IBUGW,IWRIT1,RTOL,FTOL,ITRTOL)
Check for sign change on the magic number
      IF(IDATA.NE.'Y') GO TO 82
      IF(SAV1*X1.GE.0.DO.OR.I8.EQ.1) GO TO 82

```

```

IF(IRATIO.EQ.2) BIND1=BIND1*OMEGA/KAPPA
WRITE(2) SNGL(OM),SNGL(BIND1),SNGL(X1),SNGL(PI)
CALL CLOSE(2)
CALL ASSIGN(2,'L3.DAT')
82 IF(IRATIO.EQ.2.AND.X1*SAV1.GE.0.D0) BIND1=BIND1*OMEGA/KAPPA
IF(IDATA.EQ.'Y') WRITE(2) SNGL(OM),SNGL(BIND1),SNGL(X1),SNGL(PI)
IF(LAMNUM.EQ.1) GO TO 83
Check if there are more than one BIND values to be calculated
IF(MERGE1.EQ.'Y'.AND.IDATA.EQ.'Y')
1 WRITE(3) SNGL(OM),SNGL(BIND1),SNGL(X1),SNGL(PI)
MERGE1='N'
IF(LOOP.EQ.1) BIND2=LAMBDA
IF(LOOP.EQ.2) BIND2=L
PMI=BIND2*1.001D0
CALL CRVL(PI,LAMBDA,L,RNU,LOOP,KAPPA,OMEGA,IORD,XI,PHI,RTOL,
1 FTOL,ITRTOL,IBUGL,IBUGP,IBUGW,IWRIT1,PMI,PMAX,FACTOR,1)
IF(LOOP.EQ.1) BIND2=LAMBDA
IF(LOOP.EQ.2) BIND2=L
IF(BIND2.GE.PMAX) GO TO 84
SAV2=X2
CALL MAGNUM(X2,ISIGN,IORD,TAUR,TAUI,XI,PHI,LAMBDA,L,
1 NU,RNU,LOOP,KAPPA,OMEGA,PI,IBUGM,IBUGW,IWRIT1,RTOL,FTOL,ITRTOL)
Check for sign change on the magic number
IF(IDATA.NE.'Y') GO TO 85
IF(SAV2*X2.GE.0.D0.OR.I8.EQ.1) GO TO 85
IF(IRATIO.EQ.2) BIND2=BIND2*OMEGA/KAPPA
WRITE(3) SNGL(OM),SNGL(BIND2),SNGL(X2),SNGL(PI)
CALL CLOSE(3)
CALL ASSIGN(3,'L4.DAT')
85 IF(IRATIO.EQ.2.AND.X2*SAV2.GE.0.D0) BIND2=BIND2*OMEGA/KAPPA
IF(IDATA.EQ.'Y') WRITE(3) SNGL(OM),SNGL(BIND2),SNGL(X2),SNGL(PI)
C if both roots of BIND are found
IF(IPR.EQ.'Y') WRITE(IDEV,601) OM,BIND1,X1,BIND2,X2
IF(MERGE2.NE.'Y') GO TO 86
BIND=BIND1
OME=OM
GO TO 86
C if one value of BIND exists
84 IF(IPR.EQ.'Y') WRITE(IDEV,602) OM,BIND1,X1
IF(MERGE2.NE.'Y') GO TO 86
BIND=BIND1
OME=OM
GO TO 86
C if neither root is found
81 IF(IPR.EQ.'Y') WRITE(IDEV,604) OM
GO TO 86
C if one value of BIND is to be computed
83 IF(IPR.EQ.'Y') WRITE(IDEV,603) OM,BIND1,X1,PI
IF(MERGE2.NE.'Y') GO TO 86
BIND=BIND1

```

```
      OME=OM
86    IF(ILOG.EQ.'Y') OM=DEXP(DLOG(OM)+DEL)
8      IF(ILOG.NE.'Y') OM=OM+DEL
      IF(IDATA.EQ.'Y'.AND.MERGE2.EQ.'Y'.AND.LAMNUM.EQ.2)
1    WRITE(3) SNGL(OME),SNGL(BIND),SNGL(X1),SNGL(PI)
1000  STOP
      END
```

```

SUBROUTINE BLOC(ROOT,LAMBDA,RNU,LOOP,IORD,XI,PHI,RTOL,FTOL,
  1 ITRTOL,IWRITE,IBUG,IBUGW)
C-----0-----0-----0-----0-----0-----0-----0-----0-----
C A subroutine that computes the roots of
C
C           1
C           0 = ----- + 1
C             nu*kappa
C
C for LOOP = 1, and
C
C
C           4*I
C           0 = ----- + Lambda
C             ( ( -1 ) ) 2
C             nu*(1 - (-----))
C             ( ( nu*kappa ))
C
C for LOOP = 2, using the function BLO and the secant method
C-----0-----0-----0-----0-----0-----0-----0-----
      IMPLICIT DOUBLE PRECISION(A-H,O-Z)
      DOUBLE PRECISION DABS,LAMBDA
      DIMENSION XI(5),PHI(5)
      IF(IBUG.NE.'Y') GO TO 200
      WRITE(IWRITE,101) LOOP,LAMBDA,RNU
101   FORMAT(' in BLOC ',/, ' loop type: ',I2,' Lambda = ',1PD15.5,
  2 ' nu = ',1PD15.5,/)

      IODD=MOD(IORD,2)
      DO 300 I3=1,IORD/2+IODD
300   WRITE(IWRITE,102) I3,XI(I3),PHI(I3)
102   FORMAT(' For subsystem ',I3,' xi= ',1PD15.5,' phi= ',1PD15.5)
200   VALUE=BLO(ROOT,IORD,XI,PHI,LAMBDA,RNU,LOOP,IBUG,IBUGW,IWRITE,
  1 RTOL,FTOL,ITRTOL)
      FACTOR=2.D0
      IF(LOOP.EQ.2) FACTOR=1.1D0
201   SAV=VALUE
      ROOT=FACTOR*ROOT
      VALUE=BLO(ROOT,IORD,XI,PHI,LAMBDA,RNU,LOOP,IBUG,IBUGW,IWRITE,
  1 RTOL,FTOL,ITRTOL)
      IF(ROOT.GT.1D10) GO TO 100
      IF(SAV*VALUE.GT.0.D0) GO TO 201
C-----0-----0-----0-----0-----0-----0-----0-----
Compute root using secant method
      B=ROOT
      A=ROOT/FACTOR
      FB=VALUE
      FA=SAV
      ROOT=A
      FROOT=FA
      SIGNA=DSIGN(1.D0,FA)

```

```
DO 21 I1=1,ITRTOL
IF(DABS(B-A).LT.RTOL) GO TO 202
IF(DABS(FROOT).LT.FTOL) GO TO 202
ROOT=(FA*B-FB*A)/(FA-FB)
PREV=DSIGN(1.D0,FROOT)
FROOT=BLO(ROOT,IORD,XI,PHI,LAMBDA,RNU,LOOP,IBUG,IBUGW,IWRITE,
1 RTOL,FTOL,ITRTOL)
IF(SIGMA*FROOT.LT.0.D0) GO TO 10
A=ROOT
FA=FROOT
IF(FROOT*PREV.GT.0.D0) FB=FB/2.D0
GO TO 21
10 B=ROOT
FB=FROOT
IF(FROOT*PREV.GT.0.D0) FA=FA/2.D0
21 CONTINUE
202 IF(I1.EQ.ITRTOL) WRITE(IWRITE,207)
207 FORMAT('*** MAXIMUM ITERATIONS ***')
RETURN
100 WRITE(IWRITE,103)
103 FORMAT(' no root for kappa less than 1D10')
RETURN
END
```

```

FUNCTION BLO(KAPPA,IORD,XI,PHI,LAMBDA,RNU,LOOP,
1 IBUG,IBUGW,IWRITE,RTOL,FTOL,ITRTOL)
C-----0-----0-----0-----0-----0-----0-----0-----0
C A function that computes the criterion for dynamic
C instability in the limit where pi --> 0.
C Here we want to compute
C
C      1
C      BLO = ----- + 1
C            nu kappa
C
C for LOOP = 1, and
C
C
C      4*1
C      BLO = ----- + Lambda
C      ( ( -1 ) ) 2
C      nu*(1 - (-----))
C            ( ( nu*kappa) )
C
C for LOOP = 2.
C-----0-----0-----0-----0-----0-----0-----0-----0
IMPLICIT DOUBLE PRECISION(A-H,O-Z)
DOUBLE PRECISION KAPPA,LAMBDA
DIMENSION XI(5),PHI(5)
TD=0.D0
CALL LOCIN(X4,W,IORD,XI,PHI,TD,KAPPA,RTOL,FTOL,ITRTOL,
1 IWRITE,IBUGW)
BLO=X4/(RNU*KAPPA)+1.D0
IF(LOOP.EQ.2) BLO=(4.D0*X4)/(RNU*BLO**2)+LAMBDA
IF(IBUG.EQ.'Y') WRITE(IWRITE,101) KAPPA,BLO
101 FORMAT(' kappa = ',1PD20.10,' BLO = ',1PD20.10)
RETURN
END

```

```

FUNCTION BL(KAPPA)
C-----0-----0-----0-----0-----0-----0-----0-----0
C
C      - 4*1
C      BL = -----
C      ( ( -1 ) ) 2
C      nu*(1 - (-----))
C            ( ( nu*kappa) )
C
C-----0-----0-----0-----0-----0-----0-----0-----0
IMPLICIT DOUBLE PRECISION(A-H,O-Z)
COMMON/BL/IORD,XI,PHI,LAMBDA,RNU,IBUG,IBUGW,IWRITE,

```

```
1 RTOL,FTOL,ITRTOL
      DOUBLE PRECISION KAPPA,LAMBDA
      DIMENSION XI(5),PHI(5)
      TD=0.D0
      CALL LOCIN(X4,W,IORD,XI,PHI,TD,KAPPA,RTOL,FTOL,ITRTOL,
1 IWRITE,IBUGW)
      BL=X4/(RNU*KAPPA)+1.D0
      BL=-(4.D0*X4)/(RNU*BL**2)
      IF(IBUG.EQ.'Y') WRITE(IWRITE,101) KAPPA,BL
101    FORMAT(' kappa = ',1PD20.10,' BL = ',1PD20.10)
      RETURN
      END
```

```

      SUBROUTINE CRVL(PI,LAMBDA,L,RNU,LOOP,KAPPA,OMEGA,IORD,XI,PHI,
1 RTOL,FTOL,ITRTOL,IBUGL,IBUGP,IBUGW,IWRITE,PMIN,PMAX,FACTOR,IOPT)
C-----0-----0-----0-----0-----0-----0-----0-----
C Subroutine CRITICAL Value of Lambda for loop 1
C
C A subroutine that finds the critical value of Lambda-sub-pi
C using the subroutine CRL and modified regula falsi.
C
C The parameters are
C     PMIN, PMAX : lower and upper bounds on the region to be searched
C     IOPT       : if the subroutine is to search for two initial
C                   guesses with functional values with opposite signs
C                   then IOPT= 1. If IOPT=2 then PMIN and PMAX are
C                   taken to be such guesses
C     FACTOR    : factor that Lambda is increased by during the search
C                   from the previous value, if IOPT=1.
C-----0-----0-----0-----0-----0-----0-----
      IMPLICIT DOUBLE PRECISION(A-H,O-Z)
      DOUBLE PRECISION LAMBDA,L,KAPPA,DABS,DBLE,DSIGN
      DIMENSION XI(5),PHI(5)
      IF(IBUGL.NE.'Y') GO TO 40
      WRITE(IWRITE,101) LAMBDA,L,RNU,PMIN,PMAX,LOOP,KAPPA,OMEGA,IORD
101  FORMAT(' In CRVL:',/
1     ' LAMBDA = ',1PD15.5,' L      = ',1PD15.5,' RNU    = ',1PD15.5,/,/
2     ' BIN-min= ',1PD15.5,' BIN-max= ',1PD15.5,' LOOP   = ',I15,/,/
3     ' KAPPA  = ',1PD15.5,' OMEGA  = ',1PD15.5,' ORDER  = ',I15)
      IODD=MOD(IORD,2)
      DO 90 I9=1,IORD/2+IODD
90   WRITE(IWRITE,102) I9,XI(I9),PHI(I9)
102  FORMAT(' For subsystem ',I3,' xi= ',1PD15.5,' phi= ',1PD15.5)
40   IF(IOPT.EQ.1) GO TO 20
C-----0-----0-----0-----0-----0-----0-----
C initialize regula falsi for IOPT=2
      IF(LOOP.EQ.1) LAMBDA=PMIN
      IF(LOOP.EQ.2) L=PMIN
      CALL CRL(LAMBDA,L,RNU,LOOP,KAPPA,OMEGA,IORD,XI,PHI,RTOL,FTOL,
1 ITRTOL,IBUGL,IBUGP,IBUGW,IWRITE,FA,PI,ISIGN)
      A=PMIN
      IF(LOOP.EQ.1) LAMBDA=PMAX
      IF(LOOP.EQ.2) L=PMAX
      CALL CRL(LAMBDA,L,RNU,LOOP,KAPPA,OMEGA,IORD,XI,PHI,RTOL,FTOL,
1 ITRTOL,IBUGL,IBUGP,IBUGW,IWRITE,FB,PI,ISIGN)
      B=PMAX
      GO TO 30
C-----0-----0-----0-----0-----0-----0-----
Compute an estimate of the root
20   IF(LOOP.EQ.1) LAMBDA=PMIN
      IF(LOOP.EQ.2) L=PMIN
      CALL CRL(LAMBDA,L,RNU,LOOP,KAPPA,OMEGA,IORD,XI,PHI,RTOL,FTOL,
1 ITRTOL,IBUGL,IBUGP,IBUGW,IWRITE,CRTLAM,PI,ISIGN)

```

```

BINDC=PMIN
100 SAVLAM=CRTLAM
      BINDC=FACTOR*BINDC
      IF(BINDC.GT.PMAX) GO TO 200
      IF(LOOP.EQ.1) LAMBDA=BINDC
      IF(LOOP.EQ.2) L=BINDC
      CALL CRL(LAMBDA,L,RNU,LOOP,KAPPA,OMEGA,IORD,XI,PHI,RTOL,FTOL,
1 ITRTOL,IBUGL,IBUGP,IBUGW,IWRITE,CRTLAM,PI,ISIGN)
      IF(SAVLAM*CRTLAM.GT.0.D0) GO TO 100
C-----0-----0-----0-----0-----0-----0-----0-----
C initialize regula falsi for IOPT=1
      FA=SAVLAM
      A=BINDC/FACTOR
      FB=CRTLAM
      B=BINDC
C-----0-----0-----0-----0-----0-----0-----0-----
Compute the root using modified regula falsi method
30   BINDC=A
      FLA=FA
      SIGNA=DSIGN(1.D0,FA)
      DO 300 I3=1,ITRTOL
      IF(DABS(B-A).LT.RTOL) GO TO 200
      IF(DABS(FLA).LT.FTOL) GO TO 200
      BINDC=(FA*B-FB*A)/(FA-FB)
      PREV=DSIGN(1.D0,FLA)
      IF(LOOP.EQ.1) LAMBDA=BINDC
      IF(LOOP.EQ.2) L=BINDC
      CALL CRL(LAMBDA,L,RNU,LOOP,KAPPA,OMEGA,IORD,XI,PHI,RTOL,FTOL,
1 ITRTOL,IBUGL,IBUGP,IBUGW,IWRITE,FLA,PI,ISIGN)
      IF(SIGNA*FLA.LT.0.D0) GO TO 10
      A=BINDC
      FA=FLA
      IF(FLA*PREV.GT.0.D0) FB=FB/2.D0
      GO TO 300
10    B=BINDC
      FB=FLA
      IF(FLA*PREV.GT.0.D0) FA=FA/2.D0
300  CONTINUE
200  IF(LOOP.EQ.1) LAMBDA=BINDC
      IF(LOOP.EQ.2) L=BINDC
      IF(I3.EQ.ITRTOL) WRITE(IDEV,103)
103  FORMAT('*** ITERATIONS EXCEEDED WHEN ITERATING ON LAMBDA ***')
      RETURN
      END

```

```

SUBROUTINE CRL(LAMBDA,L,RNU,LOOP,KAPPA,OMEGA,IORD,XI,PHI,RTOL,
 1 FTOL,ITRTOL,IBUGL,IBUGP,IBUGW,IWRITE,TEST,PI,ISIGN)
C-----0-----0-----0-----0-----0-----0-----0-----
C Subroutine CRIteria for Loop 1
C
C A subroutine that computes the value of the stability
C criterion
C
C           2 Omega(      nu*kappa )
C TEST = pi + ----- (2 + (1-Omega)(-----))pi
C           kappa(      1      )
C
C           Omega 2(      nu*kappa )
C           + (-----) .(1 + (-----))
C           Kappa (      1      )
C
C if LOOP = 1, and          2
C           (      Omega)   1
C TEST = pi*TEST + ( pi + ----- ) -----
C           (      Kappa) Lambda
C if LOOP = 2.
C-----0-----0-----0-----0-----0-----0-----0-----
IMPLICIT DOUBLE PRECISION(A-H,O-Z)
DOUBLE PRECISION LAMBDA,L,KAPPA
DIMENSION XI(5),PHI(5)
C solve for the product concentration
CALL STSTCO(LAMBDA,L,RNU,LOOP,KAPPA,OMEGA,RTOL,FTOL,ITRTOL,
 1 IBUGP,IWRITE,PI)
C find the locus 1
SLOPE=KAPPA/(1.D0+KAPPA*PI/OMEGA)**2
TD=0.D0
CALL LOCIN(X4,W,IORD,XI,PHI,TD,SLOPE,RTOL,FTOL,ITRTOL,
 1 IWRITE,IBUGW)
BB=X4/(RNU*KAPPA)
Compute the criterion
RATIO=OMEGA/KAPPA
TEST=PI**2+RATIO*(2.D0+(1.D0-OMEGA)/BB)*PI+
 1 RATIO**2*(1.D0+1.D0/BB)
IF(LOOP.EQ.2) TEST=PI*TEST+(PI+RATIO)**2/LAMBDA
ISIGN='-
IF(TEST.GE.0.D0) ISIGN='+
IF(IBUGL.EQ.'Y') WRITE(IWRITE,101)
101 FORMAT(' In CRL: ')
IF(IBUGL.EQ.'Y') WRITE(IWRITE,102)LAMBDA,L,TEST
102 FORMAT(1H+,' LAMBDA= ',1PD20.10,' L = ',1PD20.10,
 1 ' CRITERIA= ',1PD15.5)
RETURN
END

```



```

1  ' kappa = ',1PD15.5,' Omega = ', 1PD15.5,/
2  ' The parameters for the input rate are:',/
3  ' Lambda = ',1PD15.5,' L = ',1PD15.5,' nu = ',1PD15.5)
IF(IBUG.EQ.'Y') WRITE(IWRITE,102) IORD
102 FORMAT(' The parameters for the reaction chain are:/'
1  ' Order = ',I2)
N2=IORD/2+MOD(IORD,2)
DO 3 I2=1,N2
3  IF(IBUG.EQ.'Y') WRITE(IWRITE,109) XI(I2),PHI(I2)
109 FORMAT( ' xi = ',1PD15.5,' phi = ',1PD15.5)
DO 4 I4=1,IORD
4  IF(IBUG.EQ.'Y') WRITE(IWRITE,110) TAUR(I4),TAUI(I4)
110 FORMAT(' Tau = ',2(1PD15.5))
IF(IBUG.EQ.'Y') WRITE(IWRITE,108) PI
108 FORMAT(
2  ' The steady state concentration of product is = ',1PD15.5)
C-----0-----0-----0-----0-----0-----0-----0-----
C Derivatives of Omega(pi)
OM=KAPPA*PI/(1.D0+KAPPA*PI/OMEGA)
OM1=(OM/PI)**2/KAPPA
OM2=(2.D0*OM/(KAPPA*PI**3))*(PI*OM1-OM)
OM3=(-(3.D0*OM-PI*OM1)/PI**4)*(PI*OM1-OM)+OM*OM2/PI**2
OM3=2.D0*OM3/KAPPA
IF(IBUG.EQ.'Y') WRITE(IWRITE,103) OM,OM1,OM2,OM3
103 FORMAT(' For the removal rate:/'
1  ' rate           = ',1PD15.5,/
2  ' 1st derivative = ',1PD15.5,/
3  ' 2nd derivative = ',1PD15.5,/
4  ' 3rd derivative = ',1PD15.5)
C-----0-----0-----0-----0-----0-----0-----0-----
C Derivatives of Psi(pi)
      IF(LOOP.EQ.2) GO TO 99
      PI1=PI
      PSI=1.D0/(1.D0+(LAMBDA*PI)**NU)
      GO TO 100
99      PI1=PI+1.D0/LAMBDA
      PSI=1.D0/(1.D0+L*(1.D0+LAMBDA*PI)**NU)
100      PSI1=RNU*(PSI-1.D0)*PSI/PI1
      PSI2=(RNU/PI1)*(PSI*(1.D0-PSI)/PI1+PSI1*(2.D0*PSI-1.D0))
      PSI3=(RNU/PI1**2)*((2.D0/PI1)*(PSI-1.D0)*PSI-2.D0*PSI1*
1  (2.D0*PSI-PSI1*PI1-1.D0)+PI1*PSI2*(2.D0*PSI-1.D0))
      IF(IBUG.EQ.'Y') WRITE(IWRITE,104) PSI,PSI1,PSI2,PSI3
104      FORMAT(' For the input rate:/'
1  ' rate           = ',1PD15.5,/
2  ' 1st derivative = ',1PD15.5,/
3  ' 2nd derivative = ',1PD15.5,/
4  ' 3rd derivative = ',1PD15.5)

```

```

C-----0-----0-----0-----0-----0-----0-----0-----0-----0-----0-----0
C Frequency
      TD=0.D0
      CALL LOCIN(GAIN,W,IORD,XI,PHI,TD,OM1,RTOL,FTOL,ITRTOL,IWRITE,
1     IBUGW)
      IF(IBUG.EQ.'Y') WRITE(IWRITE,105) W,GAIN
105    FORMAT(' Frequency = ',1PD15.5,/
1           ' Gain      = ',1PD15.5)
C-----0-----0-----0-----0-----0-----0-----0-----0-----0-----0-----0
C evaluation of
C
C      n+1   tau
C      k
C SUM = SUM   ----- , PRO = -----
C      1 + iw*tau          1
C      k                   g(iw)
C
C-----0-----0-----0-----0-----0-----0-----0-----0-----0-----0-----0
Compute AA = iw
      AA(1)=0.D0
      AA(2)=W
C initialize
      SUM(1)=0.D0
      SUM(2)=0.D0
      PRO(1)=1.D0
      PRO(2)=0.D0
      DO 1 I1=1,IORD
      TAU(1)=TAUR(I1)
      TAU(2)=TAUI(I1)
Compute BB = tau*iw
      CALL CMULT(AA,TAU,BB)
Compute BB = 1 + tau*iw
      BB(1)=BB(1)+1.D0
Compute CC = tau/(1 + tau*iw)
      CALL CDIV(TAU,BB,CC)
Compute sum
      SUM(1)=SUM(1)+CC(1)
      SUM(2)=SUM(2)+CC(2)
      IF(IBUG.EQ.'Y') WRITE(IWRITE,116) I1,BB(1),BB(2),CC(1),CC(2)
116    FORMAT(' For pole   ',I5,/
1           ' 1 + tau*iw      = ',2(1PD15.5),/
2           ' tau/(1+tau*iw) = ',2(1PD15.5))
Computation of PRO = 1/g(iw)
      CC(1)=PRO(1)
      CC(2)=PRO(2)
      CALL CMULT(BB,CC,PRO)
1     IF(IBUG.EQ.'Y') WRITE(IWRITE,117) SUM(1),SUM(2),PRO(1),PRO(2)
117    FORMAT(' SUM = ',2(1PD15.5),/
2           ' PRO = ',2(1PD15.5))
C add the last term to the sum corresponding to OM1

```

```

C           n      tau
C           k
C           1/0m1
C SUM = SUM - ----- + -----
C           1 + iw#tau   1 + iw/0m1
C           k=1          k
C
Compute AA = 1 + iw/0m1
AA(1)=1.D0
AA(2)=W/OM1
Compute BB = 1/0m1
BB(1)=1.D0/OM1
BB(2)=0.D0
Compute CC = (1/0m1)/(1 + iw/0m1)
CALL CDIV(BB,AA,CC)
SUM(1)=SUM(1)+CC(1)
SUM(2)=SUM(2)+CC(2)
IF(IBUG.EQ.'Y') WRITE(IWRITE,106) SUM(1),SUM(2)
106 FORMAT(' The divider is = ',2(1PD15.5))
C-----0-----0-----0-----0-----0-----0-----0-----0
C           1
C evaluation of PRO1 = -----
C           g(2*iw)
C-----0-----0-----0-----0-----0-----0-----0-----0
Compute AA = 2*iw
AA(1)=0.D0
AA(2)=2.D0*W
C initialize
PRO1(1)=1.D0
PRO1(2)=0.D0
DO 2 I2=1,IORD
TAU(1)=TAUR(I2)
TAU(2)=TAUI(I2)
Compute BB = tau*2*iw
CALL CMULT(AA,TAU,BB)
Compute BB = 1 + tau*2*iw
BB(1)=BB(1)+1.D0
Computation of 1/g(2*iw)
IF(IBUG.EQ.'Y') WRITE(IWRITE,118) I2,BB(1),BB(2)
118 FORMAT(' For pole ',I5,'
           1 + tau*2*iw      = ',2(1PD15.5))
           CC(1)=PRO1(1)
           CC(2)=PRO1(2)
           CALL CMULT(BB,CC,PRO1)
2           IF(IBUG.EQ.'Y') WRITE(IWRITE,119) PRO1(1),PRO1(2)
119 FORMAT(' PRO1 = ',2(1PD15.5))

```

```

C-----0-----0-----0-----0-----0-----0-----0-----0-----0-----
C-----0-----0-----0-----0-----0-----0-----0-----0-----0-----
C evaluation of PRO2 = ----- = -----
C-----0-----0-----0-----0-----0-----0-----0-----0-----0-----
C-----0-----0-----0-----0-----0-----0-----0-----0-----0-----
C-----0-----0-----0-----0-----0-----0-----0-----0-----0-----
Compute BB = 1 + 2*iw/0m1
    BB(1)=0M1
    BB(2)=2.D0*W
    CALL CMULT(PRO1,BB,PRO2)
    IF (IBUG.EQ.'Y') WRITE(IWRITE,107) PRO2(1),PRO2(2)
107   FORMAT(' The inverse of g (2iw) is = ',2(1PD15.5),/
2           '           +')
C-----0-----0-----0-----0-----0-----0-----0-----0-----0-----
Compute the magic number, start by computing
C
C-----0-----0-----0-----0-----0-----0-----0-----0-----0-----
C-----0-----0-----0-----0-----0-----0-----0-----0-----0-----
C-----0-----0-----0-----0-----0-----0-----0-----0-----0-----
C-----0-----0-----0-----0-----0-----0-----0-----0-----0-----
C-----0-----0-----0-----0-----0-----0-----0-----0-----0-----
Compute numerator
    AA(1)=PSI2-0M2*PRO1(1)
    AA(2)=-0M2*PRO1(2)
Compute denominator
    PRO2(1)=PSI1-PRO2(1)
    PRO2(2)=-PRO2(2)
    CALL CDIV(AA,PRO2,CC)
C-----0-----0-----0-----0-----0-----0-----0-----0-----0-----
Compute
C-----0-----0-----0-----0-----0-----0-----0-----0-----0-----
C-----0-----0-----0-----0-----0-----0-----0-----0-----0-----
C-----0-----0-----0-----0-----0-----0-----0-----0-----0-----
C-----0-----0-----0-----0-----0-----0-----0-----0-----0-----
C-----0-----0-----0-----0-----0-----0-----0-----0-----0-----
C-----0-----0-----0-----0-----0-----0-----0-----0-----0-----
C-----0-----0-----0-----0-----0-----0-----0-----0-----0-----
C-----0-----0-----0-----0-----0-----0-----0-----0-----0-----
CC(1)=CC(1)+2.D0*((PSI2-0M2)/(PSI1-0M1))
C-----0-----0-----0-----0-----0-----0-----0-----0-----0-----
Compute
C-----0-----0-----0-----0-----0-----0-----0-----0-----0-----
C-----0-----0-----0-----0-----0-----0-----0-----0-----0-----
C-----0-----0-----0-----0-----0-----0-----0-----0-----0-----
C-----0-----0-----0-----0-----0-----0-----0-----0-----0-----
BB(1)=PSI2-0M2*PRO(1)
BB(2)=-0M2*PRO(2)

```

```

C-----0-----0-----0-----0-----0-----0-----0-----0-----0-----0-----0
Compute
C   ( Psi2-Om2   Psi2-Om2/g(2iw))(
C AA = (2#----- + -----)(Psi2 - -----)
C   ( Psi1-Om1   Psi1-1/g (2iw) )(      g(iw))
C
C-----0-----0-----0-----0-----0-----0-----0-----0-----0-----0-----0
      CALL CMULT(CC,BB,AA)
C-----0-----0-----0-----0-----0-----0-----0-----0-----0-----0-----0
Compute
C   Om3          ( Psi2-Om2   Psi2-Om2/g(2iw))(
C AA = ----- - Psi3 + (2#----- + -----)(Psi2 - -----)
C   g(iw)          ( Psi1-Om1   Psi1-1/g (2iw) )(      g(iw))
C
C-----0-----0-----0-----0-----0-----0-----0-----0-----0-----0-----0
      AA(1)=AA(1)+OM3*PRO(1)-PSI3
      AA(2)=AA(2)+OM3*PRO(2)
C-----0-----0-----0-----0-----0-----0-----0-----0-----0-----0-----0
Compute
C
C   Om3          ( Psi2-Om2   Psi2-Om2/g(2iw))(
C   ----- - Psi3 + (2#----- + -----)(Psi2 - -----)
C   g(iw)          ( Psi1-Om1   Psi1-1/g+(2iw) )(      g(iw))
C Mn = -----
C
C           n+1   tau
C           k
C           SUM -----
C           1 + iw*tau
C           k
C
C-----0-----0-----0-----0-----0-----0-----0-----0-----0-----0-----0
      CALL CDIV(AA,SUM,BB)
C then the magic number is the real part of the above number
X=BB(1)/PSI1
IF(IBUG.EQ.'Y') WRITE(IWRITE,112) X
112  FORMAT(' For the computation of the magic number',//,
1     ' The magic number is = ',1PD15.5//)
ISIGN='+''
IF(X.LT.0.D0) ISIGN='-''
RETURN
END

```

```
SUBROUTINE CMULT(A,B,C)
C-----0-----0-----0-----0-----0-----0-----0-----0-----
C A subroutine that multiplies two complex numbers A and B and
C returns the product in C
C-----0-----0-----0-----0-----0-----0-----0-----0-----
IMPLICIT DOUBLE PRECISION(A-H,O-Z)
DIMENSION A(2),B(2),C(2)
C(1)=A(1)*B(1)-A(2)*B(2)
C(2)=A(1)*B(2)+A(2)*B(1)
RETURN
END

SUBROUTINE CDIV(A,B,C)
C-----0-----0-----0-----0-----0-----0-----0-----0-----
C A subroutine that divides a complex number A with a complex number
C B and returns the quotient in C
C-----0-----0-----0-----0-----0-----0-----0-----0-----
IMPLICIT DOUBLE PRECISION(A-H,O-Z)
DIMENSION A(2),B(2),C(2)
DIV=B(1)**2+B(2)**2
C(1)=(A(1)*B(1)+A(2)*B(2))/DIV
C(2)=(A(2)*B(1)-A(1)*B(2))/DIV
RETURN
END
```

```

SUBROUTINE STSTCO(LAMBDA,L,RNU,LOOP,KAPPA,OMEGA,RTOL,FTOL,
1 ITRTOL,IBUG,IWRITE,PI)
C-----0-----0-----0-----0-----0-----0-----0-----0
C Subroutine STeady SState COncentration
C
C A subroutine that solves for the steady state concentration
C of the product which is given by (for LOOP = 1)
C
C
C     1           kappa*pi
C   ----- = -----
C     nu           kappa*pi
C   1 + (Lambda*pi)   1 + -----
C                           Omega
C
C and is for LOOP = 2
C
C     1           kappa*pi
C   ----- = -----
C     nu           kappa*pi
C   1 + L(1+Lambda*pi)   1 + -----
C                           Omega
C
C The subroutine starts with 1.d-12 as an initial guess for the steady
C state concentration of PI. It then searches for the root by increasing
C the guess by a factor of XMULT. When a sign change is detected a
C modified regula falsi method is invoked.
C-----0-----0-----0-----0-----0-----0-----0
      IMPLICIT DOUBLE PRECISION(A-H,O-Z)
      DOUBLE PRECISION LAMBDA,L,KAPPA,DSQRT,DABS,DSIGN
C-----0-----0-----0-----0-----0-----0-----0
C search for root. Initially the guess is increased by two
C orders of magnitide.
      IF(IBUG.EQ.'Y') WRITE(IWRITE,101) LAMBDA,L,RNU,KAPPA,OMEGA
101  FORMAT(/' In STSTCO: ',/
      1 ' LAMBDA = ',1PD15.5,' L      = ',1PD15.5,' RNU = ',1PD15.5,/,'
      2 ' KAPPA = ',1PD15.5,' OMEGA = ',1PD15.5/)
      XMULT=100.D0
      PI=1.D-12
      CALL MSSEQN(LAMBDA,L,RNU,LOOP,KAPPA,OMEGA,PI,FR,INEG,IBUG,
      1 IWRITE)
200  SAVE=FR
300  PI=XMULT*PI
      CALL MSSEQN(LAMBDA,L,RNU,LOOP,KAPPA,OMEGA,PI,FR,INEG,IBUG,
      1 IWRITE)
      IF(INEG.GT.0) GO TO 100
C if INEG takes a negative value it means that the modified form of
C the steady state function used by MSSEQN has to take logarithms of
C a negative value. In this case we must reduce XMULT.
      PI=PI/XMULT
      XMULT=DSQRT(XMULT)

```

```

C if the following two criteria are met terminate the search procedure
C since they are equivalent to finding the root
    IF(((XMULT-1.D0).LT.RTOL).OR.((XMULT-1.D0).LT.1D-14)) GO TO 500
    IF(DABS(FR).LT.FTOL) GO TO 500
    GO TO 300
C check for a sign change
100   IF(SAVE*FR.GT.0.D0) GO TO 200
C-----0-----0-----0-----0-----0-----0-----
C start regula falsi
B=PI
A=PI/XMULT
FB=FR
FA=SAVE
PI=A
FPI=FA
SIGNA=DSIGN(1.D0,FA)
DO 400 I1=1,ITRTOL
IF(DABS(B-A).LT.RTOL) GO TO 500
IF(DABS(FPI).LT.FTOL) GO TO 500
PI=(FA*B-FB*A)/(FA-FB)
PREV=DSIGN(1.D0,FPI)
CALL MSSEQN(LAMBDA,L,RNU,LOOP,KAPPA,OMEGA,PI,FPI,INEG,IBUG,
1  IWRITE)
IF(SIGNA*FPI.LT.0.D0) GO TO 10
A=PI
FA=FPI
IF(FPI*PREV.GT.0.D0) FB=FB/2.D0
GO TO 400
10
B=PI
FB=FPI
IF(FPI*PREV.GT.0.D0) FA=FA/2.D0
400
CONTINUE
500
IF(I1.EQ.ITRTOL) WRITE(IDEV,102)
FORMAT('*** MAXIMUM ITERATIONS WHEN SOLVING FOR PI-STST ***')
102
RETURN
END

```

```

      SUBROUTINE MSSEQN(LAMBDA,L,RNU,LOOP,KAPPA,OMEGA,PI,FR,INEG,IBUG,
1 IWRITE)
C-----0-----0-----0-----0-----0-----0-----0-----
C Subroutine Modified Steady State EQuatioN
C
C A subroutine that computes
C
C FR = nu*log(pi) + nu*log(lambda) - log(----- + ----- - 1 )
C
C if LOOP = 1, and
C
C FR = log(L) + nu*log(1+lambda*pi) - log(----- + ----- - 1 )
C
C if LOOP = 2, which is a rearranged form of the steady state equation.
C-----0-----0-----0-----0-----0-----0-----
      IMPLICIT DOUBLE PRECISION(A-H,O-Z)
      DOUBLE PRECISION LAMBDA,L,KAPPA,DLOG
      IF(IBUG.EQ.'Y') WRITE(IWRITE,101)
101    FORMAT(' In MSSEQN: ')
      INEG=1
      IF(LOOP.EQ.1) FRP=RNU*(DLOG(PI)+DLOG(LAMBDA))
      IF(LOOP.EQ.2) FRP=DLOG(L)+RNU*DLOG(1.D0+PI*LAMBDA)
      FRM=1.D0/(KAPPA*PI)+1.D0/OMEGA-1.D0
      IF(FRM.LE.0.D0) GO TO 100
      FRM=DLOG(FRM)
      FR=FRP-FRM
      IF(IBUG.EQ.'Y') WRITE(IWRITE,102) PI,FR
102    FORMAT(1H+, ' PI=',1PD20.10,' FR=',1PD20.10)
      RETURN
100   INEG=-1
      RETURN
      END

```

```

SUBROUTINE LOCIN(GAIN,W,IORD,XI,PHI,TD,OMEGAP,RTOL,FTOL,ITRTOL,
1 IWRITE,IBUG)
C-----0-----0-----0-----0-----0-----0-----0-----0
C Program that calculates the critical gain for single
C biochemical control loops of high order and with time delays.
C The program simply finds the first crossing of the imaginary
C axis and evaluates the reciprocal of that value
C
C Parameters
C     IORD : the order of the transfer function
C             describing the reaction chain
C     XI   : a vector with the damping factors
C     PHI  : a vector with the time constants
C     OMEGAP: the slope of the removal rate
C     TD   : the time delay
C
C Output
C     GAIN : the value of the critical gain
C     W    : the value of the critical frequency
C
C-----0-----0-----0-----0-----0-----0-----0-----0
      IMPLICIT DOUBLE PRECISION(A-H,O-Z)
      DOUBLE PRECISION DSQRT
      DIMENSION XI(5), PHI(5)
      IF(IBUG.NE.'Y') GO TO 30
      WRITE(IWRITE,101) OMEGAP,TD
101   FORMAT(' In LOCIN',//,' Omega-sub-pi = ',1PD15.5,
1 ' Tau-sub-d = ',1PD15.5)
      IODD=MOD(IORD,2)
      DO 40 I4=1,IORD/2+IODD
40    WRITE(IWRITE,102) I4,XI(I4),PHI(I4)
102   FORMAT(' For subsystem ',I3,' xi= ',1PD15.5,' phi= ',1PD15.5)
30    N=IORD/2
      IODD=MOD(IORD,2)
C-----0-----0-----0-----0-----0-----0-----0-----0
C estimate root
      W=1.D-5
      CALL IM(W,XI,PHI,OMEGAP,TD,N,IODD,F,IWRITE,IBUG)
10   SAVE=F
      W=10.D0*W
      CALL IM(W,XI,PHI,OMEGAP,TD,N,IODD,F,IWRITE,IBUG)
      IF(SAVE*F.GT.0.D0) GO TO 10
C-----0-----0-----0-----0-----0-----0-----0-----0
C start regula falsi
      B=W
      A=W/10.D0
      FB=FR
      FA=SAVE
      W=A
      FW=FA

```

```

SIGNA=DSIGN(1.D0,FA)
DO 100 I1=1,ITRTOL
IF(DABS(B-A).LT.RTOL) GO TO 500
IF(DABS(FW).LT.FTOL) GO TO 500
W=(FA*B-FB*A)/(FA-FB)
PREV=DSIGN(1.D0,FW)
CALL IM(W,XI,PHI,OMEGAP,TD,N,IODD,FW,IWRITE,IBUG)
IF(SIGNA*FW.LT.0.D0) GO TO 200
A=W
FA=FW
IF(FW*PREV.GT.0.D0) FB=FB/2.D0
GO TO 100
200 B=W
FB=FW
IF(FW*PREV.GT.0.D0) FA=FA/2.D0
100 CONTINUE
500 IF(I1.EQ.ITRTOL) WRITE(IDEV,103)
103 FORMAT(' MAXIMUM ITERATIONS WHEN ITERATING ON FREQUENCY ',,$)
C-----0-----0-----0-----0-----0-----0-----0-----
Compute the real part of g(iw) at w-critical
20 GAIN=1.D0/DSQRT(W**2+OMEGAP**2)
DO 3 I3=1,N
3 GAIN=GAIN/DSQRT((1.D0-(PHI(I3)*W)**2)**2+
1 (2.D0*XI(I3)*PHI(I3)*W)**2)
IF(IODD.NE.0) GAIN=GAIN/DSQRT((PHI(N+1)*W)**2+1.D0)
GAIN=-1.D0/GAIN
IF(IBUG.EQ.'Y') WRITE(IWRITE,104) W,GAIN
104 FORMAT(' The critical conditions are: ',/
1 ' Frequency = ',1PD15.5,' Psi-sub-pi = ',1PD15.5)
RETURN
END

```

```

SUBROUTINE IM(W,XI,PHI,OMEGAP,TD,N,IODD,VALUE,IWRITE,IBUG)
C-----0-----0-----0-----0-----0-----0-----0-----
C A subroutine that computes the imaginary part of g(iw)
C-----0-----0-----0-----0-----0-----0-----0-----
IMPLICIT DOUBLE PRECISION(A-H,O-Z)
DOUBLE PRECISION DATAN
DIMENSION XI(5), PHI(5)
VALUE=3.141592D0-TD*W+DATAN(-W/OMEGAP)
DO 1 I1=1,N
IF(W*PHI(I1).EQ.1.D0) GO TO 2
ANG=DATAN(-2.D0*XI(I1)*PHI(I1)*W/(1.D0-(W*PHI(I1))**2))
IF(ANG.GT.0.D0) ANG=ANG-3.141592D0
GO TO 1
2 ANG=-3.141592/2.D0
1 VALUE=VALUE+ANG

```

```
IF(IODD.NE.0) VALUE=VALUE+DATAN(-W*PHI(N+1))
IF(IBUG.NE.'Y') RETURN
WRITE(IWRITE,101) W,VALUE
101 FORMAT(' Frequency = ',1PD15.5,' Function = ',1PD15.5)
RETURN
END
```

```

DOUBLE PRECISION FUNCTION DFMIN(AX,BX,F,TOL)
C-----0-----0-----0-----0-----0-----0-----0-----
C One dimensional optimization routine. Taken from, "Mathematical
methods
C for mathematical computations", C G.E.Forsythe et al (1977) pg185-187.
C
C AX      left endpoint of initial interval
C BX      right endpoint of initial interval
C F       function subprogram that evaluates F(X) for any X in (AX,BX)
C TOL     desired lenght of the interval of uncertainty in the final
result.
C-----0-----0-----0-----0-----0-----0-----0-----
IMPLICIT DOUBLE PRECISION (A-H,O-Z)
C=.5D0*(3.D0-DSQRT(5.D0))
EPS=1.D0
10    EPS=EPS/2.D0
TOL1=1.D0+EPS
IF(TOL1.GT.1.D0) GO TO 10
EPS=DSQRT(EPS)
A=AX
B=BX
V=A+C*(B-A)
W=V
X=V
E=0.D0
FX=F(X)
FV=FX
FW=FX
20    XM=.5D0*(A+B)
TOL1=EPS*DABS(X)+TOL/3.D0
TOL2=2.D0*TOL1
IF(DABS(X-XM).LE.(TOL2-.5D0*(B-A))) GO TO 90
IF(DABS(E).LE.TOL1) GO TO 40
R=(X-W)*(FX-FV)
Q=(X-V)*(FX-FW)
P=(X-V)*Q-(X-W)*R
Q=2.D0*(Q-R)
IF(Q.GT.0.D0) P=-P
Q=DABS(Q)
R=E
E=D
30    IF(DABS(P).GE.DABS(.5D0*Q*R)) GO TO 40
IF(P.LE.Q*(A-X)) GO TO 40
IF(P.GE.Q*(B-X)) GO TO 40
D=P/Q
U=X+D
IF((U-A).LT.TOL2) D=DSIGN(TOL1,XM-X)
IF((B-U).LT.TOL2) D=DSIGN(TOL1,XM-X)
GO TO 50
40    IF(X.GE.XM) E=A-X

```

```
IF(X.LT.XM) E=B-X
D=C*E
50   IF(DABS(D).GE.TOL1) U=X+D
      IF(DABS(D).LT.TOL1) U=X+DSIGN(TOL1,D)
      FU=F(U)
      IF(FU.GT.FX) GO TO 60
      IF(U.GE.X) A=X
      IF(U.LT.X) B=X
      V=W
      FV=FW
      W=X
      FW=FX
      X=U
      FX=FU
      GO TO 20
60   IF(U.LT.X) A=U
      IF(U.GE.X) B=U
      IF(FU.LE.FW) GO TO 70
      IF(W.EQ.X) GO TO 70
      IF(FU.LE.FV) GO TO 80
      IF(V.EQ.X) GO TO 80
      IF(V.EQ.W) GO TO 80
      GO TO 20
70   V=W
      FV=FW
      W=U
      FW=FU
      GO TO 20
80   V=U
      FV=FU
      GO TO 20
90   DFMIN=X
      RETURN
      END
```

**TITLE OF THESIS:** Mathematical Modelling of Dynamics and Control

in Metabolic Networks

**MAJOR PROFESSOR** Edwin N. Lightfoot

**MAJOR DEPARTMENT** Chemical Engineering

**MINOR** Distributed

**NAME** Bernhard Orn Palsson

**PLACE AND DATE OF BIRTH** Reykjavik, Iceland feb 22, 1957

**COLLEGES AND UNIVERSITIES: YEARS ATTENDED AND DEGREES**

University of Iceland 1975-1977

University of Kansas - Lawrence 1977-1979 BS in Chemical Engng.

University of Wisconsin - Madison 1979-1984

**MEMBERSHIPS IN LEARNED OR HONORARY SOCIETIES** American Institute

of Chemical Engineers, American Association for the Advancement of  
Science.

**PUBLICATIONS** "Biomass as a Source of Chemical Feedstocks," Science  
Magazine, vol. 213, 513 (1981), with S. Fathi-Afshar and D. F. Rudd  
and E. N. Lightfoot, "Determination of Steady-state Generation Time  
Distribution from Labelled Mitosis Experimental Data," Cell and Tissue  
Kinetics, vol. 14, 365 (1981) with K. J. Himmelstein, "Mathematical  
Modelling of Dynamics and Control in Metabolic Networks. Part I. On  
Michaelis-Menten Kinetics," with E. N. Lightfoot and "Part II. Simple  
Dimeric Enzymes," with R. Jamier and E. N. Lightfoot, in press in  
the Journal of Theoretical Biology

**DATE** July 30, 1984